

1-1-2017

Development Of Tools For Phosphosite-Specific Kinase Identification And Discovery Of Phosphatase Substrates

Pavithra Maheshani Dedigama Arachchige
Wayne State University,

Follow this and additional works at: https://digitalcommons.wayne.edu/oa_dissertations

 Part of the [Biochemistry Commons](#)

Recommended Citation

Dedigama Arachchige, Pavithra Maheshani, "Development Of Tools For Phosphosite-Specific Kinase Identification And Discovery Of Phosphatase Substrates" (2017). *Wayne State University Dissertations*. 1693.
https://digitalcommons.wayne.edu/oa_dissertations/1693

This Open Access Dissertation is brought to you for free and open access by DigitalCommons@WayneState. It has been accepted for inclusion in Wayne State University Dissertations by an authorized administrator of DigitalCommons@WayneState.

**DEVELOPMENT OF TOOLS FOR PHOSPHITE-SPECIFIC KINASE
IDENTIFICATION AND DISCOVERY OF PHOSPHATASE SUBSTRATES**

by

PAVITHRA DEDIGAMA ARACHCHIGE

DISSERTATION

Submitted to the Graduate School

of Wayne State University,

Detroit, Michigan

in partial fulfillment of the requirements

for the degree of

DOCTOR OF PHILOSOPHY

2017

MAJOR: CHEMISTRY (Biochemistry)

Approved By:

Advisor

Date

DEDICATION

To all those who seek the truth

AND

To all those who shine the light where it is dark

ACKNOWLEDGEMENTS

The past few years were a very important period in my life. I learnt so much and achieved a lot as a person. Looking back at myself, I see a happy change that will stay with me for the rest of my life and will continue to improve. I owe my happiness to a lot of you. Thank you so much for creating a conducive environment where I could grow. I wish you all the happiness in the world. Although I don't have space to acknowledge all of you, I would like to mention a few names.

First of all, I would like to thank my wonderful supervisor Prof. Mary Kay Pflum. Thank you so much for being an amazing mentor! You have no idea how much of a positive impact you have had on my life. It is not an exaggeration to say that you are one of the best individuals I have met in my whole life. Thank you so much for giving me both the freedom and the support to grow, not just as a scientist but also as a person. I wish you all the happiness in the world.

Secondly, I would like to thank my lab members for their help and support. I am especially grateful to Anita Chalasani and Todd Faner for their very kind guidance during my early years in the lab. In addition, my special thanks also goes to my fantastic undergraduate student, Monika Franco for her valuable help in research work. Other members of the Pflum lab, Chamara Senevirathne, Satish Garre, Geetha Padige, Magdalene Wambua, Alexander Stark, Thilani Anthony, Maheeka Embogama, Ahmed Fouda, Dhanusha Nalawansa, Ahmed Negmeldin, Inosha Gomes, Cyprein Nanah, Ben James, Nuwan Chinthaka, Vindya Rathnayake and Aparni Gamage, thank you all so much for the fun memories and support. You all made my time in the Pflum lab highly enjoyable and exciting.

Next, I should offer my gratitude to the staff of proteomics core at Institute of Environmental Health Sciences, Wayne State University for the help in proteomics analysis. I am especially thankful to Dr. Paul Stemmer, Dr. Joseph Caruso, Dr. Nicholas Carruthers and Namhee Shin for both performing the proteomics experiments and also for offering helpful advice on data analysis.

My special thanks also go to my wonderful collaborators, Prof. Jing Liu at Northwestern University and Prof. Zhengping Yi and Dr. Xiangmin Zhang at College of Pharmacy and Health Sciences. Thank you so much for the exciting research opportunity and your valuable input on data interpretation. In addition, I would also like to convey my gratitude to my committee for their constructive comments and useful suggestions on the research work. Thank you so much for your flexibility and support.

I would also like to express my thanks to the kind, helpful staff of the Wayne State Chemistry Department. I am especially grateful to Greg Kish, Elizabeth Ries, Bonnie Cetlinski, Jason Parizon, Emil Lozanov, Melissa Barton, Yuriy Danylyuk, Olena Danylyuk, Kellie Lauder and Jacqueline Baldyga for their help in various ways. In addition, I would like to express my heartfelt gratitude to all the students and faculty of the Wayne State Chemistry Department. Even though I don't have the chance to mention you all by your names, I am very grateful to all of you in the Department for your kind help on numerous situations.

I am thankful to all my Sri Lankan friends in USA for your help throughout these years. Thank you so much for your friendship and kind help.

I am forever indebted to my parents and family for their love and support. Thanks for giving birth to me, allowing me a chance to discover the true purpose of life. My dear sisters and brother, thank you for your sweet love and company.

Last but not least, my gratitude goes to my best friend and husband, Thilina. Words can't do justice for what you have given me. Thanks for being who you are and being there with me and showing me the way.

TABLE OF CONTENTS

DEDICATION	ii
ACKNOWLEDGEMENTS	iii
LIST OF TABLES	xi
LIST OF FIGURES	xii
LIST OF ABBREVIATIONS	xv
CHAPTER 1 INTRODUCTION	1
1.1 Protein phosphorylation	1
1.2 Phosphorylation and signal transduction	2
1.3 Phosphorylation and diseases	4
1.4 Protein kinase classification, structure, mechanism and consensus sequence	4
1.5 Challenges associated with studying phosphorylation	9
1.6 γ -modified ATP analogs	9
1.6.1 ATP- γ S	10
1.6.2 Other γ -modified ATP analogs used to study phosphorylation	12
1.6.3 γ -modified ATP analogs used by Pflum and colleagues	14
1.6.3.1 ATP-biotin	14
1.6.3.2 ATP-dansyl	17
1.6.3.3 γ -modified ATP analogs with photocrosslinkers	18
1.7 Thesis Project	21
CHAPTER 2 K-CLASP (KINASE CATALYZED CROSS-LINKING AND STREPTAVIDIN PURIFICATION)	23
2.1 Current methods available for phosphosite specific kinase identification	24

2.1.1 In silico kinase prediction	24
2.1.2 Mechanism based crosslinking	25
2.2 K-CLASP strategy	27
2.3 K-CLASP using Protein Kinase A (PKA) and kemptide	29
2.3.1 In vitro crosslinking reactions with recombinant PKA and kemptide	30
2.3.2 In vitro crosslinking with recombinant CK2 and CK2 peptide	33
2.3.3 In vitro crosslinking with lysates and kemptide	33
2.3.4 K-CLASP with kemptide and lysates	36
2.4 K-CLASP to uncover the kinase/s that phosphorylate Miz1 protein	41
2.4.1 Miz1 protein	41
2.4.2 K-CLASP with Miz1 protein	42
2.5 Conclusions and Future Directions	49
2.6 Experimental Methods	51
2.6.1 Synthesis of ATP-ArN3	51
2.6.2 Peptide Synthesis and Purification	51
2.6.3 In vitro crosslinking reaction with recombinant PKA	54
2.6.4 SDS-PAGE (sodium dodecyl sulfate polyacrylamide gel electrophoresis)	55
2.6.5 Protein transfer onto a membrane	56
2.6.6 Visualization of biotin with streptavidin-Cy5 and Western blot	56
2.6.7 Sypro®Ruby staining for total protein visualization	57
2.6.8 In vitro crosslinking with PKA after pre-incubation of N-biotin peptide and ATP-ArN3	57
2.6.9 In vitro crosslinking reaction with recombinant CK2	58
2.6.10 MEF cell culture	58

2.6.11 HeLa and MEF cell lysis	59
2.6.12 Optimization of crosslinking reaction with HeLa cell lysates	59
2.6.13 In vitro crosslinking reaction with HeLa lysates	60
2.6.14 K-CLASP procedure	60
2.6.15 In gel digestion	62
2.6.16 LC-MS/MS analysis	64
2.6.17 Interactome analysis	65
CHAPTER 3: K-BIPS (KINASE-CATALYZED BIOTINYLATION TO IDENTIFY PHOSPHATASE SUBSTRATES)	66
3.1 Background	66
3.1.1 Protein Phosphatases	67
3.1.1.1 Protein Tyr phosphatases (PTPs)	67
3.1.1.2 Ser/Thr Phosphatases	68
3.1.2 Substrate trapping mutant strategy for phosphatase substrate identification ...	70
3.1.3 Phosphoproteomics for discovery of phosphatase substrates	71
3.1.4 Phosphatase activity is required for kinase-catalyzed biotinylation	72
3.1.5 The K-BIPS strategy	74
3.2 Results	75
3.2.1 K-BIPS using okadaic acid mediated phosphatase inactivation	75
3.2.1.1 K-BIPS with OA-mediated phosphatase inhibition.....	76
3.2.2 K-BIPS for PP1-Gadd34 substrate identification	81
3.2.2.1 Inactivation of PP1-Gadd34 system leads to a loss in biotinylation	83
3.2.2.2 K-BIPS with PP1-Gadd34 inactivated lysates	84
3.2.2.3 K-BIPS exposed novel roles of PP1-Gadd34 in UPR.....	88

3.2.3 K-BIPS for PP1-MYPT1 substrate identification	91
3.3.3.1 K-BIPS with PP1-MYPT1 inactivated lysates	92
3.3 Conclusions and future directions	98
3.4 Experimental methods	100
3.4.1 Synthesis of ATP-biotin	100
3.4.2 OA treatment of HeLa cells	101
3.4.3 Induction of UPR and guanabenz (Gb) treatment of HeLa cells.....	101
3.4.4 Inactivation of MYPT1 in L6 cells	102
3.4.5 Cell harvesting	102
3.4.6 Cell lysis	103
3.4.7 ATP-biotin labeling of OA treated lysates for K-BIPS	103
3.4.8 ATP-biotin labeling of PP1-Gadd34 inactivated lysates	103
3.4.9 ATP-biotin labeling of PP1-MYPT1 inactivated lysates for K-BIPS	104
3.4.10 Streptavidin purification of biotinylated proteins for K-BIPS	104
3.4.11 In gel digestion	105
3.4.12 TMT labeling of peptides and LC-MS/MS analysis for K-BIPS study with OA-mediated phosphatase inactivation	105
3.4.13 LC-MS/MS analysis for K-BIPS study with PP1-Gadd34 and PP1-MYPT1 inactivation	106
3.4.14 MS data analysis for K-BIPS study with OA-mediated phosphatase inactivation, PP1-Gadd34 and PP1-MYPT1 inactivation	107
3.4.15 Streptavidin enrichment of COPS5, WDR5, CAPRIN1 and G3BP1 from PP1-Gadd34 inactivated lysates	108
Appendix A CHAPTER 2 SUPPORTING INFORMATION	109
Appendix B CHAPTER 3 SUPPORTING INFORMATION	144
Appendix C COPYRIGHT PERMISSIONS	169

REFERENCES.....	175
ABSTRACT	199
AUTOBIOGRAPHICAL STATEMENT.....	201

LIST OF TABLES

Table1.1 Consensus sequence for some kinases	8
Table 2.1 Kinases enriched in K-CLASP	36
Table 2.2 Kinases seen in Miz1 peptide K-CLASP study	43
Table 2.3 Kinase direct interacting proteins observed by K-CLASP study with Miz1 peptide	44
Table 3.1 Known phosphatase substrates among the K-BIPS hits from OA-mediated phosphatase inactivation	78
Table 3.2 K-BIPS hits from the OA-mediated phosphatase inactivation that are not known substrates, but known to interact with phosphatase	79
Table 3.3 PP1 and Gadd34 interacting proteins among K-BIPS hits	85
Table 3.4 K-BIPS hits with biological function related to PP1	87
Table 3.5 Hits showing reproducible enrichment in all three replicates from the K-BIPS study with PP1-MYPT1 inactivated lysates	94
Table 3.6 PP1 and MYPT1 interacting proteins and proteins related to PP1-MYPT1 activity from among the K-BIPS hits enriched in only two replicates	95

LIST OF FIGURES

Figure 1.1 Protein phosphorylation	1
Figure 1.2 RAF/MEK/ERK pathway	3
Figure 1.3 Human kinase classification	5
Figure 1.4 The catalytic core of PKA and the critical active site residues.....	7
Figure 1.5 Kinase mechanism.	8
Figure 1.6 Co-substrate promiscuity of kinases.....	10
Figure 1.7 The use of ATP- γ S analog	11
Figure 1.8 The use of ATP- γ S derivative to identify substrates of CDK1.....	12
Figure 1.9 ATP-atto and ATP-ferrocene	13
Figure 1.10 Kinase labeling by ATP-acyl-biotin	14
Figure 1.11 ATP-biotin leads to phosphobiotinylation of proteins.....	15
Figure 1.12 K-BILDS procedure	16
Figure 1.13 APB	17
Figure 1.14 ATP-dansyl and its application	18
Figure 1.15 Use of photo-crosslinking ATP analogs	19
Figure 1.16 Fluorescent labeling of CK2 kinase using ATP-arylazide	20
Figure 1.17 Bifunctional ATP analog used by Cole and colleagues	21
Figure 2.1 Mechanism based crosslinking with the o-phthaldialdehyde crooslinker.....	26
Figure 2.2 Mechanism based crosslinkers developed by Shokat and colleagues	27
Figure 2.3 Mechanism based crosslinking with the methylacrylate crooslinker	27
Figure 2.4 Kinase-catalyzed labeling and the K-CLASP method.....	28
Figure 2.5 N-biotin kemptide crosslinking with recombinant PKA and lysates.....	30

Figure 2.6 Proposed nonspecific reactivity of N-biotin mutant kemptide to account for background biotinylation in Figure 2.5, lane 6.	31
Figure 2.7 In vitro crosslinking reactions with recombinant PKA with biotin peptide pre-incubated with ATP-ArN3.	32
Figure 2.8 Crosslinking reactions with recombinant CK2	33
Figure 2.9: Optimization of K-CLASP crosslinking with HeLa cell lysates.	34
Figure 2.10 N-biotin kemptide crosslinking with recombinant PKA and lysates. N-biotin kemptide crosslinking with ATP-ArN3 in HeLa lysates	35
Figure 2.11 Abundance values of the 324 K-CLASP hits	37
Figure 2.12 Kinase hits and interactome analysis of the PKA K-CLASP study	38
Figure 2.13 Direct interacting proteins of the kinases observed in K-CLASP.	40
Figure 2.14 Protein complexes identified by K-CLASP	41
Figure 2.15 Direct interacting proteins and substrates of the kinases observed in K-CLASP	45
Figure 2.16 Interacting proteins of Miz1 (ZBTB17)	47
Figure 2.17 Clusters of proteins identified by MCODE among the K-CLASP hits	48
Figure 3.1 Transmembrane receptor tyrosine phosphatases and non-receptor tyrosine phosphatases.	68
Figure 3.2 Multimeric nature of the PPP Ser/Thr phosphatase family.	69
Figure 3.3 ATP-biotin labeling requires phosphatases.	73
Figure 3.4 The K-BIPS method	74
Figure 3.5 K-BIPS study with OA.....	77
Figure 3.6 Functional classification of the proteins identified by the K-BIPS study with OA.	80
Figure 3.7 The analysis of abundance of hits from the K-BIPS study with OA-mediated phosphatase inactivation.	81
Figure 3.8 Expression of Gadd34 in HeLa lysates treated with Tm and Gb	83

Figure 3.9 Biotinylation with PP1-Gadd34 inactivated lysates.....	84
Figure 3.10 The abundance of proteins identified from the K-BIPS study with PP1-Gadd34 inactivation.....	86
Figure 3.11 Secondary validation of COPS5, WDR5, CAPRIN1 and G3BP1.....	88
Figure 3.12 Knockdown of MYPT1 in L6 lysates treated with Dox.	93

LIST OF ABBREVIATIONS

Amino Acids

A or Ala – alanine	N or Asn - asparagine
C or Cys – cycteine	P or Pro - proline
D or Asp – aspatate	Q or Gin - glutamine
E or Glu – glutamate	R or Arg - arganine
F or Phe – phenylalanine	S or Ser - serine
G or Gly – gllycine	T or Thr - threonine
H or His – histidine	V or Val - valine
I or Ile – isoleucine	W or Trp - tryptophan
K or Lys – lysine	X- any amino acid
L or Leu – leucine	Y or Try - tyrosine
M or Met – Methionine	Z – hydrophobic residue

Nucleic Acids

ADP - 5'-Adenosine diphosphate
ATP - 5'-Adenosine triphosphate
ATP- γ S- 5'-Adenosine -[γ -thio]triphosphate
APB-ATP-polyamine-biotin

Kinases

RAF- Serine/threonine-protein kinase RAF
MEK- MAPK/ERK kinase
ERK- Extra cellular signal regulated kinase
PINK1- Serine/threonine-protein kinase PINK1
LRRK2- Leucine-rich repeat serine/threonine-protein kinase 2
WNK- Protein kinase with no lysine
SPAK- STE20/SPS1-related proline-alanine-rich protein kinase
PKA-cAMP dependent Protein Kinase A
ATM- Ataxia telangiectasia mutated kinase

SGK- Serum/glucocorticoid-regulated kinase 1
CDK1- Cyclin-dependent kinase 1
CK2- Casein kinase II
CAMKII- Calcium/calmodulin-dependent protein kinase type II subunit gamma
ABL-Abelson kinase
CSK- Tyrosine-protein kinase CSK
SRC- Proto-oncogene tyrosine-protein kinase Src
AKT1- RAC-alpha serine/threonine-protein kinase
CHEK1- Checkpoint kinase-1
MAP2K7- Dual specificity mitogen-activated protein kinase kinase 7
ILK-Integrin-linked protein kinase
PBK- Lymphokine-activated killer T-cell-originated protein kinase
SLK- STE20-like serine/threonine-protein kinase
PERK- Eukaryotic translation initiation factor 2-alpha kinase 3/ PRKR-like endoplasmic reticulum kinase
EGFR- Epidermal growth factor receptor

Protein Phosphatases

PP1-Protein phosphatase 1
PP2A-Protein phosphatase 2A
PP2B- Protein phosphatase 2B
PP4- protein phosphatase 4
PP5- protein phosphatase 5
PP6- protein phosphatase 6
PP7- protein phosphatase 7
PTP1B-Protein-tyrosine phosphatase 1B
PTPN22- Tyrosine-protein phosphatase non-receptor type 22
Ptp61F- Tyrosine-protein phosphatase non-receptor type 61F

Other Proteins

CREB1- Cyclic AMP-responsive element-binding protein 1

Miz1- Myc-interacting zinc finger protein 1

Gadd34- Protein phosphatase 1 regulatory subunit 15A/ Growth arrest and DNA damage-inducible protein GADD34

MYPT1- Protein phosphatase 1 regulatory subunit 12A/ Myosin phosphatase target subunit 1

TNF- Tumor necrosis factor

HDAC1-Histone deacetylase 1

IRE1 α - Inositol-requiring enzyme 1

EIF2 α - Eukaryotic translation initiation factor 2 subunit 1 Eukaryotic translation initiation factor 2 subunit 1

Techniques

FRET- Fluorescence resonance energy transfer

UV light-Ultra violet light

HPLC-High performance liquid chromatography

SDS-PAGE- Sodiumdodecyl sulfate polyacrylamide gel electrophoresis

LC-MS/MS-Liquid chromatography, Tandem mass spectrometry

2D gel- Two dimensional gel electrophoresis

IMAC-Immobilized metal affinity chromatography

MALDI-TOF-Matrix assisted laser desorption/ionization time-of-flight

MS-Mass spectrometry

K-BILDS (Kinase-catalyzed Biotinylation with Inactivated Lysates for Discovery of Substrates)

K-CLASP (Kinase-catalyzed CrossLinking And Streptavidin Purification)

K-BIPS (Kinase-catalyzed Biotinylation to Identify Phosphatase Substrates)

Reagents

OA-Okadaic acid

Gb-guanabenz

Tm-tunicmycin

BME- β -mercaptoethanol

DMF-dimethyl formamide

FBS-Fetal bovine serum

TEAB-triethylammonium bicarbonate

TFA-trifluoro acetic acid

TRis- tris(hydroxymethyl)aminomethane

Dox-doxycycline

Other

EGF- Epidermal growth factor

MEF- Mouse embryonic fibroblasts

UPR- Unfolded protein response

ER-Endoplasmic reticulum

CHAPTER 1 INTRODUCTION

1.1 Protein phosphorylation

Proteins undergo various post translational modifications (PTMs) during their lifetime. PTMs add diversity to the 20 canonical amino acids and modulate the function of the proteins.¹ Among the various PTMs currently known, phosphorylation, the addition of a phosphoryl group onto a protein, represents an enzymatically-mediated, ubiquitous protein modification. In fact, it is estimated that 30% of cellular proteins are phosphorylated at least on one amino acid at a given time.²

Phosphorylation is a reversible chemical modification mediated by two enzyme families, kinases and phosphatases.³ Kinases use the universal phosphoryl donor ATP (5'-adenosine triphosphate) and catalyze the transfer of a phosphoryl group onto a Ser, Thr, or Tyr residue on a protein.⁴ Phosphatases remove the phosphoryl group in a process called dephosphorylation to reverse the reaction (Figure 1.1).

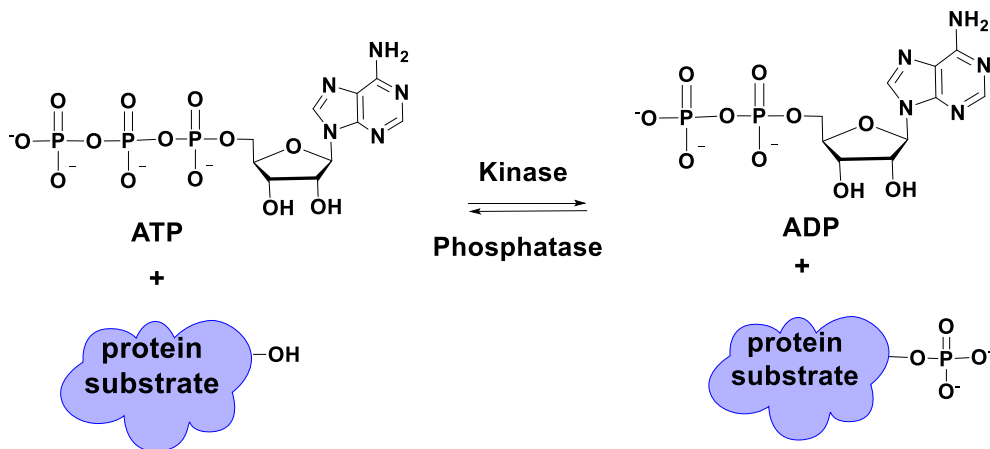


Figure 1.1: Protein phosphorylation. Kinases transfer a phosphoryl group from ATP to a hydroxyl containing amino acid on cellular proteins. ADP is produced as a side product. Phosphatases carry out dephosphorylation by removing the phosphoryl group.

Phosphorylation alters protein function by affecting activity, stability, binding, or localization.⁵ For example, the activity of the transcription factor CREB (cAMP Response Element Binding-protein) is regulated by phosphorylation. CREB is activated and promotes transcription when phosphorylated at Ser133 by Protein Kinase A.⁶ In another example, both stability and binding interactions of the tumor suppressor p53 protein are regulated by phosphorylation. Cellular levels of p53 are kept low under normal conditions by the interaction of p53 with the E3 ubiquitin ligase MDM2 (Mouse double minute 2 homolog), which targets p53 for degradation. However, when cells are stressed, p53 is phosphorylated and the interaction with MDM2 is prevented, resulting in p53 stabilization.⁷ Lastly, the microtubule-associated protein 2 (MAP2) provides a fine example of how protein localization is regulated by phosphorylation. MAP2 associates with microtubules when dephosphorylated at its KXGS motifs. When phosphorylated, MAP2 dissociates from microtubules and localizes to the actin cytoskeleton.⁸ In addition, the nuclear transport of many proteins are also known to be dependent on phosphorylation.⁹

1.2 Phosphorylation and signal transduction

Protein phosphorylation plays a prominent role in signal transduction. For example, in RAF/MEK/ERK signaling pathway (Figure 1.2), an external ligand binding to a cell surface receptor triggers the auto-phosphorylation of the receptor, providing binding sites to the adapter protein GRB2 (Growth-factor-receptor-bound protein 2). The GRB2 bound RAS exchange factor, SOS (Son of sevenless), then activates RAS protein by promoting the exchange of GDP to GTP. Activated RAS binds and activates RAF kinase. RAF in turn phosphorylates and activates MEK (MAPK/ERK kinase). Sequentially, MEK

phosphorylates and activates ERK (Extracellular signal regulated kinase). Activated ERK phosphorylates a variety of substrate proteins, including transcription factors that promotes gene transcription.^{10,11} Thus, phosphorylation is used as a medium in relaying signals in the cell. Eventually, the pathway is turned off by the activity of the PP2A phosphatase, which dephosphorylates MEK and ERK.¹² As this example illustrates, reversible phosphorylation acts as a key chemical switch in cell signaling.

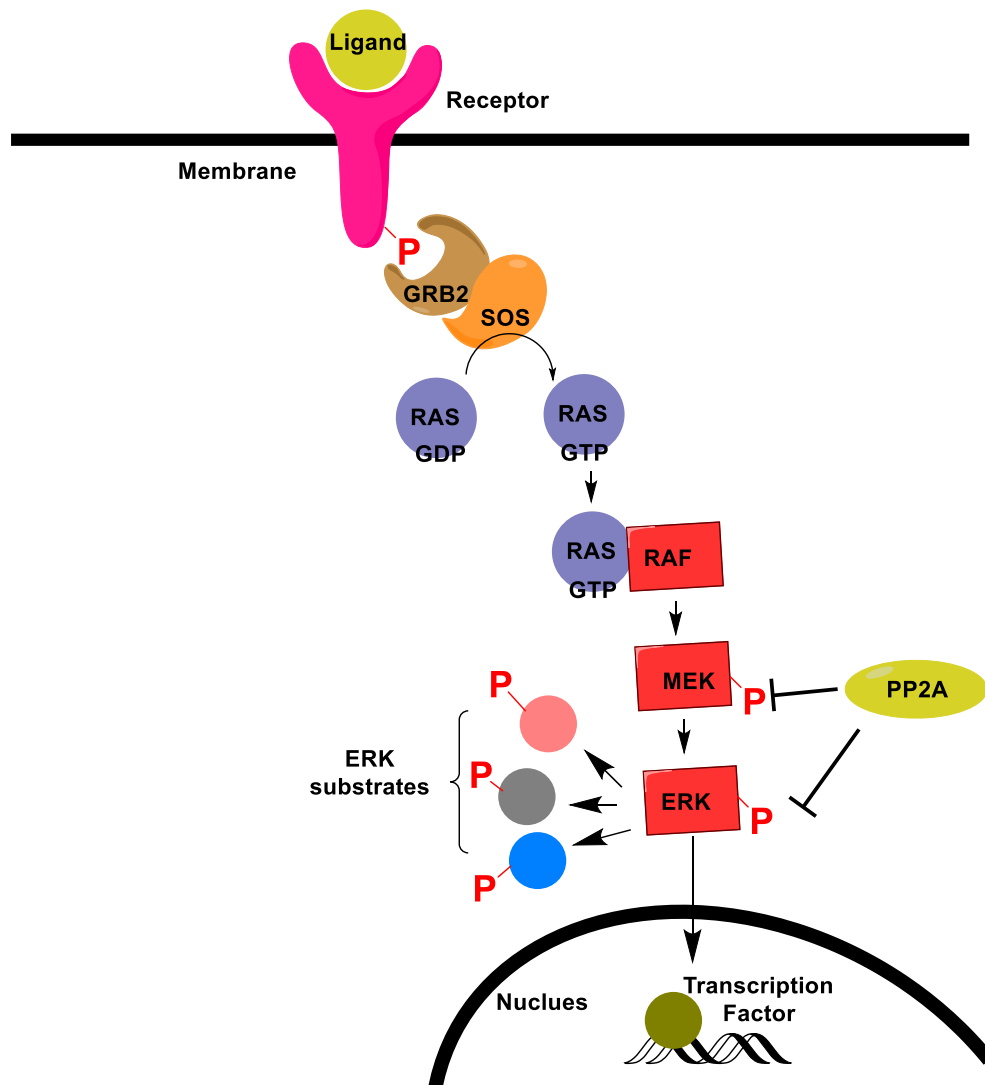


Figure 1.2: RAF/MEK/ERK pathway. See the text for a detailed description.

1.3 Phosphorylation and diseases

Owing to the profound role of phosphorylation in signal transduction and regulation of protein function in general, defects in phosphorylation are implicated in various human diseases. For example, aberrations in RAF/MEK/ERK kinase activities, either through activating mutations or the down regulation of negative regulators, such as phosphatases, have been shown to be root causes for cancer.¹³ In another example, the hyperactivity of PTP1B (protein-tyrosine phosphatase 1B) phosphatase, which is a negative regulator in insulin signaling, has been linked with obesity and diabetes.¹⁴ Further, mutations in PINK1 and LRRK2 kinases have been shown to be associated with Parkinson's disease.¹⁵ In addition, WNK and SPAK kinases have been implicated in hypertension.¹⁶ In one last example from a plethora of other available examples, the activity of PP1-Gadd34 phosphatase has been shown to be perturbed during viral transfection.¹⁷

Based on the fact that aberrant phosphorylation is a common cause of various human malignancies, kinases and phosphatases have emerged as popular drug targets in tackling diseases.¹⁸ By 2015, 28 kinase inhibitors were approved by US FDA (US Food and Drug Administration).¹⁹ Although most of the current drugs have been developed for treating cancer, a few have been approved for other diseases, such as rheumatoid arthritis and idiopathic pulmonary fibrosis. In addition, many other kinase and phosphatase inhibitors are in clinical trials.²⁰

1.4 Protein kinase classification, structure, mechanism and consensus sequence

The human proteome is estimated to include 518 protein kinases.²¹ Broadly, protein kinases are classified into two classes: Tyr kinases and Ser/Thr kinases. As the names imply, Tyr kinases phosphorylate Tyr residues while Ser/Thr kinases catalyze the

phosphorylation of Ser or Thr residues. In addition, human kinases have been classified into eight groups (Figure 1.3) depending on the sequence of the catalytic domain and structural features.²²

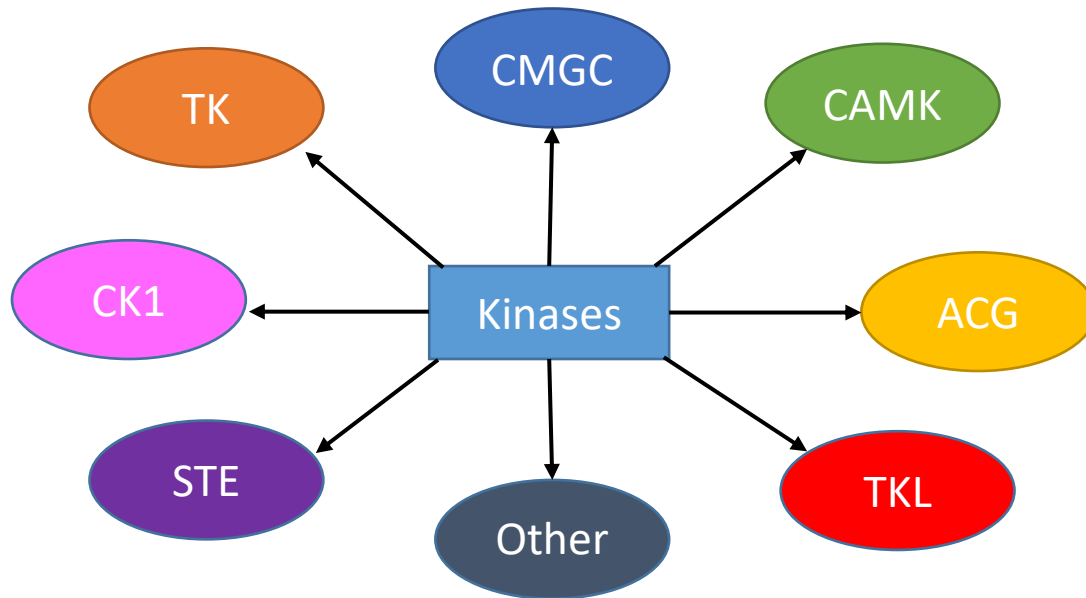


Figure 1.3: Human kinases classification. Human protein kinases are categorized into 8 groups. CAMK: Calmodulin dependent protein kinase group. ACG: Includes PKA, PKG and PKC families. TKL: Tyrosine-kinase like family. STE: Homologs of yeast Sterile 7, sterile 11 and sterile 20 kinases. CK1: Casein kinase 1 family. TK: Tyrosine kinase family. CMGC: Includes CDK, MAPK, GSK3 and CLK families. Others: kinases that does not belong to the above 7 groups.

Despite the differences in the overall structure and the substrate preferences, all eukaryotic kinases share a common catalytic core.²³ PKA (cAMP dependent Protein Kinase A), one of the first kinase structures to be solved, provides a fine example of a kinase catalytic core (Figure 1.4A). The kinase core structure is arranged as two separate lobes. The smaller lobe contains the N-terminal domain and is composed primarily of five anti-parallel β -sheets. The C-terminal domain makes up the bigger lobe and is rich in α -helices. The two lobes are connected by a linker hinge region. A deep cleft in between

the two lobes constitutes of the active site. ATP binds in the form of MgATP with the adenine ring stabilized by the linker hinge region and the γ -phosphate group extending outwards. The hinge region contains a gatekeeper residue that interacts with the adenine base. The substrate binds near the edge of the cleft.²³⁻²⁴

The residues near the kinase active site are highly conserved. A conserved glycine-rich loop called the P-loop connecting the first two β -strands (Figure 1.4A) is thought to bring the bound ATP close to the substrate.^{24a} A conserved Lys residue (Lys72 in PKA, Figure 1.4B) in the third β -strand interacts with the α and β phosphoryl groups of ATP. The conserved Lys is stabilized by a salt bridge with a Glu (Glu91 in PKA) in the C-terminal domain. The C-terminal lobe carries a metal binding loop composed of a conserved DFG domain. The Asp in the metal binding loop (Asp184 in PKA) chelates the Mg that contacts the β and γ phosphoryl groups of ATP. A second Mg is coordinated by a conserved Asn (Asn171 in PKA). A catalytic loop in the C-terminal lobe (Arg165-Asn171 in PKA) contains the residues responsible for catalysis. An invariant Asp residue (Asp166 in PKA) acts as a base by removing a proton from the hydroxyl of the substrate. A Lys residue in the catalytic loop (Lys168 in PKA) interacts with the γ -phosphoryl group and balances the negative charge. With the γ -phosphoryl of ATP being correctly oriented for nucleophilic attack by the substrate, the substrate is phosphorylated while producing ADP as a by-product (Figures 1.4B and 1.5).^{24a, 25}

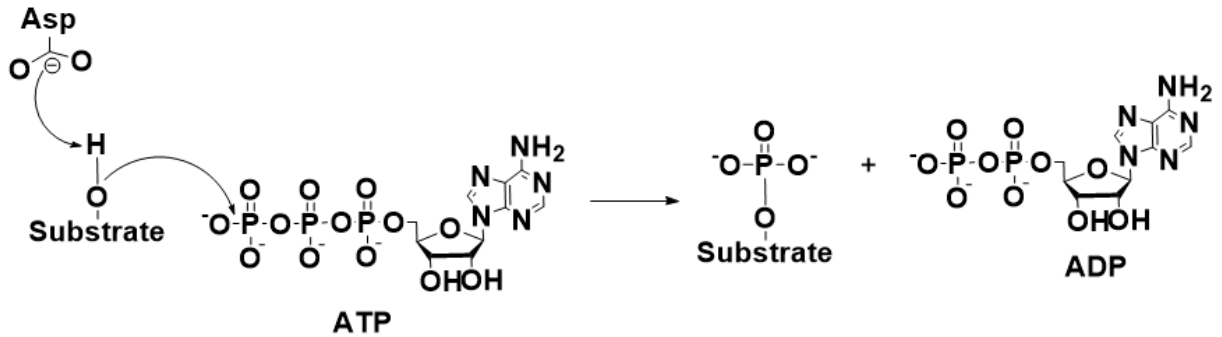


Figure 1.5: Kinase mechanism.

Although the ATP binding fold and the active site of the kinases are highly conserved, kinases show selectivity toward their substrates. Generally, the kinases recognize a conserved sequence of the substrate called the consensus sequence that flanks the phospho-site.²⁵ Consensus sequences identified for some kinases show that certain kinases depend on the presence of acidic, basic, or proline residues in the protein substrate to selectively phosphorylate a given phosphosite. For example, PKA uses a basic consensus sequence of R-R-X-S/T (X is any amino acid) to phosphorylate Ser/Thr residues of the substrates. Consensus sequences for some well-known kinases are shown below (Table 1.1).²⁵ More information on consensus sequence are provided in Chapter 2.

Table 1.1: Consensus sequence for some kinases^a

Kinase	Consensus sequence
PKA	R-R-X- S/T
ABL	I/V/L- Y -X-X-P/F
AKT1	R-X-R-XX- S/T
CDK1	S/T -P-X-R/K
CK2	S/T -X-X-D/E
ERK1	P-X- S/T -P
Aurora A	R/K/N-R-X- S/T
CHK1	R-X-X- S/T
EGFR	E-E-E- Y -F
CDK2	S/T -P-X-R/K

^aX represents any amino acid. The phosphosite is shown in bold letters.

1.5 Challenges associated with studying phosphorylation

Despite the disease relevance, understanding how phosphorylation regulates cellular processes has been challenging. The difficulties can be attributed to both the ubiquity of phosphorylation and the complicated manner by which phosphorylation is carried out. According to the PhosphoSitePlus data base, the human proteome contains about 270,000 phospho-sites,²⁶ with many novel sites being routinely discovered. In addition, a single protein can be phosphorylated on multiple residues. For example, the iPTMnet data base²⁷ reports 17 phosphosites for CREB1. Further, the same phosphosite can become phosphorylated by multiple kinases. For instance, depending on the stimuli, Ser133 on CREB1 can be phosphorylated by various kinases such as PKA,⁶ ATM²⁸ and SGK²⁹. Additionally, the human proteome carries more than 500 kinases and hundreds of different phosphatases.^{2,22} Moreover, the kinases and phosphatases in turn are regulated by various mechanisms, further complicating how phosphorylation is carried out.³⁰ As a result, the cellular phosphorylation map remains incomplete, hindering our understanding of how various diseases arise. Therefore, methods are required to study phosphorylation and determine the mechanisms behind numerous human disorders. Among the methods currently available for studying phosphorylation, γ -modified ATP analogs represent a powerful approach.³¹

1.6 γ -modified ATP analogs

An examination of the kinase crystal structure shows that ATP binds the kinase in an orientation where the γ -phosphate group is pointed outwards and is solvent exposed (Figure 1.4A). As a result, kinases also tolerate γ -modified ATP analogs and show cosubstrate promiscuity, transferring γ -modified phosphoryl groups onto substrate

proteins (Figure 1.6).^{23, 32} when used as kinase cosubstrates, ATP analogs modified at the γ position with functional groups such as biotin, represent useful tools to study phosphorylation. The next section will discuss selected γ -modified ATP analogs and their use in phosphorylation research.

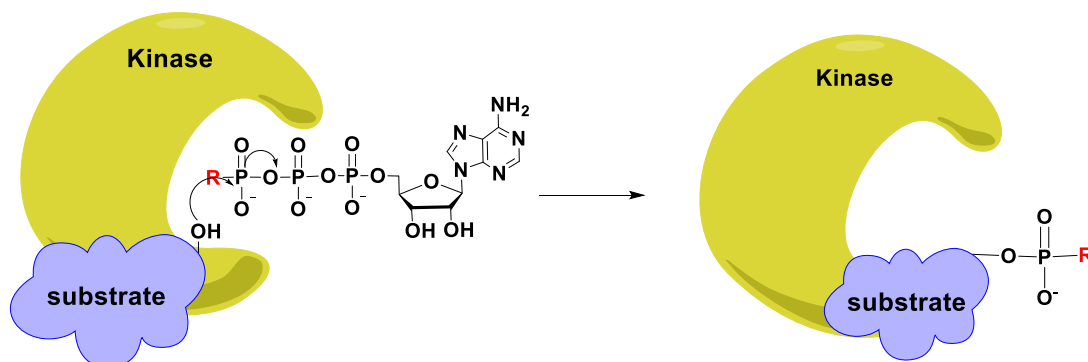


Figure 1.6: Cosubstrate promiscuity of kinases. Kinases accept γ -modified ATP analogs and transfer γ -modified phosphoryl groups onto substrate proteins.

1.6.1 ATP- γ S

The ATP- γ S analog, which leads to thiophosphorylation in a kinase reaction (Figure 1.7A), was one of the very first γ -modified ATP analogs developed.³³ Compared to ATP, ATP- γ S shows a lower catalytic efficiency.³⁴ However, the thiophosphoryl group is stable to phosphatases and can be alkylated.^{33b} Therefore, thiophosphorylation has been used as a method to purify phosphoproteins. For example, the alkylation of thiophosphorylated proteins using a biotin tagged idoacetamide derivative was used as a means of avidin enrichment of phosphoproteins (Figure 1.5B, I). In this case, low pH conditions were used to selectively alkylate the phosphorylthiol group while keeping the cysteine thiol groups unreactive.³⁵ In another example, thiophosphorylated proteins were reacted with an idoacetamide derivative conjugated with a solid phase resin (Figure 1.5B, II). Though both phosphorylthiol and cysteine thiol groups reacted with idoacetamide derivative, thio-

phosphorylated proteins were selectively eluted by peroxide assisted cleavage of the S-P bond.³⁶

Shokat and colleagues used a derivative of ATP- γ S modified at the N6 position with a bulky benzyl group (ATP- γ S*) to identify the substrates of CDK1 kinase (Figure 1.8). Here, they designed a mutant form of CDK1 kinase tolerant of the modified ATP analog. The use of the mutant CDK1 with ATP- γ S* in lysates led to the selective thiophosphorylation of only CDK1 substrates. Later, the thiophosphorylated proteins were purified by using the resin-conjugated idoacetamide derivative described above (Figure 1.7 B, II). The purified proteins were then analyzed by LC-MS/MS to reveal CDK1 substrates.³⁷

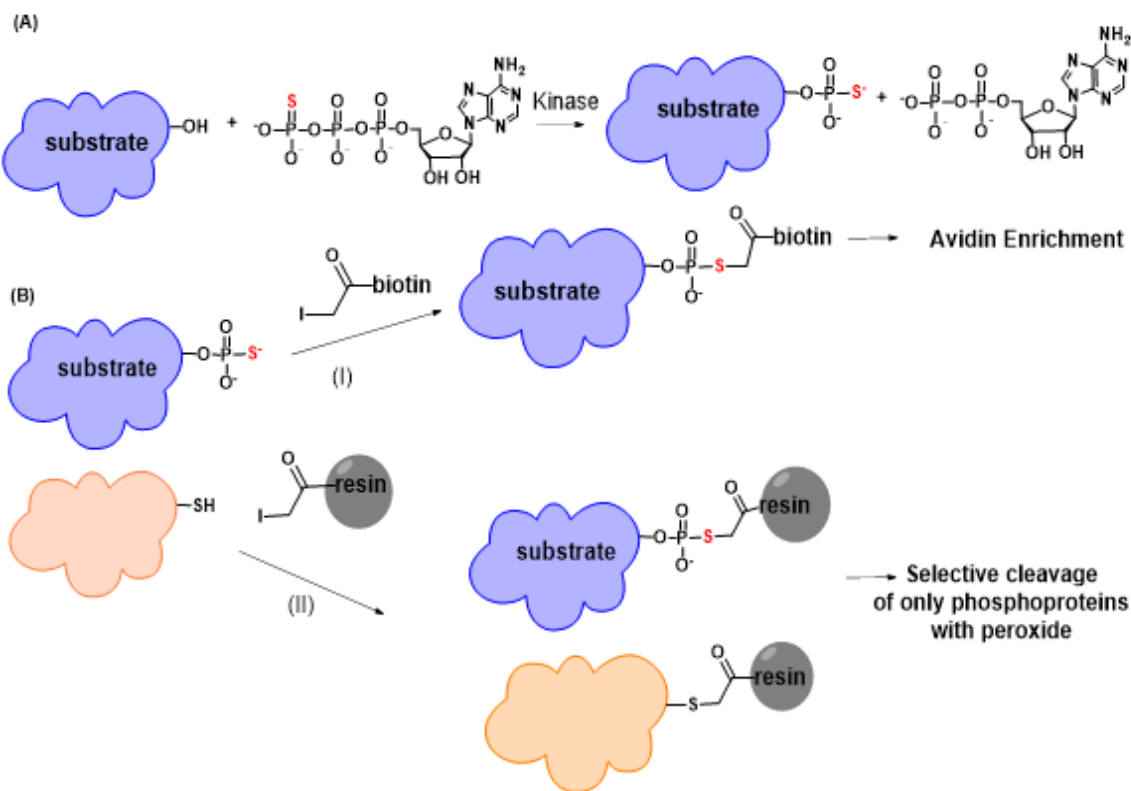


Figure 1.7: The use of ATP- γ S analog. (A) Thiophosphorylation of cellular proteins with ATP- γ S. (B) Different strategies used for the purification of thiophosphorylated proteins. Blue color shows kinase substrates while orange color shows cellular proteins with cysteine thiol groups.

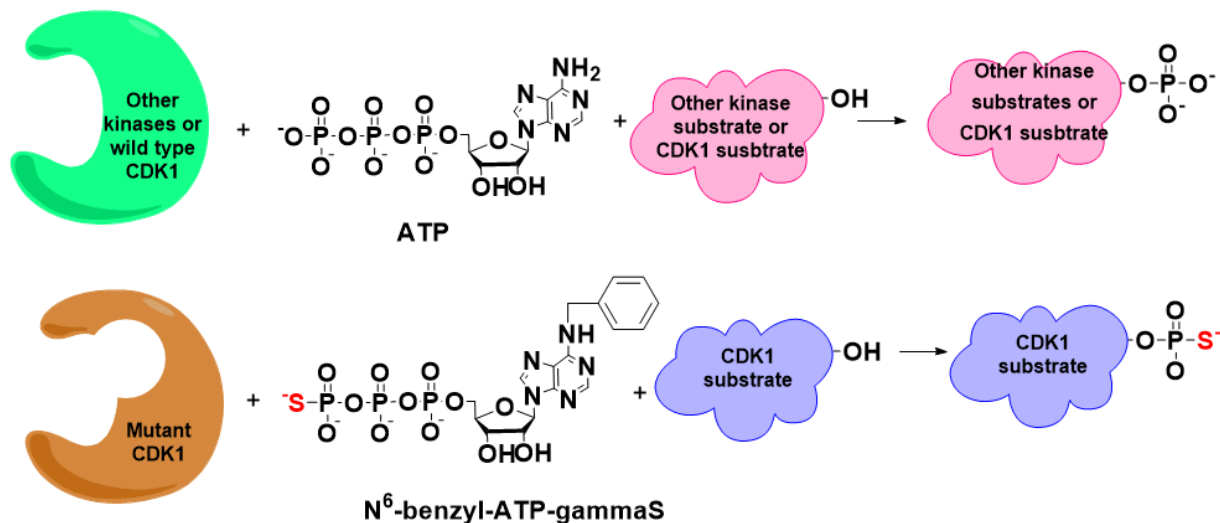


Figure 1.8: The use of ATP- γ S derivative to identify substrates of CDK1. Incubation of lysates with mutant CDK1 (brown) and ATP- γ S* (N⁶-benzyl-ATP- γ S) results in thiophosphorylation of only CDK1 substrates (blue). Wild type CDK1 and other kinases (green) are inactive towards ATP- γ S* and use ATP to phosphorylate their substrates (pink). Subsequent purification and LC-MS/MS analysis led to the discovery of CDK1 substrates.

1.6.2 Other γ -modified ATP analogs used to study phosphorylation

Other notable γ -modified ATP analogs used in phosphorylation research are ATP-Atto and ATP-ferrocene (Figure 1.9). The fluorescently active ATP-Atto analog was used in the development of a FRET (fluorescence resonance energy transfer)-based kinase assay. In this case, CK2 kinase and ATP-Atto were incubated with a CK2 substrate peptide tagged with a CdSe/ZnS quantum dot. Kinase-catalyzed transfer of the phosphoryl-Atto group onto the peptide led to a FRET signal that could be measured to study CK2 activity.³⁸

Redox active ATP-ferrocene was developed by Kraatz and colleagues to facilitate the electrochemical detection of phosphorylation. ATP-ferrocene was used to detect the activity of Protein kinase C using a surface immobilized peptide and cyclic voltammetry.³⁹

Later, anti-ferrocene antibodies were also developed to allow the visualization of the tagged phosphoproteins by Western blot.⁴⁰

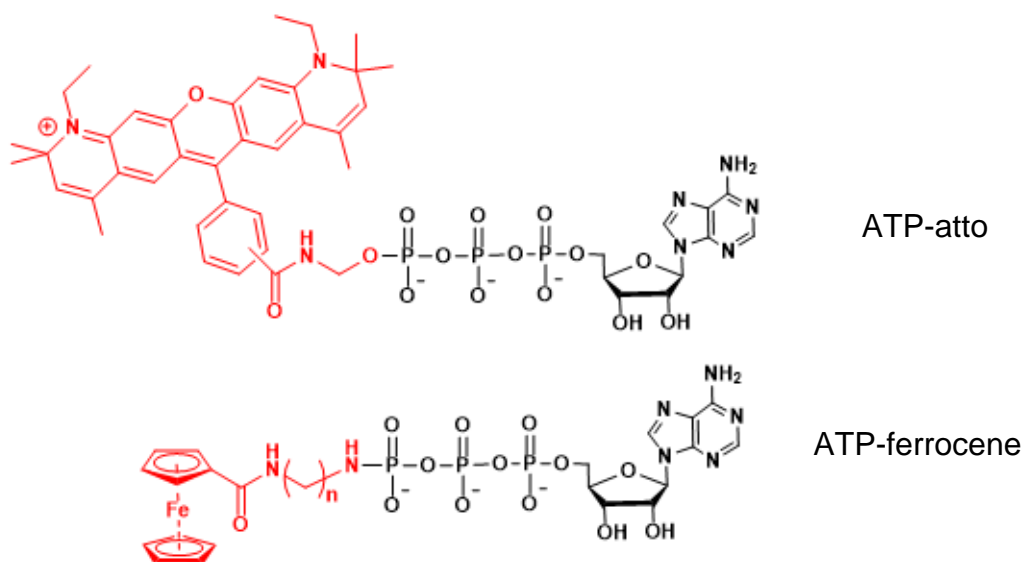


Figure 1.9: ATP-atto and ATP-ferrocene.

Commercially available ATP-acyl-biotin (Figure 1.10) is another γ -modified ATP analog that has been used. ATP-acyl-biotin differs from other γ -modified ATP analogs by modifying the kinase instead of the substrate proteins. ATP-acyl biotin binds to the kinase active site and modifies a lysine residue commonly found in the ATP binding region of kinases and other nucleotide binding proteins. Thus, ATP-acyl biotin is widely used to profile kinases and other ATP binding proteins in the cell. In an illustrative example, ATP-acyl biotin was used to study the inhibition profile of kinase inhibitors. In this case, ATP-acyl biotin was added to inhibitor-treated and untreated lysates. Since ATP-acyl biotin can only bind to kinases unoccupied by the inhibitor, only uninhibited kinases are biotinylated while inhibited kinases are unlabeled. Thus, kinases affected by the inhibitor were selectively identified.⁴¹

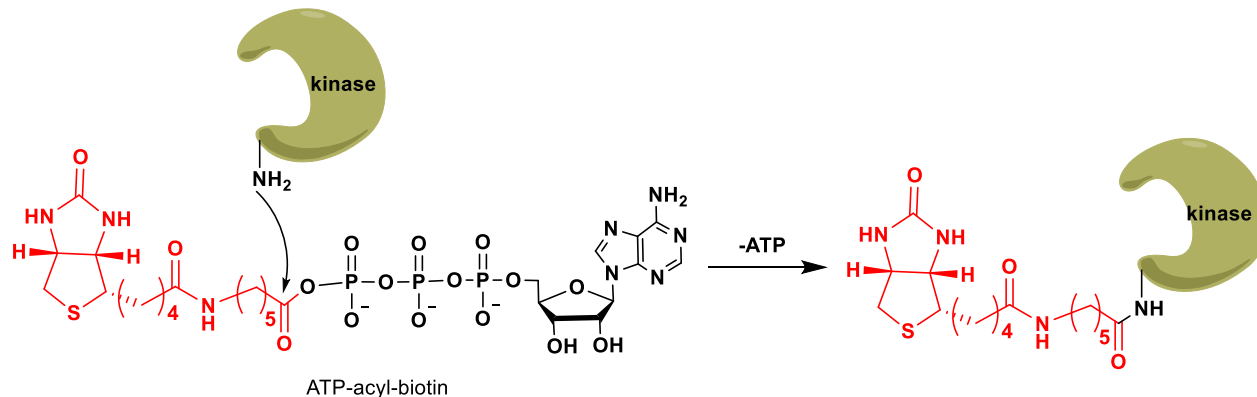


Figure 1.10: Kinase labeling by ATP-acyl-biotin

1.6.3 γ -modified ATP analogs used by Pflum and colleagues

Pflum and colleagues have developed and used a number of γ -modified ATP analogs over the years. The Pflum lab ATP analogs have been used in different applications. One such analog used by Pflum group is ATP-biotin.

1.6.3.1 ATP-biotin

The ATP-biotin analog carries a biotin group at the γ phosphate position and leads to the phosphobiotinylation of cellular proteins when used by kinases (Figure 1.11). ATP-biotin provides the advantage of directly purifying the phosphoproteins by avidin resin, compared to the two step purification with ATP- γ S (Figure 1.7).

The first reported use of ATP-biotin comes from Brust and colleagues. Here, ATP-biotin was used in a colorimetric assay to study the activity of PKA and CAMKII kinases. In this case, a gold nanoparticle decorated with substrate peptides of the tested kinase were incubated with ATP-biotin and the corresponding kinase. After the peptides were biotinylated, gold nanoparticles capped with avidin were added. Biotinylation resulted in the aggregation of the nanoparticles resulting in a colorimetric signal indicative of kinase activity.⁴² In another application, Brust and group used ATP-biotin to study the peptide substrate selectivity of protein kinases. Here, peptides were first immobilized on a solid

phase in a microarray format. Then PKA and ATP-biotin were added. Then gold nanoparticles coated with avidin were added. Biotinylated peptides that represent potential PKA substrate peptides were identified by resonance light scattering.^{42b}

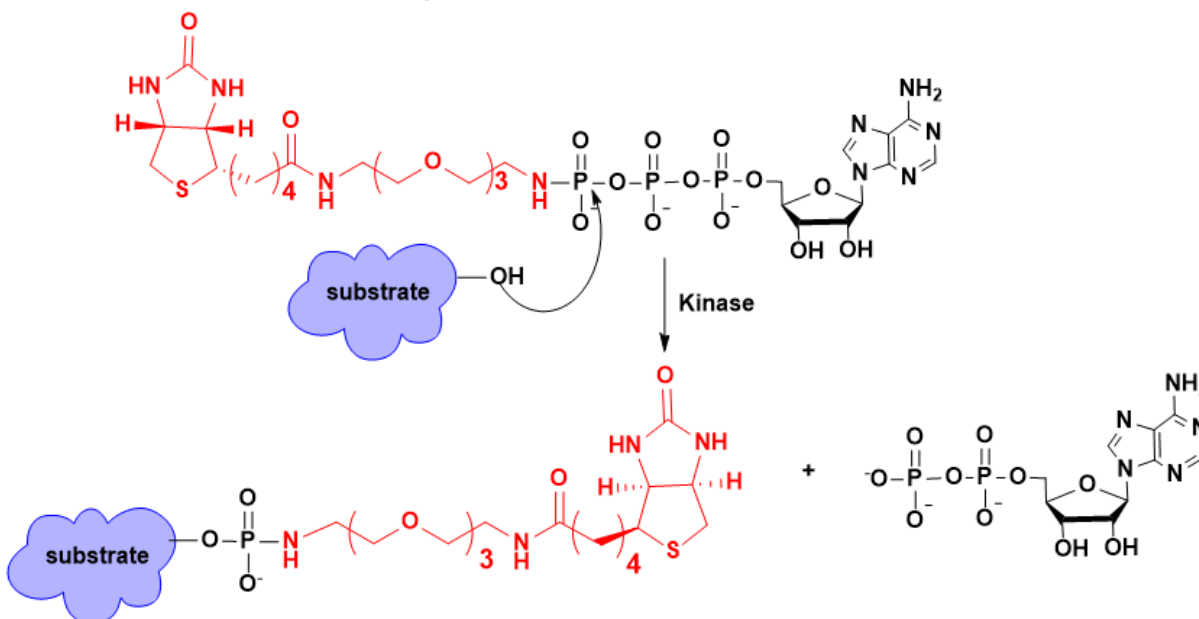


Figure 1.11: ATP-biotin leads to phosphobiotinylation of proteins.

Later, Pflum and colleagues pioneered the use of ATP-biotin as a general method of detecting phosphorylation in both simple systems, such as purified substrates, and complex mixtures, such as lysates. Specifically, recombinant kinases and ATP-biotin were incubated with either substrate peptides or full length proteins. Biotinylation was then monitored by gel based analysis using a streptavidin-cy5 conjugate. In the case of peptide substrates, biotinylation was also probed by HPLC and quantitative mass spectrometry analysis.^{32, 43} Importantly, a thorough characterization of biotinylation with 26 kinases representing the kinome showed that even though the catalytic efficiency is slightly impaired, ATP-biotin is a general cosubstrate for kinases.^{43b} In agreement, gel based visualization showed that ATP-biotin incubation with lysates leads to robust

biotinylation of cellular proteins, indicating that cellular kinases are capable of utilizing ATP-biotin.³² Similar to thiophosphorylation, phosphobiotinylation was phosphatase resistant, and therefore, suitable for phosphoprotein purification.⁴⁴

As an application of using ATP-biotin for phosphoprotein purification, Pflum and co-workers developed a technique called “K-BILDS (Kinase-catalyzed Biotinylation with Inactivated Lysates for Discovery of Substrates, Figure 1.12) for discovering kinase substrates. K-BILDS was used to identify PKA substrates. In this case, cellular kinases were inactivated by incubating the lysates with the irreversible kinase inhibitor FSBA (5'- (4-fluorosulfonylbenzoyl adenosine hydrochloride). Excess FSBA was then removed and recombinant PKA was added to the lysates, along with ATP-biotin. After exogenous PKA biotinylated its substrates, the biotinylated proteins were purified by streptavidin. Proteomics analysis was then carried out to identify the PKA substrates. K-BILDS revealed 279 PKA candidate substrates, including 57 already known PKA substrates.⁴⁵

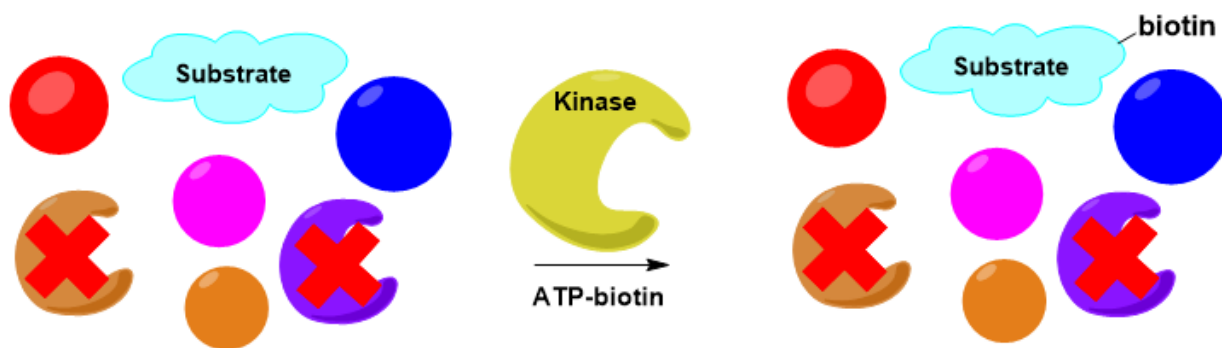


Figure 1.12: K-BILDS procedure. In K-BILDS, the cellular kinases are first inactivated (brown and purple crossed). Then an exogenous kinase (yellow) is added with ATP-biotin. The exogenous kinase biotinylated its substrates (blue). The blue, red, pink and brown circles represent other proteins in the lysates that are not substrates of the exogenous kinase.

K-BILDS demonstrates how ATP-biotin acts as a powerful tool for probing cellular phosphorylation events. However, ATP-biotin is not cell permeable and not suitable for monitoring live cell phosphorylation events. Therefore, the Pflum lab developed a cell permeable derivative of ATP-biotin called ATP-polyamine-biotin (APB) by replacing the polyethylene glycol (PEG) linker of ATP-biotin with a positively charged polyamine linker (Figure 1.13). The reduced negative charge on APB promoted its cell delivery under physiological conditions. Therefore, APB was added to live HeLa cells attached to well plates. Then cells were lysed and biotinylation was probed by gel based methods. The results showed that APB biotinylated cellular proteins, confirming that APB is cell permeable. In contrast, no biotinylation was observed when ATP-biotin was added to live cells.⁴⁶ Thus ATP-biotin has been used in multiple applications facilitating the study of phosphorylation. Chapter 3 describes another application using ATP-biotin.

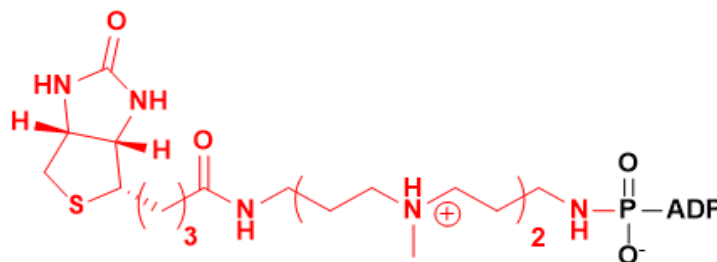


Figure 1.13: ATP-polyamine biotin (APB)

1.6.3.2 ATP-dansyl

ATP-dansyl (Figure 1.14A) developed by the Pflum lab permits modification of phospho-peptides and proteins with the fluorescently active dansyl group. Pflum and colleagues used ATP-dansyl to develop a FRET based assay for kinase activity (Figure 1.14B). Specifically, ABL kinase and ATP-dansyl were incubated with an ABL substrate peptide bearing a rhodamine tag at the N terminus. ABL-mediated dansylation of the peptide resulted in a FRET signal indicative of ABL activity. As expected, the FRET signal

was considerably reduced when kinase inhibitors were used. In a further step, the assay was also used to investigate the ABL activity in lysates. While untreated lysates produced a high FRET signal, lysate treatment with the general kinase inhibitor staurosporine led to a great reduction in the FRET signal.⁴⁷ Although no further applications of ATP-dansyl have been reported, dansylation represents a useful way of investigating phosphorylation.

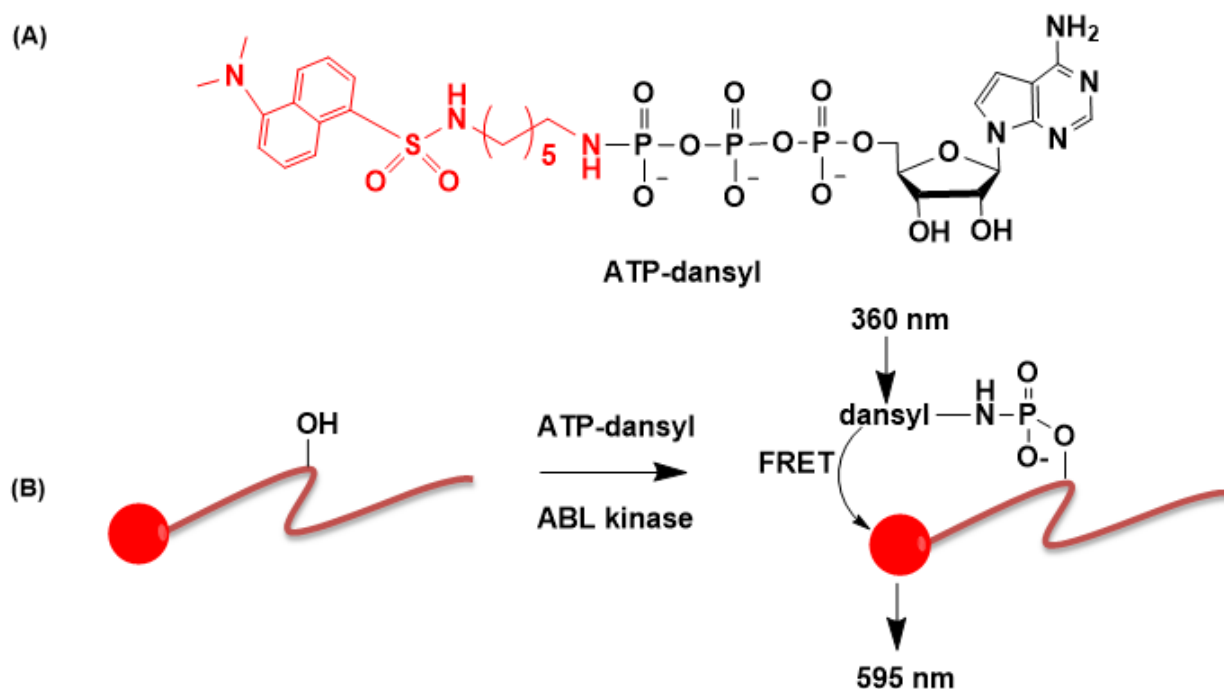


Figure 1.14: ATP-dansyl and its application. (A) Structure of ATP-dansyl (B) The FRET assay used by Pflum and colleagues to assay ABL kinase activity using ATP-dansyl. A peptide (red wavy line) carrying a rhodamine tag (red circle) was incubated with ATP-dansyl and ABL kinase. Dansylation followed by excitation with 360 nm resulted in a FRET signal (595 nm) indicative of ABL kinase activity.

1.6.3.3 γ -modified ATP analogs with photocrosslinkers

When coupled with UV irradiation, kinase-catalyzed modification of phosphoproteins with photocrosslinking groups provides the advantage of generating stable kinase-substrate pairs for later detection (Figure 1.15A). Over the years, the Pflum

lab has developed ATP-arylazide and ATP-benzophenone (Figure 1.15B) as analogs bearing photocrosslinker groups at their γ -phosphate position.⁴⁸

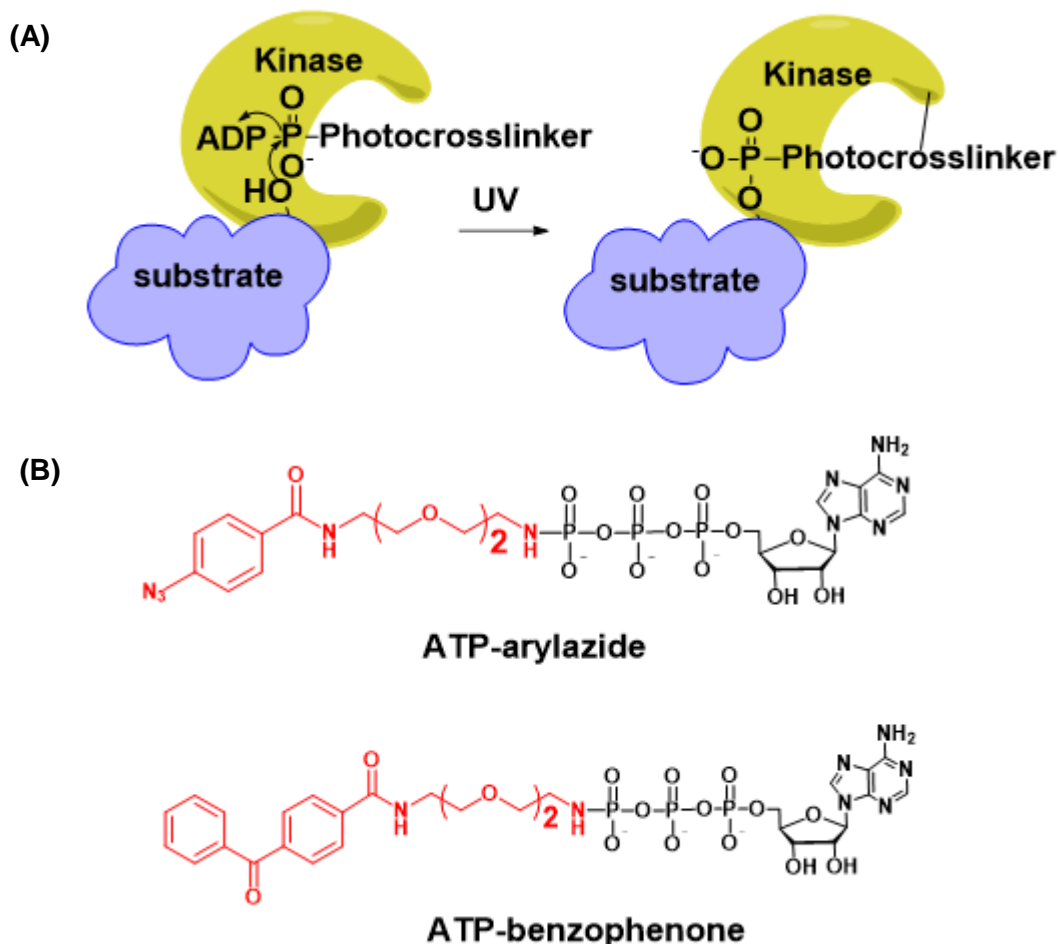


Figure 1.15: Use of photo-crosslinking ATP analogs. (A) Kinase-catalyzed modification of phosphoproteins with photocrosslinking groups leads to the generation of stable kinase-substrate complexes when UV is used. (B) Structures of ATP-arylazide and ATP-benzophenone.

In an application to show the activity of photocrosslinking ATP analogs, Pflum and colleagues incubated recombinant CK2 kinase and a rhodamine tagged CK2 substrate peptide with ATP-arylazide in the presence of UV light (Figure 1.16). When analyzed by gel methods, CK2 was shown to be fluorescently labeled, indicating that ATP-arylazide

mediated the crosslinking between the kinase and the fluorescent peptide. Similar results were obtained when another kinase-substrate pair, ABL, and its fluorophore tagged substrate peptide was used, showing that ATP-arylazide is compatible with other kinases as well. In a further step, CK2 and its protein substrate casein were incubated with ATP-arylazide in UV light. Western blot analysis of CK2 showed a higher molecular weight band corresponding to a CK2-casein complex.^{48a} Later, ATP-benzophenone was also investigated for its ability to mediate kinase-substrate crosslinking. Docking analysis and quantitative mass spectrometry analysis with a substrate peptide revealed ATP-benzophenone to be a more efficient cosubstrate compared to ATP-arylazide. However, when used for crosslinking CK2 and casein, ATP-benzophenone gave rise to multiple bands compared to a distinct band by ATP-arylazide, suggesting non-specific crosslinking.^{48b}

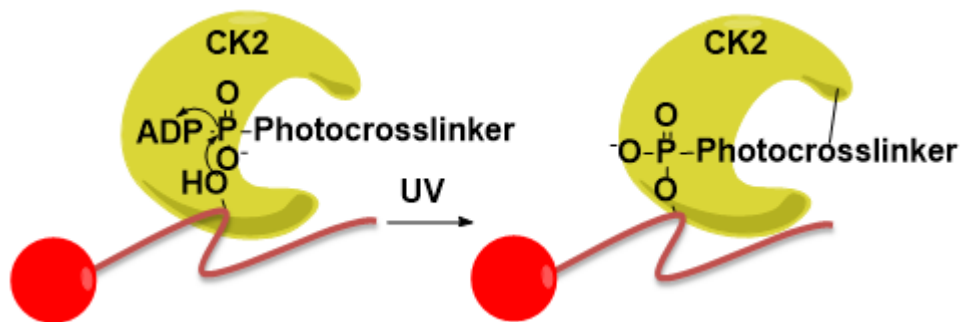


Figure 1.16: Fluorescent labeling of CK2 kinase using ATP-arylazide. CK2 kinase was incubated with ATP-arylazide and a peptide substrate (wavy red line) bearing a rhodamine tag (red circle). ATP-arylazide mediates crosslinking of CK2 with the peptide leading to fluorescent labeling of CK2 kinase.

In another application of photocrosslinking ATP analogs, the Cole lab reported the use of a bifunctional ATP analog (Figure 1.17) bearing photocrosslinking arylazide groups on both the γ phosphate position and C8 position. Unlike ATP-arylazide and ATP-benzophenone, the bifunctional analog requires only binding with the kinase and does

not depend on kinase activity for photocrosslinking. Using CSK and SRC kinases, the bifunctional analog was shown to cause the formation of high molecular weight complexes indicative of kinase-substrate crosslinking.⁴⁹ Unfortunately, no further use of this analog has been reported. In conclusion, the discussed examples show that photocrosslinking γ -modified ATP analogs have provided useful probes for studying phosphorylation. Chapter 2 describes another application of using ATP-arylazide.

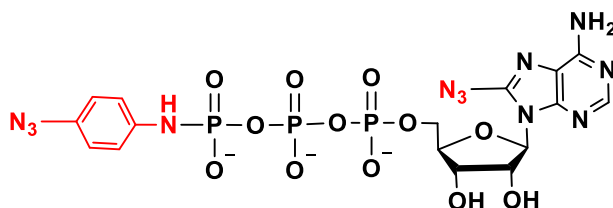


Figure 1.17: Bifunctional ATP analog used by Cole and colleagues

1.7 Thesis project

The use of γ -modified ATP analogs and other methods have facilitated the study of phosphorylation. However, phosphorylation is ubiquitous, and a staggering number of phosphorylation events are known to take place in the cell. The biological significance and the disease relevance of many of these phosphorylation events remain unknown because the methods to determine which particular kinase is responsible for the particular phosphorylation event are limited. One goal of this thesis work was to develop a method for identifying the kinase that phosphorylates a given phosphosite.

Based on our prior work with ATP-arylazide (Figure 1.16), we established a novel chemical tool called K-CLASP (Kinase-catalyzed CrossLinking And Streptavidin Purification) for phosphosite specific kinase identification. Chapter 2 describes the development and application of K-CLASP to two phosphosites. In a proof-of-concept study, the protein kinase A (PKA) peptide substrate kemptide was used to show that K-

CLASP is capable of identifying PKA as the kinase responsible for kemptide phosphorylation from cell lysates.⁵⁰ Then K-CLASP was used to identify the kinase(s) that phosphorylates Ser178 of the transcription factor called Miz1.

Although phosphorylation is a reversible process mediated by both kinases and phosphatases, the study of phosphatases has lagged behind kinases because many of the current available techniques, including γ -modified ATP analogs, are capable of interrogating only the kinases. As a result, few phosphatase substrates have been identified.⁵¹ Therefore, a second goal of this thesis work was to enable a new technique for identifying phosphatase substrates. Using ATP-biotin, we developed a method called K-BIPS (Kinase-catalyzed Biotinylation to Identify Phosphatase Substrates). Chapter 3 describes the application of K-BIPS in three biological systems. First, the general phosphatase inhibitor okadaic acid was used to show that K-BIPS is a viable tool for the discovery of phosphatase substrates. Then K-BIPS was used to explore the substrates of PP1-Gadd34 and PP1-MYPT1 phosphatase complexes. In conclusion, both K-CLASP and K-BIPS provide valuable tools to study phosphorylation and deconvolute the intricate cell signaling pathways.

CHAPTER 2 K-CLASP: KINASE CATALYZED CCROSS-LINKING AND STREPTAVIDIN PURIFICATION

Excerpts from this chapter have been reprinted or modified with permission from Dedigama-Arachchige, P. M and Pflum, M. K., K-CLASP: A tool to identify phosphosite specific kinases and interacting proteins. *ACS Chem Biol* **2016**. In press. Copyright 2016 American Chemical Society.

A significant challenge to unravel cell signaling pathways and to understand the molecular mechanism behind human diseases is to identify the kinase responsible for the phosphorylation of a given protein at a particular amino acid. Unfortunately, the methods to discover cellular proteins associated with the kinase during phosphorylation are also limited. As a solution, we developed a novel chemical tool called K-CLASP (Kinase-catalyzed CrossLinking And Streptavidin Purification) for both phosphosite specific kinase identification and the discovery of kinase associated proteins. Chapter 2 describes the development and application of K-CLASP in two systems. In a proof-of-concept study, Protein kinase A (PKA) and its known peptide substrate kemptide were used to show that K-CLASP is capable of identifying PKA as the kinase responsible for kemptide phosphorylation from cell lysates. Additionally, several protein complexes and many other proteins that associate with PKA were also discovered. Then K-CLASP was used to identify the kinase(s) that phosphorylates Ser178 of the transcription factor called Miz1. K-CLASP identified several kinases and many other cellular proteins that associate with the phosphorylation of Miz1 protein at S178.

2.1 Current methods available for phosphosite specific kinase identification

The advancement of powerful mass spectrometric techniques has facilitated the identification of novel phosphorylated amino acids or phosphosites at an unprecedented rate.⁵² The identification of these novel phosphosites poses an important question: which protein kinase catalyzes phosphorylation of a specific phosphosite? With over 500 kinases in the kinome,²² identifying the kinase that phosphorylates a specific phosphosite is a challenge. Although several methods have been established to identify the substrates of a given kinase,⁵³ fewer methods exist to identify the kinase for a specific phosphosite. One of the methods available for phosphosite specific kinase identification is *in silico* kinase prediction, as described in the next section.

2.1.1. *In silico* kinase prediction

In silico kinase prediction employs kinase consensus sequences to determine the probable kinase(s) that may phosphorylate a given site on a protein.⁵⁴ Kinase consensus sequences have been formulated based on the observation that the phosphorylation specificity of kinases depends on the primary sequence or amino acids flanking the phosphosite.⁵⁵ Benjamin Turk and colleagues have pioneered the use of the consensus sequence strategy by utilizing peptide libraries to identify consensus sequences and then using the sequence information to predict the substrates of given kinases.⁵⁶ In addition, consensus sequences have also been determined by the alignment of multiple sequences surrounding a phosphosite known to be phosphorylated by a single kinase. Subsequent studies on kinase activity and binding after mutagenesis of the sequence around the phosphosite further confirmed the consensus sequences.⁵⁷

Several bioinformatics tools are currently available that predicts kinase specificity depending on the consensus sequence.^{54, 58} However, the consensus sequences for some kinases still remain unknown, limiting the applicability of in silico kinase prediction methods. In addition, increasingly available phosphoproteomics data indicate that some kinases act on varying primary sequences and do not conform to a strict consensus sequence.⁵⁹ Further, studies also suggest that kinase specificity may be also governed by the three dimensional structure around the phosphorylation site.⁵⁹⁻⁶⁰ As a result, in silico prediction methods have limited capabilities to accurately identify the kinase of a given phosphosite.

2.1.2 Mechanism based crosslinking

Another strategy that has been reported for phosphosite specific kinase identification is a mechanism based crosslinking approach (Figure 2.1) developed by the Shokat group. This strategy uses an adenosine containing crosslinker with an o-phthaldialdehyde (Figure 2.2A) and a cysteine substituted substrate to covalently link a kinase with the substrate. Specifically, the crosslinker is expected to bind the kinase through the adenosine moiety and react with a catalytic lysine found in kinases (Figure 2.1a,b). Then the crosslinker will also react with a cysteine on the substrate to form a kinase-substrate complex (Figure 2.1c,d). Consistent with the hypothesis, the dialdehyde crosslinker led to the biotinylation of AKT1 when a biotinylated AKT1 substrate peptide bearing a cysteine substitution was used.⁶¹ However, when used in cell lysates, the dialdehyde crosslinker reacted with many proteins and proved to be non-selective. As a solution, a modified crosslinker (Figure 2.2B) with a less reactive thiophene-2,3-dicarboxaldehyde moiety was used. In addition, the weakly binding adenosine moiety was

also replaced with a kinase inhibitor scaffold to increase crosslinker binding to the kinase.⁶² Although the modified crosslinker had reduced non-specificity, its reactivity was too low to be used in biological applications. As an improvement, an ATP based crosslinker with a phosphor-anhydride group and a methylacrylate (Figure 2.2C) was developed. The modified crosslinker works by first reacting with lysine on the kinase and then with the cysteine on the substrate (Figure 2.3). In cell lysates, the modified crosslinker resulted in the isolation of exogenously added Src kinase by streptavidin

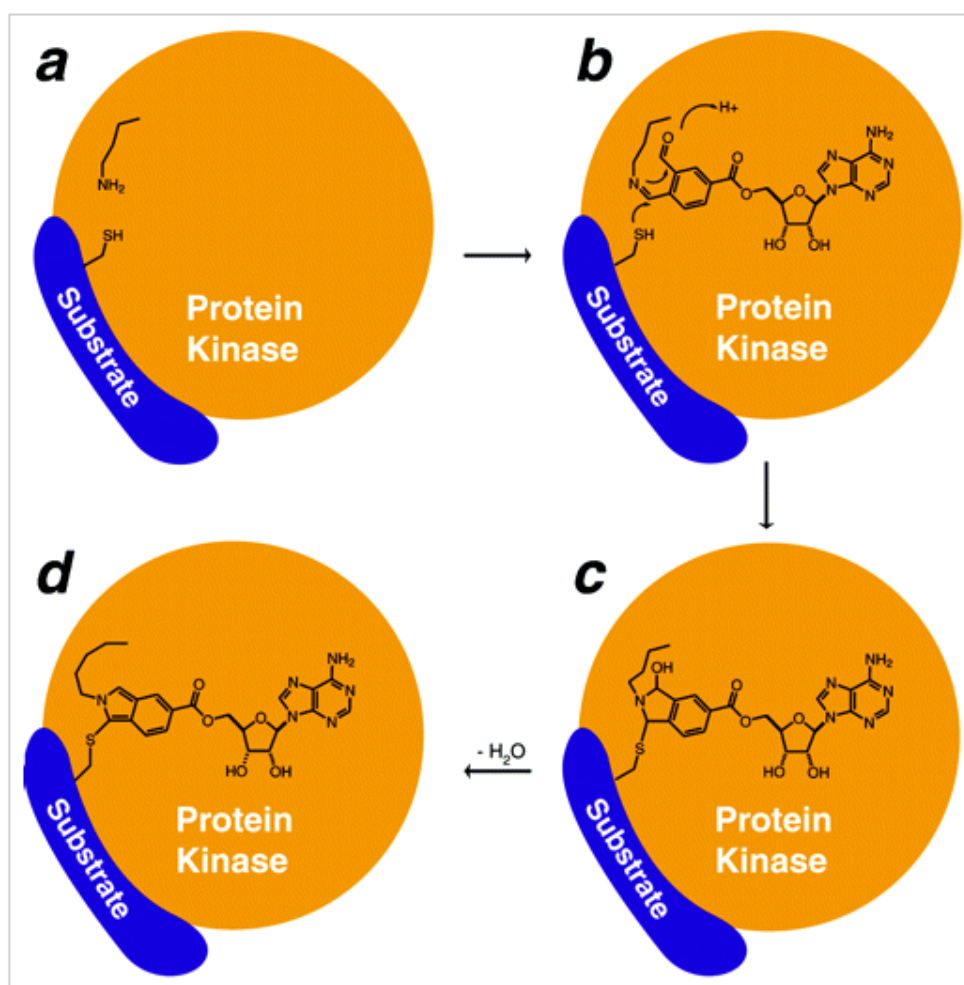


Figure 2.1: Mechanism based crosslinking with the o-phthaldialdehyde crosslinker. Reprinted with permission from Maly, D. J.; Allen, J. A.; Shokat, K. M., A mechanism-based cross-linker for the identification of kinase-substrate pairs. *J Am Chem Soc* 2004, 126 (30), 9160-1. Copyright (2004) American Chemical Society. More description is available in the text.

purification when biotinylated Src substrate peptide with a cysteine substitution was used.⁶³ However, the use of the methylacrylate crosslinker in a proteomics experiment has not been reported.

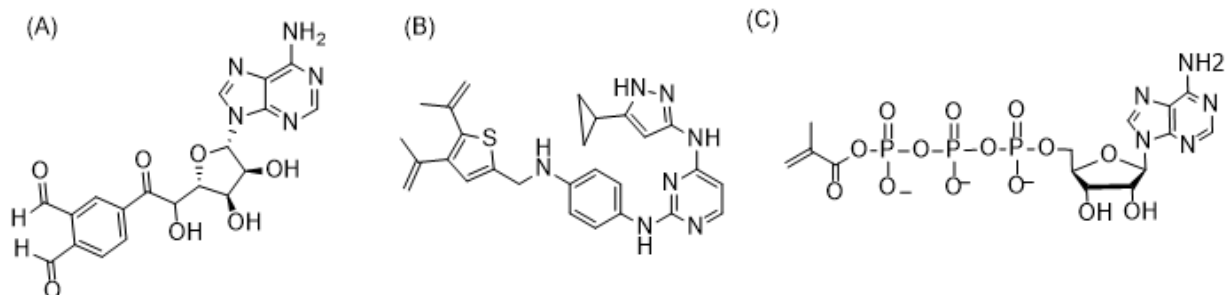


Figure 2.2: Mechanism based crosslinkers developed by Shokat and colleagues

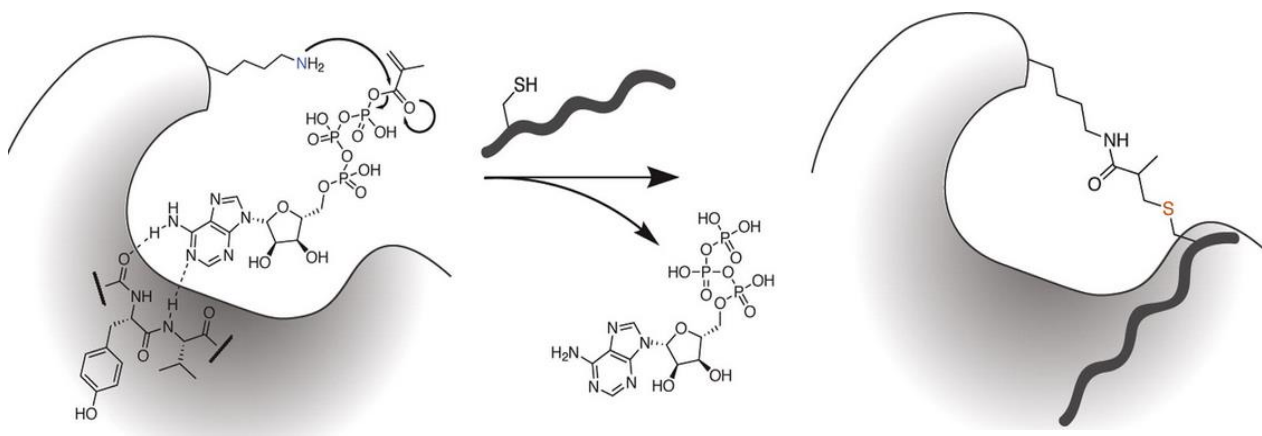


Figure 2.3: Mechanism based crosslinking with the methylacrylate crosslinker. Reprinted with permission from Riel-Mehan, M. M.; Shokat, K. M., A crosslinker based on a tethered electrophile for mapping kinase-substrate networks. *Chem Biol* 2014, 21 (5), 585-90. Copyright (2014) Elsevier. More description is available in the text.

2.2 K-CLASP strategy

The limitation of tools available for the identification of the upstream kinase of a given phosphosite has warranted the development of novel methods for phosphosite specific kinase detection. Based on kinase-catalyzed crosslinking with ATP-ArN₃, we developed a method called K-CLASP (Kinase-catalyzed CrossLinking And Streptavidin Purification) for phosphosite specific kinase identification. In the K-CLASP method, a

biotin tagged peptide containing the phosphosite of interest is incubated with a cell lysate in the presence of ATP-ArN₃ and UV irradiation. The biotinylated peptide will covalently crosslink to its respective kinase in the lysate via kinase-catalyzed phosphorylation and simultaneous UV-activated arylazide crosslinking. The covalently crosslinked complex can then be streptavidin purified and analyzed by mass spectrometry to identify the captured kinase (Figure 2.4a). However, kinase-substrate interactions are transient, allowing diffusion of the biotin-tagged peptide away from the kinase after transfer of the photocrosslinking group (Figure 2.4b). In this scenario, the biotin-tagged peptide will crosslink to proteins in close proximity of the kinase, including direct and indirect

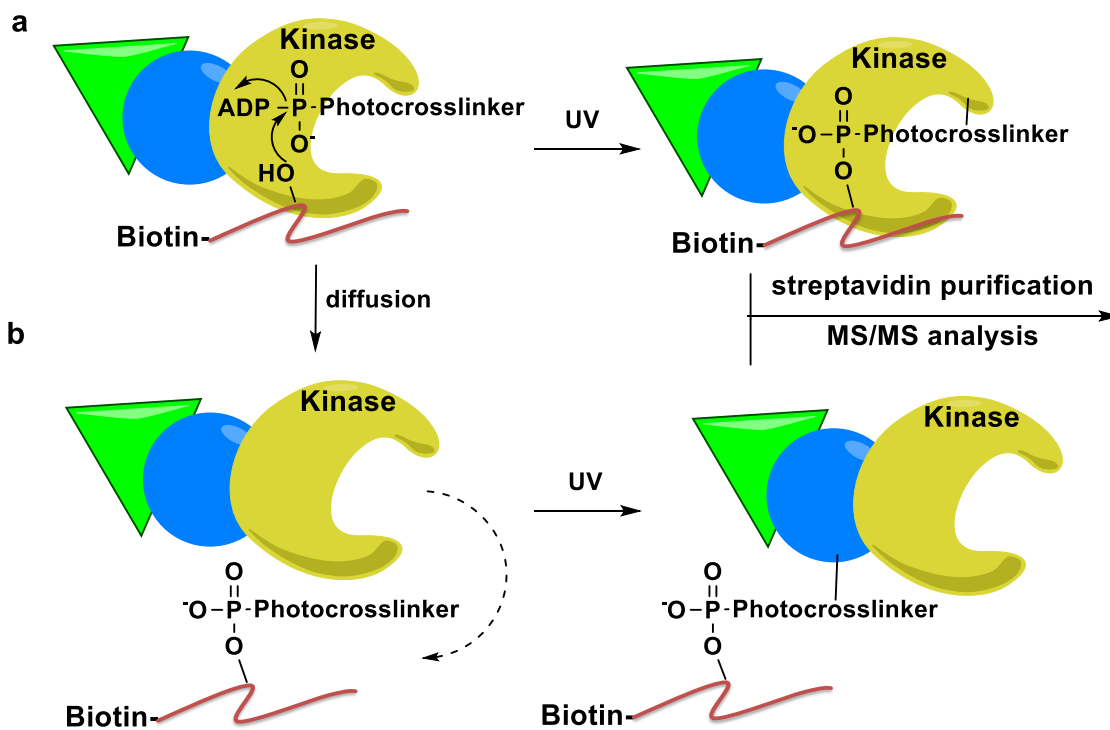


Figure 2.4: Kinase-catalyzed labeling and the K-CLASP method. (a) An N-biotinylated peptide (red) carrying a phosphosite will bind to its phosphorylating kinase (yellow) and ATP-ArN₃ in lysates. The kinase catalyzes transfer of the photocrosslinker group onto the peptide, while UV irradiation leads to covalent attachment of biotinylated peptide and kinase. The biotin-linked kinase can then be streptavidin purified and identified by MS/MS analysis. (b) Once the photocrosslinker is transferred, the N-biotinylated peptide can diffuse away from the kinase to crosslink with nearby proteins, including direct (blue) and indirect (green) associated proteins of the kinase.

associated proteins (Figure 2.4b). As a result, both the target kinase and kinase-associated proteins are purified and observed in a K-CLASP experiment. Therefore, K-CLASP has the potential to not only discover the kinase that phosphorylates a given phosphosite, but to also expose proteins interacting with the kinase under the conditions of the experiment. Given that classic methods for interacting protein identification, such as immunoprecipitation and yeast two hybrid, require stable protein-protein interactions and might miss low abundance or transient partners, K-CLASP also provides a useful tool to investigate the proteins close to the kinase during the crosslinking event.

To establish K-CLASP as a viable tool for kinase identification, we tested the well-known kinase substrate peptide pair, Protein kinase A (PKA) and its substrate kemptide (LRRASLG), in a proof-of-concept study. In addition, in a collaboration project with Prof. Jing Liu at Northwestern University, we also applied K-CLASP to identify possible kinases that phosphorylate S178 in Miz1 protein. The results from the two studies establish K-CLASP to be a useful tool for phosphosite specific kinase identification and discovery of proteins interacting with the kinase during the crosslinking event.

2.3 K-CLASP using Protein Kinase A (PKA) and kemptide

Protein kinase A (PKA) is widely reported to phosphorylate the peptide substrate kemptide (LRRASLG).⁶⁴ To show that K-CLASP can identify the kinase responsible for the phosphorylation of a given site, we used kemptide and PKA. Initially, in vitro crosslinking reactions were carried out using biotin tagged kemptide with recombinant PKA and HeLa lysates to show that ATP-ArN₃ can covalently link PKA with biotin-kemptide. Then full K-CLASP experiments were carried out after purifying crosslinked samples using streptavidin and then analyzing by tandem mass spectrometry. The

proteomics data revealed that PKA can be isolated by K-CLASP as the kinase that phosphorylates kemptide. In addition, many other proteins that interact with PKA during crosslinking were also identified establishing K-CLASP as a tool for both phosphosite specific kinase identification and the discovery of kinase interacting proteins.

2.3.1. In vitro crosslinking reactions with recombinant PKA and kemptide

As a first step to show that ATP-ArN₃ crosslinks kemptide with PKA, recombinant PKA α catalytic subunit was incubated with ATP-ArN₃ in the presence of N-biotinylated kemptide and UV irradiation. We synthesized a modified kemptide sequence containing four N-terminal glycine residues (biotin-GGGGLRRASLG) to separate the biotin tag from the phosphosite and avoid steric issues. After crosslinking, samples were separated by SDS-PAGE, transferred onto a PVDF membrane and then stained with a streptavidin–Cy5 conjugate to detect biotin-linked PKA kinase. Biotinylated PKA was observed in the presence of ATP-ArN₃ (Figure 2.5a, lane 2) but not ATP (Figure 2.5a, lane 3),

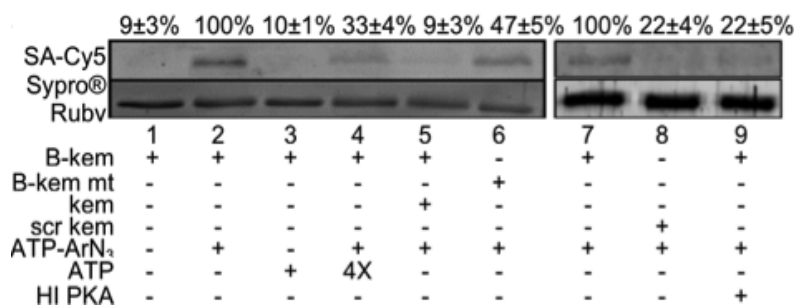


Figure 2.5: N-biotin kemptide crosslinking with recombinant PKA and lysates. Crosslinking reactions with recombinant PKA, biotinylated kemptide (B-kem), and ATP-ArN₃. Control reactions were carried out with N-biotin mutant kemptide (B-kem mt) lacking the phosphorylated Ser, 4X excess ATP, 2X excess non-biotinylated kemptide (kem), an N-biotinylated scrambled kemptide (scr kem), or heat inactivated PKA (HI PKA). Biotin signal was quantified from at least three independent trials with mean and standard error shown above each lane. The repetitive trials shown in Appendix, Figure A2.2.

demonstrating dependence on photocrosslinking. As controls, the biotin signal was reduced when excess ATP (Figure 2.5a, lane 4) or non-biotinylated kemptide (Figure

2.5a, lane 5) were included. In addition, biotinylation was also reduced when a scrambled biotin peptide (Figure 2.5a, lane 8) or heat inactivated PKA was used (Figure 2.5a, lane 9).

As a further control, we tested an N-biotinylated kemptide mutant where Ala replaced the phosphorylation site Ser (biotin-GGGGLRRAALG). PKA was biotinylated in the presence of N-biotin mutant kemptide, although at a reduced level compared to wild type kemptide ($47 \pm 5\%$, Figure 2.5, lane 6). We speculated that crosslinking of PKA with mutant kemptide is due to nonselective reactivity of the arylazide photocrosslinker with biotin-kemptide before PKA auto-phosphorylation. In this case, ATP-ArN₃ may non-specifically react with the biotin-kemptide to first form a kemptide-ATP-ArN₃ conjugate. The conjugate may act as a co-substrate for PKA and then transferred onto another PKA molecule through PKA auto-phosphorylation (Figure 2.6).

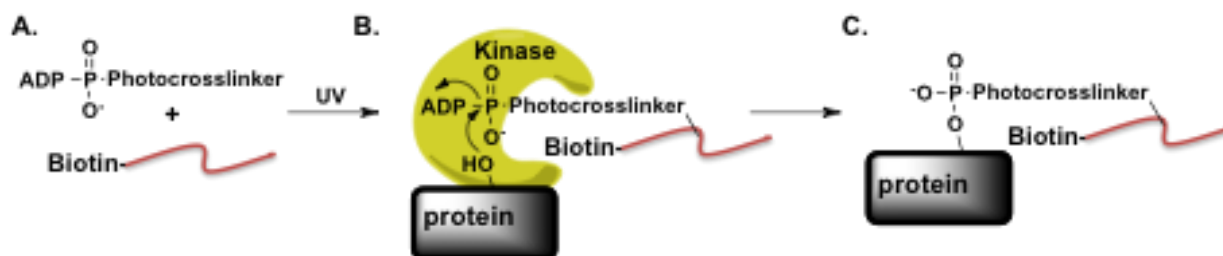


Figure 2.6: Proposed nonspecific reactivity of N-biotin mutant kemptide to account for background biotinylation in Figure 2.5, lane 6. A) Nonspecific reaction of ATP-ArN₃ and the N-biotin mutant kemptide peptide produces a peptide-ATP conjugate. B) The peptide-ATP conjugate is a cosubstrate for phosphorylation of a “protein” substrate in lysates by its kinase. C) Phosphorylation of the “protein” with the peptide-ATP conjugate produces a covalent connection between the N-biotin mutant kemptide and “protein”. To explain the labeling of PKA by mutant biotin-kemptide, “protein” is another PKA protein.

To probe our hypothesis that a pre-formed kemptide-ATP-ArN₃ results in the labeling observed for the mutant kemptide, we pre-incubated N-biotinylated kemptide with ATP-ArN₃ before adding PKA. Biotinylation was still observed for both wild type biotin-kemptide and mutant kemptide when a pre-incubated biotinylated kemptide and ATP-ArN₃ was used (Figure 2.7, lanes 2 and 3). Interestingly, when the pre-incubation was carried out with the N-biotinylated scrambled peptide, minimal PKA biotinylation was observed (Figure 2.7, lane 4), suggesting that labeling through a pre-formed kemptide-aryl azide conjugate still requires efficient kemptide-PKA interaction. The results highlighted the fact that a negative control reaction will be critical to account for and remove background crosslinking due to the highly reactive arylazide in the K-CLASP method. To be rigorous, reactions with mutant kemptide were included as critical negative controls in future experiments.

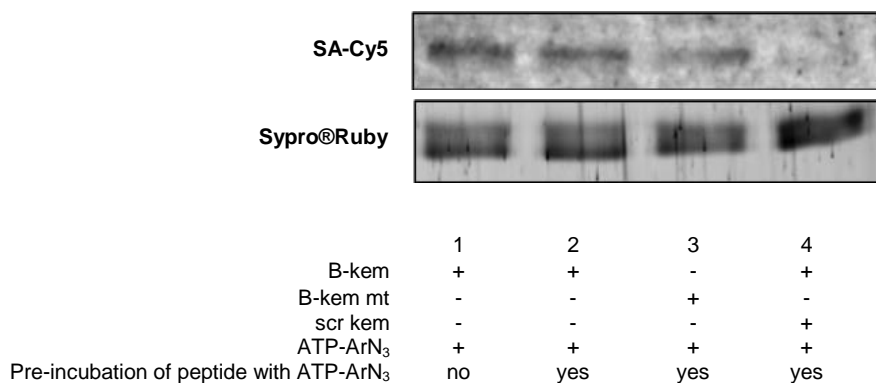


Figure 2.7: In vitro crosslinking reactions with recombinant PKA with biotin peptide pre-incubated with ATP-ArN₃. N-biotin kemptide (B-kem), N-biotin mutant kemptide (B-kem mt), or scrambled kemptide (scr kem) were separately pre-incubated with ATP-ArN₃ in the presence of UV light. Then recombinant PKA was added and crosslinking reactions were carried out. After reaction, the samples were separated by SDS-PAGE and stained with Sypro® Ruby total protein stain (bottom) or Streptavidin-Cy5 for biotinylation (top). A control reaction was carried out with N-biotin kemptide (B-kem) without pre-incubation (lane 1). The gels are representative of three independent trials (Appendix, Figure A2.3).

2.3.2 In vitro crosslinking with recombinant CK2 and CK2 peptide

To establish that K-CLASP is applicable with other kinases, we also carried out crosslinking reactions with recombinant Casein kinase II (CK2) and its N-biotinylated peptide substrate (biotin-RRREEETEEE). As observed with PKA, CK2 biotinylation was observed with ATP-ArN₃ (Figure 2.8, lane 1), but not with ATP (Figure 2.8, lane 2). Similarly, CK2 labeling was reduced when excess ATP (Figure 2.8, lane 3) or a non-biotinylated CK2 peptide (Figure 2.8, lane 4) was present. The results with CK2 demonstrate that kinase-peptide crosslinking with ATP-ArN₃ is compatible with other kinases.

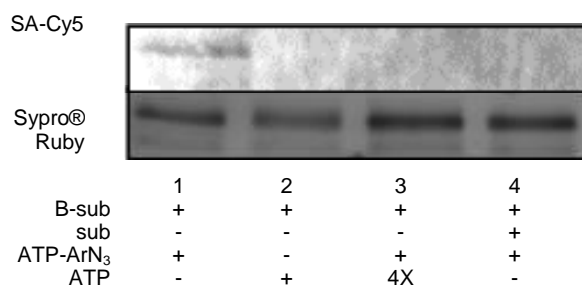


Figure 2.8: Crosslinking reactions with recombinant CK2, biotinylated CK2 substrate peptide (B-sub), and ATP-ArN₃. Control reactions were carried out with ATP, 4X excess ATP, and 2X excess non-biotinylated CK2 peptide (sub). The gels are representative of three independent trials (Appendix, Figure A2.4).

2.3.3 In vitro crosslinking with lysates and kemptide

With the ultimate goal of identifying endogenous, cellular kinases of kemptide, we carried out crosslinking in lysates. N-biotin kemptide and ATP-ArN₃ were incubated with HeLa lysates in the presence of UV before SDS-PAGE analysis. In order to optimize the reaction conditions, we performed a time course for the crosslinking reaction, with varying amounts of the N-biotin kemptide and subsequent gel analysis. The two hour reaction time with 2 mM N-biotin kemptide (Figure 2.9, Lane 8) produced an appreciable biotin

signal around ~41kDa where cellular PKA is expected. Therefore, 2 hours and 2 mM N-biotin kemptide was selected.

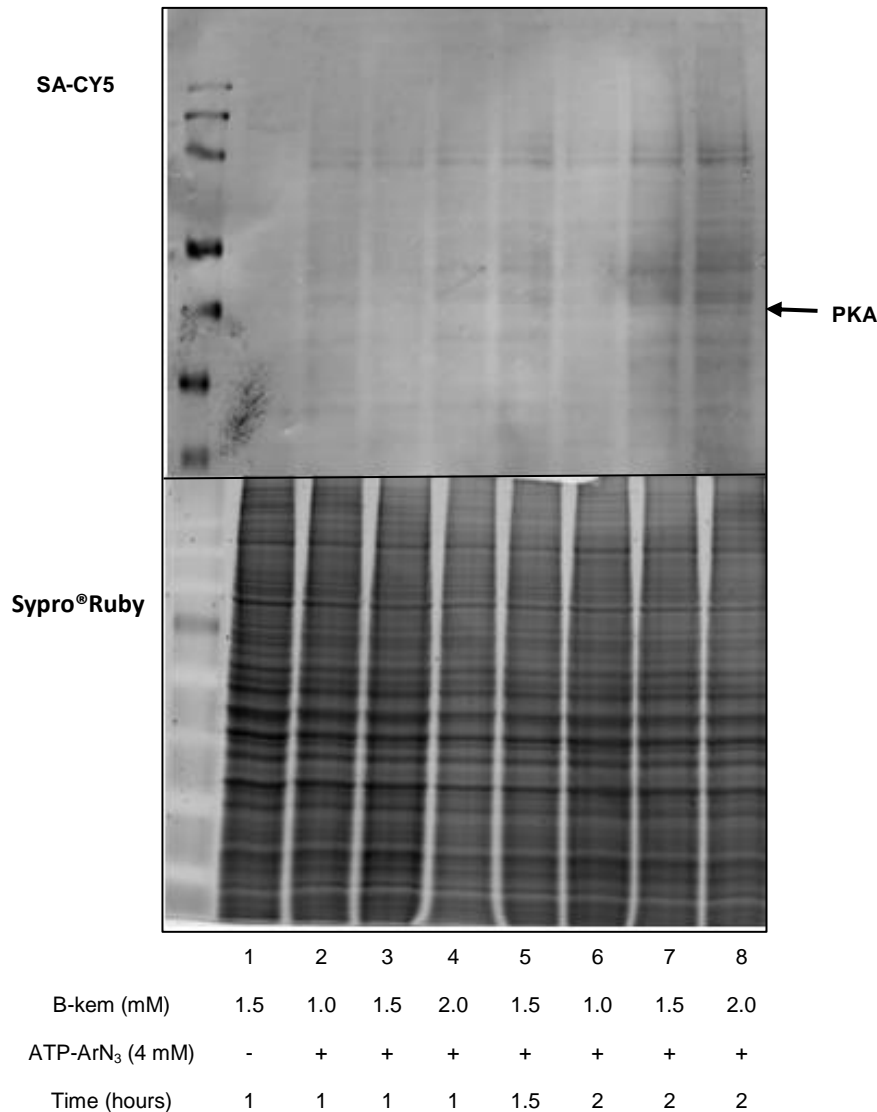


Figure 2.9: Optimization of K-CLASP crosslinking with HeLa cell lysates. HeLa cell lysates were pre-incubated with ATP in kinase buffer to activate endogenous PKA. Then, lysates were incubated with the indicated amounts of biotinylated kemptide (B-kem: 1, 1.5, or 2 mM) and ATP-ArN₃ (4 mM) under UV light for 1 hour (lanes 1-4), 1.5 hours (lane 5), or 2 hours (lanes 6-8) at 31°C. Reaction products were separated by SDS-PAGE, before visualization of biotinylated proteins using streptavidin-Cy5 (SA-Cy5) or total proteins with Sypro Ruby stain. The band at the size of PKA (~41 kDa) is indicated with an arrow. The molecular weight marking is shown on the far left side of the image, with bands corresponding to the following molecular weights: 170, 130, 95, 72, 55, 43, 34, and 26 kDa.

With the optimized conditions, *in vitro* crosslinking reactions were carried out with HeLa lysates and N-biotin kemptide. After reaction, biotinylation was visualized by gel methods. A biotinylated band at the size of the PKA catalytic subunit (~41kDa) was observed (Figure 2.10, lane 2, see arrow). In addition to PKA, many other proteins were also biotinylated (Figure 2.10, lane 2), consistent with possible diffusion of N-biotin kemptide away from the kinase after photocrosslinker transfer (Figure 2.4b). The biotin signal, including that for PKA, was lost in the absence of ATP-ArN₃ (Figure 2.10, lane 1). Reduced biotinylation was also observed with N-biotin mutant kemptide (Figure 2.10, lane 3) or in the presence of excess non-biotinylated kemptide (Figure 2.10, lane 4) or the kinase inhibitor staurosporine (Figure 2.10, lane 5). These results suggest that peptide crosslinking is kinase-dependent and phosphosite-specific in complex mixtures, such as lysates.

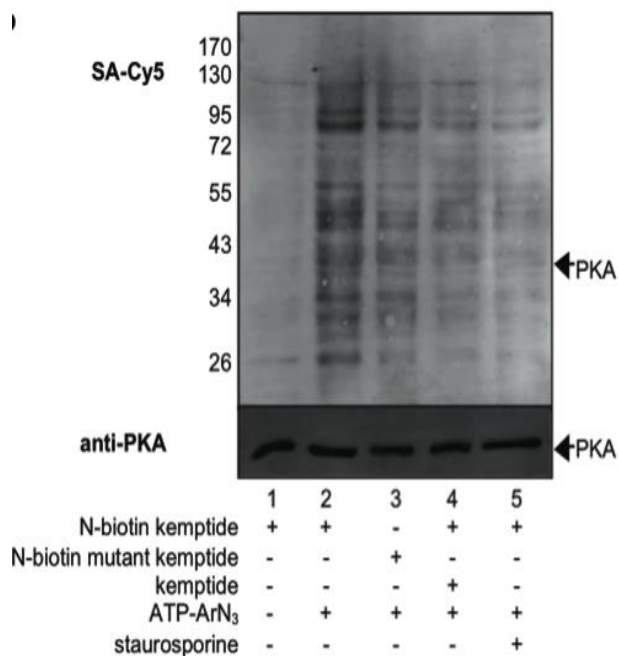


Figure 2.10: N-biotin kemptide crosslinking with recombinant PKA and lysates. N-biotin kemptide crosslinking with ATP-ArN₃ in HeLa lysates. After reaction, samples were separated by SDS-PAGE, stained with SA-Cy5 (top) or probed with a PKA antibody (anti-PKA, bottom). The gels are representative of three independent trials (Appendix, Figure A2.5).

2.3.4 K-CLASP with kemptide and lysates

To perform a full K-CLASP experiment, crosslinked complexes in lysates were purified using streptavidin resin and analyzed by tandem mass spectrometry (Figure A.2.6). Crosslinked samples from N-biotin mutant kemptide were used as the negative control to remove nonspecific background crosslinking. Compared to the mutant samples, 324 proteins were enriched in N-biotin kemptide crosslinked samples (Table A2.1). Out of the 324 proteins, only 3 were protein kinases (Table 2.1). Importantly, the known kemptide kinase PKA (alpha catalytic subunit PRKACA) was one of the three identified kinases. In addition to PKA, two other kinases; CHEK1 and MAP2K7, and many non-kinase proteins were also observed in K-CLASP.

Table 2.1: Kinases enriched in K-CLASP^a

Gene names	Trial 1 Fold enrichment	Trial 2 Fold enrichment	Trial 3 Fold enrichment
MAP2K7	∞	0	∞
CHEK1	∞	0.1	∞
PRKACA (PKA)	2.6	1.5	4.9

^a Protein kinases observed in K-CLASP. The fold enrichment for each trial is shown. Fold enrichment was calculated by dividing the peptide intensity observed for wild type crosslinking by that observed for the mutant peptide crosslinking. Infinity (∞) signifies that no peptides were observed in Mut samples, making an average ratio calculation impossible.

To rule out the possibility that K-CLASP is preferentially pulling down high abundant proteins, we analyzed the abundance of the K-CLASP hits using previously published values.⁶⁵ A range of abundance was observed among the K-CLASP hits (Figure 2.11), indicating that K-CLASP is not biased towards highly expressed proteins. Given that K-CLASP can also identify proteins associated with the kinase during crosslinking event, the many non-kinase proteins and the two other kinases observed could be either direct or indirect interactors of PKA. In this scenario, diffusion of N-biotin kemptide after PKA-catalyzed photocrosslinker labeling (Figure 2.4b) may result in the

biotinylation of the nearby proteins of PKA. To validate that CHEK1, MAP2K7, and the other proteins were biotinylated due to their proximity to PKA, we performed an interactome analysis. For the interactome analysis, protein-protein interactions among the 324 K-CLASP enriched proteins were determined using the GeneMANIA⁶⁶ application in Cytoscape. In addition, PKA, CHEK1 and MAP2K7 substrates among the enriched proteins were identified using Phosphosite Plus and KinaseNET.⁶⁷ The known substrates and interacting proteins in the K-CLASP hit list were then graphically depicted as an interactome map using Cytoscape (Figure 2.12).⁶⁸

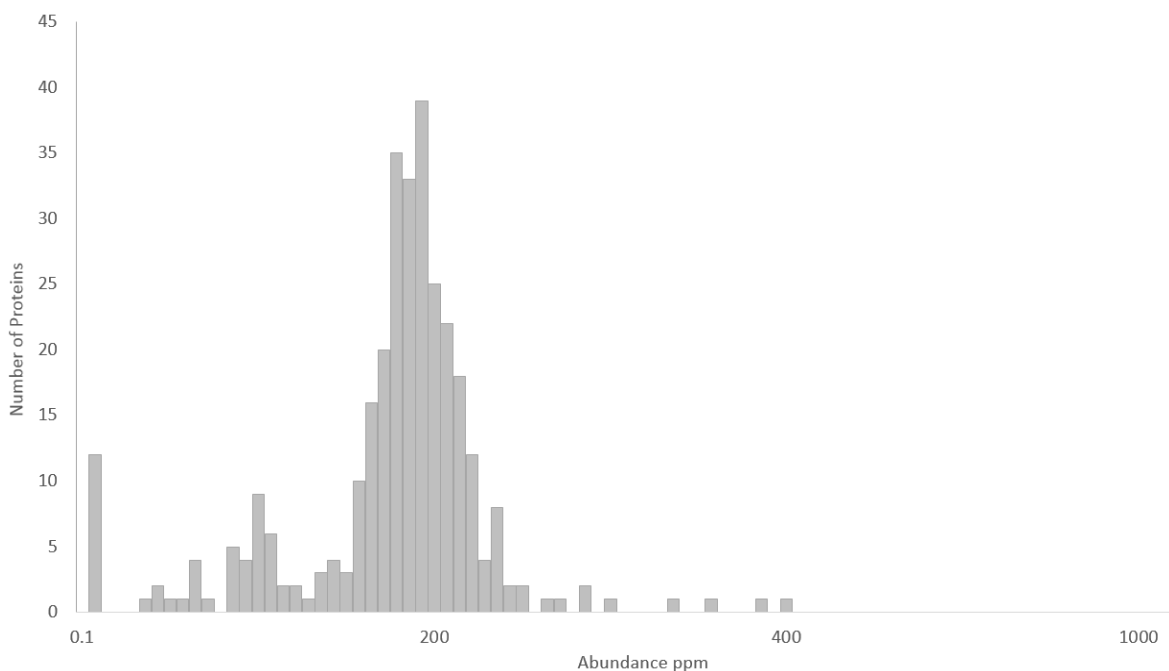


Figure 2.11: Abundance values of the 324 K-CLASP hits. Previously reported abundance levels of the K-CLASP hits in HeLa cells were plotted using Excel. K-CLASP identified proteins with a range of abundances (lowest 0.01 ppm and highest 403 ppm), which spanned the 0.01 to 10,000 possible range of all proteins. The presence of low abundance proteins among the K-CLASP hits documents that abundance is not the primary parameter for selection.

The interactome analysis confirmed that known PKA interacting proteins (Figure 2.11, dark blue circles) and substrates of PKA (Figure 2.12, light blue circles) were among the 324 K-CLASP hits. Beyond direct interacting proteins and substrates, many proteins

indirect interactors were considered, 60% of the K-CLASP hits were accounted for in the PKA interactome. The presence of direct and indirect PKA interacting proteins among the K-CLASP enriched hits is consistent with diffusion of N-biotin kemptide away from PKA after labeling (Figure 2.4b), resulting in the crosslinking and biotinylation of proteins located in close proximity to PKA.

Importantly, the interactome analysis showed that CHEK1 and MAP2K7 (Figure 2.12, orange circles) interact indirectly with PKA through common interacting partners (Figure 2.12 see blue lines). Therefore, CHEK1 and MAP2K7 biotinylation was likely due to their proximity to PKA, rather than by direct kinase-catalyzed crosslinking. In agreement, while several direct interacting proteins of PKA (Figure 2.13A, dark blue and light blue circles, green lines) were observed among the K-CLASP hits, only few direct interacting proteins were identified for CHEK1 (Figure 2.13B) and MAP2K7 (Figure 2.13C). The lack of directly associated proteins of CHEK1 and MAP2K7 among K-CLASP hits is consistent with CHEK1 and MAP2K7 being biotinylated by peptide diffusion rather than by a direct kinase labeling. Thus, the interactome analysis revealed false positive kinases. In addition to PKA, kemptide is phosphorylated by cyclic GMP-dependent protein kinase⁶⁴ and RPS6KA1⁶⁹ *in vitro*, and predicted to be phosphorylated by AKT and protein kinase C based on consensus sequence.⁷⁰ However, none of these kinases were identified by K-CLASP. Thus, K-CLASP identified PKA as the main kinase that phosphorylates kemptide in lysates. Given the wide use of kemptide in PKA studies,⁷¹ these results reinforce that PKA is the predominant kinase for kemptide.

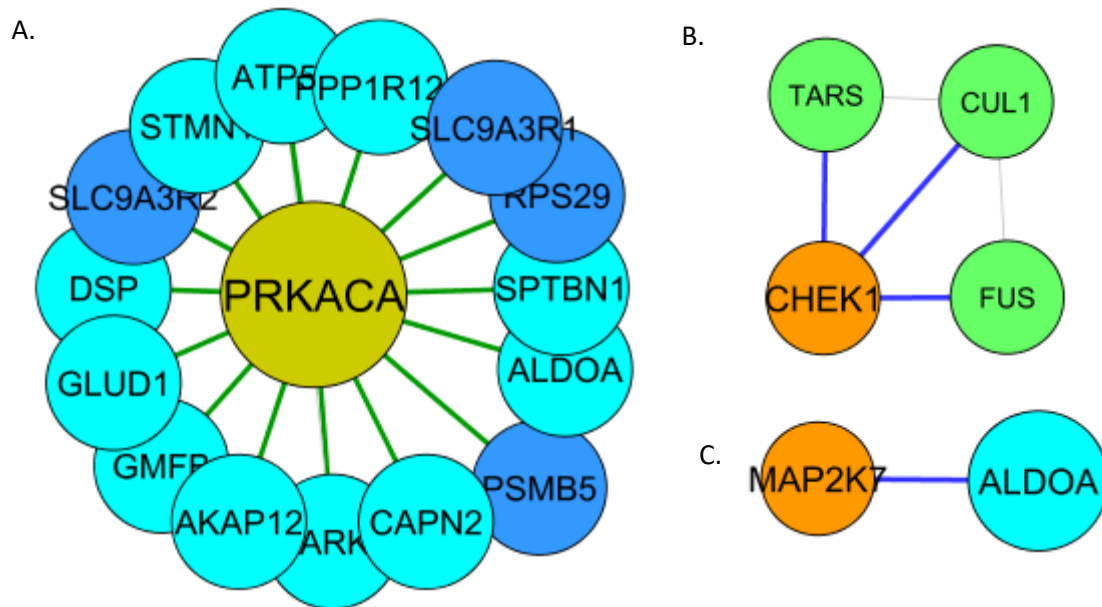


Figure 2.13: Direct interacting proteins of the kinases observed in K-CLASP. (A) Direct interacting proteins of PKA (PRKACA, yellow); binding proteins (dark blue circles) and substrates (light blue circles). (B) Direct interacting proteins of CHEK1. No substrates of CHEK1 were observed. The three CHEK1 binding proteins are indirect interacting proteins of PKA (hence green colored). (C) Direct interacting proteins of MAP2K7. No substrates of MAP2K7 were observed. The only binding protein of MAP2K7 was a known substrate of PKA (hence light blue colored). The less number of direct interacting proteins observed for CHEK1 and MAP2K7 suggests that CHEK1 and MAP2K7 were identified by K-CLASP due to their proximity to PKA and not by a kinase-catalyzed crosslinking.

In addition to eliminating false positive hits, the interactome analysis revealed several cellular complexes associated with PKA under the conditions of the experiment. For example, PKA is known to phosphorylate several proteasome subunits.⁷² In agreement, K-CLASP identified several proteins belonging to the proteasome core complex (Figure 2.14a). Additionally, many members of the ribosome complex (Figure 2.14b) were also identified, consistent with reports that PKA regulates translation in response to starvation.⁷³ Further, PKA is known to regulate the stability of the SMN complex which plays a role in the assembly of snRNPs (small nuclear Ribo Nucleo Proteins).⁷⁴ Interestingly, K-CLASP also identified several members of the SMN complex

(Figure 2.14c). While K-CLASP is primarily a tool for phosphosite-specific identification of kinases, these results demonstrate that cellular complexes containing the kinase can also be uncovered.

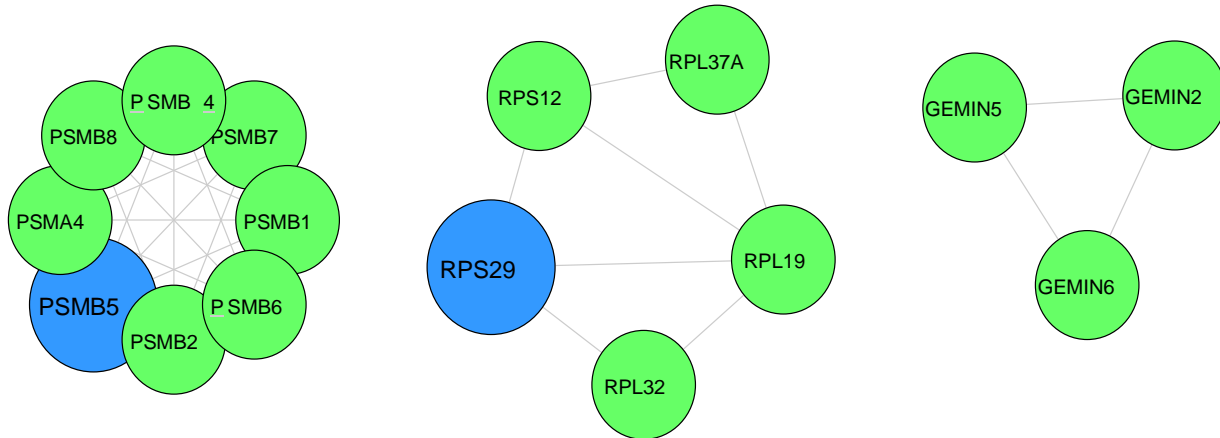


Figure 2.14: Protein complexes identified by K-CLASP. (a) Proteins belonging to the proteasome core identified by K-CLASP. (b) Proteins belonging to the ribosome complex identified by K-CLASP. (c) Proteins belonging to the SMN complex identified by K-CLASP. Green color circles indicate indirect interacting proteins of PKA and blue color circles indicate direct interacting proteins of PKA.

2.4 K-CLASP to uncover the kinase(s) that phosphorylate Miz1 protein

The proof-of-concept study with PKA and kemptide established K-CLASP as a useful tool for both phosphosite specific kinase identification and the discovery of kinase associated proteins. Next, in a collaboration project with Dr.Jing Liu at Northwestern, K-CLASP was used to uncover the kinase(s) responsible for the phosphorylation of the protein called Miz1. K-CLASP identified several kinases as potential enzymes that phosphorylate Miz1. In addition, many other proteins were also observed that could be associated proteins of the kinase.

2.4.1 Miz1 protein

Miz1, also known as ZBTB17, is a transcription factor that is involved in important cellular functions, such as cell division, differentiation and embryonic development.

Recently there have been reports that Miz1 is also involved in the attenuation of inflammation induced by TNF (tumor necrosis factor).⁷⁵ Specifically, Miz1 has been shown to bind the promoter of the inflammatory amplifier C/EBP δ during the late phase of TNF stimulation. Bound Miz1 represses the transcription of C/EBP δ by both recruiting HDAC1 and blocking the binding of the transcription factor NF-kB. The suppression of C/EBP δ resolves inflammation and prevents the tissue damage that can occur if inflammation is not regulated. Phosphorylation of Miz1 at Ser178 during TNF treatment has been shown to be essential for Miz1's role in inflammation regulation.⁷⁶ However, the particular kinase that phosphorylates Miz1 at Ser178 remains unknown, making elucidation of the signaling cascade that leads to the resolving inflammation difficult. In collaboration with Liu lab, we carried out K-CLASP to identify the kinase that phosphorylates Miz1 at Ser178 during TNF treatment.

2.4.2 K-CLASP with Miz1 protein

To carry out K-CLASP with Miz1, a biotinylated peptide carrying the Miz1 Ser178 phosphosite (biotin-GGQAESAS**S**GAEQTEK) was synthesized. Then crosslinking reactions were carried out with the N-biotinylated Miz1 peptide with MEF (mouse embryonic fibroblast) lysates derived from cells treated with or without TNF induction. A control crosslinking reaction was also carried out with a mutant variant where S178 was mutated to Ala (biotin-GGQAESAS**A**GAEQTEK). The crosslinked samples were then purified by streptavidin resin and analyzed by LC-MS/MS (Figure A.2.7).

A total of 12 kinases were reproducibly observed in two independent replicates (Table 2.2). Out of these, only five were enriched in wild type peptide crosslinked samples from TNF treated lysates compared to both the mutant peptide crosslinked sample and

TNF untreated samples in both trials (Table 2.2, green colored rows). Among the five hit kinases, SLK was the best hit based on the enrichment fold values. In addition, when both trials were considered, ILK, CDK1 and PBK also showed appreciable fold enrichment in the wild type crosslinked sample from TNF treated lysates. The fold enrichment values for PAK2, however, were not significant especially in the first trial (Table 2.2). Nevertheless, PAK2 was still kept in the list of hit kinases.

Table 2.2: Kinases seen in Miz1 peptide K-CLASP study^a

Kinase	Trial 1 Fold Enrichment	Trial 2 Fold Enrichment	Fold enrichment compared to No TNF control (Trial 1)
SLK	∞	7.4	2.9
ILK	10.4	2.7	5.5
CDK1	2.0	2.2	10.9
PBK	1.5	2.0	3.4
PAK2	1.1	3.8	4.1
MAP2K3	0.3	∞	∞
SRPK1	∞	0.9	∞
CDK4	0.7	4.8	18.9
MAPK1	4.2	0.0	1.0
MAP2K2	0.8	2.2	0.3
CAMK2D	∞	1.0	0.6
MAPK14	0.0	0.0	0.0

^aTrial 1 and Trial 2 fold changes were calculated by dividing the peptide intensity observed in the N-biotin Miz1 peptide crosslinking in TNF treated sample by the peptide intensity observed for the N-biotin mutant Miz1 peptide crosslinking in TNF treated sample. Fold change with no TNF was calculated by dividing the peptide intensity observed in the N-biotin Miz1 peptide crosslinking in TNF treated sample by the peptide intensity observed for the N-biotin Miz1 peptide crosslinking in TNF untreated sample. Infinity (∞) signifies that no peptides were observed in either the N-biotin mutant Miz1 peptide crosslinking sample or the N-biotin Miz1 peptide crosslinking in TNF untreated lysate sample. The K-CLASP hit kinases are green colored.

At a fold enrichment threshold of 2 or greater for both trials, 340 proteins were enriched in wild type peptide crosslinked samples from TNF-treated lysates compared to both the mutant peptide crosslinked sample and the TNF-untreated sample. (Table A2.2). In order to identify the most likely *in cellulo* kinase out of the five candidate kinases and to discover proteins associated with the potential kinase, we carried out an interactome

analysis using GeneMania application in Cytoscape. The substrates of ILK, SLK, CDK1, PAK2 and PBK were identified from Phosphosite Plus and added manually onto the Cytoscape map.

Table 2.3: Kinase direct interacting proteins observed by K-CLASP study with Miz1 peptide^a

Kinase	Directly Interacting proteins observed	Total number of known directly Interacting proteins	Percentage of interacting proteins observed
SLK	0	23	0
ILK	51	214	24%
CDK1	23	212	11%
PBK	9	29	31%
PAK2	13	84	15%

^aTotal number of known directly interacting proteins was obtained from the BioGrid database. Percentage of interacting proteins were calculated by dividing the number of directly interacting proteins observed in the K-CLASP study by the total number of known directly interacting proteins.

From the K-CLASP hits, 86% could be accounted for in the interactome. Except for SLK, all other kinases had a number of direct interacting proteins and substrates among the K-CLASP hits (Table 2.3, Figure 2.15). Out of all kinases, ILK had the highest number of direct interacting proteins, followed by CDK1 (Table 2.3, Figure 2.15). However, when the percentage of interacting proteins observed in K-CLASP was considered, PBK had the highest percentage (Table 2.3). Therefore, secondary validation is necessary to confirm the kinase that phosphorylates S178 of the Miz1 protein. Although SLK was the best hit when enrichment fold values were considered, SLK did not have any known interacting proteins or substrates among K-CLASP hits. This may be due to the fact that SLK is not a well characterized kinase and has only a few known substrates and interacting proteins (Table 2.3). In addition, the Miz1 peptide used for K-CLASP contained S175 that has been reported as a phosphosite.⁶⁷ Therefore, it is possible that the kinases observed in our study are responsible for the phosphorylation of S175 as well. Given that the mutated peptide with S178A was used as the negative

control in the K-CLASP study, if a K-CLASP hit kinase is confirmed to be responsible for S175 phosphorylation, it would suggest that S178 phosphorylation might be a prerequisite for S175 phosphorylation.

There were several Miz1 interacting proteins among the K-CLASP hits (Figure 2.16). Under TNF treatment, the kinase that phosphorylates Miz1 may associate with

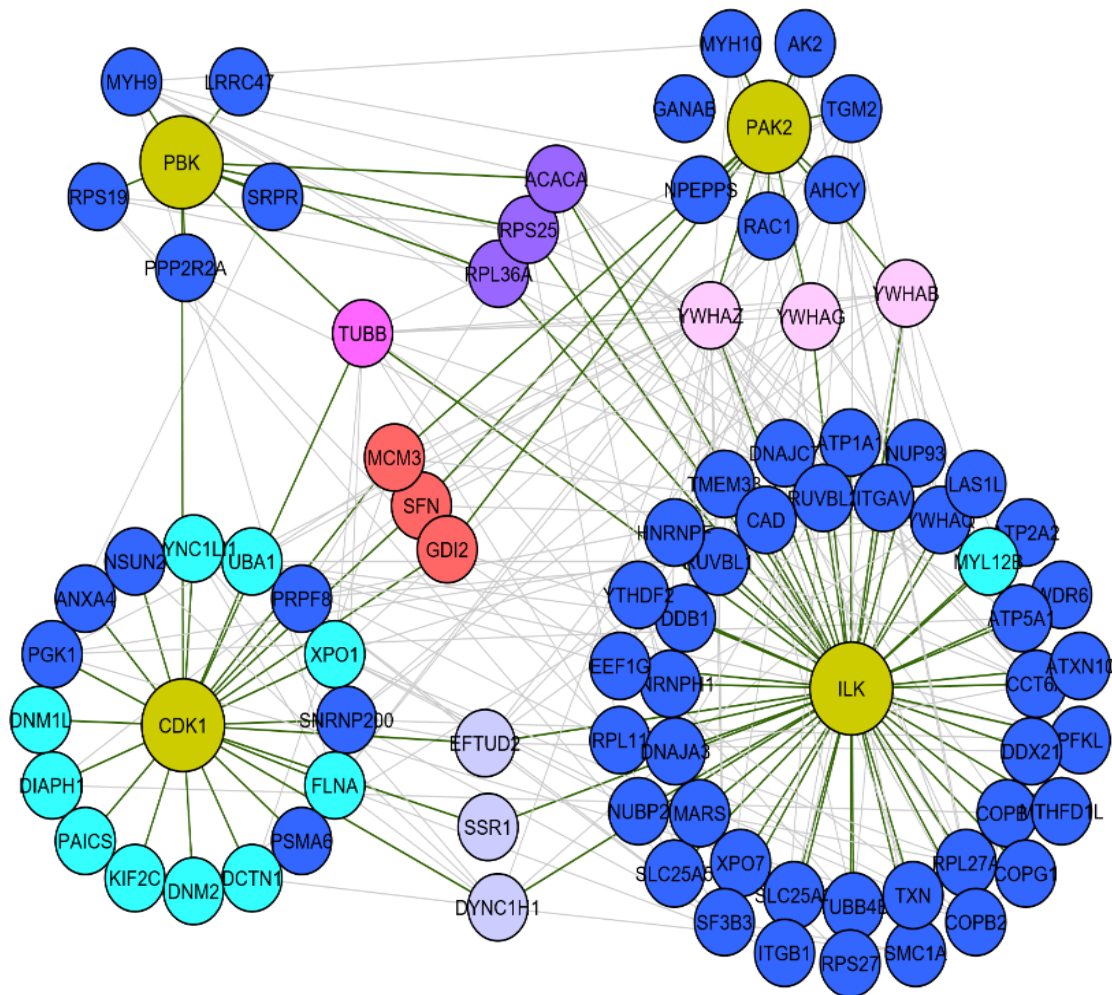


Figure 2.15: Direct interacting proteins and substrates of the kinases observed in K-CLASP. The directly interacting proteins of each kinase (yellow); binding proteins (dark blue) and substrates (light blue). SLK did not have any known interacting proteins among the K-CLASP hits. TUBB (dark pink) interacts with all four kinases. ACACA, RPS25 and RPL36A (dark purple) interact with both PBK and ILK. YWHAZ, YWHAG and YWHAB (light pink) interact with both PAK2 and ILK. MCM3, SFN and GDI2 (brick red) interact with both PAK2 and CDK1. EFTUD2, SSR1 and DYNC1H1 (light purple) interact with both CDK1 and ILK.

proteins that facilitate the delivery of Miz1 to the kinase, which explains the presence of Miz1 interacting partners among the K-CLASP hits. Out of the common interacting partners, the 14-3-3 adapter protein YWHAQ interacts directly with both ILK and Miz1. YWHAQ interacts with several other K-CLASP proteins, which in turn interact with other hit kinases (Figure 2.16). The common interacting partners of Miz1 and the kinases observed may provide clues to what other proteins are playing a role in Miz1 phosphorylation under TNF treatment. Interestingly, the Miz1 direct interacting protein HCF1 (Figure 2.16, yellow) interacts with the K-CLASP protein RELA (NF- κ B) which plays a major role as a transcription factor in TNF induced inflammatory response.⁷⁷ HCF1 may represent a scaffold between NF- κ B and Miz1 during inflammation.

To see if there are any protein complexes among the K-CLASP hits, we used the MCODE application⁷⁸ in cytoscape. MCODE identifies clusters of proteins based on the number of interactions. MCODE detected several protein clusters among the K-CLASP hits (Figure 2.17). Proteins belonging to the proteasome complex were one of the clusters identified (Figure 2.16A). TNF treatment is known to downregulate proteasome activity in cells.²¹ The MCODE analysis suggests that the Miz1 kinase may also have a role in regulating the proteasome during TNF treatment. In addition, another cluster containing several components of the COP9 signalosome (COPS3, COPS7A and GPS) and DDB1 was detected (Figure 2.17B). DDB1 is known to be associated with the COP9 signalosome.⁷⁹ The result suggests that the COP9 signalosome may play a role in TNF induced inflammation through the Miz1 kinase. Thirdly, MCODE also identified a cluster

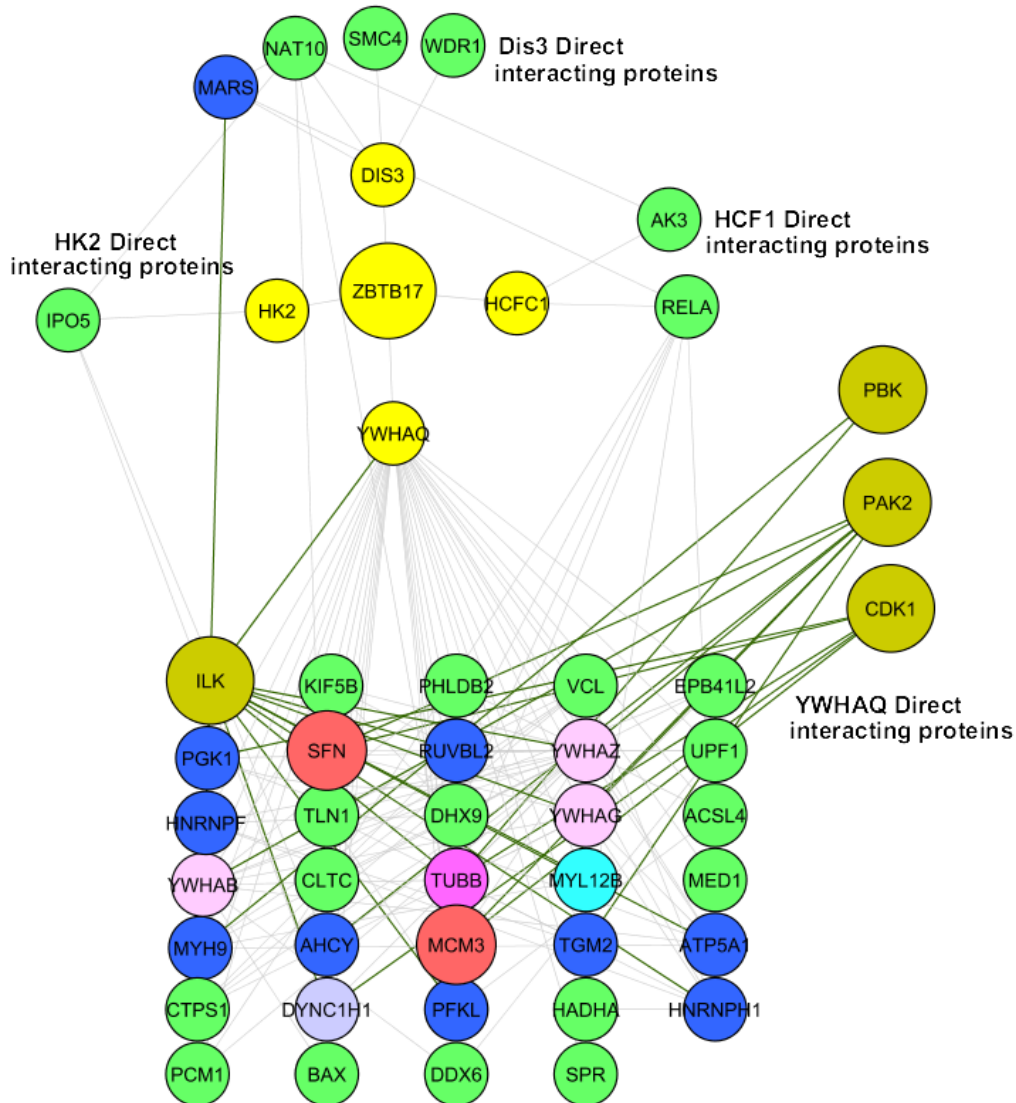


Figure 2.16: Interacting proteins of Miz1 (ZBTB17). Yellow color represents the directly interacting proteins of Miz1. The direct interacting proteins of the Miz1 interacting proteins are also shown. Miz1 direct interacting protein YWHAQ interacts directly with ILK. Some of the other YWHAQ interacting proteins also interact with PAK2, CDK1 and PBK. The common interacting partners shared with Miz1 and the K-CLASP kinases provides hints to what other proteins may be playing a role in Miz1 phosphorylation under TNF induction. Blue color represents direct interacting proteins of K-CLASP kinases (See Figure 2.14). Light blue color represents substrates of K-CLASP kinases. Brick red, light pink, light purple and dark pink are common interacting proteins of K-CLASP kinases (see Figure 2.14). The rest of the proteins are green colored.

of proteins including members of the coatamer complex (COPA, COPB1, COPB2 Figure 2.17C), which coat Golgi-derived vesicle proteins to facilitate the protein transport from the ER (endoplasmic reticulum) to the trans-Golgi network.⁸⁰ Among the other proteins in

this coatomer cluster, NSF is an ATPase involved in vesicle mediated transport.⁸¹ The rest of the members in the cluster have diverse reported functions; ACACA and IDH3G are both metabolic enzymes with carboxylase and dehydrogenase activities respectively, while DDX6 is an RNA helicase. CCT6A is a chaperone protein.⁸² Nevertheless, the MCODE result hints that the Miz1 kinase may associate with proteins in the cellular transport machinery during TNF treatment. The fourth and fifth complexes recognized by MCODE (Figure 2.17 D, E) also have proteins with diverse reported functions ranging from RNA splicing to nuclear transport of proteins. Further analysis of the MCODE complexes may reveal additional roles of the Miz1 kinase in downstream functions upon TNF treatment.

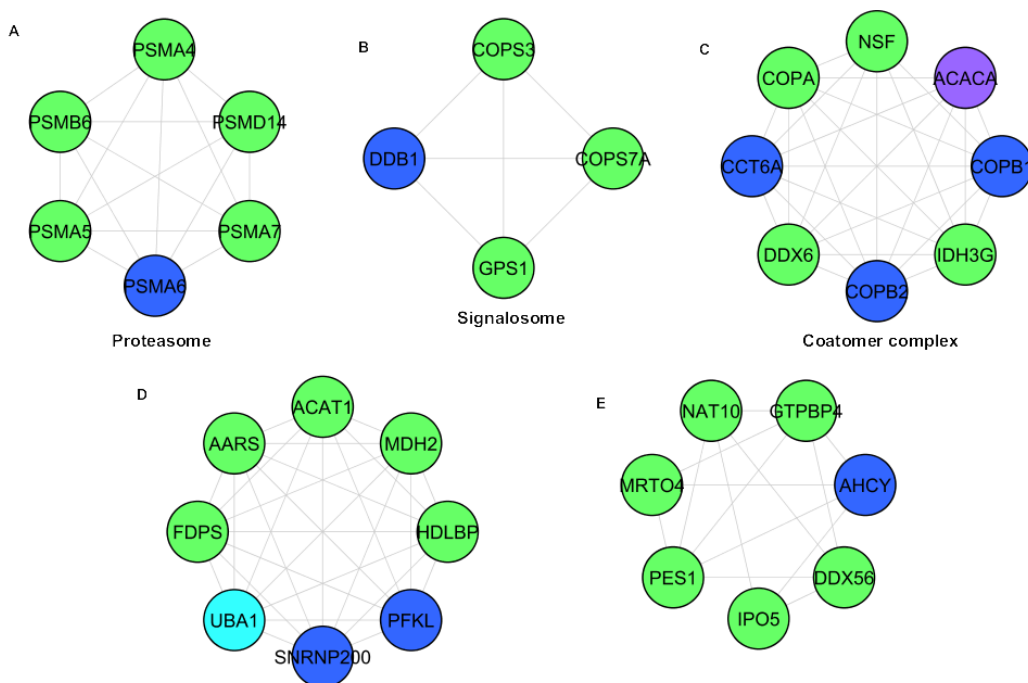


Figure 2.17: Clusters of proteins (A-E) identified by MCODE among the K-CLASP hits. Blue color represents direct interacting proteins of K-CLASP kinases (See Figure 2.11). Light blue color represents substrates of K-CLASP kinases. Dark purple represents common interacting proteins of K-CLASP kinases (see Figure 2.11). The rest of the proteins are green colored.

Overall, the K-CLASP study with the Miz1 peptide identified several kinases as candidates for S178 phosphorylation. Out of those, ILK is the best candidate given its many interacting partners observed among the K-CLASP hits. However, the K-CLASP study may also have purified a S175 kinase since S175 is a known phosphosite. Additionally, the interactome analysis revealed many other proteins and protein complexes that may link the Miz1 kinase with other cellular pathways. First the TNF-sensitive Miz1 kinase(s) has to be confirmed to use the additional information on the associated proteins provided by the K-CLASP study. Therefore validation studies are necessary to confirm the role of the identified kinases in Miz1 phosphorylation upon stimulation by TNF. These secondary validation studies are being carried out by our collaborator Dr. Jing Liu.

2.5 Conclusions and Future Directions

In conclusion, K-CLASP was developed as a discovery tool to identify the *in cellulo* kinase of a given phosphosite. In the first study with the well-known kinase-substrate pair, PKA and kemptide, K-CLASP identified PKA as the predominant cellular kinase of kemptide from a complex mixture of other proteins and kinases. In addition, interactome analysis of K-CLASP hits confirmed that peptide diffusion during crosslinking leads to the biotinylation and the subsequent identification of proteins close to the kinase. The interactome analysis identified several cellular complexes containing PKA and ruled out false positives. Identification of proteins belonging to proteasome core, ribosome and the SMN complex suggests that PKA was associated with the mentioned complexes during crosslinking. The discovery of the said complexes among the K-CLASP hits reaffirms the already known role of PKA on proteasome, ribosome, and SMN complexes. Overall, the

proof-of-concept study with PKA provided evidence for the utility of K-CALSP, while also setting parameters for identification with phosphosites without a known kinase.

In the second study, K-CLASP identified SLK, ILK, CDK1, PAK2 and PBK as potential kinases that phosphorylate S178 of Miz1 in response to TNF treatment. Interactome analysis on the K-CLASP hits revealed many other proteins and protein complexes that may associate with the Miz1 phosphorylating kinase during TNF treatment. Once the secondary validation studies confirm which kinase(s) carries out Miz1 phosphorylation, the information on the associated proteins uncovered by K-CLASP can be used to further detangle the complex cellular pathways involved in TNF induced inflammation.

In the present studies, crosslinking with a mutant peptide lacking the phosphosite was used as the negative control in K-CLASP. However, in vitro studies with PKA and mutant kemptide showed that the labeling by the mutant kemptide still requires binding to PKA (Figure 2.7). As a result, the inclusion of mutant peptide as the negative control may limit the discovery of associated proteins, although the mutant is a good control for the identification of hit kinases. As a solution, in future experiments, crosslinking with a scrambled peptide will be included to better reflect the background. While the mutant peptide control can be used to uncover the kinase(s), the scrambled peptide control may help identify the associated proteins.

In summary, the two studies show that K-CLASP is a simple, yet powerful, method to probe the activity of a specific phosphosite. Importantly, K-CLASP only requires a biotinylated peptide containing a known phosphosite and cell lysate where phosphorylation of that specific site is observed. Given the importance of studying the

many phosphorylation events in a cell, K-CLASP provides an enabling technology to understand the intricate regulatory networks governing cellular events.

2.6 Experimental Methods

2.6.1. Synthesis of ATP-ArN₃

The synthesis and characterization of ATP-ArN₃ has been previously described.^{48a} ATP-ArN₃ was dissolved in HEPES (1 mM, pH 7.4) and aliquoted (5 μ L each). Aliquots were stored at -80°C until use.

2.6.2. Peptide Synthesis and Purification

N-biotin kemptide (biotin-GGGGLRRASLG, the phosphorylation site is underlined), N-biotin mutant kemptide (biotin-GGGGLRRAALG, mutated site is underlined), non-biotinylated kemptide (GGGGLRRASLG), scrambled N-biotin kemptide (biotin-LSGARGLGGRG), N-biotin CK2 substrate peptide (biotin-RRREEEIEEE, the phosphorylation site is underlined), non-biotinylated CK2 substrate peptide (RRREEEIEEE), N-biotin Miz1 peptide (biotin-GGQAESASSGAEQTEK, the phosphorylation site is underlined) and N-biotin mutant Miz1 peptide (biotin-GGQAESASAAEQTEK, mutated site is underlined) were synthesized as previously described.⁸³ Specifically, Wang resin conjugated, Fmoc-protected C-terminal amino acid from each peptide (0.15 mmoles) and Fmoc-protected amino acids (0.45 mmoles) were used. For each coupling step, hydroxylbenzyltriazole (HOBt) (0.9 mmoles) and N,N'-Diisopropylcarbodiimide (DIPCDI, 0.6 mmoles) were used in DMF (5 mL). After final deprotection, N-biotinylation was carried out by adding D-biotin (0.75 mmoles), O-(Benzotriazol-1-yl)-N,N,N',N'-tetramethyluronium tetrafluoroborate (TBTU) (0.9 mmoles), hydroxylbenzyltriazole (HOBt) (0.9 mmoles) and N,N-Diisopropylethylamine (DIPEA) (1

mmoles) in a 1:1 mixture of DMSO and DMF (5 mL). The biotinylation reaction was incubated overnight at room temperature with shaking on a Wrist-action® shaker (Burrell). The biotinylation step was omitted to generate non-biotinylated kemptide and CK2 peptide. The product peptides were then cleaved off the resin using a trifluoroacetic acid: phenol: thioanisole: water: 1,2-ethanedithiol (82.5:5:5:5:2.5) cleavage solution (5 mL) for two hours. The cleaved product was precipitated in cold ether, washed three times with cold ether, and then dried under Argon gas. The peptides were purified by reverse phase chromatography using a C18 column (YMC America: 250x10mmI.D, S-4 μ M, 8nM) on a Waters 1525 binary HPLC pump. The flow rate was 3mL/min and the peptides were detected at 214 nm. N-biotin kemptide, N-biotin mutant kemptide and scrambled N-biotin kemptide were purified by an elution gradient that started with 95% Buffer A (99.9% water with 0.1% trifluoroacetic acid) in Buffer B (acetonitrile in 0.085% trifluoroacetic acid) and decreased to 83% Buffer A over 11 minutes, then to 81.5% Buffer A over 5 minutes, and finally to 80.6% Buffer A over 9 minutes. When characterized by MALDI-TOF, the purified N-biotin kemptide showed a $[M+H]^+$ of 1226.68 m/z ($[M+H]^+$ calculated for $C_{50}H_{88}N_{19}O_{15}S = 1226.64$, Figure A2.1.1B), while the purified N-biotin mutant kemptide showed a $[M+H]^+$ of 1210.76 ($[M+H]^+$ calculated for $C_{50}H_{88}N_{19}O_{14}S = 1210.65$, Figure A2.1.2A) and the purified scrambled N-biotin kemptide showed a $[M+H]^+$ of 1226.50 m/z ($[M+H]^+$ calculated for $C_{50}H_{88}N_{19}O_{15}S = 1226.64$, Figure A2.1.4B). The non-biotinylated kemptide was purified using an elution gradient that started with 95% Buffer A in Buffer B and ended with 75% Buffer A over 16 minutes. The purified non-biotinylated kemptide showed a $[M+H]^+$ of 1000.85 by MALDI-TOF ($[M+H]^+$ calculated for $C_{40}H_{74}N_{17}O_{13} = 1000.57$, Figure A2.1.3B). The synthesis, purification and the MALDI-TOF characterization of the scrambled N-biotin

kemptide were carried out by N.Chinthaka. N-biotin CK2 substrate peptide was purified using an elution gradient that started with 86.7% Buffer A in Buffer B and ended with 70% Buffer A in 10 minutes. Non-biotinylated CK2 substrate peptide was purified using an elution gradient that started with 95% Buffer A in Buffer B and ended with 77.5% Buffer A in 14 minutes. The purified N-biotin CK2 substrate peptide showed a $[M+H]^+$ of 1588.14 m/z ($[M+H]^+$ calculated for $C_{62}H_{101}N_{21}O_{26}S = 1588.69$, Figure A2.1.5B). The purified non-biotin CK2 substrate peptide showed a $[M+H]^+$ of 1362.36 m/z ($[M+H]^+$ calculated for $C_{52}H_{87}N_{19}O_{24} = 1362.62$, Figure A2.1.6B). The synthesis, purification and the characterization of N-biotin CK2 substrate peptide and non-biotin CK2 substrate peptide were performed by T.Faner. N-biotin Miz1 peptide was purified using an elution gradient that started with 95% Buffer A in Buffer B and ended with 75% Buffer A over 22 minutes. The purified N-biotin Miz1 peptide showed a $[M+H]^+$ of 1762.56 by MALDI-TOF ($[M+H]^+$ calculated for $C_{69}H_{111}N_{21}O_{31}S = 1762.9$, Figure A2.1.7B). N-biotin mutant Miz1 peptide was purified by using an elution gradient starting from 95% Buffer A in Buffer B and ending in 75% Buffer A over 16 minutes. The purified N-biotin mutant Miz1 showed a $[M+H]^+$ of 1747.27 by MALDI-TOF ($[M+H]^+$ calculated for $C_{69}H_{111}N_{21}O_{30}S = 1746.98$, Figure A2.1.8B). The purity of each peptide was assessed by reinjection (50 μ g of each purified peptide) on a C18 column (YMC America: J'Sphere H80, 80Å, 4 μ m, 250x4.6mm) and separation by reverse phase HPLC using a flow rate was 1 mL/min. For non-biotinylated CK2 substrate peptide, an isocratic elution at 86% of Buffer A was used for reinjection. For all other peptides, reinjection was carried out under same elution conditions used for purification (Figures A2.1.1A-A2.1.8A).

2.6.3. *In vitro* crosslinking reaction with recombinant PKA

Crosslinking reactions contained N-biotin kemptide (4 mM), ATP-ArN₃ (4 mM) and recombinant PKA (150 units/ μ L, New England BioLabs) in kinase buffer (25 mM HEPES at pH 7.5, 50 mM KCl and 10 mM MgCl₂). The final reaction volume was 25 μ L. Photocrosslinking was performed by irradiating the reaction mixtures at 365 nm for 2 hours at 31°C with shaking at 300rpm. Control reactions were performed without ATP-ArN₃ or with N-biotin mutant kemptide (4 mM) in the place of N-biotin kemptide, ATP (4mM) in the place of ATP-ArN₃, excess ATP (16 mM) in the presence of ATP-ArN₃ (4 mM), excess non-biotinylated kemptide (8 mM) in the presence of N-biotin kemptide (4 mM), N-biotin scrambled peptide (4mM) in place of N-biotin kemptide, and heat inactivated PKA (95°C, 30 minutes) in place of active PKA enzyme. After reaction, samples were boiled at 95°C for 1 minute in 1X Laemmli sample buffer (60 mM Tris-HCl pH 6.8, 2% SDS, 10% glycerol, 0.0005% bromophenol blue, 2% beta-mercaptoethanol) and separated by 10% SDS-PAGE (section 2.6.4). For visualization of biotinylation, proteins were first transferred onto a onto a PVDF membrane (section 2.6.5) and then probed with Streptavidin-Cy5 (Life Technologies, section 2.6.7). Total proteins were observed with SYPRO® Ruby stain (Thermo Fisher, section 2.6.8). After quantification of the biotin signal using ImageQuant (GE Healthcare), percent biotinylation signal intensity was determined by calculating the ratio of band intensity for each reaction compared to the band intensity with N-biotin kemptide and ATP-ArN₃ (set to 100%), and multiplying by 100. Replicate trials used to calculate the mean and standard error of percent signal intensity are shown in A2.2.

2.6.4. SDS-PAGE (sodium dodecyl sulfate polyacrylamide gel electrophoresis)

SDS-PAGE gels were produced by first preparing a lower, separating layer and then an upper, stacking layer as previously described (*Molecular cloning*, Appendix 8.40-8.45).⁸⁴ A 10% separating layer was prepared by mixing water (4.788 mL), Tris (2.5 mL, 1.5M, pH 8.8), and 40% w/v 37:1 acrylamide:bisacrylamide (2.513 mL, OmniPur® EMD Milipore). The mixture was then de-gassed under vacuum for about 10 minutes. Next, SDS (100 µL from 10% w/v SDS in water, Fisher Scientific), and Ammonium persulfate (APS, 100 µL from 10% w/v APS in water, Fisher Scientific) were added. Finally, tetramethylethylenediamine (TEMED, 4 µL, Acros Organics) was added to initialize polymerization. The mixture was then immediately poured onto a gel set up and was overlaid with methanol (100%). The separating layer was then allowed to polymerize for at least 2 hours at room temperature. After polymerization, methanol was removed and the top of the gel was briefly washed with deionized water. A stacking layer was then prepared by mixing water (2.913 mL), Tris (0.5 mL, 1 M, pH 6.8) and 40% w/v 37:1 acrylamide:bisacrylamide (0.488 mL). The mixture was de-gassed for 10 minutes. SDS (40 µL from 10% SDS in water) and APS (40 µL from 10% APS in water) were added. After adding TEMED (4 µL), the mixture was immediately added to the gel set up. For protein separation, samples were loaded onto the gel after boiling in 1X Laemmli buffer (section 2.6.3) along with a molecular weight marker (1 µL, EZ-run™ Prestained Rec Protein Ladder, Fisher). The gel was run first at 110V for 10 minutes and then at 200V for 1 hour on a gel electrophoresis system (BioRad) in running buffer (1X, 25 mM Tris, 192 mM glycine and 0.1% SDS).

2.6.5. Protein transfer onto a membrane

After protein separation by SDS-PAGE (section 2.6.4), the gel was briefly washed in water (~10 mL) and then equilibrated in transfer buffer (10 mL, 1X, 25 mM Tris, 192 mM glycine and 10% v/v methanol) for 5-10 minutes. A PVDF membrane cut to the size of the gel (Immobilon-P, Milipore) was first washed with methanol (~10 mL, 100%), water (~10 mL) and equilibrated in transfer buffer (10 mL) for 5-10 minutes. Then the gel and the membrane were assembled onto a transfer apparatus (Mini-Transblot Electrophoretic Transfer Cell apparatus, BioRad) as described by the manufacturer. Transfer was carried out at 90V for 2 hours on ice in the transfer buffer.

2.6.6. Visualization of biotin with streptavidin-Cy5 and Western blot

After transfer (2.6.5), the membrane was rocked in non-fat dry milk (Meijer, 5% w/v) in 1X PBST (15 mL, phosphate buffered saline with tween, 0.1% v/v Tween-20 in 1X PBS buffer: 137 mM NaCl, 2.7 mM KCl, 10 mM Na₂HPO₄, 2 mM KH₂PO₄, pH 7.4) at room temperature overnight. The membrane was briefly washed with 1X PBST (15 mL) and fresh non-fat dry milk (3-5% w/v in 1X PBST (15 mL) was added. Then streptavidin-Cy5 (7.5 µL, 1:2000 dilution, ZyMax Grade, ThermoFisher Scientific, catalog number- 438316) was added in dark. The container carrying the membrane was covered in foil and rocked at room temperature for 1 hour. Then the milk was removed and the membrane was briefly washed first in 1X PBST (~20 mL) and then in 1X PBS (~ 20 mL). The biotin signal was then visualized using a Typhoon imager (635 nm laser, 500 PMT, 50 µm pixel size, Typhoon FLA 9500, GE Healthcare) and ImageQuant (GE Healthcare).

2.6.7. Sypro®Ruby staining for total protein visualization

After protein separation (section 2.6.5), the gel was fixed by rocking at room temperature in a fixing solution (~30 mL, 50% methanol and 7% acetic acid in water) for 1 ½- 2 hours. Then the gel was rocked in Sypro®Ruby stain (~ 30 mL, BioRad) at room temperature for overnight. The Sypro®Ruby stain was removed the next day and the gel was destained by rocking in a destaining solution (~ 30 mL, 10% methanol and 7% acetic acid in water) at room temperature for 30 minutes. Then the gel was washed two times in water (~30 mL) by rocking at room temperature for 5 minutes each time. Next the Sypro®Ruby signal was visualized on Typhoon imager (532 nm, 500 PMT, 100 µm pixel) and ImageQuant.

2.6.8. *In vitro* crosslinking with PKA after pre-incubation of N-biotin peptide and ATP-ArN₃

N-biotin kemptide, N-biotin mutant kemptide, or scrambled N-biotin peptide (4 mM) was pre-incubated with ATP-ArN₃ (4 mM) in kinase buffer for 15 minutes at 31°C under UV irradiation at 365nm with shaking at 300rpm. Then recombinant PKA (150 units/µL) was added and the reaction mixtures were further irradiated at 365 nm for 2 hours at 31°C with shaking at 300rpm. The final reaction volume was 25 µL. As a control, crosslinking reactions were performed with N-biotin kemptide (4 mM) without pre-incubation. After the reaction, samples were boiled at 95°C for 1 minute in Laemmli sample buffer and separated by 10% SDS-PAGE (section 2.6.4). Total proteins were observed with SYPRO® Ruby stain (section 2.6.7). Biotinylation was visualized with Streptavidin-Cy5 (section 2.6.6). A Typhoon imager was used for gel band visualization.

2.6.9. *In vitro* crosslinking reaction with recombinant CK2

Crosslinking reactions were carried out with N-biotin CK2 substrate peptide (0.76 mM), ATP-ArN₃ (2 mM), and recombinant CK2 (20 units/ μ L, New England BioLabs) in kinase buffer. The final reaction volume was 25 μ L. Photocrosslinking was performed by irradiating the reaction mixtures at 365nm for 2 hours at 31°C with shaking at 300rpm. Control reactions were performed with ATP (2 mM) in the place of ATP-ArN₃, excess ATP (8 mM) in the presence of ATP-ArN₃ (2 mM), and excess non-biotinylated CK2 substrate peptide (1.52 mM) in the presence of N-biotin CK2 peptide (0.76 mM). After reaction, samples were boiled at 95°C for 1 minute in Laemmli sample buffer and separated by 10% SDS-PAGE (section 2.6.4). Total proteins were observed with SYPRO® Ruby stain (section 2.6.7). Biotinylation was visualized with Streptavidin-Cy5 (section 2.6.6). A Typhoon imager was used to visualize the gel bands.

2.6.10. MEF cell culture

MEF (Mouse Embryonic Fibroblasts) cells were a gift from Dr. Jing Liu at Northwestern University. MEF cells (8×10^6) were grown in DMEM media (45 mL, ThermoFisher, catalog number 12430104) supplemented with 10% FBS (fetal bovine serum, ThermoFisher, catalog number 16000044) and 1X antibiotic/antimycotic solution (ThermoFisher, catalog number 15240062). After 24 hours of cell growth, cells were serum starved overnight by placement in DMEM media with 1% FBS without antibiotic/antimycotic mixture (45 mL). The next day, cells were treated with TNF α (10ng/mL in DPBS, Dulbecco's Phosphate Buffered Saline, Hyclone) or without TNF (DPBS,) for 15 minutes at 37°C in the cell incubator. Then cells were briefly washed with DPBS (10 mL). The cells were then treated with trypsin-EDTA (0.25%, 12 mL,

ThermoFisher, catalog number 25200072) for 5 minutes. Next cold DPBS (15 mL) was added to the cells to stop trypsin reaction. The cells were collected into a centrifuge tube and spun at 1000 rpm, at 4°C for 5 minutes. The supernatant was discarded and the cells were re-suspended in cold DPBS (2mL). The cells were again spun at 1000 rpm, at 4°C for 5 minutes. The supernatant was discarded and the cell pellet was either stored at -80°C or immediately lysed.

2.6.11. HeLa and MEF cell lysis

HeLa cells (20 X 10⁶) purchased from National Cell Culture Center (Biovest) were lysed in lysis buffer (4 mL; 25 mM HEPES at pH 7.4, 150 mM NaCl, 0.5% Triton X-100, 10% glycerol, and 1X protease inhibitor cocktail (GenDepot)) at 4°C for 10 minutes with rotation. For MEF cells (20 X 10⁶), 250 µL of lysis buffer was used. Cell debris was removed by centrifugation at 13,200 rpm at 4°C for 10 minutes. The protein concentration was assessed by Bradford assay (Biorad) per manufacturer's instructions. The lysates were aliquoted and stored at -80°C or immediately used.

2.6.12. Optimization of crosslinking reaction with HeLa cell lysates

HeLa cell lysates (3.75 mg/mL) were initially incubated with ATP (12 mM) in kinase buffer for 15 minutes at room temperature to activate endogenous PKA. Then, the lysates were incubated with the indicated amounts of biotinylated kemptide (B-kem: 1, 1.5, or 2 mM) and ATP-ArN₃ (4 mM) under UV light for 1 hour, 1.5 hours, or 2 hours at 31°C in a final reaction volume of 40 µL. Reaction products were separated by 10% SDS-PAGE (section 2.6.4), before visualization of biotinylated proteins using streptavidin-Cy5 (SA-Cy5, section 2.6.6) or total proteins with Sypro®Ruby stain (section 2.6.7).

2.6.13. In vitro crosslinking reaction with HeLa lysates

Before crosslinking, HeLa lysates (3.75 mg/mL) were incubated with ATP (12 mM) in kinase buffer for 15 minutes at room temperature to activate endogenous PKA. Then ATP-ArN₃ (4 mM) and N-biotin kemptide (2 mM) were added. The final reaction volume was 40 μ L. Crosslinking reactions were performed by irradiating the reaction mixtures at 365nm for 2 hours at 31°C with shaking at 300rpm. Control reactions were carried out without ATP-ArN₃, with N-biotin mutant kemptide (2 mM) in place of N-biotin kemptide, or non-biotinylated kemptide (2 mM) in the presence of biotin-kemptide (2 mM). For the staurosporine control reaction, HeLa lysate was pre-incubated with staurosporine (1 mM) at 37°C for 1 hour before the crosslinking reaction. After the reaction, the samples were boiled at 95°C for 1 minute in Laemmli sample buffer and separated on 10% SDS-PAGE gels (section 2.6.4). Total proteins were observed with SYPRO®Ruby stain (section 2.6.7). After transfer onto PVDF membranes, biotinylated proteins were visualized with Streptavidin-Cy5 (section 2.6.6), whereas PKA was observed with an antibody to PKA α catalytic subunit (Santa Cruz Biotechnology- catalog number sc-28315). Gel bands were visualized using a Typhoon imager.

2.6.14. K-CLASP procedure

For the kemptide K-CLASP study, HeLa lysates (7.5 mg/mL, 450 μ g) were incubated with ATP (12 mM) in kinase buffer at room temperature for 15 minutes to activate endogenous PKA. Then, kinase-catalyzed crosslinking was initiated by adding ATP-ArN₃ (5 mM) and N-biotin kemptide (4.1 mM) in a total volume of 60 μ L. Control reactions were performed without ATP-ArN₃ or with N-biotin mutant kemptide (4.1 mM) in the place of biotin-kemptide. For the Miz1 peptide K-CLASP study, MEF lysates (6.6

mg/mL, 400 μ g), ATP-ArN₃ (5 mM) and N-biotin Miz1 peptide (1.9 mM) were used in a total volume of 60 μ L. Control reactions were performed with N-biotin mutant Miz1 peptide (1.9mM) in the place of N-biotin Miz1 peptide and TNFalpha untreated MEF lysates (6.6 mg/mL) in the place of TNFalpha treated lysate with N-biotin Miz1 peptide (1.9mM). Crosslinking was carried out by incubating reaction mixtures at 31°C for 2 hours with shaking at 300rpm under UV irradiation at 365nm. After reaction, excess N-biotin peptide and endogenous biotin were removed by filtration using 3 KDa centiprep spin columns (Millipore). Specifically, the sample was diluted into water (total volume 400 μ L) and then spun at 12,300 rpm at 4 °C for 20 minutes. After spin, the samples were diluted again in water (total volume 400 μ L) and spun again under same conditions mentioned before. The same procedure was repeated again. After the third spin, the filtered samples were collected into clean centrifuge tubes by turning the filter upside down and spinning at 2300 rpm at 4 °C for 2 minutes. The samples were then diluted into phosphate binding buffer (total volume of 250 μ L, 0.1 M phosphate pH 7.2, 0.15 M NaCl). Streptavidin resin (250 μ L packed beads, Genscript) was washed 3 times in phosphate binding buffer. Then the samples were incubated with streptavidin resin for 20 minutes at room temperature with rotation in phosphate binding buffer. The resin was washed ten times with phosphate binding buffer (250 μ L) and then four times with water (250 μ L). Each wash was done with centrifugation at 2300 rpm at room temperature for 1 minute. The proteins were eluted by boiling in 2% SDS in water (250 μ L) for 8 minutes. The eluate was concentrated and excess SDS was partially removed by filtering using 3 KDa Centiprep spin columns. Specifically, the elution was diluted with water (final volume 400 μ L) and spun at 12, 300 rpm at room temperature for 30 minutes. Then the concentrated samples were collected

by spinning at 2.3 rpm at room temperature for 2 minutes as described before. The concentrated elution was then boiled at 95°C for 1 minute in Laemmli sample buffer and separated on 10% SDS-PAGE gels (section 2.6.4). For in gel digestion (2.6.15), gels were run halfway. Total proteins were visualized with SYPRO®Ruby stain (section 2.6.7). In kemptide K-CLASP study, PKA was visualized with an antibody to PKA α catalytic subunit (Santa Cruz Biotechnology- catalog number sc-28315,) after transfer onto PVDF membranes (section 2.6.5). Gel bands were visualized using a Typhoon imager.

2.6.15. In gel digestion

The proteins in eluate lanes from the wild type and mutant samples described in the procedure (section 2.5.10) were excised from the SYPRO®Ruby stained gel (preserved in destaining solution—section 2.6.7 for no more than two weeks at 4 °C) and in gel digested as previously described.⁸⁵ For PKA-kemptide K-CLASP study, gels from three independent trials were used, whereas for Miz1 gels from two independent replicates were used. Specifically, gels were washed twice in deionized water (~ 30 mL). Then each half run, eluate lane was sliced into four gel pieces using separate ethanol cleaned razor blades for each lane. Each gel piece was then cut into smaller pieces and transferred into 1.5 mL Eppendorf™ LoBind Microcentrifuge Tubes (Fisher Scientific). The gel pieces were then soaked in a 1:1 mixture of NH_4HCO_3 (50 mM, 150 -200 μL , volume required to submerge the gel pieces, freshly prepared in a 50 mL total volume) and acetonitrile (100%, 150-200 μL , LC-MS grade, Sigma Aldrich) for 5 minutes at room temperature. The solution was removed and then NH_4HCO_3 (50 mM, 150-200 μL) was added followed by acetonitrile (100%, 150-200 μL) after 5 minutes. The gel pieces were then left in the solution mixture for 15 minutes at room temperature. Next, the solutions

were removed and acetonitrile (100%, 150-200 μL) was added. After gel pieces became white and shrunken, the solution was removed and the gel pieces were dried under vacuum. Then a solution of TCEP (tris(2-carboxyethyl)phosphine, 150-200 μL , 50 mM in 25 mM NH_4HCO_3) was added and incubated for 10 minutes at room temperature. After removing the solution, iodoacetamide (150-200 μL , 55 mM in 50 mM NH_4HCO_3) was added to the gel pieces in dark. The tubes were wrapped in foil and incubated at room temperature for 30 minutes with shaking on a platform shaker. Next, the solution was removed and NH_4HCO_3 (50 mM, 150-200 μL) was added with acetonitrile (100%, 150-200 μL). After 5 minutes, the solution was removed and gel pieces were soaked in acetonitrile (100%, 150-200 μL) until white. The solution was then pipetted out and the gel pieces were dried under vacuum. A fresh trypsin solution (20 $\mu\text{g}/\text{mL}$ final concentration) was prepared by the sequential addition of HCl (100 μL , 1 mM) and then of NH_4HCO_3 (50 mM, 810 μL) and acetonitrile (90 μL of 100% to obtain a final concentration of 9%) to a vial of trypsin (20 μg , Sigma-Aldrich). Trypsin solution (30-50 μL) was added to the gel pieces. Then digestion buffer (2.5 fold of the trypsin volume, 40 mM NH_4HCO_3 in 9% acetonitrile in water) was added to submerge the gel pieces. After a brief spin at ~ 1000 rpm, the tubes containing the gel pieces were placed on a centrifuge tube rack and incubated at 37°C wrapped in foil. After 30 minutes, the tubes were checked to see if the gel pieces are fully submerged. If not, more digestion buffer was added as needed. Then the gel pieces were incubated at 37°C overnight. The next day, formic acid (volume required to get a final concentration of 0.1% using a 10% stock, proteomics grade, Proteochem) was added to the gel pieces. After brief vortex, the solution containing the peptides were transferred into new 0.5 mL Eppendorf™ LoBind

Microcentrifuge Tubes (Fisher Scientific). A solution of 0.1% formic acid in 50% acetonitrile (100 μ L) was added to the gel pieces. The gel pieces were then sonicated at 37°C for 10 minutes to extract any remaining peptides. The solution was then transferred to the Lobind tubes containing the tryptic-digestion. Finally, the gel pieces were shrunk by adding acetonitrile (100%, 100 μ L) and the acetonitrile solution carrying any more peptides were added to the Lobind tubes containing the tryptic-digestion. The collected peptides were then dried under vacuum. The dried peptides were stored at -20°C until submission for LC-MS/MS analysis.

2.6.16. LC-MS/MS analysis

LC-MS/MS analysis was performed by Dr. Joseph Caruso at the Proteomics core facility, Wayne State University. In Digested peptides were separated by reverse phase chromatography (Acclaim PepMap100 C18 pre-column, Acclaim PepMapRSLC C18 analytical column, Thermo) using an EASY nLC-1000 UHPLC system (Thermo). The gradient used started with 95% Buffer A (0.1% formic acid in water) in Buffer B (acetonitrile) and decreased to 95% Buffer A in 2 minutes, then to 68% Buffer A over 30 minutes. The flow rate used was 300nL/min. The peptides were ionized using a Nanospray Flex Ion Source (Proxeon Biosystems A/S) and analyzed on a Q-Exactive mass spectrometer (Thermo). MS1 profiling was carried out over a 375-1600 m/z range at a resolution of 70,000. MS2 fragmentation was performed using higher energy collision induced dissociation (HCD) on the top 15 ions using a 1.6 m/z window and normalized collision energy of 29. Dynamic exclusion was turned on (15 s). MS raw data was processed using MaxQuant (version 1.5.2.8) against a human protein database from UniProt (downloaded 2016.04.07, 20159 entries). Searches included up to 2 missed

tryptic cleavages. Mass tolerances for parent ions were 20 ppm for the first search and 4.5 ppm for the second search and 20 ppm for fragment ions. The iodoacetamide derivative of cysteine was specified as a fixed modification. Oxidation of methionine and acetylation of protein N-termini were set as variable modifications. Minimum protein and peptide identification probabilities were set at $\leq 1\%$ false discovery rate (FDR) as determined by a reversed database search and proteins required just 1 unique peptide. All other parameters were left at their default settings. Fold enrichment was calculated by dividing the peptide intensity observed for wild type crosslinking by that observed for the mutant peptide crosslinking. For the kemptide K-CLASP study, a hit list was constructed by identifying proteins with at least 2 fold enrichment in wild type crosslinked sample compared to the mutant crosslinked samples in at least two replicates. For Miz1 peptide K-CLASP study, all kinases that showed fold enrichment greater than 1 compared to both the mutant crosslinked sample and the No TNF treated lysate crosslinking samples were considered as K-CLASP hit kinases. For the rest of the proteins, a hit list was constructed by identifying proteins with at least 2 fold enrichment in wild type crosslinked sample compared to both the mutant crosslinked samples and the No TNF treated lysate crosslinking samples.

2.6.17. Interactome analysis

The known physical protein-protein interactions among the proteins identified by K-CLASP were mapped using the GeneMANIA application in Cytoscape 3.3.0.⁶⁶ Known substrates of the hit kinases K-CLASP hits were identified from Phospho Site plus and kinaseNET.⁶⁷ The identified substrates were then manually added. MCODE application was used to identify the potential cellular complexes among K-CLASP hits.

CHAPTER 3 K-BIPS (KINASE-CATALYZED BIOTINYLATION TO IDNENTIFY PHOSPHATASE SUBSTRATES)

Excerpts from this chapter have been taken from two manuscripts submitted for publication. Dedigama-Arachchige, P. M.; Chinthaka, N.; Pflum, M. K., K-BIPS, a method for phosphatase substrate identification. Dedigama-Arachchige, P. M.; Zhang, X.; Yi, Z.; Pflum, M. K., Kinase-catalyzed biotinylation reveals novel substrates of PP1-MYPT phosphatase.

Protein phosphatases are key players in cell signaling pathways with implications in human diseases. However, understanding the precise cellular functions of phosphatases has been hampered by the scarcity of tools to identify phosphatase substrates. In addition, most cellular phosphatases exist in multimeric complexes, further complicating the efforts of developing phosphatase substrate identification methods. As a solution, we developed a method called K-BIPS (Kinase-catalyzed Biotinylation to Identify Phosphatase Substrates). Chapter 3 describes the application of K-BIPS in three biological systems. First, in a proof-of-concept study, K-BIPS was used to identify the substrates of okadaic acid-sensitive phosphatases (section 3.6). Then K-BIPS was used to explore the substrates of PP1-Gadd34 (section 3.7) and PP1-MYPT1 (section 3.8) phosphatase complexes. The results from the three studies established K-BIPS as a viable tool for phosphatase substrate identification, while also uncovering previously known functions for the tested phosphatase systems.

3.1 Background

The following section details protein phosphatases and methods available for phosphatase substrate identification.

3.1.1 Protein Phosphatases

Phosphatases catalyze dephosphorylation or removal of phosphoryl groups from cellular proteins, and thus play an essential role in signal transduction in the cell (Section 1.2).⁸⁶ When phosphatase function is altered either due to inactivation or over-expression, proper cell signaling is perturbed and results in various human diseases.⁸⁷ For example, PP2A phosphatase malfunction has been reported as a cause for tumor invasiveness and metastasis.⁸⁸ In addition, the hyperactivity of PTP1B phosphatase has been linked with diabetes and obesity.⁸⁹ Consequently, phosphatases have been identified as drug targets.⁹⁰

3.1.1.1 Protein Tyr phosphatases (PTPs)

Broadly, protein phosphatases are classified into two families; Protein Tyr phosphatases (PTP) and Ser/Thr phosphatases.⁹¹ The PTP super family is further divided into two main branches: Tyr phosphatases and dual specificity phosphatases. Tyr phosphatases, as the name implies, act on phosphorylated Tyr residues and exist either as transmembrane receptors or non transmembrane proteins (Figure 3.1).⁹² Dual specificity phosphatases act on both Tyr and Ser/Thr substrates. The well-known mitogen activated protein kinase phosphatase family (MKPs) provide an example for dual specificity phosphatases.⁹³ Structure wise, PTPs contain a single subunit comprising one or more catalytic domains and regulatory domains.⁹⁴ Although the catalytic domain is conserved throughout different members of tyrosine phosphatase family, the regulatory domains generate structural diversity and dictate the activity, localization, and substrate specificity.^{92, 95} For example, the non-receptor Tyr phosphatase, PTP1B contains multiple

regulatory domains that can participate in specific protein-protein interactions and a number of post translational modifications through which its activity is regulated.⁹⁶

3.1.1.2 Ser/Thr Phosphatases

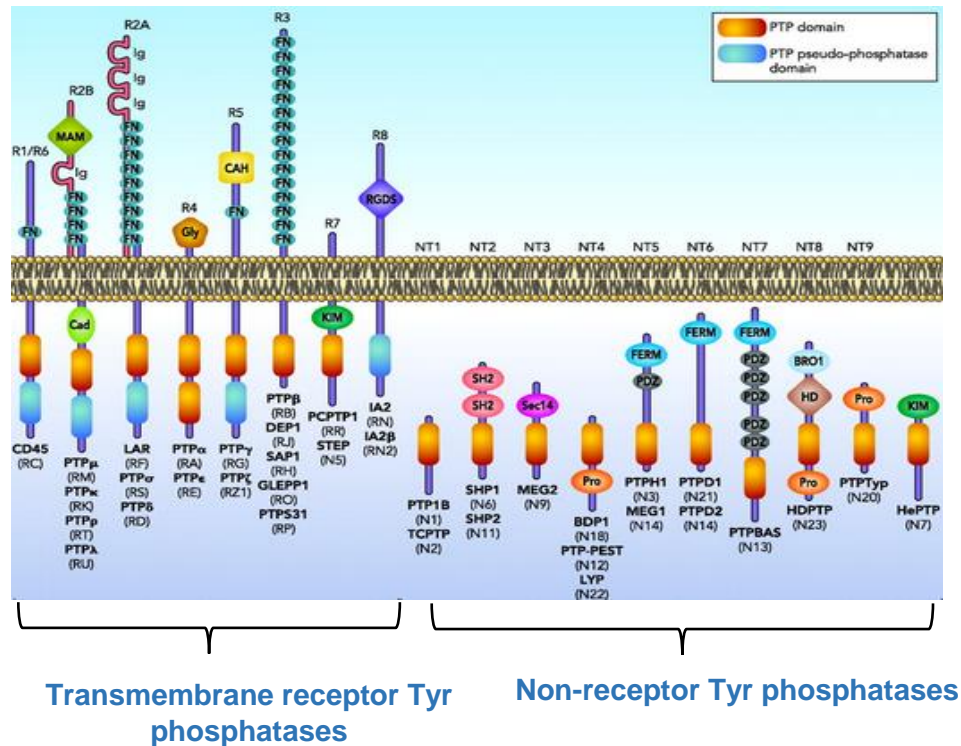


Figure 3.1: Transmembrane receptor tyrosine phosphatases and non-receptor tyrosine phosphatases. Adapted with permission from Soulsby, M.; Bennett, A. M., Physiological signaling specificity by protein tyrosine phosphatases. *Physiology* 2009, 24, 281-9.

Ser/Thr phosphatases dephosphorylate phosphorylated Ser/Thr residues and are further classified into PPP and PPM families. The PPP family consists of PP1, PP2A, PP2B, PP4, PP5, PP6 and PP7 phosphatases, while the PPM family includes PP2C phosphatase.⁹⁴ Out of these, PP1 and PP2A are most abundant and carry out more than 90% of Ser/Thr dephosphorylation in cells.⁸⁸ PPP family members are evolutionarily related and exist in multimeric complexes. For example, PP1 phosphatase comprises different phosphatase complexes composed of a common catalytic subunit and different regulatory subunits (Figure 3.2). The catalytic subunit binds the phosphorylated protein

substrate and catalyzes the dephosphorylation. The substrate specificity is governed by the assembly of different regulatory subunits with the common catalytic subunit.⁹⁷In addition to the regulatory subunit, other accessory subunits, such as adapters, also associate with the multimeric phosphatase complexes. Remarkably, it is known that more than a hundred regulatory subunits exists for PP1 alone.^{48a} PP2C phosphatase, however, is distinct from the PPP family phosphatases in that they occur as single subunit proteins containing both a catalytic domain and diverse regulatory domains.⁹⁴

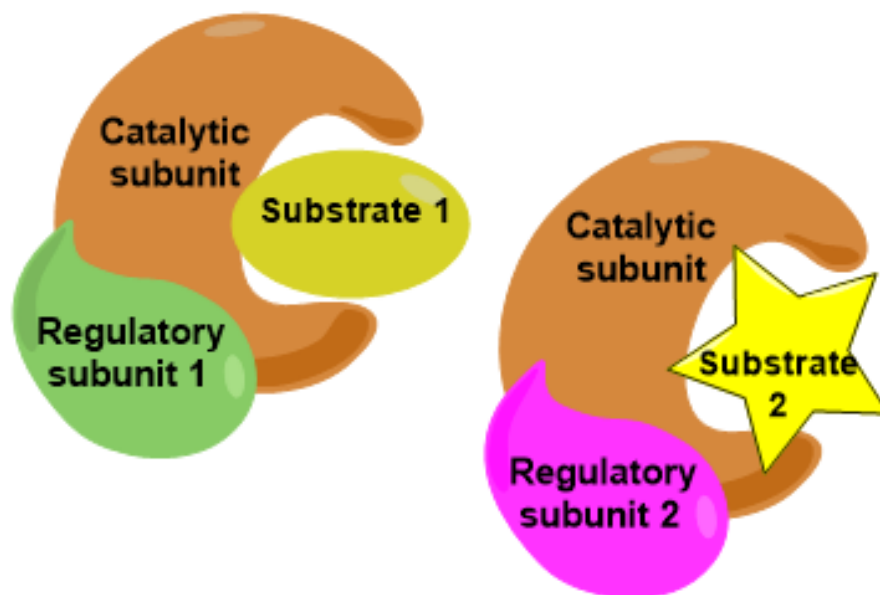


Figure 3.2: Multimeric nature of the PPP Ser/Thr phosphatase family. PPP phosphatases exist in multimeric complexes where a common catalytic subunit is shared to form different phosphatase complexes by associating with different regulatory subunits. The substrate specificity is usually determined by the regulatory subunit.

Despite the importance of phosphatases in cell signaling, research progress on phosphatase has been slow compared to the kinases. As a result, very few methods have been developed for phosphatase substrate identification. Currently available methods include substrate trapping mutants for Tyr phosphatases and phosphoproteomics studies following inactivation for Ser/Thr phosphatases, as discussed in the next sections.

3.1.2 Substrate trapping mutant strategy for phosphatase substrate identification

The substrate trapping strategy was pioneered by Tonks and colleagues for the identification of protein tyrosine phosphatases. The technique employs catalytically inactive tyrosine phosphatase mutants that bind more tightly to their phosphorylated substrates compared to the wild type phosphatase. The stabilized phosphatase-substrate complexes with mutants can be later isolated. Although most trapping mutants have been generated by mutating the catalytic Cys, other residues have also been used.⁹⁸

The first reported study of substrate trapping mutants led to the identification of EGFR as a novel substrate of PTP1B phosphatase. In this case, an Asp residue that acts as a general acid during catalysis was mutated to an Ala to produce a substrate trapping variant of PTP1B. Then the mutated PTP1B was expressed in COS cells. The cells were next treated with EGF to discover EGF sensitive PTP1B substrates. The cells were lysed, immunoprecipitated using a PTP1B antibody and the effect on tyrosine phosphorylation was monitored by Western blot. A band corresponding to the size of EGFR showed increasing tyrosine phosphorylation. Further validation experiments confirmed that EGFR is a PTP1B substrate.⁵¹

Later, the substrate trapping strategy was coupled with affinity purification and MS/MS analysis to enable the unbiased discovery of tyrosine phosphatase substrates. In an illustrative example, an Asp/Cys double mutant was used to identify the substrates of PTPN22 phosphatase. In this example, Jurkat cells were first treated with the tyrosine phosphatase inhibitor pervandate to promote phosphorylation. Then cells were lysed and recombinant PTPN22 mutant was incubated with the lysates. PTPN22 was then affinity

purified and the potential substrates co-purified were analyzed by MS/MS. The study revealed three novel and two previously known PTPN22 substrates.⁹⁹

The substrate trapping technique has been a valuable tool in producing the substrate profile of as many as 20 tyrosine phosphatases.⁹⁸ However, substrate trapping has not been used for studying Ser/Thr phosphatase. While the ability to generate trapping mutations in Ser/Thr phosphatases has not been explored, the major obstacle of using trapping for Ser/Thr phosphatases can be attributed to their multimeric nature, where the substrate specificity is dictated by regulatory subunits. In this case, trapping by the mutant phosphatase cannot distinguish substrates of different regulatory complexes.

3.1.3 Phosphoproteomics for discovery of phosphatase substrates

Although not widely reported, phosphoproteomics following phosphatase inactivation represents a possible method for looking at Ser/Thr phosphatases. A few studies have reported the use of phosphoproteomics for discovering both tyrosine and Ser/Thr phosphatase substrates. In these cases, the phosphatase of interest was inactivated and the effect on phosphorylation was studied by isolating phosphopeptides using IMAC (Immobilized metal affinity chromatography) and then MS analysis. As an example, phosphoproteomics was used to discover possible substrates of PP6 phosphatase. Here, the catalytic subunit of PP6 was silenced and phosphoproteomics was carried out. The study revealed 220 proteins with increased phosphorylation.¹⁰⁰

In another report, the *Drosophilla* tyrosine phosphatase Ptp61F was knocked down and phosphoproteomics studies were carried out. The study uncovered 288 phosphosites affected by Ptp61F knockdown.¹⁰¹ A recent study detailed the application of phosphoproteomics with the inactivation of a regulatory subunit of PP1 phosphatase. In

this study, which will be further discussed in section 3.8, the PP1 regulatory subunit, MYPT1 was knocked down. The resulting proteomics study disclosed many novel proteins as candidate PP1-MYPT1 substrates.¹⁰²

Although phosphoproteomics presents a useful tool, it has not been widely employed for discovering phosphatase substrates. One limitation of phosphoproteomics strategies is the inability to distinguish dynamic phosphorylation events from static events. Since the majority of phosphosites are non-dynamic,¹⁰²⁻¹⁰³ the detection of dynamic phosphorylation events, especially low abundance phosphosites, can be difficult with IMAC-based phosphopeptide purification. In addition, IMAC has also been shown to have a bias towards peptides with acidic residues.¹⁰⁴ Furthermore, phosphatase inactivation during phosphoproteomics may increase the phosphorylation status of some kinases, leading to increased phosphorylation of some proteins through kinase activation. In such cases, phosphoproteomics strategies are incapable of distinguishing direct phosphatase substrates from proteins indirectly affected by the inactivated phosphatase. Therefore, to provide an alternative, general method for phosphatase substrate identification, we developed a novel method based on our prior work on kinase-catalyzed ATP-biotin labeling of phosphoproteins.

3.1.4 Phosphatase activity is required for kinase-catalyzed biotinylation

Kinase cosubstrate promiscuity has allowed the usage of ATP-biotin to label phosphoproteins in complex mixtures, such as lysates. Detailed studies of ATP-biotin labeling of cellular phosphoproteins revealed that, while the phosphobiotin tag was insensitive to phosphatases, efficient biotinylation indeed required the activity of phosphatases.⁴⁴ Specifically, in prior work published by Pflum lab, 2D gel analysis of the

ATP and ATP-biotin labeling reactions were carried out with HeLa lysates with and without phosphatase inhibitors.⁴⁴ In the case of ATP, the phosphate signal (Pro-Q-Diamond Stain) was increased in the presence of phosphatase inhibition (Figure 3.3A, compare boxed regions), indicating increased phosphorylation. However, for ATP-biotin labeling, the biotin signal (Streptavidin-Cy5) was reduced when the lysate was treated with phosphatase inhibitors (Figure 3.3B, compare boxed regions), suggesting that the activity of phosphatases is required for biotinylation. Based on the observation that phosphatases are required for efficient biotinylation, we developed a novel method for phosphatase substrate identification called K-BIPS.

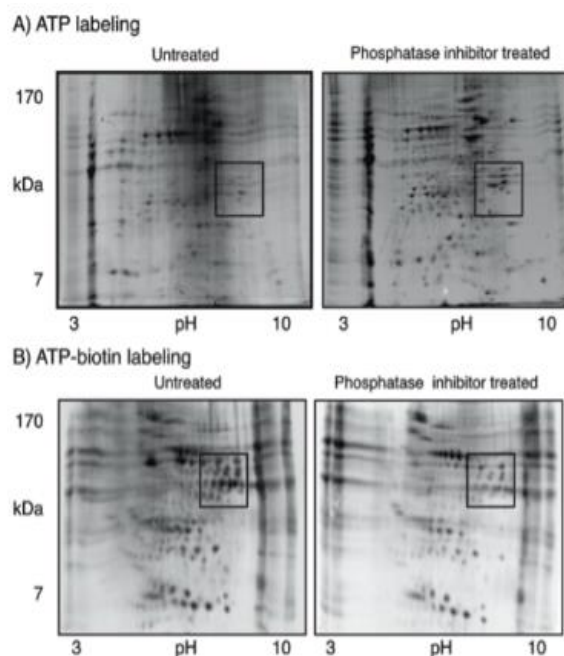


Figure 3.3: ATP-biotin labeling requires phosphatases. 2D gel analysis of HeLa lysate phosphobiotinylation with and without phosphatase inhibitor treatment.³⁰ Boxed region highlights changes in ATP and ATP-biotin labeling with and without phosphatase inhibitor treatment. Senevirathne, C.; Pflum, M. K., Biotinylated phosphoproteins from kinase-catalyzed biotinylation are stable to phosphatases: implications for phosphoproteomics. *Chembiochem* 2013, 14 (3), 381-7. Copyright Wiley-VCH Verlag GmbH & Co. KGaA. Reproduced with permission.

3.1.5 The K-BIPS strategy

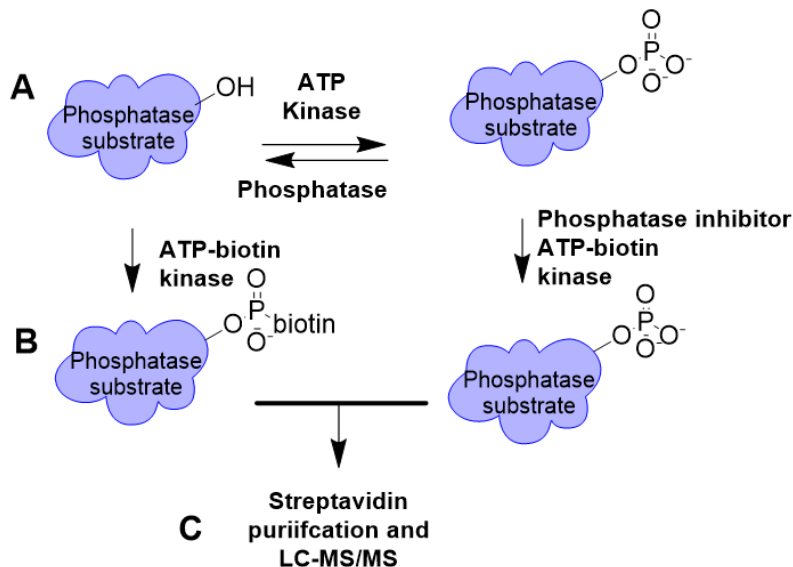


Figure 3.4: The K-BIPS method. (A) A phosphatase removes phosphate groups from its substrate (blue). When the particular phosphatase is inactivated, its substrate is maintained in the phosphorylated form. (B) When biotinylation is carried out, the dephosphorylated substrate is biotinylated, while the phosphorylated substrate is prevented from biotinylation. (C) The biotinylated proteins are then purified from both samples and analyzed by LC-MS/MS to reveal the proteins that showed reduced biotinylation in the phosphatase-inactivated sample.

To provide an alternative tool for the discovery of phosphatase substrates, we developed a new method called K-BIPS (Kinase-catalyzed Biotinylation to Identify Phosphatases Substrates). We reasoned that phosphate groups present on cellular proteins have to be removed in order for biotinylation to occur (Figure 3.3A). Therefore, in K-BIPS, biotinylation is carried out with ATP-biotin in lysates with and without inactivating a phosphatase of interest (Figure 3.3B). In the phosphatase-inactivated sample, the substrates of the inactivated phosphatase will remain phosphorylated and will be immune to biotinylation. Therefore, phosphatase substrates will be less biotinylated in the phosphatase-inactive sample compared to the phosphatase-active sample. Then, the biotinylated proteins are purified by streptavidin resin and analyzed by

liquid chromatography tandem mass spectrometry (LC-MS/MS, Figure 3.3C). Finally, the candidate substrates of the inactivated phosphatase can be identified by detecting the proteins that showed a loss in biotinylation in the phosphatase-inactive sample. Further validation studies must then be carried out to confirm the identified proteins as the substrates of a particular phosphatase.

To establish K-BIPS as a viable method for the identification of phosphatase substrates, we used K-BIPS with three Ser/Thr phosphatase systems. Although K-BIPS is amenable to both Tyr and Ser/Thr phosphatases, we specifically selected Ser/Thr phosphatases due to the fact that Ser/Thr phosphatases are less studied than Tyr phosphatases. In the first study, we used the general phosphatase inhibitor okadaic acid to inactivate a majority of PPP family phosphatases and used K-BIPS in a proof-of-concept experiment (section 3.2.1). Then in a discovery approach, we used K-BIPS to explore possible substrates of PP1-Gadd34 complex in the context of unfolded protein response (section 3.2.2). Finally, in a collaboration project with Dr.Zhengping Yi at College of Pharmacy and Health Sciences at Wayne State University, we used K-BIPS to uncover novel substrates of PP1-MYPT1 system (3.2.3).

3.2 Results

3.2.1 K-BIPS using okadaic acid mediated phosphatase inactivation

As a proof of concept study to demonstrate that K-BIPS is a feasible method, the well-known phosphatase inhibitor okadaic acid (OA) was used. OA is a broad phosphatase inhibitor that inhibits a majority of the PPP family phosphatases, including PP1 and PP2A.¹⁰⁵ Given that PP1 and PP2A phosphatases have a large number of known substrates, K-BIPS with OA will serve as a validation method for the feasibility of

K-BIPS for phosphatase substrate identification. Specifically, by comparing known substrates of PPP phosphatases with the substrates identified by K-BIPS, the viability of our method can be determined. In addition, unknown substrates of PPP family phosphatases can also be identified.

3.2.1.1 K-BIPS with OA-mediated phosphatase inhibition

To show that K-BIPS is a viable method for phosphatase substrate identification, we inhibited cellular phosphatases with OA and probed the levels of biotinylation by streptavidin purification after treatment with ATP-biotin. OA inhibits PP2A, PP4, PP5 and PP6 at a concentration of 1-2 nM, while PP1 is inhibited at around 1 μ M.¹⁰⁶ We carried out K-BIPS with OA treatment in HeLa lysates. HeLa cells were untreated or treated with OA at either 10 nM or 1 μ M concentrations to differentially influence PP2A and PP1. After cell lysis, biotinylation was carried out by incubating each lysate sample with ATP-biotin either in the absence or the presence of OA to keep the phosphatases activity consistent. The biotinylated proteins were then purified by streptavidin resin and separated by gel. The amounts of protein eluted were visualized using Sypro®Ruby total protein stain. As expected, reduced protein levels were observed in the elution of OA-treated compared to untreated lysates (Figure 3.5 and B.1, compare lanes 4, 5, 6), confirming that inactivation of phosphatases results in less biotinylation. As anticipated, the sample treated with 1 μ M OA showed the most reduction (Figure 3.5 and B.1, compare lane 4 to 5 and 6). The results confirmed that efficient biotinylation requires the activity of phosphatases, and inactivation of phosphatases leads to a reduction in biotinylation.

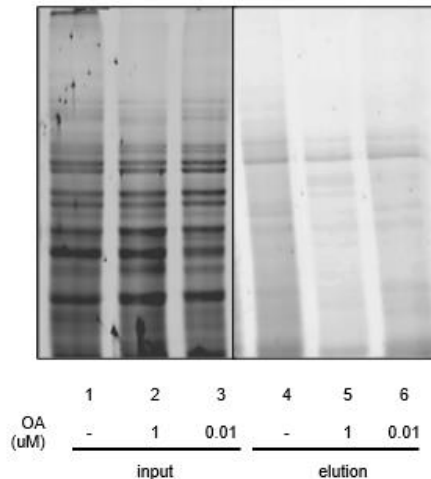


Figure 3.5: K-BIPS study with OA. Streptavidin purification of biotinylated proteins after kinase-catalyzed biotinylation. Biotinylation was carried out with lysates from cells treated with (1 μM or 10 nM) or without OA (input in lanes 1-3). After reaction, biotinylated proteins were enriched (elution in lanes 4-6), separated by SDS-PAGE, and stained for total proteins using SYPRO® Ruby stain. Replicates are shown in Figure B.1.

To identify the substrates of phosphatases inhibited by OA, we next performed LC-MS/MS analysis after in-gel digesting the proteins eluted from 1 μM OA-treated and untreated samples (Figure 3.5, lanes 4 and 5). TMT (Tandem mass tag™)-based quantitation was used to select proteins enriched by at least 1.5-fold in the phosphatase-active compared to the OA-treated sample. K-BIPS identified 71 proteins as hits (Table B.1).

A literature search revealed that 15 proteins from the K-BIPS hits (21% of hits, Table 3.1, Table B.1-green colored rows) are known PP1 or PP2A substrates, showing that K-BIPS is capable of discovering known phosphatase substrates. In addition, 18 of the remaining proteins (25% of the hits, Table 3.2, Table B.1-blue colored rows) were known interactors of PP1, PP2A, PP4, PP5 and PP6 catalytic subunits or their regulatory subunits. In fact, most of the known substrates also directly interact with the catalytic or

regulatory subunits (Table 3.1, Table B1-green colored rows). Therefore, the 18 K-BIPS hits known to interact with the inactivated phosphatases (Table 3.2) are also likely substrates. Overall, 46% from the K-BIPS hits were either known substrates or had known interactions with the inhibited phosphatase complexes.

Table 3.1: Known phosphatase substrates among the K-BIPS hits from OA-mediated phosphatase inactivation^a

Protein	Gene	Substrate of	Interactions	
			Catalytic subunits	Regulatory subunits
Structural maintenance of chromosomes protein 1A ¹⁰⁷	SMC1A	PP1 or PP2A		
Eukaryotic translation initiation factor 2 subunit 1 ¹⁰⁸	EIF2S1	PP1	PPP1CC	PPP1R7
Tubulin beta chain ¹⁰⁹	TUBB	PP1 or PP2A	PPP1CC	PPP2R2A
60 kDa heat shock protein, mitochondrial ¹¹⁰	HSPD1	PP2A		PPP2R1B PPP2R1A PPP2R2C
Nucleolin ¹¹¹	NCL	PP1 or PP2A	PPP1CB	RRP1B
Ezrin ¹¹²	EZR	PP1		
Voltage-dependent anion-selective channel protein 1 ¹¹³	VDAC1	PP2A		
DNA replication licensing factor MCM3 ¹¹⁴	MCM3	PP2A		PPP2R1B PPP2R1A
HORMA domain-containing protein 1 ¹¹⁵	HORMAD1	PP1		
Brefeldin A-inhibited guanine nucleotide-exchange protein 2 ¹¹⁶	ARFGEF2	PP1 and PP2A		
Ryanodine receptor 2 ¹¹⁷	RYR2	PP1 or PP2A	PPP1CA PPP1CB PPP1CC PPP2CA	
Elongation factor 2 ¹¹⁸	EEF2	PP2A	PPP2CA	PPP2R1B PPP2R1A PPP2R2B
Moesin ¹¹⁹	MSN	PP1		PPP1R2
Calreticulin ¹²⁰	CALR	PP2A		
Pyruvate kinase PKM ¹²¹	PKM	PP1	PPP1CA	

^aThe primary literature demonstrating the K-BIPS hits as known phosphatase substrates is cited. The interaction information was obtained from Uniprot and BioGrid databases.¹²² The gene names of phosphatase catalytic and regulatory subunits are shown. For example, PPP1CA refers to PP1 alpha isoform of catalytic subunit whereas PPP2CA refers to PP2A alpha isoform of catalytic subunit. PPP1R7 refers to Regulatory subunit 7 of PP1.

The identification of K-BIPS hits, PCNA (Table 3.2, Table B1 entry #22) and LDHA (Table B1, entry #40) further supported the conclusion that K-BIPS discovered proteins that are potential phosphatase substrates. In addition to being a known interacting protein of PP2A (Table 3.2, Table B1 entry #22), the nuclear transport of PCNA has been shown to be inhibited by OA and regulated by a PP2A-mediated mechanism.¹²³ The observation of PCNA among the K-BIPS hits suggests that PCNA may be a PP2A substrate and PP2A may dephosphorylate PCNA to effect nuclear transport. Further, the K-BIPS hit, LDHA (Table B1, entry #40) could also be a possible PP2A substrate as the knock down of CIP2A, the endogenous inhibitor of PP2A, is known to reduce LDHA activity.¹²⁴ Functional analysis using Gene Ontology¹²⁵ revealed that K-BIPS hits belonged to diverse functions, such as metabolism, cellular processes and localization (Figure 3.6), consistent with the wide spectrum of biological roles associated with phosphatases.¹²⁶ Finally, to dismiss the possibility that K-BIPS hits were identified due to their high abundance, the abundance of the K-BIPS hits were also analyzed by using previously reported values.⁶⁵ The results showed that proteins with low abundance were identified (Figure 3.7), demonstrating that K-BIPS is not abundance dependent. Overall, the results confirm that K-BIPS identified phosphatase substrates.

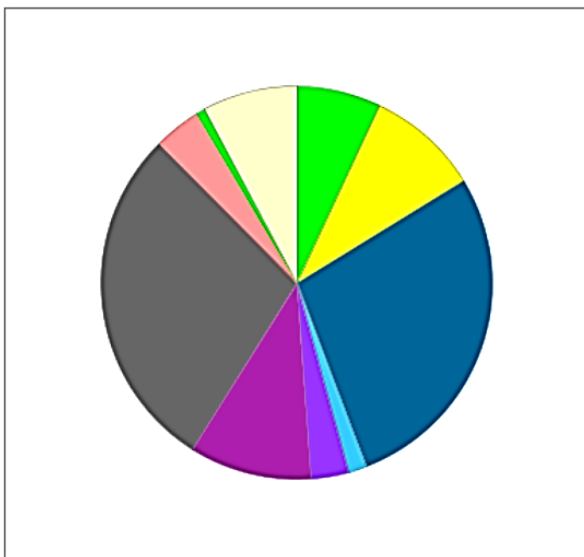
Table 3.2: K-BIPS hits from the OA-mediated phosphatase inactivation that are not known substrates, but known to interact with phosphatase^a

Protein	Gene	Known interactions	
		Catalytic Subunits	Regulatory Subunits
Complement component 1 Q subcomponent-binding protein, mitochondrial	C1QBP		PPP2R1A RRP1B PPP2R2A
Translational activator GCN1	GCN1L1		PPP6R1
Heat shock protein HSP 90-beta	HSP90AB1	PPP5C	PPP6R3
Eukaryotic initiation factor 4A-III	EIF4A3		PPP6R3

ATP-dependent RNA helicase DDX1	DDX1	PPP1CA	PPP1R8
HLA class I histocompatibility antigen, B-59 alpha chain	HLA-B	PPP2CB	PPP1R16A
ATP-dependent RNA helicase A	DHX9	PPP1CB	
Proliferating cell nuclear antigen	PCNA	PPP1CA PPP1CC	PP2A
Exostosin-like 3	EXTL3		PPP6R2
Endoplasmin ¹²⁷	HSP90B1	PPP5C	
Calnexin	CANX		PPP2R1A
Ral GTPase-activating protein subunit alpha-1	RALGAPA1		RRP1B
Importin subunit beta-1 ¹²⁸	KPNB1	PPP2CA	PPP2R2A
Trifunctional enzyme subunit alpha, mitochondrial	HADHA		PPP6R1
CAD protein	CAD	PPP1CA PPP2CA	
Trifunctional enzyme subunit beta, mitochondrial	HADHB		PPP6R1
60S ribosomal protein L27 ¹²⁹	RPL27	PPP1CC	REPOMAN
Protein PML ¹³⁰	PML	PPP1CA	

^aExcept when cited, the information on interactions were obtained from Uniprot and BioGrid database.¹²²Gene names are shown in the "Interactions" column.

Select Ontology: View:
PANTHER GO-Slim Biological Process
 Total # Genes: 79 Total # process hits: 129



Click to get gene list for a category:

- [biological regulation \(GO:0065007\)](#)
- [cellular component organization or biogenesis \(GO:0071840\)](#)
- [cellular process \(GO:0009987\)](#)
- [developmental process \(GO:0032502\)](#)
- [immune system process \(GO:0002376\)](#)
- [localization \(GO:0051179\)](#)
- [metabolic process \(GO:0008152\)](#)
- [multicellular organismal process \(GO:0032501\)](#)
- [reproduction \(GO:0000003\)](#)
- [response to stimulus \(GO:0050896\)](#)

Color picker powered by Web Colors by VisiBone

**Chart tooltips are read as: Category name (Accession): # genes; Percent of gene hit against total # genes; Percent of gene hit against total # Process hits

Figure 3.6: Functional classification of the proteins identified by the K-BIPS study with OA. The proteins were classified based on their biological processes by the enrichment analysis tool available on Gene Ontology Consortium.

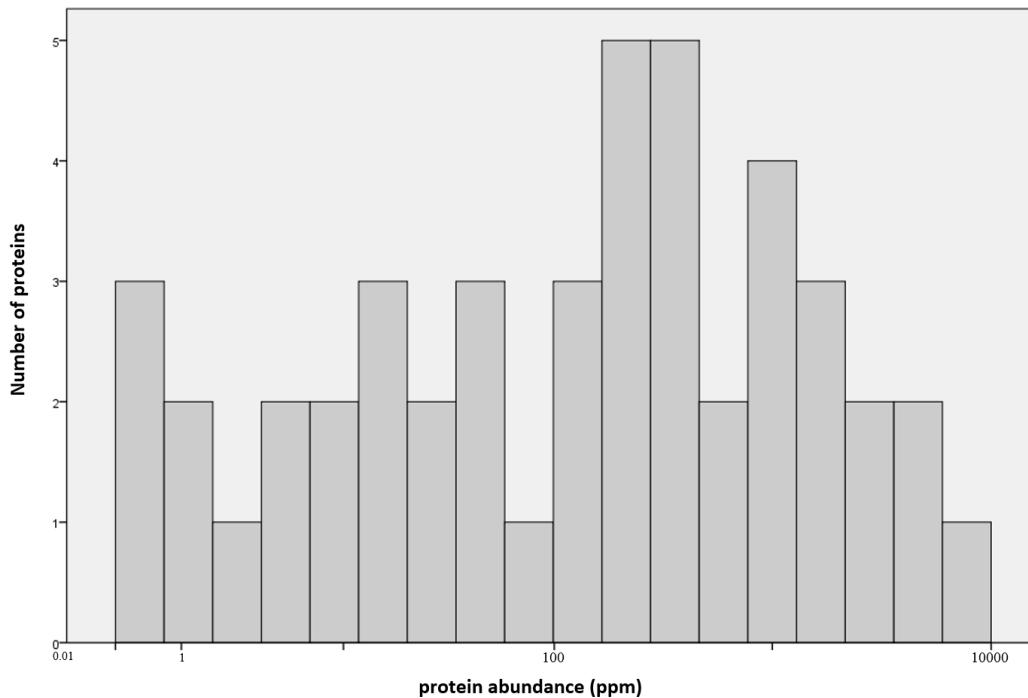


Figure 3.7: The analysis of abundance of hits from the K-BIPS study with OA-mediated phosphatase inactivation. Proteins with a range of abundance values (0.01-8785ppm) were identified by K-BIPS from HeLa cells which carries proteins with abundances ranging from 0.01 to 10,000. The abundance data was obtained from previously published values⁶⁵ available on Pax database.¹³¹

In summary, K-BIPS was carried out after inactivating phosphatases with OA. While gel-based experiments confirmed that phosphatase activity is necessary for efficient biotinylation, proteomics studies revealed both known phosphatase substrates and proteins that are potential phosphatase substrates. Together, the study with OA showed that K-BIPS is an applicable method for phosphatase substrates identification.

3.2.2: K-BIPS for PP1-Gadd34 substrate identification

Having established that K-BIPS is a viable strategy for phosphatase substrate identification, we used K-BIPS to discover potential substrates of the PP1-Gadd34 phosphatase complex. Gadd34 (PPP1R15A) is a regulatory subunit of PP1 that plays a key role during unfolded protein response (UPR).^{108, 132} UPR is induced when cells are

faced with various insults that disrupt correct protein folding. As a result, misfolded proteins accumulate in the ER (endoplasmic reticulum) causing ER stress. Consequently, ER stress triggers the activation of three main stress sensors in the cell, IRE1 α , PERK and ATF6, to induce a cascade of downstream pathways in the UPR. In a bid to restore cellular protein homeostasis and save the cell from apoptosis, UPR promotes the expression of a series of proteins involved in various restorative processes, such as protein folding, protein degradation, and apoptosis suppression. In addition, through PERK-mediated phosphorylation of the translation initiation factor EIF2 α , UPR also blocks the synthesis of new proteins by stalling translation and allowing the cell to recover from stress. As cells rebound from stress, Gadd34 is induced in a feedback loop. The PP1-Gadd34 complex acts to dephosphorylate EIF2 α and remove the block on translation.¹³²⁻¹³³ Thus PP1-Gadd34 functions a key modulator of UPR and has been implicated in various neurodegenerative diseases, cancer and viral infections.^{17, 133b, 134} Despite being a feedback regulator of UPR, surprisingly, the only known UPR-involved PP1-Gadd34 substrate is EIF2 α .

Given the disease relevance of the PP1-Gadd34 phosphatase, we aimed to use K-BIPS to explore unknown substrates of PP1-Gadd34 in the context of the UPR. To inhibit the PP1-Gadd34 complex for K-BIS-Phos, we used the small molecule guanabenz (Gb), which was reported to inactivate the PP1-Gadd34 complex by disrupting the binding of Gadd34 with the PP1 catalytic subunit.¹³⁵ To create the conditions to promote UPR, we also used the known ER stressor tunicmycin (Tm).¹³⁵

3.2.2.1: Inactivation of PP1-Gadd34 system leads to a loss in biotinylation

As a first step, we tested if inactivation of the PP1-Gadd34 complex by Gb leads to a reduction in biotinylation of cellular proteins. We treated HeLa cells with or without Gb to inactivate PP1-Gadd34. Since our goal was to identify the PP1-Gadd34 substrates in the context of UPR, cells were also simultaneously stressed with Tm. Then, cells were lysed and the expression of Gadd34 was monitored by Western blot. The results showed that Gb treatment did not affect Gadd34 expression (Figure 3.8, compare lanes 2 & 3).

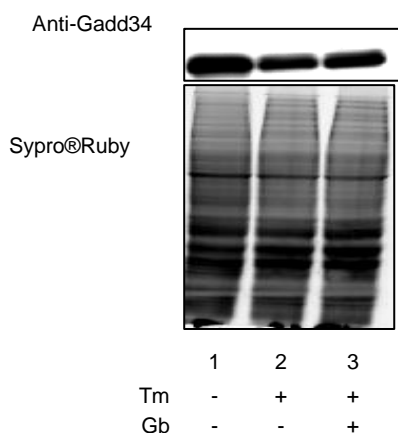


Figure 3.8: Expression of Gadd34 in HeLa lysates treated with Tm and Gb. Gadd34 expression was probed with Western blot (Top gel) in untreated cells (Lane 1), cells treated with only Tm (Lane 2) and cell treated with both Tm and Gb (Lane 3). The bottom Sypro-Ruby stained gel shows equal protein loading. Replicates and full gel images shown in Figure B.2.

Biotinylation was next carried out by incubating treated lysates with ATP-biotin. For the Gb treated samples, Gb was also added to the lysates to maintain the PP1-Gadd34 complex in a dissociated state during biotinylation. After reaction, cellular proteins were separated by SDS-PAGE, transferred to a membrane, and then probed with streptavidin-cy5 to detect biotinylation. A reduction in biotinylation was observed in the Gb-treated lysate compared to the untreated lysate (Figure 3.9, Compare bracketed region and

regions pointed by arrow in lanes 2 & 3), consistent with the expectation that inactivation of PP1-Gadd34 leads to loss of biotinylation.

3.2.2.2: K-BIPS with PP1-Gadd34 inactivated lysates

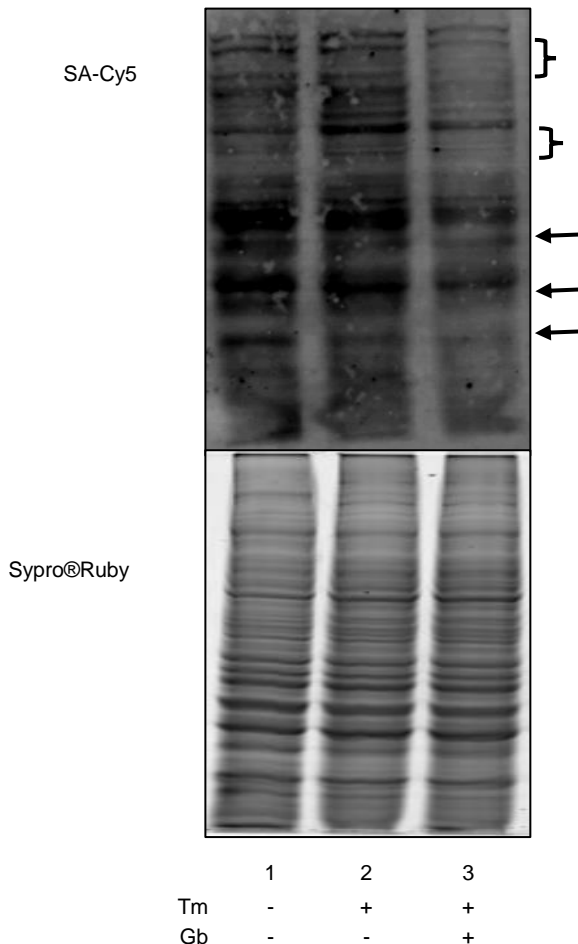


Figure 3.9: Biotinylation with PP1-Gadd34 inactivated lysates. Biotinylation was carried out with ATP-biotin and PP1-Gadd34 active and inactive HeLa lysates. A Control reaction was also carried out with HeLa lysates untreated with both Tm and Gb. After biotinylation, proteins were separated on SDS-PAGE and visualized with Streptavidin-Cy5 (Top) and SyproRuby (bottom). Replicates shown in Figure B.3.

To perform a full K-BIPS experiment and identify UPR-implicated PP1-Gadd34 substrates, biotinylated proteins obtained from UPR-induced lysates treated with or without Gb were purified with streptavidin resin. The purified proteins were then separated by SDS-PAGE (Figure B.4) and analyzed by LC-MS/MS. After analysis with label free

quantitation, 130 proteins (Table B2) reproducibly enriched by at least 1.3-fold in the untreated versus the Gb-treated sample were identified as PP1-Gadd34 candidate substrates. Importantly, the known PP1-Gadd34 substrate, EIF2 α (EIF2S1, Table 3.3, Table B.2, green colored) was among the enriched proteins (Table 3.3), confirming the ability of K-BIPS to discover PP1-Gadd34 substrates. In addition to EIF2 α , three other proteins involved in translation initiation¹³⁶ (EIF4G3, EIF3M and EIF3G, Table B2) were also observed among the enriched proteins, consistent with the role of PP1-Gadd34 in translation. Further, ribosomal proteins RPS12, RPL10A, RPL26L1 and RPLP0 (Table B2) were also among the enriched proteins. Additionally, several K-BIPS identified proteins were known interactors of either the catalytic subunit of PP1 or Gadd34 (Table 3.3) and hence possible substrates. Overall, the results suggest that K-BIPS revealed new candidate PP1-Gadd34 substrates.

Table 3.3: PP1 and Gadd34 interacting proteins among K-BIPS hits^a

Protein (Gene name)	Fold Enrichment		Interactions
	Trial 1	Trial 2	
EIF2 α	2.4	2.3	PPP1CC,GADD34
CTBP2	4.9	∞	GADD34
MAPK1	2.9	∞	PPP1CA,PPP1CC
PPP2R4	∞	2.5	PPP1CA
MYO18A	2.0	∞	PPP1CB
SYNCRIP	∞	1.8	PPP1CA
WDR5	∞	1.4	PPP1CB
COPS5	∞	1.3	PPP1CC, GADD34
UBE2Z	18.4	3.0	PPP1CA
PPA1	15.2	1.6	PPP1CC
NACA	10.1	1.3	PPP1CC
PRKAR2A	6.0	1.3	PPP1CB
SFPQ	3.3	1.3	PPP1CA
PRKAR1A	3.2	1.3	PPP1CA

^aFold enrichment was calculated by dividing the peptide intensity in the Gb-untreated sample by that of the treated sample. Fold enrichment of infinity (∞) was observed when the protein was identified only in the Gb-untreated sample. Interaction information was obtained from Uniprot and BioGrid databases.¹²²

To verify that the identification of the 130 K-BIPS hits was not abundance dependent, we performed an abundance analysis using reported values.⁶⁵ The data showed that K-BIPS hits belonged to a range of abundance (Figure 3.10), indicating that abundance was not a factor for K-BIPS identification. Then we carried out a literature search to see if the K-BIPS hits have biological functions related to PP1-Gadd34. In fact, many K-BIPS hits had known roles in UPR, ER stress and stress granules (Table 3.4), confirming that K-BIPS discovered likely PP1-Gadd34 substrates.

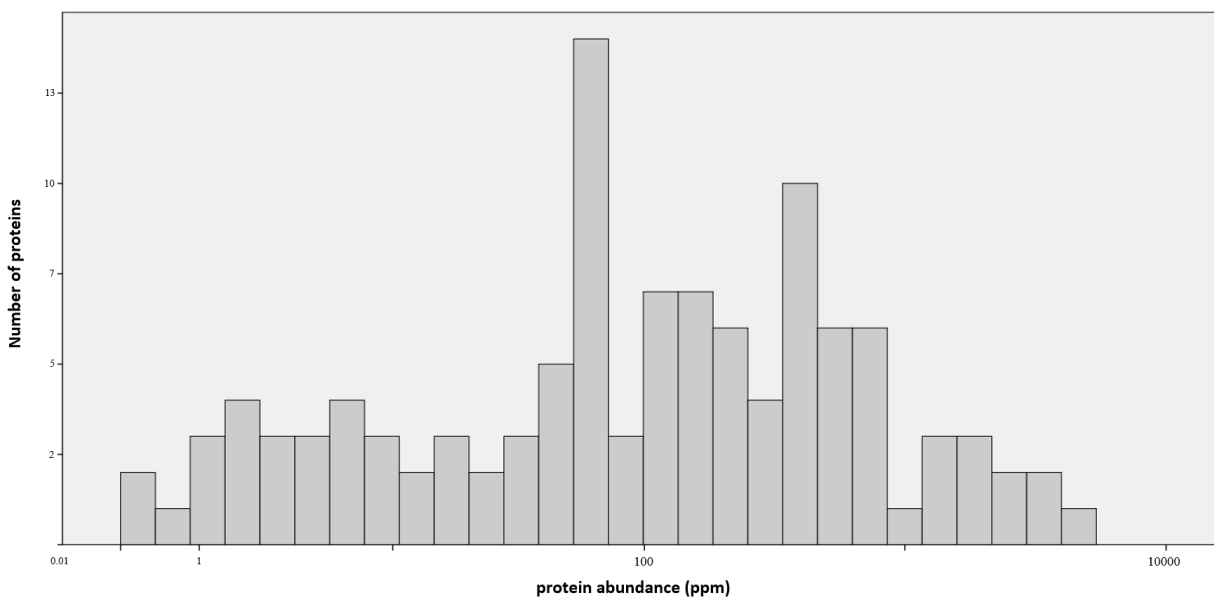


Figure 3.10: The abundance of proteins identified from the K-BIPS study with PP1-Gadd34 inactivation. K-BIPS identified proteins with a range of abundance (0.02-5188). The reported range of abundance in HeLa cells is from 0.01 to 10,000. The abundance values were obtained from previous data⁶⁵ deposited on Pax database.¹³¹

To further validate the K-BIPS results, we selected a few hits that are known to have cellular functions similar to that of Gadd34, but have not been previously identified as PP1-Gadd34 substrates. Specifically, the K-BIPS hits, COPS5 and WDR5 represented strong candidates to be PP1-Gadd34 substrates. Besides being known interacting proteins of PP1 (Table 3.3), COPS5 and WDR5 also had known roles in UPR¹³⁷ (Table

3.4). In addition, COPS5 was also known to associate with Gadd34 (Table 3.3). Therefore, COPS5 and WDR5 were picked for further validation. In addition, the K-BIPS hits, CAPRIN1 and G3BP1 were also selected. Both CAPRIN1 and G3BP1 were known to be involved in the formation of stress granules¹³⁸(Table 3.4), a downstream event in the UPR cascade. In fact, K-BIPS identified several stress granule proteins, suggesting an unprecedented role for PP1-Gadd34 in stress granule formation. Therefore CAPRIN1 and WDR5 were also selected for validation experiments.

Table 3.4: K-BIPS hits with biological function related to PP1-Gadd34^a

Associated with	K-BIPS hits
UPR	COPS5,DNAJB11,ATP6V0D1,WDR5,CSNK2A3,EIF2S1,FKBP10
ER stress	ERLIN1,ITPR1,RELA,CAPN2,RNF213,IDH3A,HM13,PSMC2,UBQLN2,PDIA6,PSMC3,MAPK1
Stress granules	CAPRIN1,TIAL1,IGF2BP3,G3BP1,FXR1
Oxidative stress	PRDX4,PGAM1

^aInformation on function was obtained from Uniprot.

For secondary validation of K-BIPS results, we checked the differential biotinylation of COPS5, WDR5, CAPRIN1 and G3BP1 by gel methods. Specifically, proteins from untreated and Gb-treated lysates were biotinylated using ATP-biotin. Then the biotin-labeled proteins were purified by streptavidin resin and separated on SDS-PAGE. After transfer of the proteins onto a membrane, the levels of each protein was checked by Western blot. The results showed reproducible loss in all selected proteins in the Gb-treated sample compared to the untreated sample (Figure 3.11, compare lanes 3 and 4), confirming that PP1-Gadd34 affects phosphorylation of the selected proteins. Notably, the validation of COPS5 and WDR5, which showed only modest enrichment in the proteomics experiment (Table 3.3, fold enrichment 1.3 and 1.4 respectively), also rationalized the 1.3-fold threshold enrichment used for K-BIPS hit selection. Importantly,

the data also showed that the levels of tested proteins in lysates were equal in the samples treated with and without Gb (Figure 3.11, compare lanes 1 and 2), verifying that the changes in biotinylation was not due to Gb-mediated differences in expression. Altogether, the results validate COPS5, WDR5, CAPRIN1 and G3BP1 as previously unknown PP1-Gadd34 substrates and establish K-BIPS as a method for phosphatase substrate identification.

3.2.2.3 K-BIPS exposed novel roles of PP1-Gadd34 in UPR

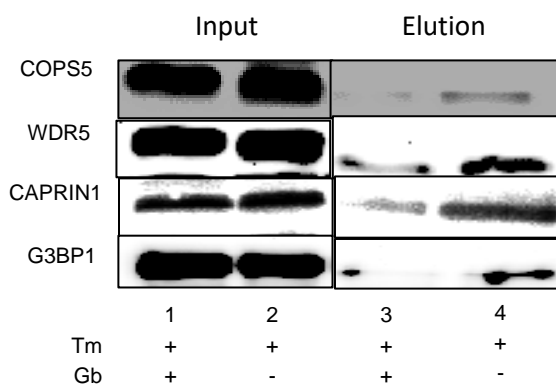


Figure 3.11: Secondary validation of COPS5, WDR5, CAPRIN1 and G3BP1. Biotinylation was carried out with ATP-biotin and PP1-Gadd34 active and inactive HeLa lysates. Biotin tagged proteins were enriched by streptavidin and probed by Western blot after separated on SDS-PAGE. Replicates shown in figures B.5-B.8.

The use of K-BIPS with PP1-Gadd34 inactivation resulted in the enrichment of many candidate UPR-related PP1-Gadd34 substrates. Notably, K-BIPS with Gb identified the known PP1-Gadd34 substrate EIF2 α . In addition, many other UPR related proteins were also observed. Among these were chaperone proteins, such as PDIA6, FKBP10 and DNABJ11, which assist in protein refolding during UPR. Another chaperone enriched was DNAJA1, though it was not previously known to be involved in UPR. The E3 ligase RNF213 is known to play a role in ER stress and was also observed. RNF213 may ubiquitinate misfolded proteins to facilitate their degradation. Although not previously implicated in UPR, another E3 ligase UBE3A and the E2 ubiquitin conjugating enzyme

UBE2Z were also among the enriched proteins. Additionally, the UPR-associated protein UBQLN2, which is thought to mediate the transfer of ubiquitinated proteins from the ER to the cytosolic proteasome complex for degradation, was also among the enriched proteins. The discovery of UPR-related proteins by K-BIPS validates that the identified hits are likely to be PP1-Gadd34 substrates. In addition, the data also suggest that PP1-Gadd34 may be involved in other UPR-related functions besides EIF2 α dephosphorylation.

Cellular stress conditions that cause the stalling of translation, such as Tm treatment, are also known to cause the formation of cytoplasmic bodies called stress granules in cells. Stress granules contain transient aggregates of mRNA and translation pre-initiation complexes, and allow the rapid recovery of translation once the stress is resolved.¹³⁹ Overexpression of Gadd34 has been shown to reduce the formation of stress granules under conditions that otherwise promote stress granule formation, suggesting a role for Gadd34 in the dissociating of stress granules. In agreement, treatment with Gb was also shown to increase the formation of stress granules.¹⁴⁰ Interestingly, several stress granule proteins, such as TIAL1,^{139b} G3BP1, CAPRIN1,¹³⁸ FMR1, FXR1^{139b} and IGF2BP3,¹⁴¹ were identified by K-BIPS. Importantly, both CAPRIN1 and G3BP1 were further validated by gel methods. Overall the K-BIPS data suggests a model where Gadd34 may regulate stress granule assembly as cells recover from stress by affecting their phosphorylation status.

UPR is a tightly regulated process that culminates in either cell survival or cell death depending on the severity of the stress.¹⁴² A recent study reported crosstalk between UPR and Hippo pathway. The pro-apoptotic Hippo pathway promotes the

phosphorylation of the transcriptional coactivator YAP1 and blocks its nuclear translocation, suppressing the proliferative activities of YAP1. Expression of Gadd34 was previously shown to correlate with increased phosphorylation and cytoplasmic retention of YAP1 under Tm treatment, suggesting a link between UPR and Hippo pathways.¹⁴³ Notably, the Hippo pathway kinase STK3 (MST2), which promote phosphorylation of Yap1 through LATS kinase, was one of the K-BIPS hits. The identification of STK3 by K-BIPS suggests a possible mechanism where Gadd34 may indirectly affect the phosphorylation of YAP1 through dephosphorylation of STK3. The crosstalk between UPR and the pro-apoptotic Hippo pathway may represent a regulatory mechanism through which the balance between cell survival and cell death under cell stress conditions is determined. Beyond the Hippo pathway, STK3 is known to interact with the scaffolding protein SLC9A3R1, which in turn associates with PKA through cytoplasmic proteins EZR and RDX.¹⁴⁴ Interestingly, K-BIPS also identified SLC9A3R1 and PKA regulatory subunits, PRKAR1A and PRKAR2A, suggesting connections between the Hippo pathway and PKA signaling during UPR.

The Gadd34 interacting protein COPS5 (JAB1) identified by K-BIPS is both a transcriptional coactivator and a component of the COP9 signalosome. COPS5 is known to regulate key cellular processes, such as cell proliferation, apoptosis and cell cycle arrest.¹⁴⁵ COPS5 plays a role in ER stress through association with the ER stress modulating protein IRE1 α . COPS5 interacts with IRE1 α under normal conditions, but dissociates when ER stress is induced. The dissociation of COPS5 was shown to be necessary for the downstream activation of IRE1 α during UPR.^{137b} Importantly, validation experiments further confirmed that PP1-Gadd34 affects COPS5 phosphorylation. The

identification of COPS5 as a likely substrate of PP1-Gadd34 hints of a possible mechanism where reversible phosphorylation may mediate the role of COPS5 during UPR. Phosphorylation may regulate IRE1 α binding of COPS5 under ER stress conditions, controlling both activation of IRE1 α and COPS5 activities in UPR. Once the UPR is resolved, Gadd34 may dephosphorylate COPS5 and allow association of COPS5 with IRE1 α restoring regular cellular processes.

Overall, the K-BIPS study with Gb revealed many potential proteins that could be substrates of PP1-Gadd34. Notably, K-BIPS identified the known PP1-Gadd34 substrate, EIF2 α and several proteins with functions in translation initiation, protein folding, protein degradation and stress granule formation, consistent with the role of Gadd34 in UPR. The presence of PP1 and Gadd34 interacting proteins among the K-BIPS data further suggests that identified K-BIPS hits are likely PP1-Gadd34 substrates. Interestingly, the K-BIPS study also detected the Hippo pathway kinase STK3 and PKA regulatory subunits, suggesting potential crosstalk between UPR and other cellular pathways. Finally, the discovery of COPS5 as a substrate of Gadd34 may represent additional regulatory mechanisms of the UPR process. Altogether, the K-BIPS study indicates a bigger role for PP1-Gadd34 in UPR than previously appreciated and further validates the use of K-BIPS as a phosphatase substrate identification method.

3.2.3: K-BIPS for PP1-MYPT1 substrate identification

MYPT1, which is also known as Myosin phosphatase targeting subunit 1 or PPPR12A, is a regulatory subunit of PP1. The most known function of the PP1-MYPT1 complex, which is also known as the Myosin light chain phosphatase (MLCP), is to trigger muscle relaxation in smooth muscle cells by dephosphorylating S19 on the myosin

regulatory light chain(MLC20).^{146,147} Given that the cytoskeleton is composed of an actomyosin (actin-myosin) network, PP1-MYPT1 has also been implicated in cytoskeleton organization, with roles in cell migration and adhesion. In agreement, either the knock down or the impaired expression of MYPT1 has been shown to disrupt the cytoskeletal architecture of the cell.¹⁴⁸ Further, a prior study also showed that disassembly of microtubules affects the polymerization of actomyosin and formation of stress fibers through promoting the phosphorylation of MYPT1, suggesting effects of PP1-MYPT1 on microtubules as well.¹⁴⁹ Besides myosin light chain, the other reported substrates of PP1-MYPT1 are merlin¹⁵⁰, retinoblastoma protein¹⁵¹ and PLK1.¹⁵² PLK1 (Polo Like Kinase 1) is a key kinase involved in mitosis. Additionally, MYPT1 has also been reported to interact with Shugoshin, a protein known to protect centromeres.¹⁵³ Together, the reports suggests a role for PP1-MYPT1 in cell division. Recently, the Yi lab at Wayne State University, College of Pharmacy and Health Sciences identified that MYPT1 interacts with the insulin responsive protein IRS1, implying a possible role of PP1-MYPT1 in insulin signaling as well.¹⁵⁴ Given the interesting biological roles of PP1-MYPT1, we used K-BIPS to explore the unknown substrates of the PP1-MYPT1 complex in a collaborative project with Prof. Yi.

3.2.3.1: K-BIPS with PP1-MYPT1 inactivated lysates

In order to use K-BIPS and identify PP1-MYPT1 substrates, we generated MYPT1 inactivated lysates using a L6 muscle cell line transected with an inducible knock down MYPT1 plasmid that we received from Prof. Yi.¹⁰² Specifically, MYPT1 knock down was induced in L6 myoblast cells by treatment with doxycycline. Then cells were harvested and lysed. Control lysates were prepared from untreated cells. The knock down of MYPT1

was confirmed in lysates by Western Blot. The results showed reduced MYPT1 levels in Dox treated lysates (Figure 3.12, compare lanes 1 and 2), confirming MYPT1 knock down. Biotinylation was then carried out with ATP-biotin in Dox-treated and untreated lysates. Biotinylated proteins were purified using streptavidin resin, separated by SDS-PAGE (Figure B.10) and analyzed by LC-MS/MS using three independent replicates. Label free quantitation was then used to select for proteins that were enriched in the MYPT1-active sample compared to the MYPT1-inactivated sample.

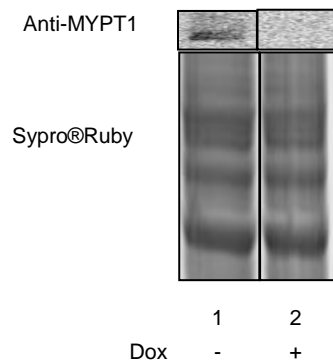


Figure 3.12: Knockdown of MYPT1 in L6 lysates treated with Dox. MYPT1 knock down was assessed using Western blot (Top gel) in untreated cells (lane 1), and Dox treated cells (Lane 2). The bottom Sypro-Ruby stained gel shows equal protein loading. Full gel image and repetitive trials shown in Figure B.9.

From the K-BIPS enriched proteins, fourteen proteins showed reproducible enrichment in all three replicates (at least 2 unique peptides, P value < 0.05 on the t-test, 1.5 average fold enrichment, Table 3.5, Table B.3) in the MYPT1-active sample and represented strong candidates to be PP1-MYPT substrates. In addition, 161 proteins showed significant enrichment (fold enrichment of at least 2, Table B.4) in at least two trials. Out of the 161 proteins, 12 (Table 3.6, green rows) were known interacting proteins of PP1 while 3 were known to interact with MYPT1 (PPP1R12A, Table 3.6, green rows) itself. Additionally, many of the 161 proteins had roles in cytoskeleton organization, cell

adhesion, motility and cell division (Table 3.6), consistent with the known activities of MYPT1 and, therefore, representing likely substrates of the PP1-MYPT1 complex.

Table 3.5: Hits showing reproducible enrichment in all three replicates from the K-BIPS study with PP1-MYPT1 inactivated lysates^a

Entry	Protein	Gene	Trial 1	Trial 2	Trial 3	Average	Interactions
1	Coatomer subunit gamma-2	Copg2	1.3	∞	1.4	∞	
2	Annexin A1	anxa1	1.1	2.7	2.6	2.1	
3	RAT Glutamate dehydrogenase 1, mitochondrial	Glud1	1.2	2.6	2.2	2.0	
4	Protein disulfide-isomerase A3	Pdia3	1.5	3.5	2.6	2.5	
5	2,3-cyclic-nucleotide 3-phosphodiesterase	Cnp	2.7	∞	1.8	∞	PPP1CA
6	RAC-alpha serine/threonine-protein kinase	Akt1	∞	∞	1.4	∞	PPP1CA PPP1CB PPP1CC
7	Neuroplastin	Nptn	7.4	12.9	1.5	7.3	
8	Actin-related protein 2	Actr2	1.3	7.2	1.8	3.4	
9	Fragile X mental retardation syndrome-related protein 1	Fxr1	1.4	3.2	2.7	2.4	
10	Protein disulfide-isomerase A6	Pdia6	1.1	2.1	1.6	1.6	
11	Peptidyl-prolyl cis-trans isomerase FKBP9	Fkbp9	2.1	3.1	1.4	2.2	
12	COP9 signalosome complex subunit 4	Cops4	1.1	5.5	2.0	2.9	
13	BRCA1-A complex subunit BRE	Bre	1.1	3.2	1.4	1.9	
14	4-trimethylaminobutyraldehyde dehydrogenase	Aldh9a1	1.2	1.8	9.1	4.0	

^aThe fold enrichment for each replicate is shown. The fold enrichment was calculated by dividing the peptide intensity observed in the MYPT1-active sample by that of the MYPT1-inactive sample. ∞ was observed when the protein was only observed in the MYPT1-active sample. The interaction information was obtained from BioGrid database.¹²²

From the fourteen K-BIPS hits enriched in all three replicates, the Ser/Thr kinase AKT1 (Table 3.5, Entry # 6) is known to regulate the cytoskeleton during cell movement and adhesion.¹⁵⁵ Importantly, AKT1 is known to associate with and be dephosphorylated by PP1 catalytic subunit as well.¹⁵⁶ Further, previous studies have shown that silencing

of AKT leads to an increase in the inhibitory phosphorylation of MYPT1, consistent with a role of AKT in MYPT1 regulation.¹⁵⁷ Therefore, AKT1 is a likely substrate and a regulator of PP1-MYPT1 complex, possibly through a feedback mechanism. Additionally, GSK3A, a known substrate of AKT¹⁵⁸ was enriched in two replicates (Table B.4). The data suggests that MYPT1 may affect the phosphorylation of GSK3A either directly or indirectly through AKT1.

The activity of MYPT1 is regulated by the RhoA protein. RhoA affects MYPT1 activity by associating with ROCK1 kinase and mediating the inhibitory phosphorylation of MYPT1.¹⁵⁹ Further, RhoA levels in the cell are regulated through degradation by the neddylated CUL3 ubiquitin ligase.¹⁶⁰ The neddylation of CUL3 is controlled by COP9 signalosome,¹⁶¹ and hence COP9 signalosome indirectly affect RHOA and MYPT1 activity. The inhibition of either CUL3 or neddylation has been shown to induce morphological changes in the cytoskeleton, further demonstrating involvement of CUL3 and the COP9 signalosome in MYPT1 related activities.^{160, 162} Interestingly, the COP9 signalosome subunit, COPS4 was enriched in K-BIPS in all three replicates (Table 3.5, entry # 12). Additionally, COPS3 and COPS8 (Table B.4), other subunits of the signalosome complex along with CUL3 and RhoA (Table 3.6), were observed among the 161 proteins showing enrichment in two replicates. Consequently, the discovery of RhoA, CUL3 and COP9 subunits as possible PP1-MYPT1 substrates suggests a feedback mechanism where MYPT1 may regulate itself and affect cytoskeleton arrangement.

Table 3.6: PP1 and MYPT1 interacting proteins and proteins related to PP1-MYPT1 activity from among the K-BIPS hits enriched in only two replicates

Protein	Gene Name	Interactions	Involved In
GrpE protein homolog 1, mitochondrial	Grpel1	PPP1CC	

RNA polymerase II subunit A C-terminal domain phosphatase	Ssu72	PPP1CC	
Cullin-3	Cul3	PPP1CA,PP P1CB	Cytoskeleton organization via RhoA ¹⁶⁰
Focal adhesion kinase 1	Ptk2	PPP1CA,PP P1CB	Cell adhesion and motility
Amyloid beta A4	App	PPP1CC	Cell adhesion and motility
Actin, cytoplasmic 1	Actb	PPP1CA, PPP1CC	Cytoskeleton
Calcineurin B homologous protein 1	Chp1	PPP1CB	
Platelet-activating factor acetylhydrolase IB subunit alpha	PAFAH1 B1	PPP1CA	Microtubule arrangement
Actin-related protein 2/3 complex subunit 2	Arcp2	PPP1R12A	Cytoskeleton organization
Interferon-induced, double-stranded RNA-activated protein kinase	Eif2ak2	PPP1CA, PPP1CC	
Alpha-amino adipic semialdehyde dehydrogenase	Aldh7a1	PPP1CA	
Serine--tRNA ligase, cytoplasmic	Sars	PPP1CC	
Serine/threonine-protein kinase WNK1	Wnk1	PPP1CA	
Prolyl 3-hydroxylase 1	Lepre1	PPP1R12A	
Transforming protein RhoA	Rhoa	PPP1R12A	Cytoskeleton organization through ROCK1 ¹⁵⁹
Shootin-1	SHTN1		Cytoskeleton organization
Afadin	Mlt4		Cell junction
1-phosphatidylinositol 4,5-bisphosphate phosphodiesterase gamma-1	Plcg1		Cytoskeleton organization, cell motility
Glycogen synthase kinase-3 alpha	Gsk3a		Regulates cell plasticity
Programmed cell death protein 10	Pdcd10		Cell motility
Nek7	Nek7		Regulates microtubule activity during cell division
Microtubule-actin cross-linking factor 1	Macf1		Cytoskeleton organization
Protein kinase C iota type	Prkci		Cytoskeleton organization
Myc box-dependent-interacting protein 1	Bin1		Mediates actomyosin filament assembly into sarcomeres
Kinesin-like protein KIF3C	Kif3c		Microtubule associated motor protein
Kinesin-like protein KIF1B	Kif1b		Microtubule associated motor protein
Integrin alpha-1	Itga1		Cell adhesion
Tyrosine-protein phosphatase non-receptor type 1	Ptpn1		Cell adhesion and motility
Ezrin	Ezr		Cytoskeleton organization
Caspase-3	Casp3		Cell adhesion

Kinetochores protein Spc25	Spc25		Associated with microtubules during cell division
Kinesin-like protein KIF2C	Kif2c		Associated with microtubules during cell division
Dihydropyrimidinase-related protein 3	Dpysl3		Cytoskeleton organization
Gelsolin	Gsn		Cytoskeleton organization
Actin-related protein 2/3 complex subunit 1A	Arpc1a		Cytoskeleton organization
Alpha-actinin-1	Actn1		Cytoskeleton organization

^a Except when referenced, the information on interactions and functional association with PP1-MYPT1 was obtained from Uniprot and BioGrid database.¹²² The proteins in green colored rows are known to interact with either PP1 or MYPT1 (PPP11R12A).

The finding of many actin-regulating proteins, such as ARPC1A, ARPC2 and MACF1 (Table 3.6), among K-BIPS data suggests the possibility that PP1-MYPT1 may dephosphorylate other actomyosin-related proteins beside myosin regulatory light chain to affect the cytoskeleton organization. Thus the data predicts a more prominent role for PP1-MYPT1 complex in cytoskeletal arrangement than previously appreciated. In addition, PP1-MYPT1 is known to influence cell division by acting on PLK1 and shugoshin. The discovery of several cell division associated proteins, such as NEK7, SPC25 and KIF2C, by K-BIPS hints that PP1-MYPT1 may be a bigger player in cell division than anticipated. Thus K-BIPS data reveals unknown functions of PP1-MYPT1 complex.

Another PP1 interacting kinase enriched by K-BIPS is the tyrosine kinase PTK2 (FAK1, Table 3.6). PTK2 is known to be present on focal adhesions, which are adhesive contact points where the actomyosin stress fibers of the cytoskeleton are bridged to the extracellular matrix through transmembrane integrin proteins. PTK2 has been shown to affect actomyosin assembly directly through phosphorylation of stress fiber associated protein ACTN1 (alpha-actinin) and indirectly through regulating the activity of MYPT1 via

ROCK1 mediated MYPT1 phosphorylation.¹⁶³ In addition to PTK2, K-BIPS identified both ACTN1 and the integrin protein ITGA1 (Table 3.6) as possible substrates, indicating a previously unknown role for MYPT1 in cytoskeletal organization at focal adhesions.

In summary, the K-BIPS study with MYPT1 inactivation uncovered many possible substrates of the PP1-MYPT1 complex. Importantly, the study identified many proteins that have diverse roles in cytoskeleton regulation, further emphasizing the involvement of PP1-MYPT1 complex in various aspects of cytoskeleton rearrangement with effects on cell migration, adhesion and cell division. In addition, some of the proteins uncovered by K-BIPS were already established interacting partners of either PP1 or MYPT1, increasing the likelihood they are PP1-MYPT1 substrates. Interestingly, the study also revealed MYPT1-regulating proteins also as potential substrates, suggesting that MYPT1 may regulate itself through feedback mechanisms. Overall, the K-BIPS study with MYPT1 inactivation helped identify novel substrates and shed further light on the cellular roles of PP1-MYPT1.

3.3 Conclusions and future directions

In conclusion, we used kinase-catalyzed biotinylation to develop K-BIPS as a tool for discovering phosphatase substrates. The application of K-BIPS to three Ser/Thr phosphatase systems established the use of K-BIPS, while also revealing novel biological functions of phosphatases. In the first K-BIPS study, OA-mediated phosphatase inactivation led to the identification of already known phosphatase substrates and many other candidate substrates. K-BIPS with PP1-Gadd34 inactivated lysates revealed many potential substrates, while also suggesting a bigger role for PP1-Gadd34 in UPR than previously appreciated. Importantly, K-BIPS also identified the known substrate EIF2S1,

confirming the use of K-BIPS as a tool for phosphatase substrate identification. Lastly, the K-BIPS study with PP1-MYPT1 inactivated lysates identified many likely substrates with roles in cytoskeleton and cell division, implying PP1-MYPT1 as a key modulator in cytoskeleton organization. Overall, the studies established K-BIPS as a discovery tool for phosphatase substrate identification.

Given that K-BIPS depends on the inactivation of a given phosphatase, K-BIPS provides a general substrate discovery method applicable to both Tyr and Ser/Thr phosphatases. Although the present study focused on three Ser/Thr phosphatase systems, future experiments with inactivation of Tyr phosphatases will confirm the general use of K-BIPS to discover the substrates of all protein phosphatases. Compared to the currently available phosphoproteomic methods, K-BIPS has the advantage of detecting dynamically changing phosphorylation events due to the use of kinase-catalyzed biotinylation. Therefore, K-BIPS also discovered substrates of low abundance. In contrast, IMAC purification used in phosphoproteomics enrich all phosphoproteins regardless of dynamics. Similar to the phosphoproteomics, K-BIPS may also discover both direct phosphatase substrates and proteins indirectly affected by the inactivated phosphatase through kinase activation. However, kinase activation will lead to increased biotinylation in K-BIPS compared to increased phosphorylation in the case of phosphoproteomics. While phosphoproteomics strategies rely on the identification of proteins with increased phosphorylation in the phosphatase-inactive sample as candidate substrates, K-BIPS selects for proteins showing reduced biotinylation. Therefore, K-BIPS will not discover proteins with increased phosphorylation by kinases as substrates. As a result, K-BIPS is expected to produce fewer false positive hits compared to

phosphoproteomics. However, false positives may be observed in K-BIPS due to expression differences of proteins in the phosphatase-active and inactive samples. Therefore, secondary studies are necessary to confirm that discovered proteins are the substrates of a particular phosphatase.

A deficiency in the present K-BIPS studies was the identification of full length protein substrates, in contrast to phosphopeptides, which will enable the recognition of the phosphosite dephosphorylated by the tested phosphatase. Given that a single protein may carry more than one phosphosite, the phosphorylation status, and hence the biotinylation status of a protein, might be regulated by other kinases and phosphatases in addition to the inactivated phosphatase. Therefore, in future experiments, proteins from the phosphatase-active and inactive samples will be trypsin-digested after ATP-biotin labeling. The biotinylated peptides can be then purified by streptavidin enrichment. Subsequent LC-MS/MS studies will reveal both the phosphatase substrate and the phosphosite affected by the inactivated phosphatase.

In addition to its use in exploring substrates, K-BIPS may also serve as a validation tool for substrate confirmation. While the current validation methods usually require in vitro incubation of candidate substrates with purified phosphatases, K-BIPS only requires phosphatase inactivation and can be used in lysate conditions. Taken together, K-BIPS provides an enabling tool to explore the biological role of phosphatases. Given the importance of protein phosphatases in cell signaling, K-BIPS will assist in unraveling the complex regulatory network in the cell to reveal mechanisms behind human diseases.

3.4 Experimental methods

3.4.1. Synthesis of ATP-biotin

The synthesis and characterization of ATP-biotin has been previously described.³² Purified ATP-biotin was dissolved in deionized water and aliquoted (5 μ L each). Aliquoted ATP-biotin was stored at -80°C until use.

3.4.2. OA treatment of HeLa cells

HeLa cells (20×10^6) were grown in F12 media (45 mL, ThermoFisher, catalog number 11765070) containing 10% FBS (fetal bovine serum, ThermoFisher, catalog number 16000044) and 1X antibiotic/antimycotic solution (ThermoFisher, catalog number 15240062). When cells reached 80% confluency, cells were serum starved overnight in F12 media (45 mL) without FBS or antibiotic/antimycotic. The next day cells were treated with OA (1 μM or 10nM in ethanol, 45 μL , Santa Cruz Biotechnology, catalog number SC-3513) or without OA (0.1% ethanol, EMD) in F12 media without FBS or antibiotic/antimycotic for 30 minutes at 37°C in the cell incubator. Cells were harvested as described in section 3.4.5.

3.4.3. Induction of UPR and guanabenz (Gb) treatment of HeLa cells

HeLa cells (20×10^6) plated in F12 media (45 mL) supplemented with 10% FBS and 1X antibiotic/antimycotic solution were allowed to grown to at least 80% confluence. Then all cells were treated with Tunicamycin (Tm, 2.5 $\mu\text{g}/\text{mL}$ in DMSO, 45 μL , Sigma, catalog number T7765). At the same time, cells were also treated with Guanabnez (Gb, 50 μM in ethanol, 45 μL , Sigma-Aldrich, catalog number G110) or without Gb (0.1 % ethanol, EMD and 0.1% DMSO, ATCC). The cells were then incubated at 37°C for 6 hours and harvested as described in section 3.4.5.

3.4.4. Inactivation of MYPT1 in L6 cells

L6 muscle cell line stably transected with an inducible knock down MYPT1 plasmid was a gift from Prof. Zhengping Yi.¹⁰² L6 cells were grown in DMEM media (45 mL, ThermoFisher, catalog number 12430104) containing 10% FBS and 1X antimycotic antibiotic solution. When cells became ~80% confluent, doxycycline (45 μ L, 100 μ g/mL dissolved in DMEM media without FBS and antibiotic) was added. Two days later, the media was removed and fresh media containing doxycycline (45 μ L, 100 μ g/mL dissolved in same DMEM media without FBS and antibiotic) was added. The next morning, cells were serum starved with FBS-free DMEM containing doxycycline (45 μ L, 100 μ g/mL dissolved in same DMEM media without FBS and antibiotic) and 0.1% BSA (Bovine serum albumin, GenDEPOT, catalog number A0100-010). Then cells were kept at 37°C for 4 hours and harvested as detailed in section 3.4.5.

3.4.5: Cell harvesting

After cell treatment (sections 3.4.2, 3.4.3 and 3.4.4), media was removed. Then the adherent cells were briefly washed once with DPBS (Dulbecco's Phosphate Buffered Saline, 10 mL, ThermoFisher, catalog number SH30028FS). The cells were then incubated with trypsin-EDTA (0.25%, 12 mL, ThermoFisher, catalog number 25200072) for 5 minutes at 37°C. Next, cold DPBS (15 mL) was added to the cells to stop the trypsin reaction. The released cells were collected into a centrifuge tube and spun at 1000 rpm, at 4°C for 5 minutes. The supernatant was discarded and the cells were resuspended in cold DPBS (2mL). The cells were again spun at 1000 rpm, at 4°C for 5 minutes. The supernatant was discarded and the cell pellet was either stored at -80°C or immediately lysed.

3.4.6: Cell lysis

The cell pellets were resuspended in lysis buffer (150-300 μ L, 50mM Tris pH 7.5, 150mM NaCl, 0.5% Triton X-100 and 10% glycerol), and rocked at 4^oC for 20 minutes. Then the samples were spun at 13.2 rpm for 20 minutes. The supernatant was aliquoted into single reaction volumes and saved at -80^oC. Protein concentration was determined by Bradford assay (BioRad) per manufacturer's instructions.

3.4.7: ATP-biotin labeling of OA treated lysates for K-BIPS

Lysates from OA-treated cells (500 μ g total protein) were pre-incubated with OA (1 μ M or 10nM in water) for 10 minutes at room temperature. Lysates from untreated cells were also incubated for 10 minutes at room temperature. Biotinylation was initiated by adding ATP-biotin (2 mM) to the lysates in a final reaction volume of 60 μ L. Reactions were incubated for 2 hours at 31^oC. Then biotinylated proteins were purified by streptavidin affinity chromatography as described in section 3.4.10.

3.4.8: ATP-biotin labeling of PP1-Gadd34 inactivated lysates

Lysates from Tm and Gb-treated cells were pre-incubated with Gb (50 μ m in 0.1 % ethanol) at room temperature for 15 minutes. Lysates from only Tm treated cells were pre-incubated with vehicle (0.1% ethanol) at room temperature for 15 minutes as well. For biotinylation reactions that did not include streptavidin purification (Figure 3.9), lysates (100 μ g) were used in a final volume of 20 μ L with ATP-biotin (2 mM). After reaction, samples were separated by 10% SDS-PAGE (section 2.6.4). Total proteins were visualized by Sypro®Ruby gel stain (section 2.6.7). For visualizing biotin, proteins were transferred onto a PVDF membrane (section 2.6.5) and probed with a Streptavidin-Cy5 conjugate (section 2.6.6). For K-BIPS reactions (Figure B.3), lysates (500 μ g) were used

in a volume of 30 μ L with ATP-biotin (2 mM). Biotinylation reactions were carried out for 2 hours at 31 $^{\circ}$ C. Then biotinylated proteins were purified by streptavidin resin as described in section 3.4.10.

3.4.9: ATP-biotin labeling of PP1-MYPT1 inactivated lysates for K-BIPS

L6 lysates (600 μ g) with and without MYPT1 knocked down were incubated with ATP-biotin (2 mM) for 2 hours at 31 $^{\circ}$ C in a final reaction volume of 32 μ L. Then biotinylated proteins were isolated by streptavidin enrichment as described in section 3.4.10.

3.4.10: Streptavidin purification of biotinylated proteins for K-BIPS

After biotinylation, a fraction of lysates (80 μ g for OA treated lysates and PP1-Gadd34 inactivated lysates and 100 μ g for PP1-MYPT1 inactivated lysates) was saved to be analyzed as the input. The rest of the lysates were filtered using 3 KDa centiprep spin columns (section 2.6.14) to remove excess ATP-biotin and endogenous biotin. Streptavidin resin (200 μ L of packed beads for OA treated lysates and PP1-Gadd34 inactivated lysates and 250 μ L for PP1-MYPT1 inactivated lysates, Genscript) was washed three times with phosphate binding buffer (200-250 μ L; 0.1 M phosphate pH 7.2, 0.15 M NaCl). The filtered samples were then allowed to bind to the streptavidin resin by rotating for 1 hour at room temperature. The flow through was collected by spinning at 2300 rpm at room temperature for 1 minute and streptavidin beads were washed with phosphate binding buffer (200-250 μ L) ten times and four times with water (200-250 μ L). Each wash was performed by spinning at 2300 rpm at room temperature for 1 minute. The final wash was collected. The bound, biotinylated proteins were eluted by boiling the beads in 2% SDS in water (200 μ L for OA treated lysates and PP1-Gadd34 inactivated

lysates and 250 μ L for PP1-MYPT1 inactivated lysates) for 8 minutes. The eluate was then concentrated to dryness by lyophilization. The dried eluate was re-suspended in water (\sim 30 μ L). The input, flow through, last wash, and the concentrated eluate were boiled at 95°C for 1 min in Laemmli sample buffer and separated by 10% SDS-PAGE (section 2.6.4) gels. SYPRO®Ruby stain was used to visualize total proteins (section 2.6.7).

3.4.11: In gel digestion

The proteins in eluate lanes from gels described in section 3.4.10 were excised and in gel digested, as described in section 2.6.15.⁸⁵ For OA-inactivated and PP1-Gadd34 inactivated K-BIPS studies, gels from two independent replicates were used. For MYPT1 knocked down K-BIPS study, gels from three independent trials were used. In all the K-BIPS studies, gels were run completely the whole length and each eluate lane was cut into 8 gel slices. Only for the OA-inactivated K-BIPS study, the peptide samples derived from each lane (after digestion of the 8 slices) were combined into single tubes resulting in four separate tubes containing digested peptides representing the two samples (OA-untreated, OA-treated) in two trials.

3.4.12: TMT labeling of peptides and LC-MS/MS analysis for K-BIPS study with OA-mediated phosphatase inactivation

Digested dry peptides (section 3.4.11) were then resuspended in TEAB (triethylammonium bicarbonate, 30 μ L, 100 mM) and labeled with TMT (0.5 mg of tag, Tandem Mass Tag™, ThermoFisher Scientific) per manufacturer's instructions. Specifically, the peptides from the OA-untreated sample from the two trials were labeled with TMT reporters 127N and 128N respectively. The peptides derived from the OA-

treated samples from the two trials were labeled with the TMT tags 127C and 128C. After labeling for 1 hour at room temperature, the reactions were quenched by adding hydroxylamine (8 μ L, 5% w/v) and maintaining the sample at room temperature for 15 minutes. The TMT labeled peptide samples representing each trial were pooled into a single tube for LC-MS/MS analysis. LC-MS/MS analysis was carried out by Dr. Joseph Caruso at Proteomics Core Facility at Wayne State University. The peptides were first separated by reverse phase chromatography over a 90 min gradient (5% - 28% acetonitrile in 0.1% formic acid) followed by a 20 min gradient (28% - 40% acetonitrile in 0.1% formic acid) using an Easy-nLC pump (Thermo) at 300 nl/min. Peptides were analyzed with an Orbitrap Fusion Tribrid mass spectrometer (Thermo). MS1 scans were performed within the orbitrap at a 120,000 resolution and 350-1600 m/z scan range. The top 10 ions with a charge of +2 to +7 were isolated in the ion trap and fragmented with CID (30% collision energy; activation Q = 0.25). Dynamic exclusion was turned on (after 1 isolation the ion was excluded for analysis for 30 s). Quantitation of isobaric TMT tags was performed with MS3 scans. The top 10 fragment ions were isolated, re-fragmented by HCD (65% collision energy) and sent to the orbitrap for analysis (60,000 resolution over a scan range of 100-500 m/z).

3.4.13: LC-MS/MS analysis for K-BIPS study with PP1-Gadd34 and PP1-MYPT1 inactivation

Biotinylated proteins from eluate lanes from gels described in section 3.4.10 were excised from gel and trypsin digested as previously described in section 2.6.15.⁸⁵ LC-MS/MS analysis was performed by Dr. Joseph Caruso at Proteomics Core Facility at Wayne State University as described in section 2.6.16.

3.4.14: MS data analysis for K-BIPS study with OA-mediated phosphatase inactivation, PP1-Gadd34 and PP1-MYPT1 inactivation

MS raw data was analyzed by MaxQuant (version 1.5.2.8). A human protein database from UniProt (downloaded 2016.04.07, 20159 entries) was used for the K-BIPS studies with HeLa. A rat database from Uniprot was used for K-BIPS study with L6 lysates. Searches allowed 2 missed tryptic cleavages. The iodoacetamide derivative of cysteine was set as a fixed modification, while oxidation of methionine and acetylation of protein N-termini were set as variable modifications. Mass tolerances for parent ions were 20 ppm for the first search and 4.5 ppm for the second search and 20 ppm for fragment ions. Minimum protein and peptide identification probabilities were specified at $\leq 1\%$ false discovery rate (FDR) as determined by a reversed database search and proteins required 1 unique peptide. All other parameters were used at their default settings. Fold enrichment for OA-mediated K-BIPS study was calculated by dividing the TMT reporter intensity observed for the OA-untreated sample by that of the OA-treated sample. Proteins showing fold enrichment of at least 1.5 in both replicates were considered as K-BIPS hits. For PP1-Gadd34 inactivated K-BIPS study, fold enrichment was calculated by dividing the peptide intensity observed in the PP1-Gadd34-active sample by that observed for the PP1-Gadd34-inactive sample. Proteins showing fold enrichment of at least 1.3 in both replicates in the PP1-Gadd34 active sample compared to the PP1-Gadd34 inactive sample were considered hits (Table B.2). For K-BIPS study with MYPT1 knock down, first proteins showing enrichment in all three trials (fold enrichment > 1) were selected. Then, Student's paired t-test with a two-tailed distribution was carried out and the average fold enrichment was calculated. Fourteen proteins showing P value > 0.05 ,

average fold enrichment >1.5 and at least 2 unique peptides were selected as the best candidates (Table 3.5 and B.3). In addition proteins that showed at least 2-fold enrichment in the MYPT1-active sample compared to the MYPT1-inactive sample in at least out of the three replicates were also considered as potential hits (Table 3.6 and B.4).

3.4.15: Streptavidin enrichment of COPS5, WDR5, CAPRIN1 and G3BP1 from PP1-Gadd34 inactivated lysates

Biotinylated proteins from section 3.4.8 (using 16.7 mg/mL lysates) were streptavidin enriched as described in section 3.4.10. The eluted proteins (30% of eluate for COPS5 and 100% for WDR5, CAPRIN1 and G3BP1) and the input, flow through, and the last wash from streptavidin enrichment (section 3.4.10) were separated on SDS-PAGE (section 2.6.4). The proteins were then transferred onto a PVDF membrane and probed by specific antibodies; COPS5 (Santa Cruz-SC-9074, 1:200 dilution), WDR5 (Bethyl Laboratories, A302-429A-T, 1:1000 dilution), CAPRIN1 (Bethyl Laboratories, A303-881A-T, 1:1000 dilution), G3BP1 (Bethyl Laboratories, A302-033, 1:1000 dilution).

APPENDIX A – CHAPTER 2 SUPPORTING INFORMATION

A2.1 Peptide characterization

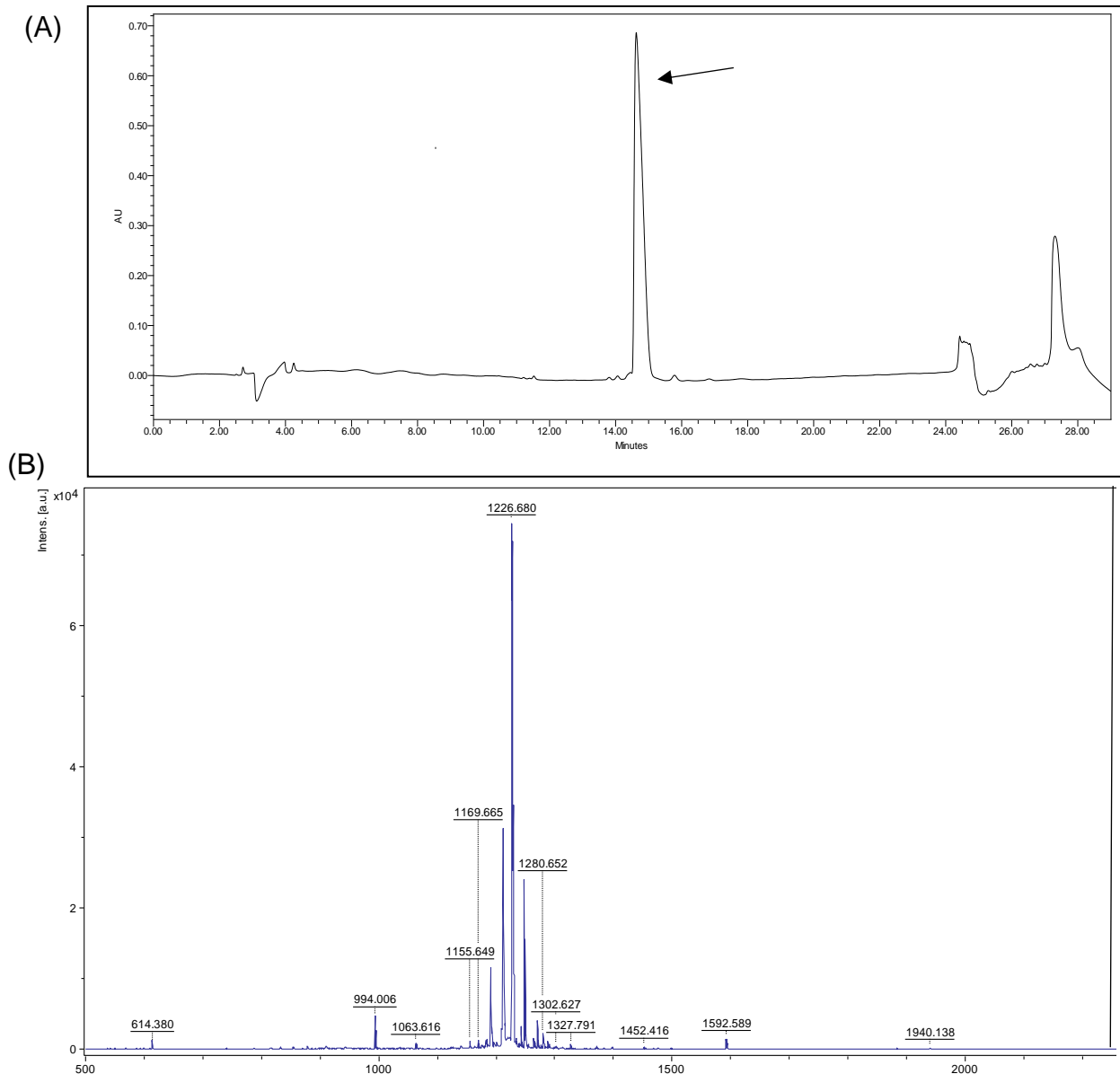


Figure A2.1.1: Characterization of N-biotin kemptide (biotin-GGGGLRRASLG). (A) Reinjection of 50ug of purified N-biotin kemptide (arrow). Elution gradient used started with 95% Buffer A (99.9% water with 0.1% trifluoroacetic acid) in Buffer B (acetonitrile in 0.085% trifluoroacetic acid) and decreased to 83% Buffer A over 11 minutes, then to 81.5% Buffer A over 5 minutes, and finally to 80.6% Buffer A over 9 minutes. The flow rate was 1mL/min and the peptides were detected at 214 nM. (B) When characterized by MALDI-TOF, the purified N-biotin kemptide showed a $[M+H]^+$ of 1226.68 m/z ($[M+H]^+$ calculated for $C_{50}H_{88}N_{19}O_{15}S = 1226.64$).

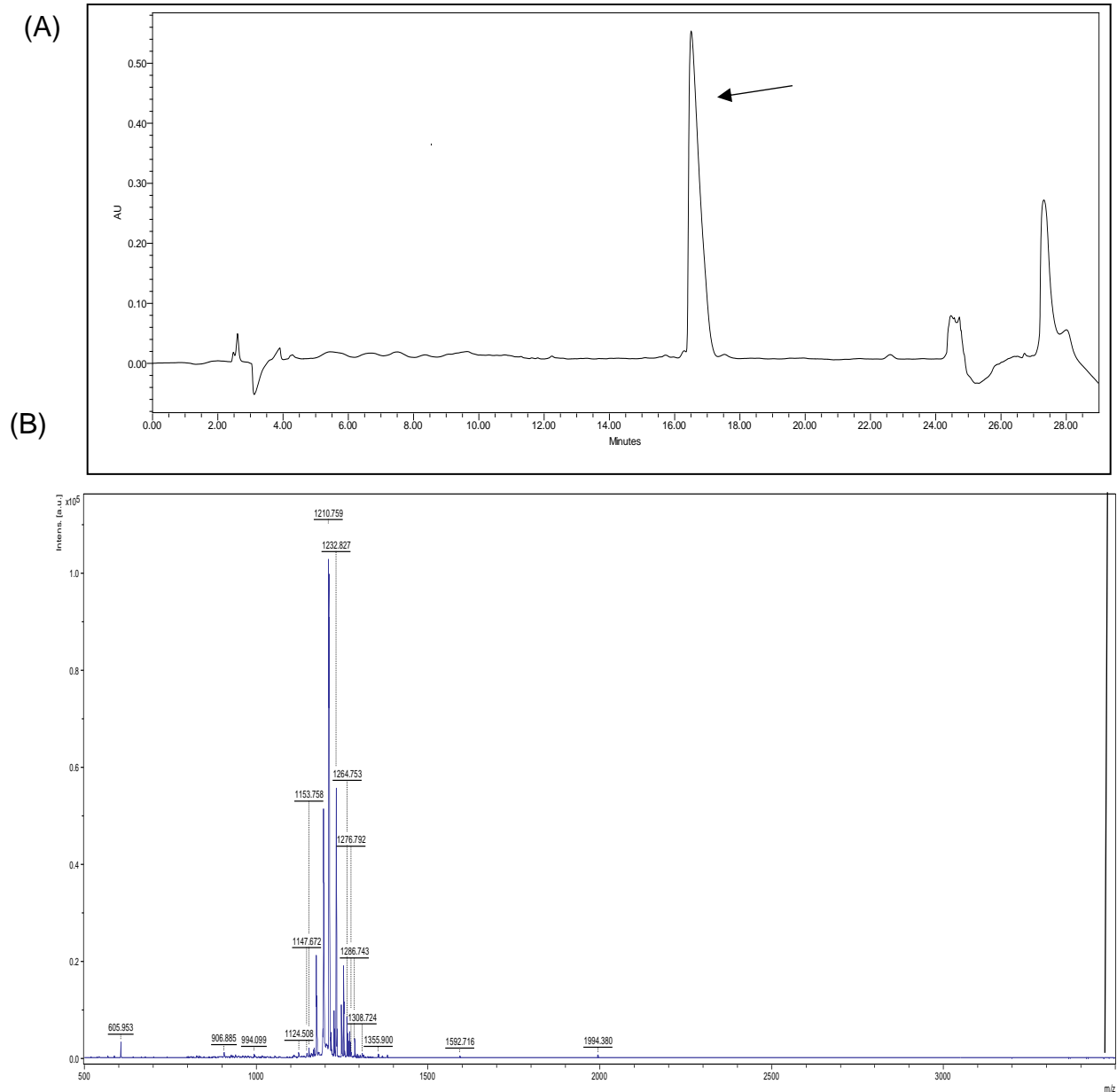


Figure A2.1.2: Characterization of N-biotin mutant kemptide (biotin-GGGGLRRAALG). (A) Reinjection of 50ug of purified N-biotin mutant kemptide (arrow). Elution gradient used started with 95% Buffer A in Buffer B and decreased to 83% Buffer A over 11 minutes, then to 81.5% Buffer A over 5 minutes, and finally to 80.6% Buffer A over 9 minutes. The flow rate was 1mL/min and the peptides were detected at 214 nM. (B) When characterized by MALDI-TOF, the peptide showed a $[M+H]^+$ of 1210.76 ($[M+H]^+$ calculated for $C_{50}H_{88}N_{19}O_{14}S = 1210.65$).

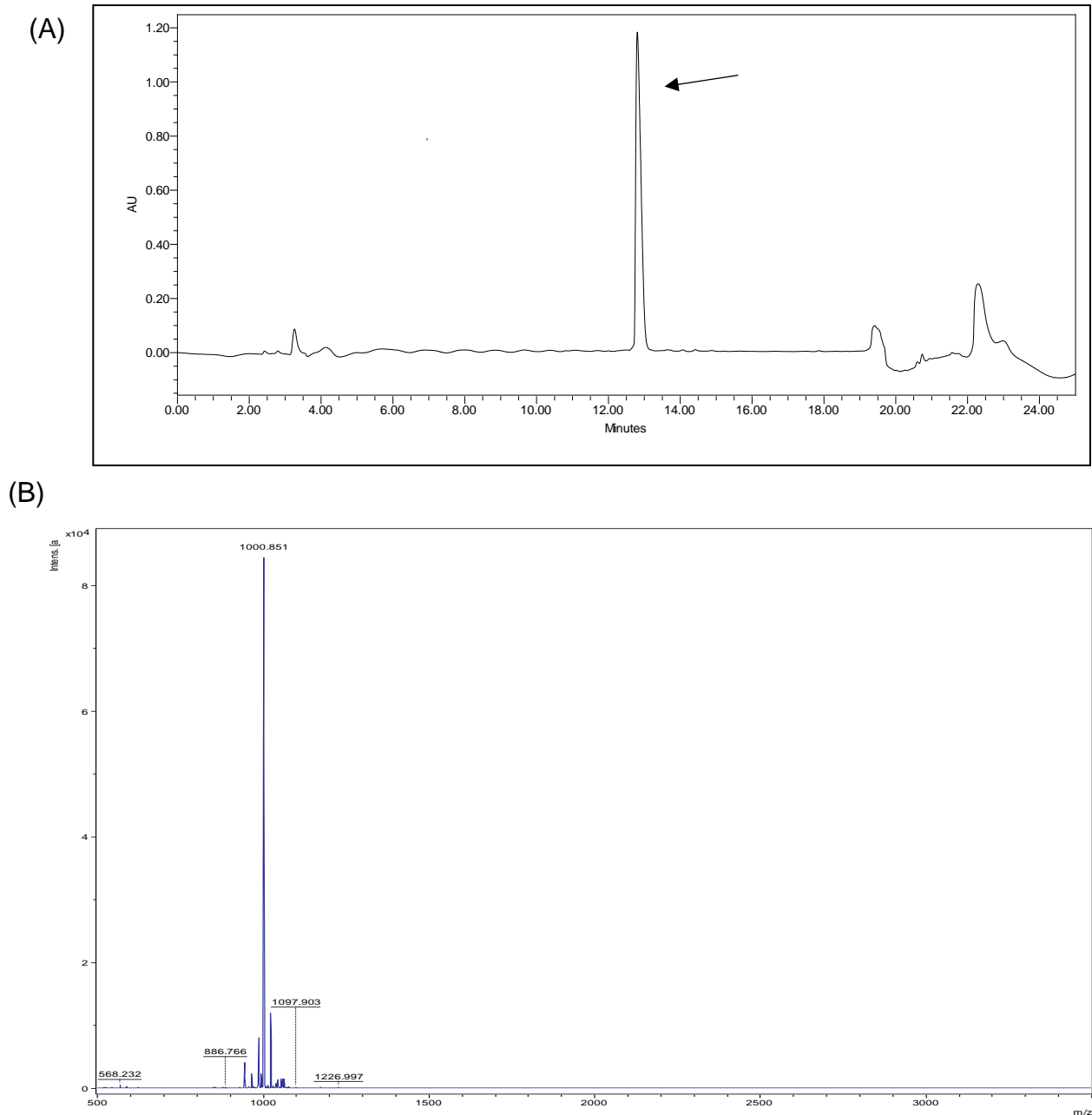


Figure A2.1.3: Characterization of non-biotinylated kemptide (GGGGLRRAALG). (A) Reinjection of 50 μ g of purified non-biotinylated kemptide (arrow). Elution gradient used started with 95% Buffer A in Buffer B and ended in 75% Buffer A over 16 minutes. The flow rate was 1 mL/min and the peptides were detected at 214 nM. (B) When characterized by MALDI-TOF, the peptide showed a $[M+H]^+$ of 1000.85 ($[M+H]^+$ calculated for $C_{40}H_{74}N_{17}O_{13} = 1000.57$).

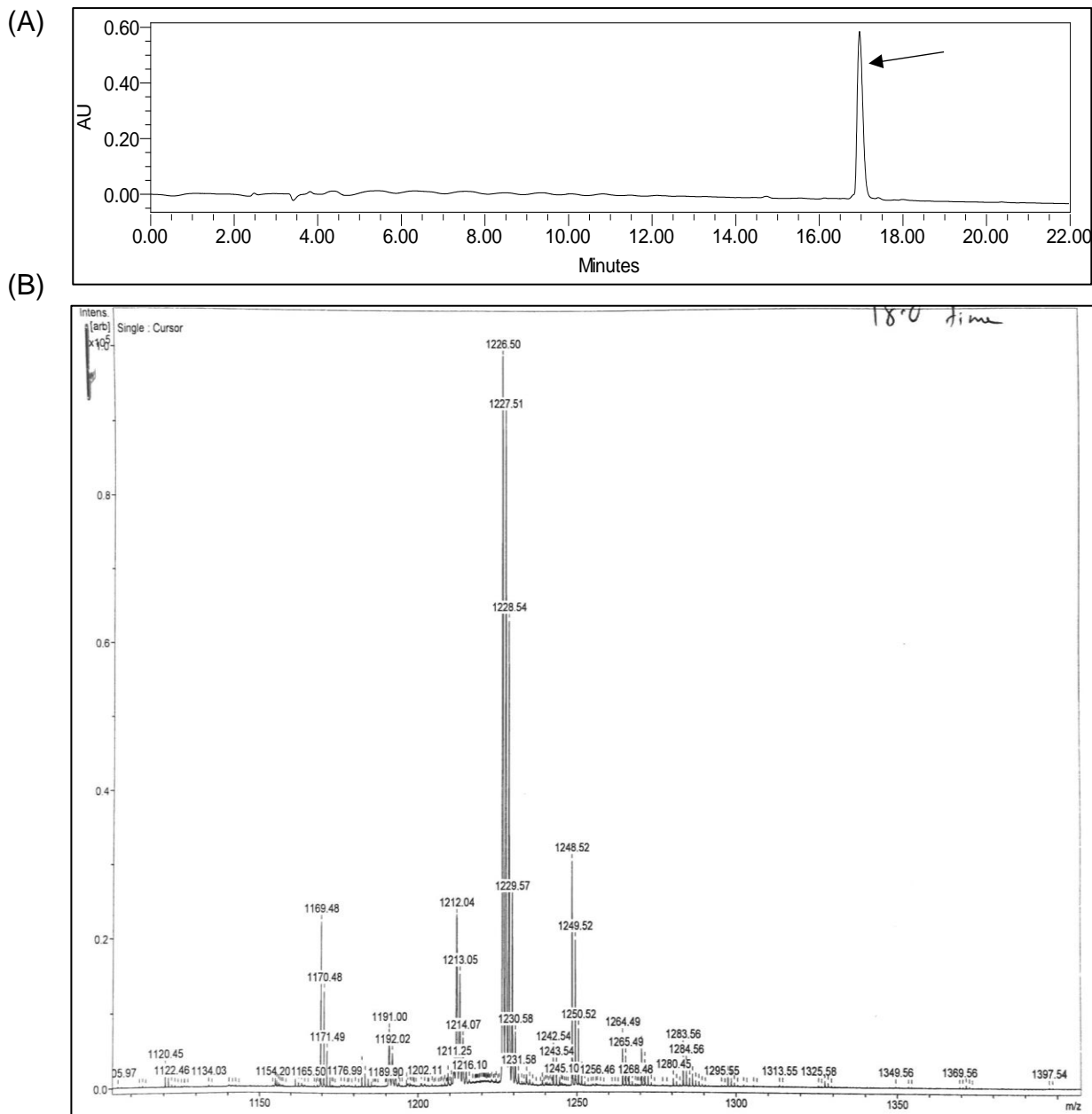


Figure A2.1.4: Characterization of scrambled N-biotin kemptide (biotin-LSGARGLGGRG). (A) Reinjection of 50ug of purified scrambled N-biotin kemptide (arrow). Elution gradient used started with 95% Buffer A in Buffer B and decreased to 83% Buffer A over 11 minutes, then to 81.5% Buffer A over 5 minutes, and finally to 80.6% Buffer A over 9 minutes. The flow rate was 1mL/min and the peptides were detected at 214 nM. (B) When characterized by MALDI-TOF (performed by N.Chinthaka), the peptide showed a $[M+H]^+$ of 1226.50 ($[M+H]^+$ calculated for $C_{50}H_{88}N_{19}O_{15}S = 1226.64$).

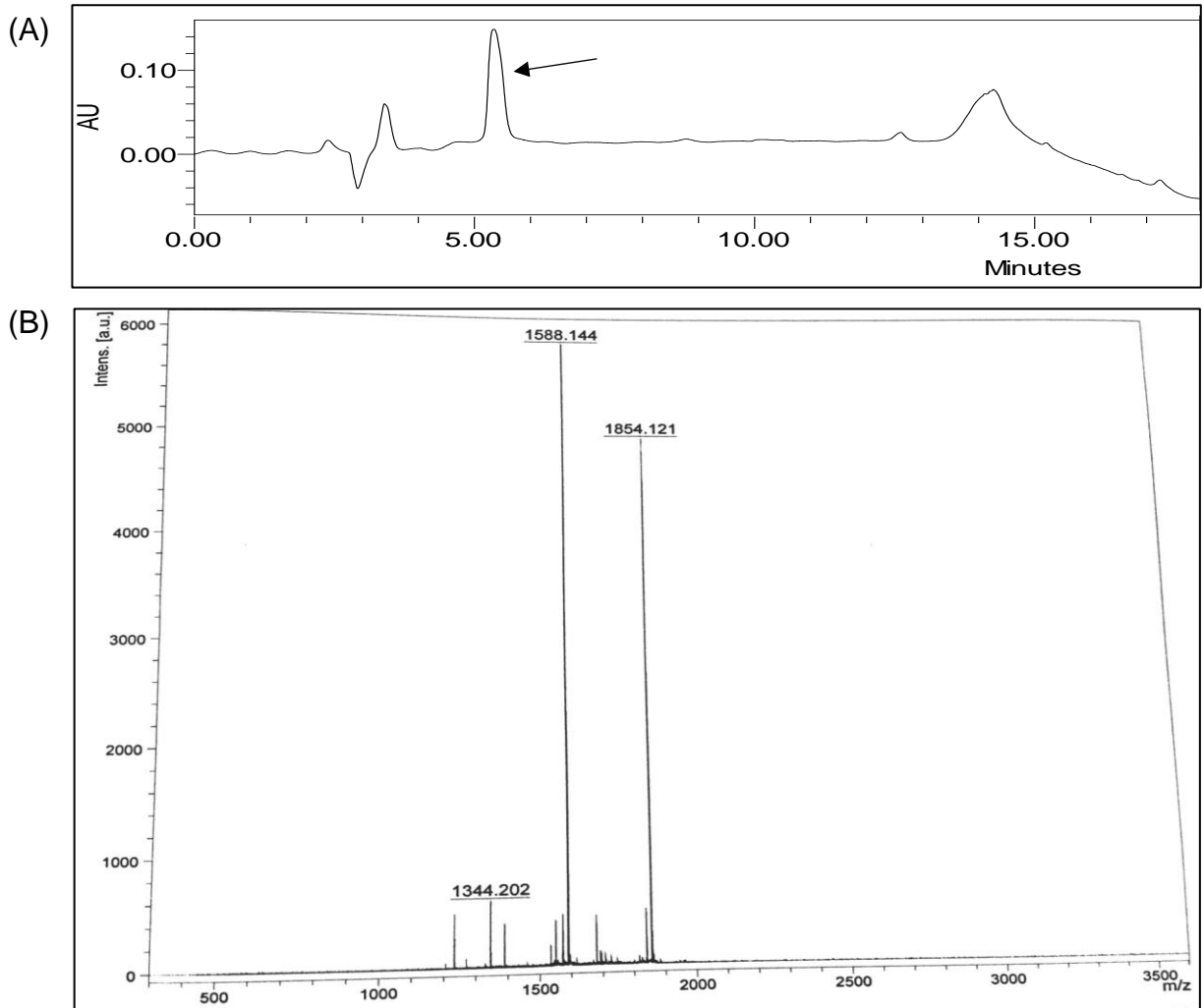


Figure A2.1.5: Characterization of N-biotin CK2 substrate peptide (biotin-RRREEETEEE, performed by T.Faner). (A) Reinjection of 50ug of purified N-biotin CK2 substrate peptide (arrow). Elution gradient used started with 86.7% Buffer A in Buffer B and decreased to 70% Buffer A over 10 minutes. The flow rate was 1mL/min and the peptides were detected at 214 nM. (B) When characterized by MALDI-TOF, the peptide showed a $[M+H]^+$ of 1588.14 ($[M+H]^+$ calculated for $C_{62}H_{101}N_{21}O_{26}S = 1588.69$).

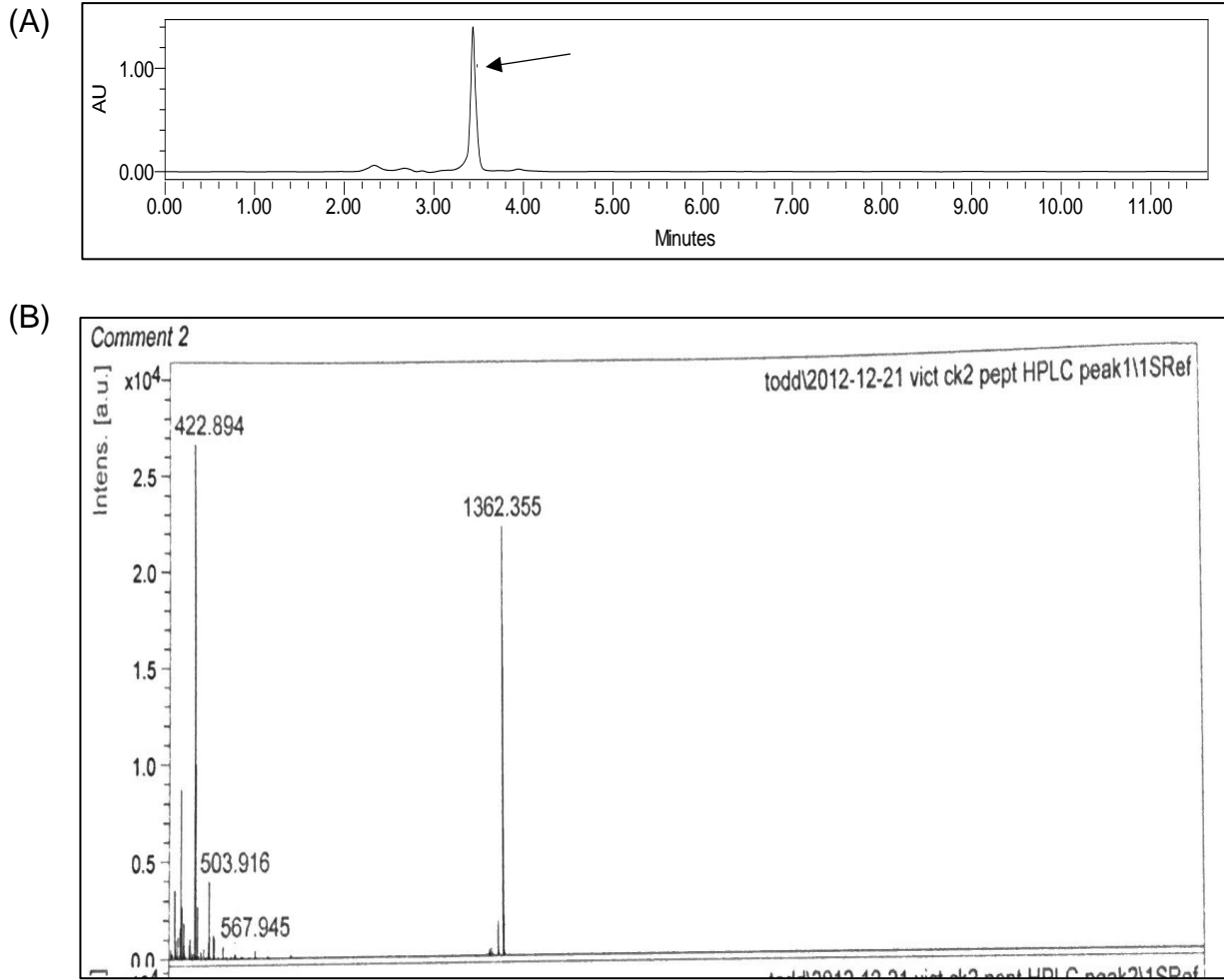


Figure A2.1.6: Characterization of Non-biotinylated CK2 substrate peptide (RRREEETEEE, performed by T.Faner). (A) Reinjection of 50ug of purified non-biotinylated CK2 substrate peptide (arrow). Isocratic elution at 86% was used. The flow rate was 1mL/min and the peptides were detected at 214 nM. (B) When characterized by MALDI-TOF, the peptide showed a $[M+H]^+$ of 1362.36 ($[M+H]^+$ calculated for $C_{52}H_{87}N_{19}O_{24} = 1362.62$).

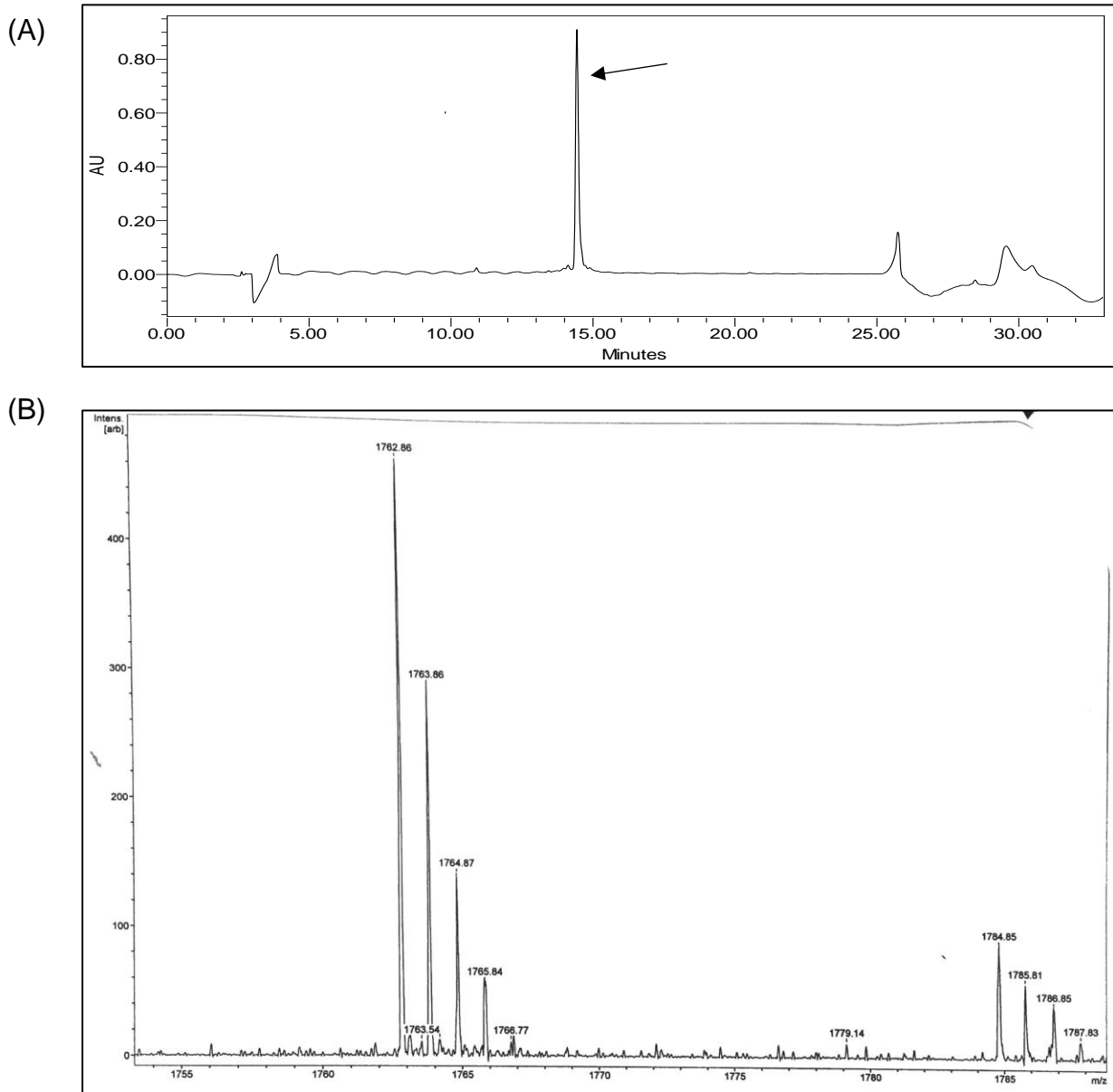


Figure A2.1.7: Characterization of N-biotin Miz1 peptide (biotin-GGQAESASSGAEQTEK). (A) Reinjection of 50ug of purified N-biotin Miz1 peptide (arrow). Elution gradient used started with 95% Buffer A in Buffer B and decreased to 75% Buffer A over 22 minutes. The flow rate was 1mL/min and the peptides were detected at 214 nM. (B) When characterized by MALDI-TOF, the peptide showed a $[M+H]^+$ of 1762.56 ($[M+H]^+$ calculated for $C_{69}H_{111}N_{21}O_{31}S = 1762.90$).

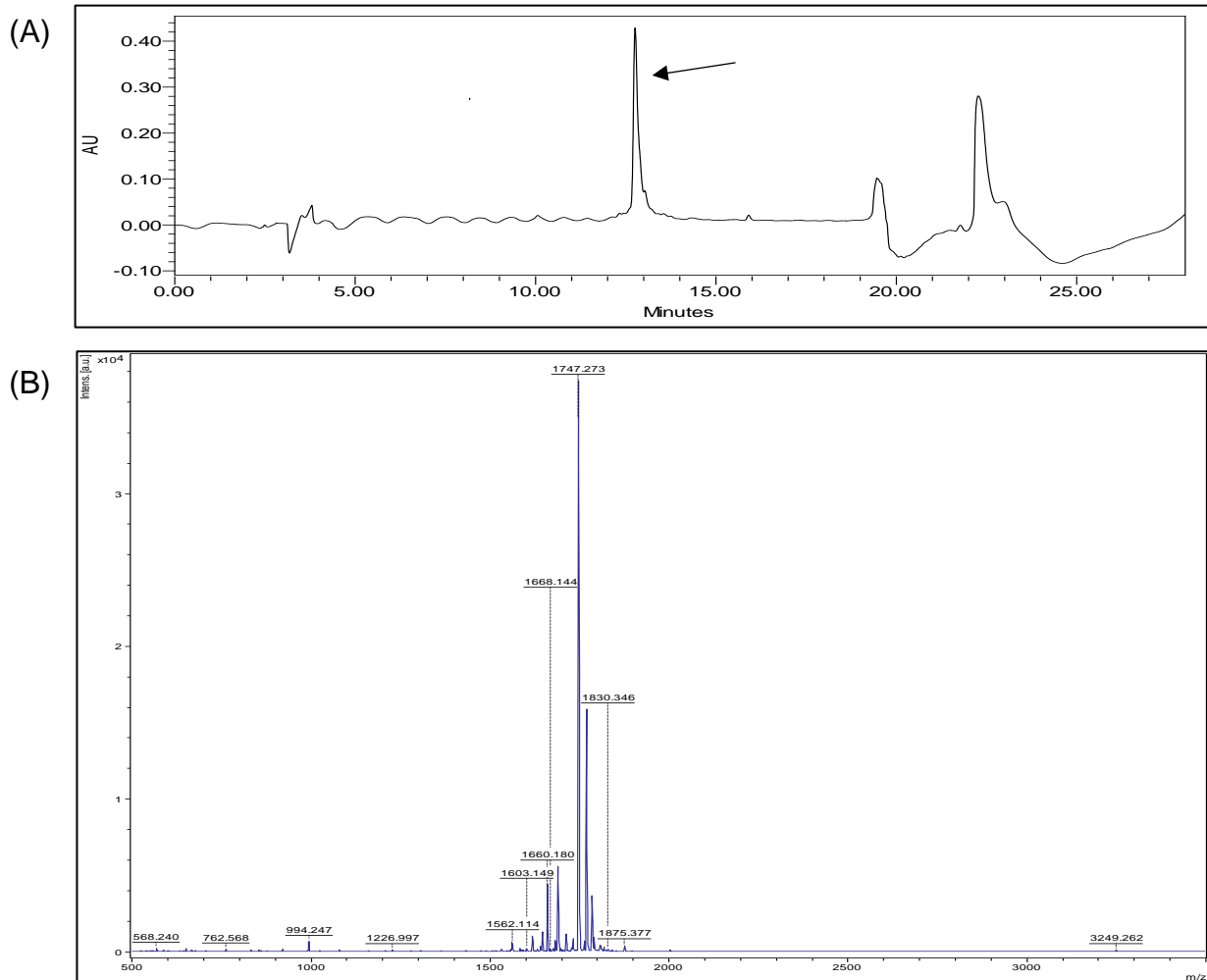
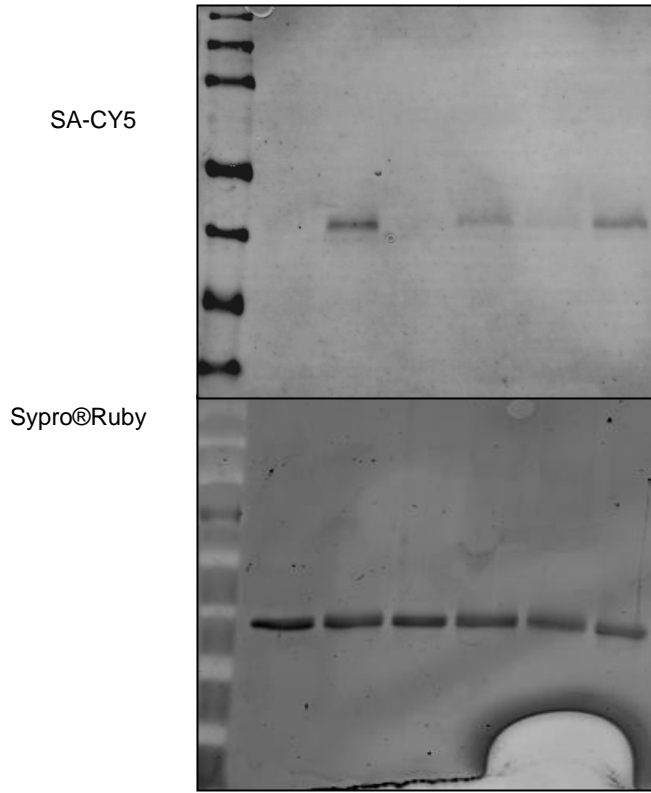
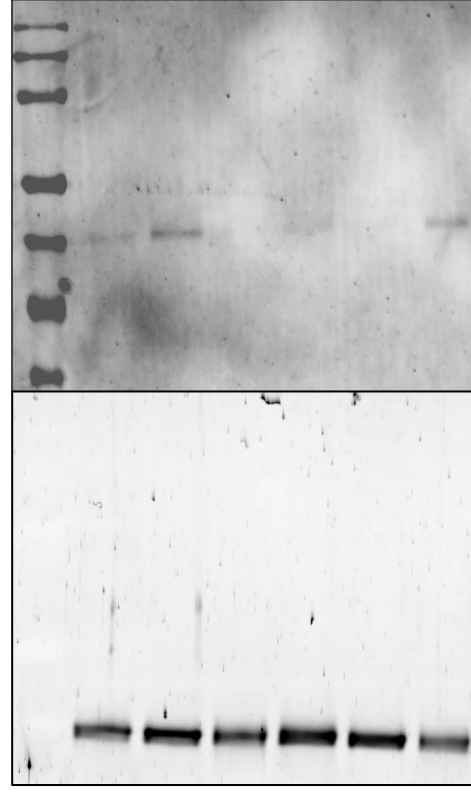


Figure A2.1.8: Characterization of N-biotin mutant Miz1 peptide (biotin-GGQAESASAGAEQTEK). (A) Reinjection of 50ug of purified N-biotin mutant Miz1 peptide (arrow). Elution gradient used started with 95% Buffer A in Buffer B and decreased to 75% Buffer A over 16 minutes. The flow rate was 1mL/min and the peptides were detected at 214 nM. (B) When characterized by MALDI-TOF, the peptide showed a $[M+H]^+$ of 1747.27 ($[M+H]^+$ calculated for $C_{69}H_{111}N_{21}O_{30}S = 1746.98$).

(A) 11% 100% 12% 35% 14% 46%

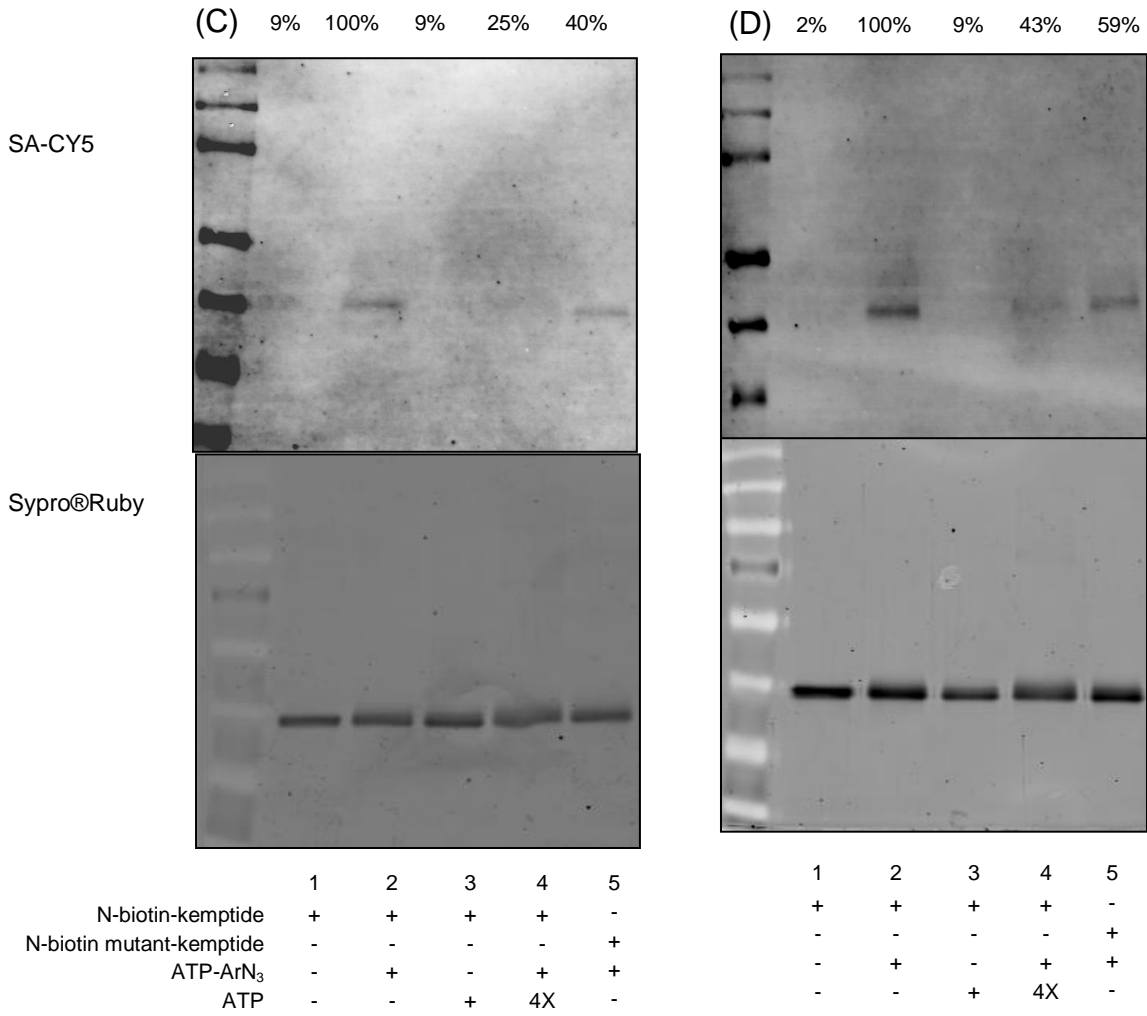


(B) 15% 100% 10% 30% 10% 42%



	1	2	3	4	5	6
N-biotin-kemptide	+	+	+	+	+	-
N-biotin mutant-kemptide	-	-	-	-	-	+
kemptide	-	-	-	-	2X	-
ATP-ArN ₃	-	+	-	+	+	+
ATP	-	-	+	4X	-	-

	1	2	3	4	5	6
N-biotin-kemptide	+	+	+	+	+	-
N-biotin mutant-kemptide	-	-	-	-	-	+
kemptide	-	-	-	-	2X	-
ATP-ArN ₃	-	+	-	+	+	+
ATP	-	-	+	4X	-	-



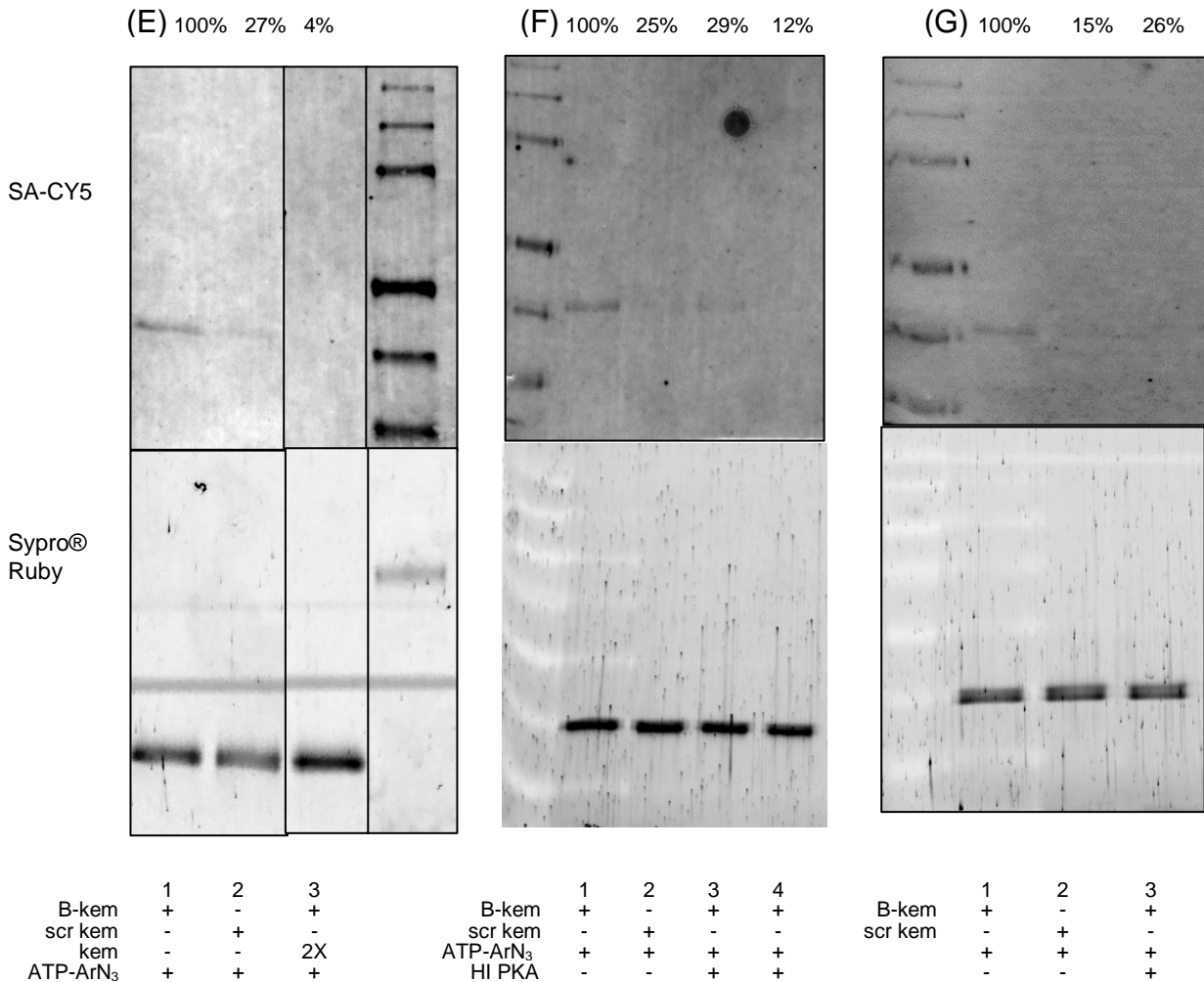


Figure A.2.2: Replicates (A-G) of in vitro crosslinking reactions with recombinant PKA shown in Figure 2.5. Crosslinking reactions were carried out with recombinant PKA, N-biotin kemptide (B-kem) and ATP-ArN₃. After reaction, the samples were separated by SDS-PAGE and stained with Sypro® Ruby total protein stain (bottom) or Streptavidin-Cy5 for biotinylation (top). Control reactions were carried out with a mutant biotin kemptide lacking the phosphorylated Ser (B-kem mt), 4X excess ATP, 2X excess non-biotinylated kemptide (kem), with N-biotin scrambled peptide (scr kem) and heat inactivated PKA (HI PKA). Trial A and F are shown in Figure 2.5. The molecular weight marker is shown, with bands corresponding to the following molecular weights: 170, 130, 95, 72, 55, 43, 34, and 26 kDa.

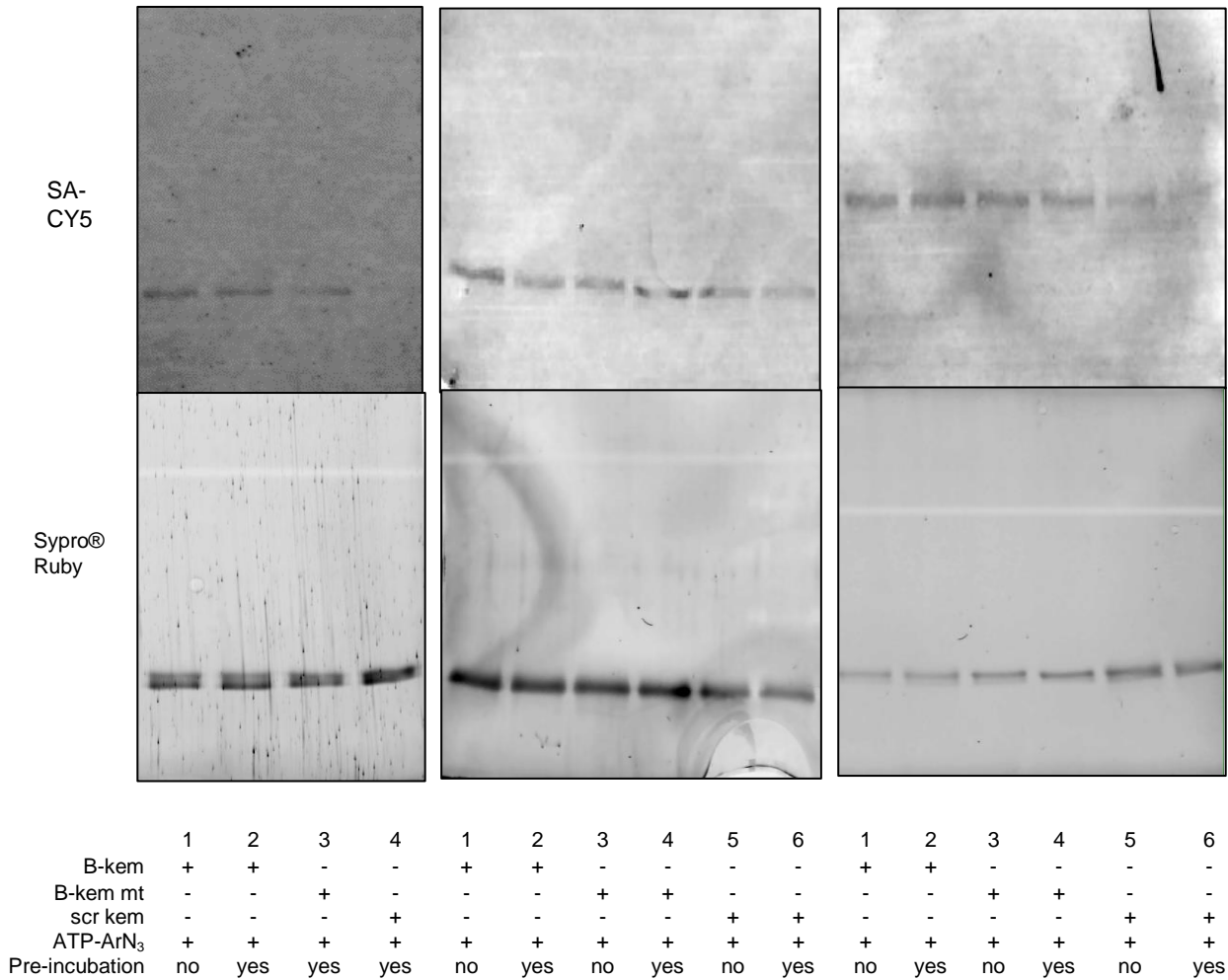


Figure A.2.3: Replicates of in vitro crosslinking reactions with recombinant PKA with biotin peptide pre-incubated with ATP-ArN₃ shown in Figure 2.7. N-biotin kemptide (B-kem), N-biotin mutant kemptide (B-kem mt), or scrambled kemptide (scr kem) was pre-incubated with ATP-ArN₃ in the presence of UV light. Then recombinant PKA was added and crosslinking reactions were carried out. After reaction, the samples were separated by SDS-PAGE and stained with Sypro® Ruby total protein stain (bottom) or Streptavidin-Cy5 for biotinylation (top). Control reactions were carried out without pre-incubation. The first trial is shown in Figure 2.7.

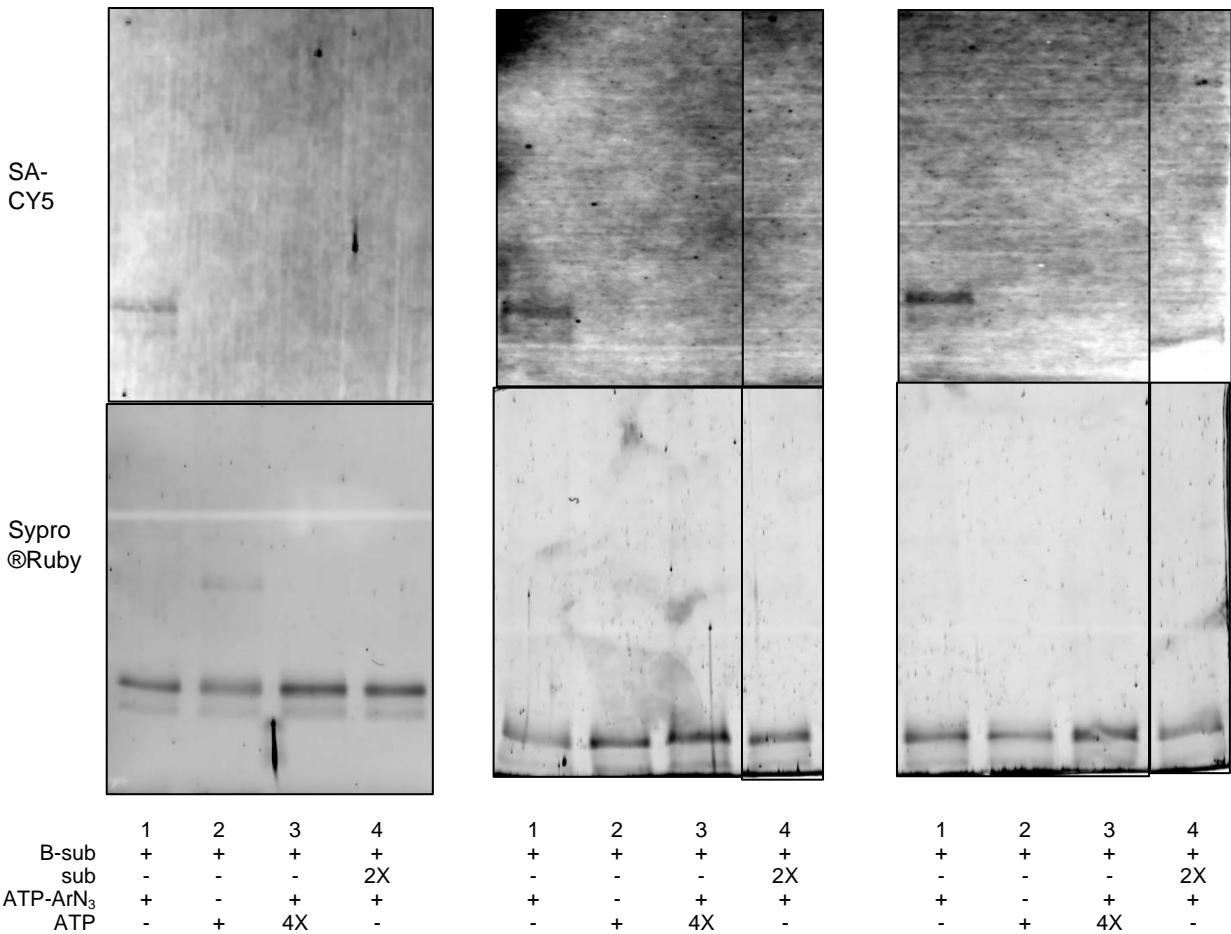


Figure A.2.4: Replicates of in vitro crosslinking reactions with recombinant CK2 shown in Figure 2.8. Crosslinking reactions were carried out with recombinant CK2, N-biotin CK2 substrate peptide (B-sub) and ATP-ArN₃. After reaction, the samples were separated by SDS-PAGE and stained with Sypro® Ruby total protein stain (bottom) or Streptavidin-Cy5 for biotinylation (top). Control reactions were carried out with ATP, 4X excess ATP and 2X excess non-biotinylated CK2 substrate peptide (sub). Trial 1 is shown in Figure 2.8.

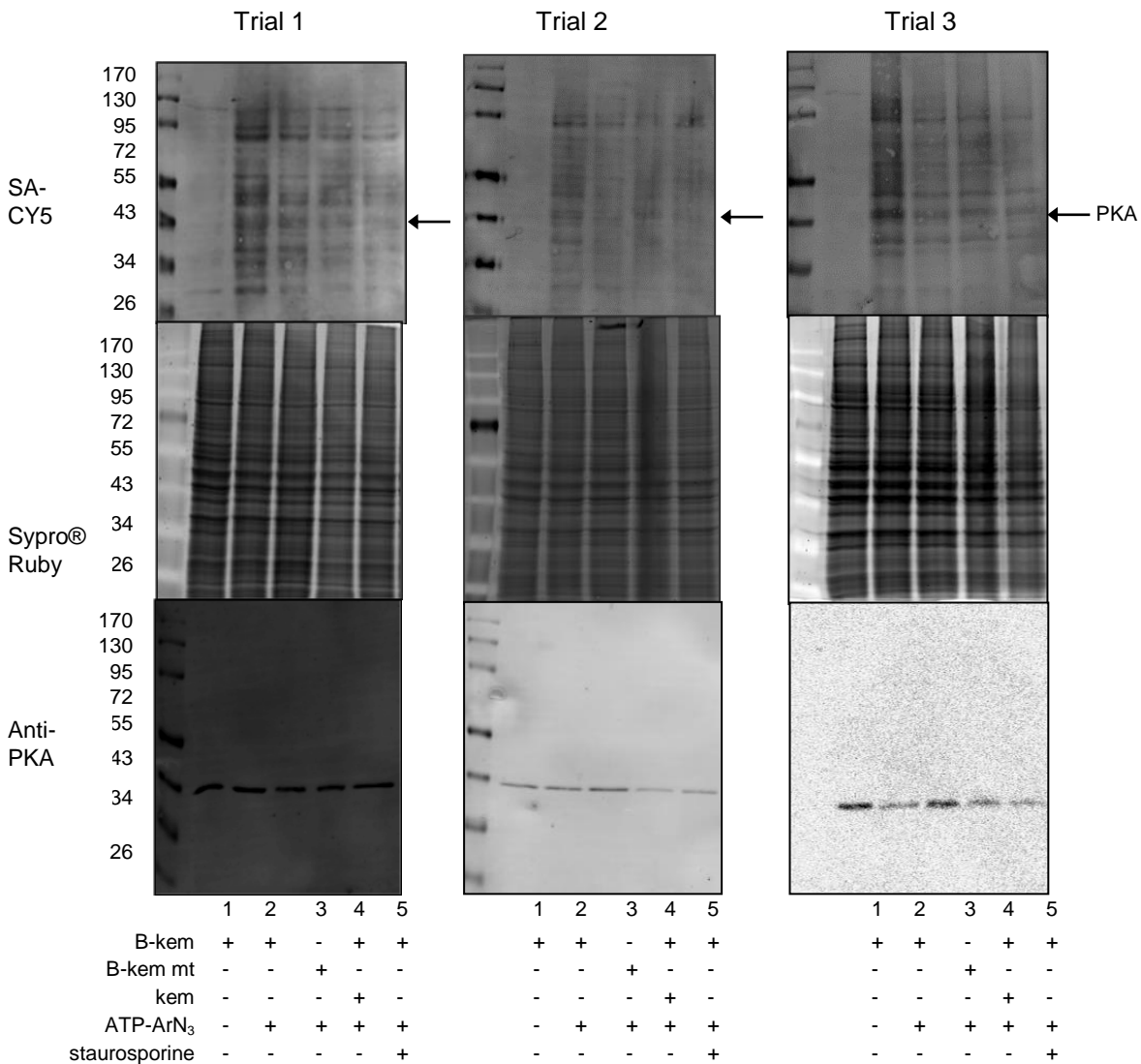


Figure A.2.5: Three replicates of crosslinking reactions in HeLa lysates shown in Figure 2.10. Crosslinking reactions contained HeLa lysates, N-biotin kemptide (B-kem), and ATP-ArN₃ (lane 2). Control reactions were carried out with a N-biotin mutant kemptide lacking Ser (B-kem mt, lane 3), in the presence of 1X non-biotinylated kemptide (kem, lane 4), or after pre-incubation with the kinase inhibitor staurosporine (lane 5). The top gel was Streptavidin-Cy5 stained to visualize biotinylated proteins, the middle gel was SYPRO® Ruby stained to observe all proteins, and the bottom gel was immunoblotted with an anti-PKA antibody to assure the presence of PKA. Trial 1 is shown in Figure 2.10.

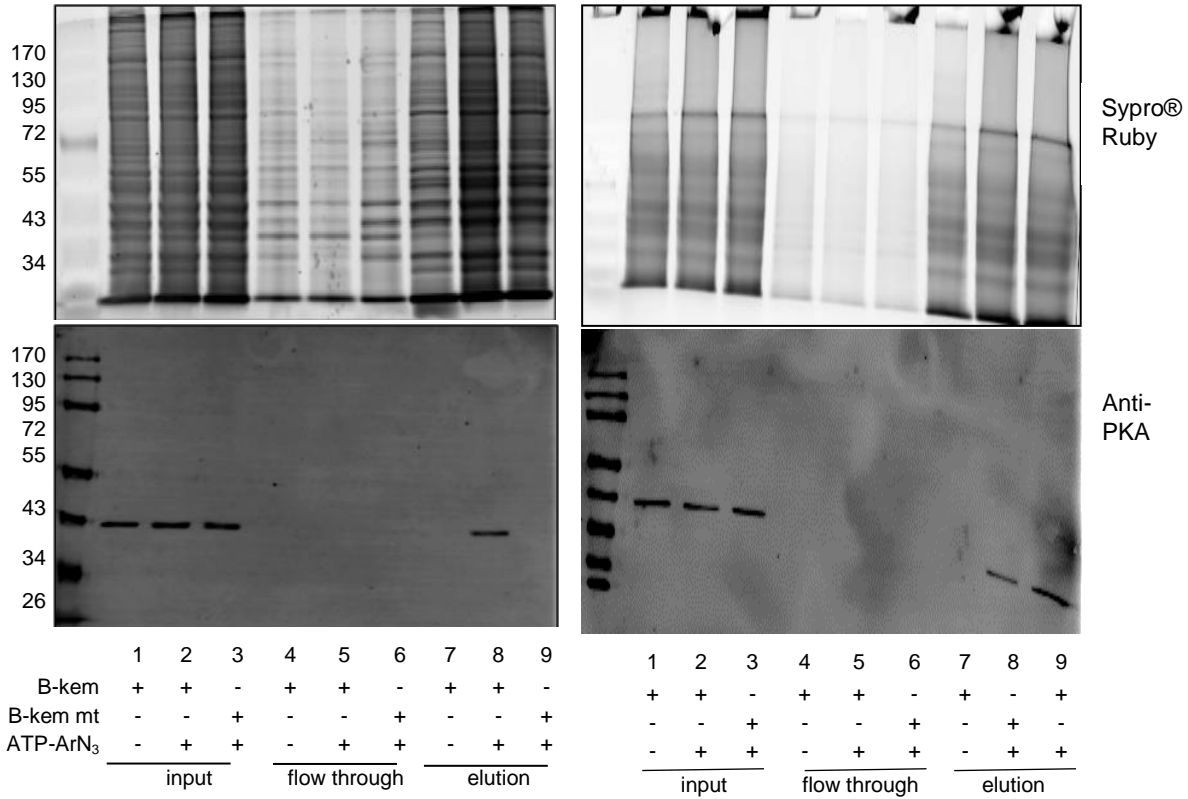


Figure A.2.6: Gel images from the kemptide K-CLASP experiment. Crosslinking reactions were carried out with HeLa lysate and N-biotin kemptide (B-kem) in the presence of ATP-ArN₃ (lanes 2, 5, and 8 in first gel and lanes 2, 5, and 9 in second gel). Control reactions were performed without ATP-ArN₃ (lanes 1, 4, and 7) or with N-biotin mutant kemptide (B-kem mt) in place of N-biotin kemptide (lanes 3, 6, and 9 in first gel and lanes 2, 5, and 7 in second gel). After reaction, biotinylated proteins were enriched using streptavidin resin. The input before streptavidin enrichment (11% loaded per gel, lanes 1-3), flow through (8% loaded per gel, lanes 4-6), and the elution from each sample (33% loaded per gel, lanes 7-9) were separated by SDS-PAGE and then stained for total proteins using SYPRO® Ruby stain (top gel). PKA was visualized using an anti-PKA antibody (bottom gel). The shown gels were used in LC-MS/MS analysis.

Table A.2.1: Full listing of the 324 kemptide K-CLASP hits^a

Gene name	T1 WT	T2 MT	T2 WT	T2 MT	T3 WT	T3 MT	T1 fold change	T2 fold change	T3 fold change
SNAP23	3.8E+08	3.2E+08	2.3E+07	0.0E+00	2.5E+08	1.1E+08	1.2	∞	2.4
PSMD9	5.6E+07	2.2E+07	2.7E+06	1.1E+07	2.8E+07	0.0E+00	2.5	0.3	∞
GAPDHS	2.7E+07	0.0E+00	2.2E+07	0.0E+00	1.8E+07	0.0E+00	∞	∞	∞
AP3D1	1.9E+07	3.1E+06	0.0E+00	0.0E+00	2.7E+07	1.1E+07	6.1	0	2.5
CCS	1.1E+08	0.0E+00	0.0E+00	5.0E+07	1.7E+07	0.0E+00	∞	0	∞
MAP2K7	1.7E+07	0.0E+00	0.0E+00	0.0E+00	3.9E+07	0.0E+00	∞	0	∞
PDCD5	1.7E+09	1.7E+08	5.0E+07	4.6E+07	1.6E+07	5.3E+06	10.4	1.1	3
SLC9A3R1	3.5E+08	9.7E+07	7.8E+07	0.0E+00	8.4E+07	0.0E+00	3.7	∞	∞
CHEK1	6.2E+06	0.0E+00	9.0E+05	9.5E+06	7.4E+07	0.0E+00	∞	0.1	∞
GEMIN2	5.4E+07	8.4E+07	7.9E+06	0.0E+00	1.3E+07	0.0E+00	0.7	∞	∞
GIPC1	1.4E+08	1.7E+08	4.5E+07	1.8E+07	1.5E+08	6.9E+07	0.9	2.5	2.3
PPP1R12A	2.0E+07	2.0E+06	0.0E+00	0.0E+00	3.3E+07	1.5E+07	10	0	2.2
PFAS	6.8E+07	0.0E+00	0.0E+00	1.5E+07	9.7E+08	1.1E+07	∞	0	86.2
SCAMP1	4.7E+07	0.0E+00	6.6E+06	0.0E+00	1.3E+08	6.8E+07	∞	∞	1.9
CTAGE5	4.4E+07	0.0E+00	0.0E+00	0.0E+00	2.3E+07	1.2E+07	∞	0	2
ZW10	3.6E+07	1.6E+07	0.0E+00	0.0E+00	1.3E+08	5.1E+07	2.3	0	2.6
TPD52L2	4.1E+09	1.7E+09	6.4E+08	5.1E+08	1.1E+09	5.4E+08	2.5	1.3	2.1
EPB41L2	3.6E+08	6.4E+06	4.0E+06	0.0E+00	1.7E+08	1.1E+08	55.8	∞	1.6
DENR	6.9E+07	3.2E+08	4.8E+07	7.1E+06	7.1E+08	2.8E+08	0.3	6.9	2.6
HTATSF1	4.8E+08	2.7E+07	1.8E+07	0.0E+00	3.8E+08	2.8E+08	17.9	∞	1.4
NUDT21	1.6E+09	1.1E+09	1.3E+08	3.1E+07	4.7E+08	1.5E+08	1.5	4.2	3.2
LANCL1	4.9E+08	2.1E+08	1.5E+08	2.8E+08	4.1E+08	1.9E+08	2.4	0.6	2.2
RAD21	1.0E+08	2.9E+07	1.1E+08	0.0E+00	1.1E+08	1.2E+08	3.6	∞	0.9
GMFB	1.9E+08	7.8E+07	0.0E+00	0.0E+00	6.9E+07	0.0E+00	2.4	0	∞
EIF4E2	1.7E+07	5.2E+06	0.0E+00	0.0E+00	3.7E+07	0.0E+00	3.3	0	∞
DNAJA2	4.8E+08	1.8E+08	3.2E+07	4.6E+07	4.1E+08	2.0E+08	2.7	0.8	2.1
CUTA	1.5E+08	1.0E+08	6.8E+06	0.0E+00	2.1E+08	6.7E+07	1.5	∞	3.1
CLASP2	1.1E+07	0.0E+00	0.0E+00	0.0E+00	2.7E+06	0.0E+00	∞	0	∞
NDUFS7	1.7E+07	0.0E+00	2.4E+07	0.0E+00	0.0E+00	0.0E+00	∞	∞	0
ZPR1	6.5E+07	2.1E+07	4.3E+06	0.0E+00	3.4E+07	8.6E+07	3.1	∞	0.4
ERLIN1	4.2E+07	0.0E+00	0.0E+00	0.0E+00	1.9E+07	0.0E+00	∞	0	∞
TIPRL	1.1E+08	6.9E+07	1.4E+07	0.0E+00	1.2E+08	1.3E+07	1.6	∞	9.6
NUP155	1.2E+08	4.7E+06	9.4E+06	2.3E+06	6.4E+08	4.5E+08	26.5	4.1	1.5
DCTN3	1.2E+09	4.2E+08	2.8E+07	4.1E+07	7.7E+07	2.2E+07	2.8	0.7	3.5
SNCG	2.3E+08	2.3E+07	8.9E+05	0.0E+00	0.0E+00	3.7E+07	10.2	∞	0
UBXN7	3.3E+07	0.0E+00	2.3E+07	0.0E+00	9.1E+07	7.8E+07	∞	∞	1.2
PROSC	1.5E+08	7.6E+07	6.1E+07	8.2E+07	1.9E+08	8.4E+07	2	0.8	2.3
GLS	4.5E+08	8.2E+07	0.0E+00	0.0E+00	5.5E+08	1.3E+08	5.5	0	4.3

Gene name	T1 WT	T2 MT	T2 WT	T2 MT	T3 WT	T3 MT	T1 fold change	T2 fold change	T3 fold change
HEXIM1	9.4E+07	0.0E+00	2.0E+07	2.2E+07	4.8E+07	1.8E+07	∞	1	2.6
KIF4A	1.3E+07	4.8E+06	0.0E+00	0.0E+00	2.7E+08	8.1E+07	2.9	0	3.4
PGM3	1.2E+08	1.6E+08	1.5E+08	5.8E+07	2.2E+08	8.3E+07	0.8	2.6	2.7
UTS2	0.0E+00	0.0E+00	1.3E+09	2.0E+07	3.9E+07	0.0E+00	0	69.1	∞
TDP2	2.0E+07	0.0E+00	8.9E+06	0.0E+00	2.0E+07	2.8E+07	∞	∞	0.8
DDAH2	6.3E+07	0.0E+00	1.3E+07	6.5E+06	1.4E+07	5.3E+07	∞	2	0.3
ACTL6A	4.4E+08	1.7E+08	2.6E+07	1.4E+08	1.1E+09	1.6E+08	2.7	0.2	7.2
GLUD1	4.6E+08	7.5E+08	6.5E+08	1.5E+08	1.9E+09	1.1E+08	0.7	4.3	17.1
HPRT1	1.8E+09	3.5E+08	2.9E+08	1.2E+08	3.1E+08	2.3E+07	5.1	2.6	13.7
AK1	1.1E+09	5.4E+08	1.9E+08	4.3E+07	3.1E+08	2.9E+07	2.2	4.5	10.6
ALDOA	4.8E+10	2.9E+10	1.2E+10	5.4E+09	5.7E+10	4.9E+09	1.7	2.2	11.6
SOD2	2.1E+09	2.2E+09	2.2E+08	7.9E+07	2.9E+09	3.5E+08	1	2.9	8.5
EIF2S1	4.0E+09	3.0E+09	1.9E+09	9.8E+08	4.0E+09	1.7E+09	1.4	2	2.5
S100A6	4.4E+10	2.3E+10	6.9E+09	2.5E+08	6.5E+08	1.3E+10	2	27.4	0.1
EPHX1	3.4E+07	0.0E+00	3.4E+07	0.0E+00	8.6E+07	3.6E+07	∞	∞	2.5
ANXA2	4.0E+10	2.7E+10	1.1E+10	4.1E+09	4.4E+10	2.2E+09	1.6	2.8	20.1
APRT	1.6E+09	7.9E+08	4.4E+08	2.4E+08	1.5E+09	4.4E+08	2.1	1.9	3.4
SNRNP70	0.0E+00	1.9E+07	8.3E+07	3.8E+07	6.9E+07	3.3E+07	0	2.2	2.2
ANXA5	7.7E+09	6.0E+09	1.7E+09	4.5E+08	9.3E+09	4.2E+09	1.3	3.8	2.3
HMGB1	1.1E+09	1.3E+09	1.3E+08	5.5E+07	1.8E+09	6.4E+08	0.9	2.4	2.9
DLD	1.3E+08	3.8E+08	8.5E+08	3.6E+08	2.7E+09	5.9E+08	0.4	2.4	4.6
SNRPA1	1.2E+09	1.0E+09	3.0E+08	1.3E+08	8.0E+08	2.0E+08	1.2	2.3	4.1
ALDOC	3.8E+09	1.8E+09	6.8E+08	5.5E+08	3.2E+09	3.8E+08	2.1	1.3	8.4
CHTF8	0.0E+00	0.0E+00	3.0E+07	0.0E+00	3.6E+07	0.0E+00	0	∞	∞
DLAT	1.3E+08	2.1E+08	3.3E+07	8.3E+06	5.5E+08	2.8E+08	0.7	4.1	2
ESD	6.1E+08	4.0E+08	1.2E+07	0.0E+00	1.2E+08	0.0E+00	1.6	∞	∞
IGF2R	1.4E+08	1.1E+07	2.9E+06	0.0E+00	2.1E+08	1.7E+08	12	∞	1.3
CKMT1A	2.3E+07	0.0E+00	8.7E+06	0.0E+00	4.0E+07	0.0E+00	∞	∞	∞
APEH	3.9E+07	0.0E+00	9.2E+07	7.1E+07	3.7E+08	1.8E+08	∞	1.3	2
ENO3	3.2E+08	7.8E+07	2.0E+07	1.2E+07	7.0E+08	3.6E+08	4.1	1.7	2
MTHFD2	1.5E+08	3.1E+07	1.1E+07	0.0E+00	9.3E+07	1.2E+08	4.8	∞	0.8
FDPS	4.2E+09	5.1E+08	3.2E+08	1.8E+08	1.5E+09	3.6E+08	8.3	1.9	4.2
CPM	2.6E+07	1.4E+07	2.2E+06	0.0E+00	4.8E+07	0.0E+00	1.9	∞	∞
CD46	4.3E+08	2.0E+08	8.4E+07	1.4E+07	8.1E+07	5.2E+07	2.2	6.1	1.6
NME1	5.2E+09	1.8E+09	7.1E+08	4.2E+07	1.6E+09	4.8E+08	3	17	3.4
DSP	5.1E+07	1.9E+06	0.0E+00	8.8E+06	1.9E+08	6.6E+07	27.1	0	3
NQO2	5.3E+08	1.5E+08	5.7E+07	1.7E+07	5.5E+07	0.0E+00	3.5	3.4	∞
FAH	0.0E+00	1.6E+07	2.3E+07	1.1E+07	1.8E+07	5.3E+06	0	2.1	3.5
STMN1	8.5E+08	4.4E+08	1.1E+08	1.0E+08	2.3E+08	8.6E+07	2	1.1	2.7

Gene name	T1 WT	T2 MT	T2 WT	T2 MT	T3 WT	T3 MT	T1 fold change	T2 fold change	T3 fold change
ITGA2	2.3E+08	0.0E+00	0.0E+00	2.5E+07	6.0E+08	3.1E+08	∞	0	2
PRKACA	3.0E+08	1.2E+08	5.6E+06	3.8E+06	4.4E+08	9.0E+07	2.6	1.5	4.9
CAPN2	0.0E+00	0.0E+00	1.2E+07	0.0E+00	7.6E+07	3.9E+07	0	∞	2
LGALS3	4.6E+09	1.9E+09	2.4E+08	4.6E+08	4.0E+09	1.3E+09	2.5	0.6	3.1
ATP5J	1.3E+08	4.0E+07	0.0E+00	6.0E+05	3.6E+07	0.0E+00	3.3	0	∞
PSMB1	1.5E+09	1.8E+09	5.9E+08	1.8E+08	8.0E+08	1.8E+08	0.9	3.4	4.5
ATP6V1C1	3.4E+08	1.0E+08	1.2E+06	0.0E+00	1.3E+08	1.6E+08	3.4	∞	0.9
SCP2	2.1E+08	1.0E+08	0.0E+00	0.0E+00	3.1E+07	0.0E+00	2.2	0	∞
NME2	6.5E+07	7.3E+07	2.6E+07	0.0E+00	1.3E+08	0.0E+00	0.9	∞	∞
FDXR	2.8E+07	0.0E+00	9.4E+06	2.5E+06	3.7E+07	3.1E+07	∞	3.8	1.3
TUBG2	1.5E+08	2.6E+07	7.4E+06	0.0E+00	7.6E+06	0.0E+00	5.9	∞	∞
NFYA	2.3E+07	0.0E+00	0.0E+00	0.0E+00	1.4E+07	0.0E+00	∞	0	∞
ACP1	2.3E+09	9.3E+08	3.2E+08	1.8E+08	7.1E+08	1.7E+08	2.5	1.8	4.2
MPST	3.2E+08	3.8E+08	5.9E+07	1.6E+07	1.1E+08	2.4E+07	0.9	3.8	4.4
RPS12	1.1E+10	4.7E+09	1.3E+09	6.1E+08	3.4E+09	1.2E+09	2.3	2.2	2.9
PSMA4	8.3E+08	5.7E+08	3.3E+08	1.6E+08	1.5E+09	3.3E+08	1.5	2.1	4.6
S100P	4.2E+09	1.7E+07	7.3E+08	9.3E+08	2.1E+09	1.1E+09	248.6	0.8	2
TARS	2.8E+09	1.2E+09	1.5E+09	1.4E+09	6.7E+09	1.6E+09	2.3	1.1	4.3
PSMB8	2.6E+08	1.3E+08	4.7E+07	1.3E+07	1.3E+08	0.0E+00	2	3.7	∞
PSMB4	2.1E+09	2.0E+09	9.6E+08	4.1E+08	1.0E+09	2.5E+08	1.1	2.4	4.3
PSMB6	2.3E+09	2.2E+09	1.0E+09	4.6E+08	1.2E+09	2.2E+08	1.1	2.3	5.5
PSMB5	1.4E+09	1.1E+09	7.8E+08	2.6E+08	1.6E+09	1.0E+08	1.3	3	16.1
TM4SF1	0.0E+00	0.0E+00	3.6E+07	0.0E+00	8.9E+06	0.0E+00	0	∞	∞
CASP14	2.4E+08	1.7E+07	0.0E+00	1.2E+07	3.4E+08	3.4E+07	14.4	0	10
KIF5B	2.3E+08	4.3E+07	4.5E+07	1.6E+07	8.1E+08	1.9E+09	5.4	2.8	0.5
SPR	5.5E+08	2.2E+08	3.6E+07	1.0E+08	8.3E+07	0.0E+00	2.6	0.4	∞
FUS	1.1E+09	2.0E+08	2.1E+07	6.0E+07	1.8E+08	8.4E+07	5.7	0.4	2.2
GLRX	2.8E+08	1.4E+07	7.2E+06	0.0E+00	0.0E+00	0.0E+00	20	∞	0
ARL2	2.7E+08	2.8E+07	5.0E+07	3.0E+07	1.5E+08	0.0E+00	9.8	1.7	∞
NUDT1	4.5E+08	2.5E+07	2.8E+07	0.0E+00	0.0E+00	0.0E+00	17.7	∞	0
NUP62	3.8E+07	0.0E+00	0.0E+00	1.6E+07	5.5E+07	0.0E+00	∞	0	∞
TXLNA	1.8E+07	1.2E+08	4.2E+07	1.9E+07	1.7E+08	7.0E+07	0.2	2.2	2.4
NAA10	5.3E+08	1.6E+08	0.0E+00	3.6E+07	4.6E+08	1.9E+08	3.4	0	2.5
PPP1R2P3	5.1E+08	1.2E+07	0.0E+00	1.6E+07	5.6E+08	1.6E+08	43.7	0	3.7
STAT1	5.3E+07	8.0E+07	4.8E+07	1.1E+07	3.3E+08	1.5E+08	0.7	4.6	2.3
EPS15	3.9E+07	0.0E+00	0.0E+00	5.0E+06	5.5E+07	2.6E+07	∞	0	2.2
CRKL	1.5E+08	2.0E+08	1.7E+07	0.0E+00	3.8E+07	0.0E+00	0.8	∞	∞
ALDH9A1	9.3E+07	1.3E+08	1.9E+07	0.0E+00	6.3E+08	4.8E+07	0.8	∞	13.2
DHPS	8.2E+07	0.0E+00	1.2E+07	0.0E+00	0.0E+00	0.0E+00	∞	∞	0

Gene name	T1 WT	T2 MT	T2 WT	T2 MT	T3 WT	T3 MT	T1 fold change	T2 fold change	T3 fold change
PRIM1	2.1E+07	9.0E+06	1.1E+07	0.0E+00	2.4E+07	3.0E+07	2.4	∞	0.8
PSMB2	1.4E+09	4.4E+08	1.7E+08	1.3E+08	4.7E+08	1.0E+08	3.3	1.4	4.7
EIF2B2	1.0E+08	4.4E+08	4.3E+07	0.0E+00	1.6E+08	5.2E+07	0.3	∞	3.1
NUP153	3.8E+07	0.0E+00	0.0E+00	0.0E+00	2.0E+07	0.0E+00	∞	0	∞
NT5C2	1.6E+07	0.0E+00	5.7E+06	0.0E+00	3.1E+07	1.0E+07	∞	∞	3
SEPHS1	8.4E+07	7.0E+06	2.3E+07	0.0E+00	2.1E+07	0.0E+00	12	∞	∞
KNTC1	1.9E+07	2.6E+07	8.1E+07	0.0E+00	3.4E+08	1.5E+08	0.8	∞	2.3
PPT1	5.5E+08	0.0E+00	3.1E+07	0.0E+00	7.7E+07	3.1E+07	∞	∞	2.6
FXR2	3.6E+07	0.0E+00	2.2E+06	0.0E+00	2.2E+07	4.4E+07	∞	∞	0.6
MMP15	0.0E+00	0.0E+00	1.1E+07	0.0E+00	7.2E+07	3.8E+07	0	∞	2
SMARCA4	2.2E+07	0.0E+00	0.0E+00	5.4E+06	8.0E+07	3.0E+07	∞	0	2.7
METAP1	6.4E+07	0.0E+00	2.5E+07	1.8E+07	1.2E+08	0.0E+00	∞	1.4	∞
BID	2.0E+08	2.6E+07	1.9E+07	0.0E+00	3.2E+07	6.2E+07	8	∞	0.6
KCNQ4	7.1E+08	7.0E+08	4.6E+07	0.0E+00	3.9E+08	0.0E+00	1.1	∞	∞
SEC61G	1.9E+08	0.0E+00	0.0E+00	4.1E+06	3.7E+07	1.3E+07	∞	0	2.9
CXCR4	0.0E+00	6.2E+07	3.2E+07	1.4E+07	9.8E+07	0.0E+00	0	2.4	∞
UBE2K	3.6E+08	5.7E+08	5.1E+08	1.8E+08	3.2E+08	8.2E+07	0.7	2.9	3.9
RPL37A	6.9E+08	1.3E+09	1.7E+08	7.7E+07	5.6E+08	2.6E+08	0.6	2.2	2.3
HSPE1	1.4E+09	6.7E+08	3.5E+08	2.7E+08	5.6E+08	1.2E+08	2.2	1.3	4.7
SUMO2	1.2E+09	0.0E+00	1.4E+08	1.0E+08	2.8E+08	8.4E+07	∞	1.4	3.4
RPS29	8.0E+08	3.5E+08	4.4E+07	1.2E+07	9.6E+08	6.6E+07	2.4	3.7	14.6
CNBP	9.8E+07	5.8E+07	4.9E+06	0.0E+00	6.2E+07	2.8E+07	1.8	∞	2.3
RPL32	2.8E+09	3.3E+09	2.5E+08	5.8E+07	2.7E+09	1.1E+09	0.9	4.4	2.6
DYNLT1	2.0E+08	4.7E+07	0.0E+00	1.6E+07	1.6E+07	7.5E+06	4.3	0	2.2
UBE2I	6.6E+08	2.6E+08	1.5E+07	0.0E+00	1.4E+08	2.0E+07	2.6	∞	7.2
HIST2H3A	1.5E+09	5.4E+08	3.8E+08	5.5E+08	1.5E+09	7.1E+08	2.8	0.7	2.2
GSTO1	1.6E+09	3.2E+08	1.2E+08	4.2E+07	9.1E+07	1.1E+08	4.9	2.8	0.9
MRPS34	1.7E+08	2.5E+08	2.1E+07	0.0E+00	2.4E+08	1.2E+08	0.7	∞	2.1
RPL36AL	1.2E+09	1.9E+09	1.9E+08	4.9E+07	6.6E+08	2.9E+08	0.7	4	2.3
RPL19	4.7E+09	1.2E+09	8.3E+08	9.7E+08	4.2E+09	8.9E+08	4.1	0.9	4.8
SPTBN1	4.4E+08	0.0E+00	2.9E+08	1.4E+08	5.5E+08	6.5E+08	∞	2.1	0.9
HMGCS1	2.2E+07	0.0E+00	1.3E+07	0.0E+00	1.1E+08	1.4E+08	∞	∞	0.9
AKAP12	2.8E+08	1.6E+07	3.9E+07	3.2E+07	5.1E+08	2.0E+08	16.8	1.3	2.6
GLO1	4.0E+09	1.2E+09	9.6E+08	6.2E+08	1.4E+09	5.9E+08	3.5	1.6	2.4
PLP2	1.4E+09	5.5E+08	9.4E+06	0.0E+00	1.9E+08	3.3E+08	2.7	∞	0.6
TJP1	4.8E+07	1.2E+07	0.0E+00	0.0E+00	1.7E+08	6.3E+07	4	0	2.7
KLC1	4.2E+07	0.0E+00	0.0E+00	0.0E+00	5.1E+07	2.1E+07	∞	0	2.4
DHX9	6.6E+08	1.6E+08	5.2E+08	1.6E+08	1.8E+09	1.9E+09	4.2	3.4	1
CRYZ	7.5E+08	3.5E+08	1.2E+08	9.3E+07	6.0E+08	8.3E+06	2.2	1.3	71.7

Gene name	T1 WT	T2 MT	T2 WT	T2 MT	T3 WT	T3 MT	T1 fold change	T2 fold change	T3 fold change
HDHD1	1.0E+08	1.3E+08	4.4E+07	0.0E+00	2.9E+07	0.0E+00	0.8	∞	∞
AP1B1	8.8E+06	0.0E+00	0.0E+00	0.0E+00	2.2E+08	3.7E+07	∞	0	6
LMAN2	1.3E+09	6.7E+08	1.6E+08	1.1E+09	2.5E+09	5.2E+08	2	0.2	4.9
ANK3	1.0E+07	0.0E+00	0.0E+00	0.0E+00	1.6E+07	7.7E+06	∞	0	2.1
MTAP	1.6E+08	1.8E+07	0.0E+00	0.0E+00	5.2E+06	0.0E+00	8.8	0	∞
SRSF6	0.0E+00	3.7E+08	3.0E+07	1.4E+07	2.3E+08	3.0E+07	0	2.2	7.7
PDAP1	4.2E+08	1.1E+08	5.6E+07	3.1E+07	4.6E+07	1.7E+07	3.7	1.9	2.8
CUL1	9.3E+07	3.6E+07	4.8E+06	6.1E+06	4.1E+08	1.3E+08	2.6	0.8	3.1
FHL3	5.1E+07	7.4E+07	4.2E+07	0.0E+00	6.0E+07	0.0E+00	0.7	∞	∞
COTL1	2.5E+09	1.9E+09	6.2E+08	5.9E+07	6.1E+08	1.8E+08	1.4	10.6	3.5
IL18	2.1E+08	5.0E+07	5.0E+06	0.0E+00	3.3E+07	0.0E+00	4.3	∞	∞
SCRIB	2.9E+07	0.0E+00	1.8E+07	0.0E+00	1.4E+08	1.5E+08	∞	∞	1
ENDOG	3.6E+07	0.0E+00	1.1E+07	1.5E+06	7.6E+06	0.0E+00	∞	7.2	∞
SMC1A	8.6E+08	1.4E+08	1.6E+07	8.6E+07	2.0E+09	8.1E+08	6.2	0.2	2.5
EXOSC7	9.6E+07	8.5E+07	5.3E+06	0.0E+00	3.0E+07	1.2E+07	1.2	∞	2.6
ARL6IP1	2.1E+08	0.0E+00	5.7E+06	0.0E+00	1.0E+08	2.9E+07	∞	∞	3.5
RAB3GAP 1	1.7E+07	0.0E+00	0.0E+00	0.0E+00	2.9E+07	0.0E+00	∞	0	∞
PAFAH1B3	5.3E+07	0.0E+00	1.3E+08	1.1E+08	1.1E+08	5.0E+07	∞	1.3	2.2
PPA1	5.2E+09	2.1E+09	3.0E+08	3.1E+08	1.3E+09	4.5E+08	2.5	1	3
RSU1	2.5E+08	4.2E+07	5.0E+06	0.0E+00	2.3E+08	2.7E+08	6	∞	0.9
SEC23B	0.0E+00	2.1E+07	2.9E+07	8.6E+06	1.7E+08	3.8E+07	0	3.4	4.4
SKIV2L	9.9E+07	0.0E+00	0.0E+00	0.0E+00	8.8E+07	3.1E+07	∞	0	2.9
SLC9A3R2	8.7E+07	0.0E+00	2.1E+07	0.0E+00	9.0E+07	5.0E+07	∞	∞	1.8
SF1	5.4E+08	1.5E+08	2.8E+08	7.4E+07	2.8E+08	6.3E+08	3.7	3.9	0.5
UBE2V2	6.4E+08	4.9E+08	2.7E+08	7.5E+07	1.4E+08	6.8E+07	1.4	3.6	2.1
FXN	1.9E+07	1.8E+08	2.4E+06	0.0E+00	6.6E+07	0.0E+00	0.2	∞	∞
DECR1	8.4E+08	1.7E+08	2.1E+07	9.7E+07	1.4E+08	6.6E+07	5	0.3	2.1
TST	3.4E+08	1.3E+08	1.7E+07	1.4E+07	2.6E+08	1.1E+08	2.6	1.2	2.5
GUK1	5.6E+07	0.0E+00	3.8E+07	1.2E+07	5.4E+07	4.1E+07	∞	3.2	1.4
HAGH	5.8E+07	0.0E+00	4.2E+07	4.9E+07	7.2E+07	0.0E+00	∞	0.9	∞
IMMT	3.2E+07	3.5E+06	1.0E+08	4.5E+07	2.6E+08	1.2E+08	9.3	2.3	2.1
HFE	1.4E+07	0.0E+00	0.0E+00	0.0E+00	3.2E+07	1.6E+07	∞	0	2
NADK2	1.3E+08	2.1E+08	3.3E+07	1.4E+07	2.1E+08	3.9E+07	0.7	2.3	5.6
TBC1D10B	3.4E+07	4.6E+07	7.1E+07	0.0E+00	1.2E+08	4.8E+07	0.8	∞	2.6
HS1BP3	2.0E+07	0.0E+00	0.0E+00	0.0E+00	1.3E+07	0.0E+00	∞	0	∞
RRP12	6.0E+06	0.0E+00	6.3E+06	0.0E+00	1.4E+08	6.6E+07	∞	∞	2.2
EXOSC6	6.8E+08	6.7E+08	7.9E+07	5.2E+06	1.7E+08	1.1E+07	1.1	15.2	16.3
HP1BP3	0.0E+00	5.2E+07	8.0E+07	1.7E+07	2.8E+08	1.2E+08	0	4.8	2.4
RARS2	1.0E+07	0.0E+00	0.0E+00	0.0E+00	7.6E+05	0.0E+00	∞	0	∞

Gene name	T1 WT	T2 MT	T2 WT	T2 MT	T3 WT	T3 MT	T1 fold change	T2 fold change	T3 fold change
UBAP2	4.1E+06	0.0E+00	0.0E+00	0.0E+00	3.0E+07	0.0E+00	∞	0	∞
KIF24	3.4E+08	1.3E+08	1.2E+08	9.0E+07	5.2E+08	4.9E+07	2.8	1.4	10.7
NT5DC1	1.5E+08	1.8E+08	9.8E+07	3.9E+07	6.1E+08	2.6E+08	0.9	2.5	2.4
RNF20	2.3E+07	0.0E+00	0.0E+00	4.6E+07	2.4E+08	1.2E+08	∞	0	2
LYPLAL1	5.8E+07	1.3E+07	0.0E+00	0.0E+00	2.7E+07	0.0E+00	4.5	0	∞
RRAGA	3.2E+07	4.7E+07	1.5E+07	0.0E+00	1.8E+07	0.0E+00	0.7	∞	∞
RNF213	9.0E+07	3.0E+07	6.7E+06	0.0E+00	0.0E+00	5.2E+06	3.1	∞	0
NSUN5P2	0.0E+00	0.0E+00	1.0E+07	0.0E+00	1.7E+07	0.0E+00	0	∞	∞
FAM91A1	0.0E+00	0.0E+00	2.6E+06	0.0E+00	8.9E+07	2.1E+07	0	∞	4.3
MZT2B	2.5E+07	3.0E+07	1.6E+06	0.0E+00	1.1E+08	4.3E+07	0.9	∞	2.7
MRPL14	1.3E+06	0.0E+00	5.9E+06	0.0E+00	2.3E+07	1.4E+07	∞	∞	1.7
METTL2B	7.3E+07	0.0E+00	3.5E+07	1.5E+07	7.2E+07	6.7E+07	∞	2.5	1.1
PGM2L1	5.6E+07	0.0E+00	0.0E+00	0.0E+00	6.7E+07	0.0E+00	∞	0	∞
RANBP10	6.0E+07	0.0E+00	1.8E+07	0.0E+00	9.0E+07	0.0E+00	∞	∞	∞
QSOX2	2.4E+07	1.3E+07	0.0E+00	0.0E+00	1.9E+06	0.0E+00	2	0	∞
UBE2R2	1.4E+08	6.4E+07	5.0E+06	0.0E+00	0.0E+00	0.0E+00	2.3	∞	0
NUP54	2.2E+07	0.0E+00	0.0E+00	0.0E+00	1.9E+07	0.0E+00	∞	0	∞
NUFIP2	1.7E+07	0.0E+00	4.9E+07	6.2E+06	0.0E+00	2.0E+07	∞	8.1	0
IRF2BP2	2.0E+08	1.1E+08	1.1E+07	0.0E+00	5.5E+07	7.9E+07	2	∞	0.8
GLRX5	1.1E+08	3.8E+08	5.0E+07	2.1E+07	7.8E+07	0.0E+00	0.3	2.4	∞
SETD3	2.7E+07	0.0E+00	2.7E+07	3.9E+06	3.0E+07	1.7E+07	∞	7	1.8
ZC3H18	9.5E+06	0.0E+00	0.0E+00	0.0E+00	4.2E+07	1.4E+07	∞	0	3
ERC1	1.0E+08	0.0E+00	0.0E+00	0.0E+00	4.3E+08	4.0E+07	∞	0	10.7
CCAR1	1.4E+07	0.0E+00	0.0E+00	8.3E+06	4.9E+07	2.6E+07	∞	0	2
SUPV3L1	1.4E+08	1.4E+08	1.4E+07	0.0E+00	9.1E+07	3.5E+07	1.1	∞	2.6
PHACTR4	0.0E+00	0.0E+00	9.0E+06	0.0E+00	2.9E+07	9.3E+06	0	∞	3.1
EHP1L1	7.2E+07	3.0E+07	3.9E+06	0.0E+00	5.3E+08	1.4E+08	2.4	∞	3.7
TTC9C	1.2E+08	5.9E+07	7.9E+06	0.0E+00	7.6E+07	5.3E+07	2.1	∞	1.5
NPEPL1	9.6E+06	0.0E+00	0.0E+00	5.2E+07	1.1E+08	1.5E+07	∞	0	7.4
MRPL30	3.5E+07	1.2E+08	1.1E+07	3.8E+06	5.0E+06	0.0E+00	0.3	3.1	∞
CEP192	3.8E+07	0.0E+00	0.0E+00	0.0E+00	2.8E+08	1.7E+07	∞	0	16.3
GEMIN5	5.3E+07	0.0E+00	1.4E+07	3.7E+06	3.8E+08	2.6E+08	∞	3.8	1.5
SHROOM3	7.5E+06	0.0E+00	1.6E+08	3.4E+05	0.0E+00	0.0E+00	∞	459.2	0
PTPMT1	2.2E+07	0.0E+00	0.0E+00	4.9E+06	4.9E+07	2.2E+07	∞	0	2.3
LEO1	4.6E+07	2.0E+07	7.3E+06	6.7E+06	1.4E+08	6.7E+07	2.3	1.1	2.1
PCNP	8.1E+08	1.9E+08	0.0E+00	0.0E+00	1.3E+07	0.0E+00	4.3	0	∞
NELFB	1.7E+08	6.3E+07	8.2E+07	4.3E+07	2.5E+08	2.8E+08	2.7	2	0.9
GEMIN6	2.1E+08	1.1E+08	0.0E+00	0.0E+00	2.4E+07	0.0E+00	2.1	0	∞
DDX1	5.8E+08	2.3E+08	2.3E+08	5.4E+08	2.6E+09	1.0E+09	2.5	0.5	2.6

Gene name	T1 WT	T2 MT	T2 WT	T2 MT	T3 WT	T3 MT	T1 fold change	T2 fold change	T3 fold change
ANP32B	4.0E+09	2.1E+09	3.1E+08	5.4E+08	3.2E+09	1.4E+09	2	0.6	2.4
DLG3	2.2E+07	9.3E+06	0.0E+00	0.0E+00	1.5E+07	0.0E+00	2.4	0	∞
ZNF622	2.0E+07	0.0E+00	9.2E+06	0.0E+00	1.4E+07	1.9E+07	∞	∞	0.8
PSMG2	1.0E+08	1.7E+07	3.0E+07	0.0E+00	1.6E+08	0.0E+00	6.3	∞	∞
ISOC2	5.7E+07	1.9E+07	0.0E+00	0.0E+00	3.6E+07	0.0E+00	3	0	∞
FERMT2	2.8E+07	0.0E+00	6.3E+07	6.8E+06	1.1E+08	1.4E+08	∞	9.4	0.8
ISOC1	5.3E+08	1.1E+08	9.8E+07	2.0E+07	3.1E+08	1.2E+08	4.9	4.9	2.6
FLYWCH2	1.4E+09	1.7E+08	1.4E+08	6.8E+07	7.1E+07	4.8E+07	8.2	2.1	1.5
MALSU1	9.0E+07	2.5E+07	6.7E+06	6.0E+06	5.7E+07	0.0E+00	3.6	1.2	∞
DAZAP1	9.1E+07	0.0E+00	0.0E+00	0.0E+00	4.6E+07	2.2E+07	∞	0	2.1
MED30	5.3E+07	0.0E+00	2.4E+05	1.4E+07	4.9E+07	0.0E+00	∞	0.1	∞
PGAM5	1.7E+08	1.8E+05	3.6E+07	3.4E+07	1.3E+08	0.0E+00	928.3	1.1	∞
DDRKG1	6.7E+07	2.1E+08	1.2E+08	4.5E+07	1.3E+08	2.6E+07	0.4	2.8	5
TMX3	0.0E+00	0.0E+00	4.8E+07	0.0E+00	2.7E+08	0.0E+00	0	∞	∞
PRRC1	2.2E+07	0.0E+00	0.0E+00	0.0E+00	9.2E+06	3.5E+06	∞	0	2.7
C16orf13	1.2E+07	0.0E+00	0.0E+00	0.0E+00	4.0E+07	0.0E+00	∞	0	∞
ADO	1.2E+08	0.0E+00	1.9E+07	0.0E+00	0.0E+00	0.0E+00	∞	∞	0
MMS19	1.2E+06	0.0E+00	0.0E+00	0.0E+00	1.6E+07	0.0E+00	∞	0	∞
MYCBP	2.8E+08	1.3E+08	1.8E+07	0.0E+00	6.4E+07	2.5E+07	2.3	∞	2.6
PSMB7	1.2E+07	7.7E+07	5.0E+07	1.1E+07	1.3E+08	2.4E+07	0.2	4.6	5.6
PARK7	2.2E+09	9.3E+08	1.1E+08	3.9E+07	1.7E+08	9.6E+07	2.4	2.9	1.8
TSG101	0.0E+00	7.4E+07	8.7E+06	0.0E+00	2.0E+08	3.6E+07	0	∞	5.6
BAG1	4.9E+08	2.2E+08	3.0E+07	1.5E+07	7.4E+08	9.2E+07	2.3	2.1	8.1
MACROD1	2.7E+07	0.0E+00	2.4E+07	1.0E+07	4.4E+08	2.3E+08	∞	2.4	2
VKORC1	9.3E+07	2.4E+08	4.2E+06	0.0E+00	6.6E+07	0.0E+00	0.4	∞	∞
TXNDC17	1.5E+08	7.5E+07	1.6E+07	0.0E+00	2.6E+07	0.0E+00	2	∞	∞
ADPGK	0.0E+00	1.7E+07	5.4E+06	0.0E+00	3.1E+07	0.0E+00	0	∞	∞
NTPCR	1.5E+08	2.3E+07	0.0E+00	0.0E+00	2.0E+08	0.0E+00	6.7	0	∞
MED18	3.5E+07	0.0E+00	0.0E+00	0.0E+00	1.1E+07	0.0E+00	∞	0	∞
HNRNPUL1	0.0E+00	2.0E+07	1.2E+07	0.0E+00	2.3E+08	7.5E+07	0	∞	3.2
HTATIP2	9.3E+08	9.5E+08	4.3E+08	2.0E+08	9.0E+08	4.5E+08	1	2.3	2
APOO	1.9E+08	7.8E+07	1.2E+07	1.9E+07	3.3E+07	0.0E+00	2.5	0.6	∞
WDR18	0.0E+00	2.6E+07	2.3E+07	0.0E+00	1.3E+08	2.3E+07	0	∞	5.7
KIFC3	2.1E+08	0.0E+00	0.0E+00	0.0E+00	7.3E+07	1.8E+06	∞	0	40.2
SFXN3	5.1E+07	3.9E+07	3.0E+06	0.0E+00	1.6E+08	5.3E+07	1.3	∞	3
AP1M1	2.3E+08	5.3E+07	0.0E+00	0.0E+00	2.0E+08	8.5E+07	4.4	0	2.4
NUF2	3.8E+07	3.2E+07	3.8E+07	0.0E+00	5.6E+07	0.0E+00	1.2	∞	∞
SH3BGRL3	0.0E+00	0.0E+00	5.6E+07	0.0E+00	5.4E+07	2.2E+07	0	∞	2.5

Gene name	T1 WT	T2 MT	T2 WT	T2 MT	T3 WT	T3 MT	T1 fold change	T2 fold change	T3 fold change
PDCL3	2.6E+07	1.8E+08	1.7E+07	0.0E+00	2.4E+08	6.2E+07	0.2	∞	3.9
RAB3GAP2	1.4E+07	0.0E+00	0.0E+00	0.0E+00	1.5E+08	7.0E+07	∞	0	2.2
PPA2	4.5E+08	4.6E+08	8.9E+07	1.8E+07	1.6E+08	4.0E+07	1	5	4
RABEP2	0.0E+00	0.0E+00	1.6E+07	0.0E+00	3.7E+07	1.3E+07	0	∞	2.8
RANBP3	5.4E+07	1.1E+07	1.5E+07	7.7E+06	1.1E+08	2.8E+07	5.1	2	3.9
DCTPP1	3.9E+08	2.6E+07	0.0E+00	0.0E+00	4.4E+07	0.0E+00	14.7	0	∞
L2HGDH	3.4E+07	2.4E+08	6.6E+07	1.7E+07	2.1E+08	7.4E+07	0.2	3.9	3
COPS7B	3.5E+07	0.0E+00	4.4E+07	0.0E+00	8.5E+07	2.1E+08	∞	∞	0.4
C12orf10	1.6E+08	8.1E+07	4.4E+06	0.0E+00	3.2E+08	7.5E+06	2	∞	42.9
SDF2L1	1.4E+08	1.8E+08	4.7E+07	0.0E+00	4.5E+07	0.0E+00	0.8	∞	∞
SRA1	9.3E+07	1.7E+07	1.3E+07	0.0E+00	0.0E+00	0.0E+00	5.5	∞	0
CHMP1A	2.2E+07	0.0E+00	2.9E+07	0.0E+00	0.0E+00	0.0E+00	∞	∞	0
VTA1	4.4E+08	4.6E+08	1.1E+08	4.4E+07	3.6E+08	1.3E+08	1	2.6	2.7
MRPS30	2.8E+07	5.3E+05	0.0E+00	1.3E+07	4.4E+07	5.4E+06	52.5	0	8.3
DMAP1	0.0E+00	0.0E+00	1.4E+07	0.0E+00	2.2E+08	4.3E+07	0	∞	5.3
ANLN	1.4E+08	5.7E+07	0.0E+00	1.8E+07	1.6E+08	1.1E+07	2.5	0	14.1
ACSS2	0.0E+00	0.0E+00	4.0E+06	0.0E+00	5.4E+07	2.0E+07	0	∞	2.7
DIABLO	7.1E+08	2.5E+08	6.3E+07	0.0E+00	2.2E+08	7.1E+07	2.9	∞	3.1
OSTC	0.0E+00	0.0E+00	6.2E+06	0.0E+00	5.1E+07	0.0E+00	0	∞	∞
DROSHA	2.0E+09	0.0E+00	0.0E+00	0.0E+00	2.4E+07	0.0E+00	∞	0	∞
IARS2	2.3E+07	0.0E+00	4.0E+07	0.0E+00	2.8E+08	2.2E+08	∞	∞	1.3
ABCF3	2.7E+07	1.8E+07	1.8E+07	0.0E+00	1.5E+08	7.2E+07	1.6	∞	2.1
NUDT15	6.6E+07	0.0E+00	8.3E+06	1.6E+07	7.3E+07	0.0E+00	∞	0.6	∞
FANCI	7.1E+06	0.0E+00	0.0E+00	0.0E+00	1.8E+08	4.6E+07	∞	0	3.9
NLE1	0.0E+00	1.1E+08	5.5E+07	9.6E+05	2.2E+07	0.0E+00	0	56.9	∞
GIN1	0.0E+00	0.0E+00	2.0E+07	1.9E+06	3.2E+08	1.3E+08	0	10.4	2.5
BRE	5.3E+07	1.9E+07	3.3E+06	0.0E+00	6.6E+07	6.0E+07	2.9	∞	1.1
CDKN2AIP	2.3E+08	2.3E+08	1.3E+08	2.9E+07	3.5E+08	3.4E+07	1	4.4	10.6
DNAJB12	9.7E+07	4.5E+07	0.0E+00	4.1E+07	1.6E+08	3.9E+07	2.2	0	4.2
PPP4R2	3.2E+07	0.0E+00	0.0E+00	0.0E+00	2.8E+07	0.0E+00	∞	0	∞
MRPL39	6.0E+07	3.4E+07	9.6E+05	0.0E+00	1.2E+08	8.0E+06	1.8	∞	15
FKBP11	1.8E+08	0.0E+00	6.6E+07	3.1E+07	6.5E+07	3.1E+07	∞	2.2	2.1
FAM120A	1.0E+08	1.5E+07	1.0E+07	3.4E+07	4.5E+08	2.2E+08	6.9	0.3	2.1
SPG21	0.0E+00	4.1E+07	1.6E+07	0.0E+00	1.4E+07	0.0E+00	0	∞	∞
TMEM9	0.0E+00	0.0E+00	2.5E+07	0.0E+00	3.9E+07	0.0E+00	0	∞	∞
DIP2B	1.9E+07	0.0E+00	0.0E+00	0.0E+00	9.2E+07	4.3E+07	∞	0	2.2
STARD9	5.3E+07	6.3E+07	3.1E+07	0.0E+00	7.2E+07	1.6E+07	0.9	∞	4.7
NRBP1	3.6E+07	0.0E+00	2.6E+07	2.1E+07	1.6E+08	7.0E+07	∞	1.3	2.4
VPS51	6.6E+06	0.0E+00	7.6E+06	1.4E+07	1.0E+08	5.7E+05	∞	0.6	182.5

Gene name	T1 WT	T2 MT	T2 WT	T2 MT	T3 WT	T3 MT	T1 fold change	T2 fold change	T3 fold change
AK3	3.0E+08	1.5E+08	0.0E+00	1.6E+07	2.0E+07	6.0E+06	2.1	0	3.4
MRT04	1.6E+08	3.0E+08	1.4E+08	5.4E+07	3.0E+08	7.4E+07	0.6	2.7	4.1
TMCO1	6.8E+07	3.2E+07	7.4E+06	0.0E+00	1.8E+08	8.5E+07	2.2	∞	2.1
LIMCH1	2.3E+07	0.0E+00	0.0E+00	0.0E+00	1.3E+08	6.4E+07	∞	0	2.1
VDAC3	9.0E+07	5.8E+07	1.5E+07	6.6E+06	3.3E+07	0.0E+00	1.6	2.3	∞
GDA	5.6E+07	0.0E+00	1.2E+07	0.0E+00	1.5E+08	3.6E+07	∞	∞	4.3
YARS2	2.7E+07	1.4E+08	1.5E+07	0.0E+00	2.2E+08	7.5E+07	0.2	∞	2.9
SBDS	3.7E+08	5.5E+07	3.1E+08	1.3E+07	3.2E+08	1.4E+08	6.8	23.8	2.3
RRP15	2.0E+07	0.0E+00	0.0E+00	5.3E+06	1.6E+07	0.0E+00	∞	0	∞
RNF114	4.6E+07	0.0E+00	2.1E+07	0.0E+00	3.9E+07	3.4E+07	∞	∞	1.2
NUB1	6.1E+07	0.0E+00	0.0E+00	0.0E+00	6.6E+07	2.5E+07	∞	0	2.7
NUBP2	1.9E+08	1.1E+08	3.1E+07	0.0E+00	2.2E+08	3.4E+07	1.9	∞	6.5
NFS1	1.5E+08	2.6E+07	1.0E+07	1.2E+07	4.2E+07	0.0E+00	5.6	0.9	∞
TEX264	2.1E+08	0.0E+00	0.0E+00	0.0E+00	1.0E+08	0.0E+00	∞	0	∞

^a Protein hits observed in the kemptide K-CLASP study. The peptide intensity observed for each sample (WT: N-biotin kemptide crosslinking, MT: N-biotin mutant kemptide crosslinking) for the three trials (T1: trial 1, T2: trial 2, T3: trial 3) is shown. Fold change for each trial was calculated by dividing the peptide intensity observed in the N-biotin kemptide crosslinking reaction by the peptide intensity observed for the N-biotin mutant kemptide crosslinking reaction. Infinity (∞) signifies that no peptides were observed in N-biotin mutant kemptide sample, making a numeric ratio calculation impossible. The three K-CLASP hit kinases are yellow colored.

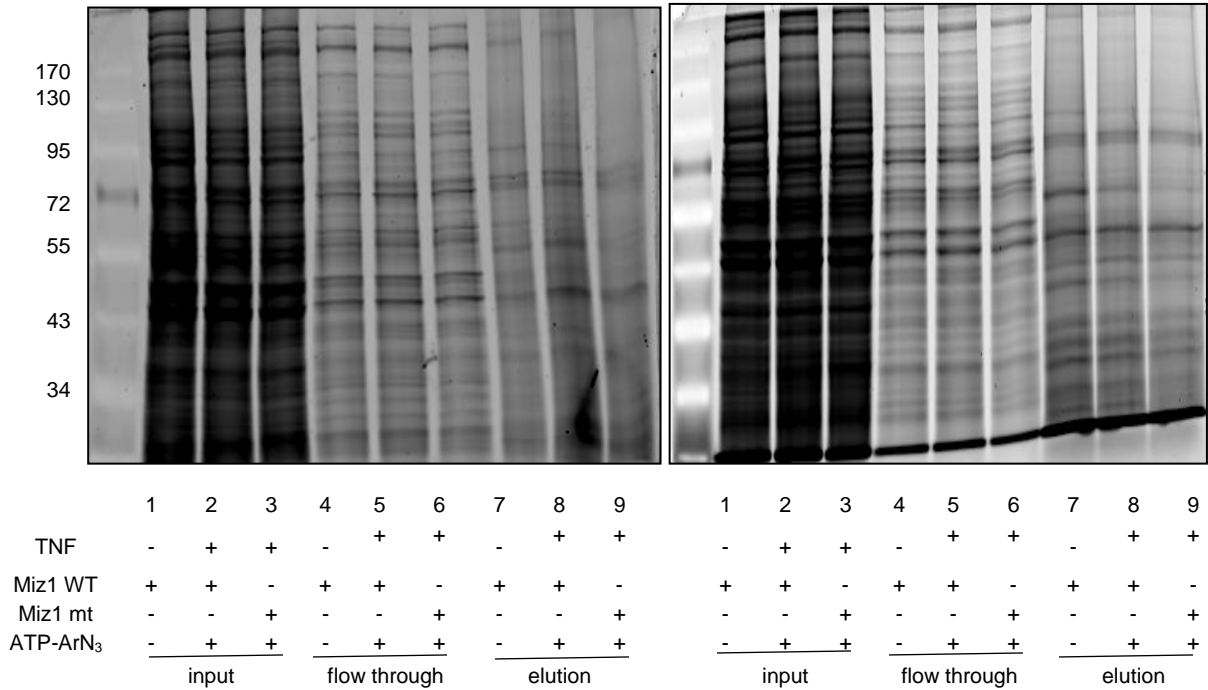


Figure A.2.7: Gel images from two replicates of the Miz1 K-CLASP experiment. Crosslinking reactions were carried out with MEF lysate and N-biotin Miz1 peptide (Miz1 WT) in the presence of ATP-ArN₃ (lanes 2, 5, and 8). Control reactions were performed with TNF untreated lysate and N-biotin Miz1 peptide (lanes 1, 4, and 7) or with N-biotin mutant Miz1 peptide (Miz1 mt) in place of N-biotin Miz1 peptide (lanes 3, 6, and 9). After reaction, biotinylated proteins were enriched using streptavidin resin. The input before streptavidin enrichment (11% loaded per gel, lanes 1-3), flow through (8% loaded per gel, lanes 4-6), and the elution from each sample (33% loaded per gel, lanes 7-9) were separated by SDS-PAGE and then stained for total proteins using SYPRO[®] Ruby stain (top gel). The shown gels were used in LC-MS/MS analysis.

Table A.2.2: Full listing of the 340 Miz1 K-CLASP hits^a

Gene names	T1 MT	T1 WT	T2 MT	T2 WT	T1 No TNF	T1 Fold change	T2 Fold change	Fold change with No TNF
Kif1b	0.0E+00	6.0E+09	1.1E+07	2.4E+07	0.0E+00	∞	2.2	∞
Rps19	0.0E+00	3.0E+07	0.0E+00	2.3E+09	0.0E+00	∞	∞	∞
Rab11b	1.8E+08	5.3E+08	0.0E+00	1.5E+09	1.7E+08	2.9	∞	3.1
Rpl36a	0.0E+00	8.5E+06	0.0E+00	1.3E+09	1.3E+06	∞	∞	6.5
Lamp1	1.5E+09	7.0E+09	0.0E+00	1.3E+09	3.3E+09	4.6	∞	2.1
Txn	0.0E+00	8.0E+07	0.0E+00	8.5E+08	3.6E+06	∞	∞	21.9
H3f3a	0.0E+00	1.4E+07	0.0E+00	8.9E+08	0.0E+00	∞	∞	∞
Cd63	0.0E+00	7.9E+08	5.3E+07	1.2E+08	7.9E+07	∞	2.4	10.0
Sfn	1.9E+08	1.8E+09	0.0E+00	7.6E+08	4.4E+08	9.6	∞	4.2
Rac1	0.0E+00	1.6E+08	0.0E+00	5.2E+08	1.6E+06	∞	∞	104.0
Gps1	0.0E+00	5.1E+08	1.3E+07	1.2E+08	9.1E+07	∞	9.0	5.5
Hnrnpf	1.0E+08	3.5E+08	0.0E+00	5.1E+08	4.9E+07	3.5	∞	7.2
Ubr4	1.8E+07	4.2E+08	0.0E+00	4.8E+08	8.0E+07	23.1	∞	5.3
Tagln2	2.8E+06	2.2E+07	0.0E+00	4.8E+08	3.7E+06	7.6	∞	5.8
Rela	0.0E+00	4.2E+08	0.0E+00	1.6E+07	4.4E+07	∞	∞	9.5
Mme	0.0E+00	1.5E+08	0.0E+00	2.1E+08	4.6E+06	∞	∞	32.4
Wdr1	0.0E+00	3.3E+08	0.0E+00	1.8E+07	6.5E+07	∞	∞	5.1
Mad2l1	1.5E+07	3.5E+07	0.0E+00	2.9E+08	0.0E+00	2.4	∞	∞
Aco2	0.0E+00	2.8E+08	7.7E+06	5.6E+07	2.4E+07	∞	7.2	11.9
Tmem109	0.0E+00	5.0E+06	0.0E+00	2.7E+08	0.0E+00	∞	∞	∞
Zbtb17	0.0E+00	2.5E+08	0.0E+00	1.7E+07	4.3E+07	∞	∞	5.9
Psma5	2.6E+08	5.4E+08	0.0E+00	2.6E+08	1.1E+08	2.1	∞	4.9
Ywhag	2.3E+08	5.9E+08	0.0E+00	2.4E+08	1.2E+08	2.6	∞	5.0
Rab8a	0.0E+00	9.5E+06	0.0E+00	2.3E+08	0.0E+00	∞	∞	∞
Sgpl1	0.0E+00	2.4E+08	5.3E+07	2.1E+08	6.2E+07	∞	4.0	3.8
Mrps34	6.1E+06	1.5E+07	0.0E+00	2.2E+08	6.5E+06	2.5	∞	2.4
Tardbp	4.7E+06	6.8E+07	0.0E+00	2.2E+08	3.6E+07	14.5	∞	1.9
Rab11fip1	2.7E+07	4.2E+08	0.0E+00	2.1E+08	0.0E+00	15.7	∞	∞
Hmmr	0.0E+00	1.8E+08	0.0E+00	2.9E+07	7.2E+06	∞	∞	24.3
Mrc2	0.0E+00	1.9E+08	0.0E+00	1.3E+07	6.7E+06	∞	∞	28.2
Sar1a	2.8E+07	1.2E+08	0.0E+00	2.0E+08	1.4E+07	4.4	∞	9.1
Cnn2	0.0E+00	3.7E+06	0.0E+00	1.8E+08	0.0E+00	∞	∞	∞
Dync1i2	0.0E+00	1.6E+08	0.0E+00	2.5E+07	8.9E+07	∞	∞	1.8
Rps21	0.0E+00	3.1E+06	0.0E+00	1.8E+08	0.0E+00	∞	∞	∞
Mrps26	0.0E+00	5.0E+07	0.0E+00	1.3E+08	1.9E+07	∞	∞	2.6
Psma7	1.0E+08	2.5E+08	0.0E+00	1.7E+08	6.9E+06	2.5	∞	37.0
Msh6	0.0E+00	1.4E+08	0.0E+00	3.0E+07	2.8E+07	∞	∞	4.9

Gene names	T1 MT	T1 WT	T2 MT	T2 WT	T1 No TNF	T1 Fold change	T2 Fold change	Fold change with No TNF
Arhgef40	0.0E+00	1.6E+08	0.0E+00	7.6E+06	5.8E+06	∞	∞	27.1
Slk	0.0E+00	1.6E+08	1.6E+07	1.2E+08	5.5E+07	∞	7.4	2.9
Uba6	0.0E+00	1.3E+08	0.0E+00	2.7E+07	4.8E+07	∞	∞	2.8
Slc25a3	5.6E+06	1.8E+07	0.0E+00	1.6E+08	0.0E+00	3.2	∞	∞
Smchd1	0.0E+00	1.3E+08	0.0E+00	2.9E+07	2.0E+07	∞	∞	6.7
Rab6a	2.0E+07	2.1E+08	0.0E+00	1.6E+08	1.2E+07	10.8	∞	17.7
Pitrm1	0.0E+00	1.4E+08	0.0E+00	1.4E+07	4.3E+07	∞	∞	3.3
Stat3	0.0E+00	1.6E+08	6.1E+06	9.8E+07	2.9E+07	∞	16.0	5.4
Pus1	0.0E+00	4.4E+07	0.0E+00	1.0E+08	1.9E+07	∞	∞	2.3
Pdlim5	0.0E+00	2.1E+07	0.0E+00	1.3E+08	0.0E+00	∞	∞	∞
Fam83h	0.0E+00	9.7E+07	0.0E+00	4.2E+07	3.5E+07	∞	∞	2.8
Las1l	0.0E+00	1.1E+08	0.0E+00	2.3E+07	1.4E+07	∞	∞	8.2
Iars	4.7E+07	3.4E+08	0.0E+00	1.3E+08	8.4E+07	7.1	∞	4.0
Mrpl18	0.0E+00	3.7E+06	0.0E+00	1.3E+08	0.0E+00	∞	∞	∞
Ranbp3	0.0E+00	6.8E+07	0.0E+00	5.9E+07	9.2E+06	∞	∞	7.4
Timm13	0.0E+00	6.3E+07	0.0E+00	5.9E+07	1.5E+07	∞	∞	4.3
Nptn	0.0E+00	1.0E+08	0.0E+00	1.4E+07	2.9E+07	∞	∞	3.6
Bax	0.0E+00	6.7E+07	0.0E+00	5.1E+07	4.4E+07	∞	∞	1.5
Pcyox1l	0.0E+00	1.2E+08	3.3E+06	2.5E+07	3.5E+07	∞	7.5	3.3
Pdcd10	6.1E+06	1.5E+08	0.0E+00	1.1E+08	2.3E+07	24.3	∞	6.4
Hk2	0.0E+00	8.3E+07	0.0E+00	2.8E+07	1.6E+07	∞	∞	5.1
Dync1li1	4.4E+07	1.0E+08	0.0E+00	1.0E+08	7.8E+06	2.3	∞	13.0
Mars	2.5E+07	2.1E+08	0.0E+00	1.0E+08	7.4E+07	8.2	∞	2.8
Tspan3	0.0E+00	5.8E+07	0.0E+00	4.0E+07	4.7E+07	∞	∞	1.2
Dnm1l	2.2E+07	8.3E+07	0.0E+00	9.7E+07	3.0E+07	3.8	∞	2.7
Impact	0.0E+00	9.7E+07	8.2E+06	2.2E+07	1.1E+07	∞	2.6	8.9
UPF0568	4.6E+07	1.8E+08	0.0E+00	9.5E+07	1.5E+07	4.0	∞	12.4
Atp1b1	0.0E+00	6.9E+07	0.0E+00	2.3E+07	3.7E+07	∞	∞	1.9
Cops7a	4.8E+07	1.7E+08	0.0E+00	9.2E+07	0.0E+00	3.7	∞	∞
Lrp1	6.7E+07	4.5E+08	0.0E+00	9.0E+07	6.6E+07	6.7	∞	6.8
Acaa2	4.2E+06	2.2E+07	0.0E+00	8.8E+07	0.0E+00	5.2	∞	∞
Diaph1	2.0E+07	2.5E+08	0.0E+00	8.7E+07	4.3E+07	12.7	∞	6.0
Adsl	1.7E+07	7.7E+07	0.0E+00	8.6E+07	6.7E+07	4.5	∞	1.1
Atp6v1d	0.0E+00	9.9E+06	0.0E+00	7.1E+07	0.0E+00	∞	∞	∞
Inf2	3.4E+07	2.2E+08	0.0E+00	7.9E+07	7.1E+07	6.4	∞	3.1
Ly75	0.0E+00	2.9E+07	0.0E+00	4.9E+07	2.9E+06	∞	∞	10.2
Pcolce	0.0E+00	4.3E+07	0.0E+00	3.4E+07	6.1E+06	∞	∞	7.1
Gdi2	4.5E+06	1.7E+08	0.0E+00	7.4E+07	1.2E+08	38.5	∞	1.4

Gene names	T1 MT	T1 WT	T2 MT	T2 WT	T1 No TNF	T1 Fold change	T2 Fold change	Fold change with No TNF
Uggt1	2.3E+07	9.6E+07	0.0E+00	7.4E+07	3.2E+07	4.2	∞	3.1
Ddx42	0.0E+00	7.4E+07	1.7E+07	3.7E+07	3.8E+07	∞	2.2	1.9
Ctnna1	0.0E+00	3.2E+07	0.0E+00	4.1E+07	9.1E+06	∞	∞	3.6
Pcm1	0.0E+00	1.9E+07	0.0E+00	5.4E+07	0.0E+00	∞	∞	∞
Psmb6	0.0E+00	2.6E+07	0.0E+00	4.7E+07	9.7E+06	∞	∞	2.6
Adam9	0.0E+00	5.0E+07	0.0E+00	2.3E+07	9.0E+06	∞	∞	5.5
Psm6	9.2E+07	3.6E+08	0.0E+00	7.3E+07	1.0E+07	3.9	∞	35.5
Ahcy	3.5E+07	2.8E+08	0.0E+00	7.0E+07	2.0E+08	8.2	∞	1.4
Xpo7	0.0E+00	3.7E+07	0.0E+00	2.9E+07	8.6E+06	∞	∞	4.3
Ykt6	0.0E+00	3.0E+07	0.0E+00	3.5E+07	1.7E+07	∞	∞	1.8
Pelp1	0.0E+00	3.6E+07	0.0E+00	2.7E+07	2.0E+06	∞	∞	18.2
Etfdh	0.0E+00	5.0E+07	0.0E+00	1.2E+07	6.8E+06	∞	∞	7.3
Stt3b	0.0E+00	1.3E+07	0.0E+00	4.9E+07	0.0E+00	∞	∞	∞
Sf3b1	0.0E+00	4.5E+07	0.0E+00	1.6E+07	1.6E+06	∞	∞	29.2
Npepps	3.1E+06	2.4E+08	0.0E+00	6.0E+07	5.6E+07	78.6	∞	4.3
Prdx6	1.2E+08	3.0E+08	0.0E+00	6.0E+07	1.4E+08	2.4	∞	2.1
Farsb	0.0E+00	5.9E+07	4.5E+06	5.0E+07	1.8E+07	∞	11.2	3.3
Tpp2	0.0E+00	5.0E+07	0.0E+00	8.1E+06	1.5E+07	∞	∞	3.4
Wdr6	0.0E+00	5.8E+07	1.5E+07	3.6E+07	1.8E+07	∞	2.4	3.2
Trip13	0.0E+00	4.1E+07	0.0E+00	1.7E+07	1.9E+07	∞	∞	2.2
Hcfc1	0.0E+00	2.6E+07	0.0E+00	3.1E+07	2.3E+06	∞	∞	11.6
Ak3	0.0E+00	3.4E+07	0.0E+00	2.2E+07	8.5E+06	∞	∞	4.0
Sec22b	0.0E+00	9.9E+06	0.0E+00	4.6E+07	0.0E+00	∞	∞	∞
Kif2a	0.0E+00	5.5E+07	1.0E+07	2.9E+07	2.6E+07	∞	2.8	2.1
Gstp1	6.5E+07	3.2E+08	0.0E+00	5.5E+07	1.6E+07	4.9	∞	19.9
Tmem33	0.0E+00	4.2E+06	0.0E+00	5.0E+07	0.0E+00	∞	∞	∞
Pex5	0.0E+00	3.7E+07	0.0E+00	1.7E+07	0.0E+00	∞	∞	∞
Sdf2	0.0E+00	2.4E+07	0.0E+00	3.0E+07	0.0E+00	∞	∞	∞
Acsl4	1.1E+06	1.8E+08	0.0E+00	5.3E+07	3.3E+07	157.6	∞	5.4
Wdr26	0.0E+00	4.8E+07	0.0E+00	4.7E+06	2.4E+07	∞	∞	2.0
Csrp2	0.0E+00	1.3E+06	0.0E+00	5.1E+07	0.0E+00	∞	∞	∞
Baspl	0.0E+00	5.2E+07	1.2E+07	2.5E+07	1.8E+07	∞	2.2	2.9
Rala	5.7E+07	1.6E+08	0.0E+00	5.2E+07	3.1E+07	2.7	∞	4.9
Med1	0.0E+00	3.0E+07	0.0E+00	2.0E+07	0.0E+00	∞	∞	∞
Nsf	3.6E+07	7.5E+07	0.0E+00	4.9E+07	4.7E+06	2.1	∞	15.9
Phldb2	0.0E+00	6.2E+06	0.0E+00	4.2E+07	0.0E+00	∞	∞	∞
Ddx6	0.0E+00	1.4E+07	0.0E+00	3.2E+07	6.7E+06	∞	∞	2.0
Plxnb2	3.5E+07	1.2E+08	0.0E+00	4.6E+07	2.3E+07	3.5	∞	5.4

Gene names	T1 MT	T1 WT	T2 MT	T2 WT	T1 No TNF	T1 Fold change	T2 Fold change	Fold change with No TNF
Esyt1	2.2E+06	7.6E+07	0.0E+00	4.4E+07	1.4E+07	35.4	∞	5.4
Exoc4	6.6E+06	3.8E+07	0.0E+00	4.3E+07	3.9E+06	5.8	∞	9.6
Usp10	4.4E+06	1.4E+07	0.0E+00	4.2E+07	0.0E+00	3.3	∞	∞
Golga3	1.1E+07	5.2E+07	0.0E+00	4.1E+07	3.4E+07	4.7	∞	1.5
Sec23b	4.2E+06	8.4E+07	0.0E+00	4.1E+07	7.0E+07	19.8	∞	1.2
Mgea5	0.0E+00	2.0E+07	0.0E+00	2.1E+07	8.3E+06	∞	∞	2.4
Setd3	0.0E+00	3.3E+07	0.0E+00	4.1E+06	9.3E+06	∞	∞	3.6
Tkt	2.5E+08	7.1E+08	0.0E+00	3.7E+07	1.0E+08	2.9	∞	6.8
Eif2b5	0.0E+00	3.2E+07	0.0E+00	4.4E+06	3.3E+06	∞	∞	9.6
Aco1	0.0E+00	2.1E+07	0.0E+00	1.6E+07	7.7E+06	∞	∞	2.7
Atp6v1c1	0.0E+00	1.9E+07	0.0E+00	1.7E+07	0.0E+00	∞	∞	∞
Nr2f2	0.0E+00	3.1E+07	0.0E+00	5.1E+06	0.0E+00	∞	∞	∞
Idh3g	2.1E+07	2.1E+08	0.0E+00	3.4E+07	3.8E+07	9.7	∞	5.4
Ddx17	0.0E+00	3.4E+07	2.5E+07	6.7E+07	3.2E+07	∞	2.7	1.1
Ak2	6.4E+06	2.7E+07	0.0E+00	3.4E+07	1.9E+07	4.2	∞	1.5
Gtpbp4	0.0E+00	3.3E+07	1.4E+07	5.5E+07	2.8E+07	∞	3.8	1.2
Snx4	0.0E+00	3.2E+07	1.5E+07	7.9E+07	2.2E+07	∞	5.1	1.5
Fam3c	4.3E+07	1.8E+08	0.0E+00	3.2E+07	2.9E+07	4.1	∞	6.1
Mob1a	3.4E+07	7.6E+07	0.0E+00	3.2E+07	1.4E+07	2.2	∞	5.3
Smarcd2	0.0E+00	2.1E+07	0.0E+00	1.0E+07	0.0E+00	∞	∞	∞
Kif2c	8.8E+06	5.5E+07	0.0E+00	3.1E+07	1.0E+07	6.3	∞	5.5
Phb	6.0E+07	2.3E+08	0.0E+00	3.1E+07	4.1E+07	3.9	∞	5.6
Sugt1	2.5E+07	1.1E+08	0.0E+00	3.1E+07	3.4E+07	4.5	∞	3.4
Eci1	0.0E+00	9.2E+06	0.0E+00	2.1E+07	0.0E+00	∞	∞	∞
Plekhf1	0.0E+00	6.5E+06	0.0E+00	2.4E+07	4.4E+06	∞	∞	1.5
Chmp4b	0.0E+00	2.9E+07	2.1E+07	4.7E+08	9.8E+05	∞	22.2	29.7
Nemf	0.0E+00	1.2E+07	0.0E+00	1.7E+07	1.1E+07	∞	∞	1.1
Ist1	3.0E+07	8.8E+07	0.0E+00	2.8E+07	6.8E+07	3.0	∞	1.3
Hspg2	0.0E+00	2.4E+07	0.0E+00	1.7E+06	1.2E+07	∞	∞	2.0
Timm44	5.5E+07	2.8E+08	0.0E+00	2.5E+07	0.0E+00	5.1	∞	∞
Nubp2	5.3E+06	3.5E+07	0.0E+00	2.5E+07	0.0E+00	6.5	∞	∞
Atp6v1h	5.6E+06	2.2E+08	0.0E+00	2.4E+07	1.4E+07	40.0	∞	16.6
Dis3	7.5E+06	6.1E+07	0.0E+00	2.4E+07	3.2E+07	8.1	∞	1.9
Smc1a	1.6E+07	1.9E+08	0.0E+00	2.3E+07	1.3E+07	12.1	∞	15.4
Dhrs1	3.1E+07	1.1E+08	0.0E+00	2.2E+07	1.9E+07	3.7	∞	6.2
Vps16	0.0E+00	9.8E+06	0.0E+00	1.1E+07	0.0E+00	∞	∞	∞
Ncstn	3.5E+06	1.5E+08	0.0E+00	2.0E+07	7.5E+07	43.0	∞	2.0
Lrrc47	0.0E+00	1.2E+07	0.0E+00	7.8E+06	0.0E+00	∞	∞	∞

Gene names	T1 MT	T1 WT	T2 MT	T2 WT	T1 No TNF	T1 Fold change	T2 Fold change	Fold change with No TNF
Ppm1a	0.0E+00	1.9E+07	7.5E+06	2.4E+07	3.3E+06	∞	3.2	5.7
Aaas	0.0E+00	1.9E+07	1.3E+07	5.0E+07	0.0E+00	∞	3.8	∞
Ythdf2	2.9E+07	1.3E+08	0.0E+00	1.8E+07	5.0E+07	4.7	∞	2.7
Cnot10	0.0E+00	1.4E+07	0.0E+00	1.9E+06	0.0E+00	∞	∞	∞
Rps27	0.0E+00	1.6E+07	3.3E+07	4.5E+09	0.0E+00	∞	137.4	∞
Qki	0.0E+00	1.5E+07	4.0E+06	2.3E+07	8.3E+06	∞	5.7	1.8
Emc1	1.2E+07	9.9E+07	0.0E+00	1.5E+07	4.5E+06	8.2	∞	21.8
Mia3	8.4E+06	3.4E+07	0.0E+00	1.4E+07	1.9E+07	4.0	∞	1.8
Smad3	0.0E+00	1.4E+07	6.7E+06	2.5E+07	3.2E+06	∞	3.7	4.4
Myo1c	5.9E+06	1.7E+08	0.0E+00	1.4E+07	0.0E+00	29.0	∞	∞
Agps	1.5E+07	5.8E+07	0.0E+00	1.3E+07	5.9E+06	4.0	∞	9.9
Aldh16a1	8.4E+06	7.0E+07	0.0E+00	1.3E+07	1.7E+07	8.4	∞	4.2
Tex10	0.0E+00	5.4E+06	0.0E+00	8.0E+06	4.6E+06	∞	∞	1.2
Fam98a	0.0E+00	1.3E+07	2.9E+07	6.3E+07	1.0E+07	∞	2.2	1.3
Hdgfrp2	0.0E+00	1.9E+06	0.0E+00	9.9E+06	0.0E+00	∞	∞	∞
Myl12b	0.0E+00	1.1E+07	1.1E+07	1.2E+09	0.0E+00	∞	112.6	∞
S100a11	3.4E+06	2.5E+07	0.0E+00	1.1E+07	2.2E+07	7.3	∞	1.1
Cnot1	3.4E+06	3.9E+07	0.0E+00	1.1E+07	0.0E+00	11.4	∞	∞
Psm4	6.9E+06	1.6E+08	0.0E+00	9.8E+06	5.1E+07	22.8	∞	3.1
Anpep	0.0E+00	7.5E+06	0.0E+00	1.9E+06	0.0E+00	∞	∞	∞
Ganab	1.9E+07	2.6E+08	0.0E+00	8.7E+06	7.6E+07	13.6	∞	3.5
Snrnp200	1.1E+07	4.1E+07	0.0E+00	8.6E+06	5.7E+06	3.9	∞	7.2
Cwc22	0.0E+00	5.8E+06	0.0E+00	2.1E+06	0.0E+00	∞	∞	∞
Cyfp1	5.6E+05	5.8E+07	0.0E+00	7.7E+06	1.8E+07	102.7	∞	3.2
Cs	1.2E+07	4.9E+07	0.0E+00	7.5E+06	4.7E+07	4.1	∞	1.0
Nat10	1.4E+07	8.7E+07	0.0E+00	6.4E+06	4.2E+06	6.0	∞	20.8
Eif3j1	0.0E+00	5.6E+06	2.2E+07	1.1E+08	0.0E+00	∞	5.1	∞
Aebp1	0.0E+00	1.6E+06	0.0E+00	2.8E+06	0.0E+00	∞	∞	∞
Rnf213	9.7E+06	7.9E+07	0.0E+00	3.5E+06	1.1E+07	8.2	∞	6.9
Pes1	2.0E+06	2.2E+07	0.0E+00	3.5E+06	0.0E+00	10.8	∞	∞
Ipo11	5.2E+06	2.5E+07	0.0E+00	2.9E+06	4.4E+06	4.8	∞	5.7
Impa1	2.3E+07	1.9E+08	0.0E+00	2.6E+06	6.2E+07	8.1	∞	3.0
Eea1	1.8E+06	1.0E+07	0.0E+00	1.3E+06	1.1E+06	5.9	∞	9.7
S100a6	7.3E+06	2.5E+08	1.3E+07	2.5E+09	2.2E+08	34.0	185.4	1.1
Mvp	2.8E+06	4.3E+08	1.1E+07	4.1E+07	2.4E+07	155.0	3.9	17.7
Hist1h2ah	5.1E+06	2.5E+07	1.5E+07	1.6E+09	1.7E+07	5.0	110.2	1.4
Txlna	4.7E+06	4.0E+08	1.4E+08	5.4E+08	1.2E+08	84.5	3.8	3.4
Edc4	3.6E+07	1.9E+08	6.5E+06	5.1E+08	5.9E+07	5.3	79.0	3.2

Gene names	T1 MT	T1 WT	T2 MT	T2 WT	T1 No TNF	T1 Fold change	T2 Fold change	Fold change with No TNF
Ube4b	7.7E+05	5.6E+07	6.2E+06	2.4E+07	7.2E+06	73.2	3.9	7.9
Rpl11	8.0E+07	2.1E+08	9.2E+07	6.5E+09	1.2E+08	2.6	71.0	1.8
Tfrc	5.4E+08	2.7E+09	2.1E+08	1.4E+10	6.6E+08	5.0	66.6	4.1
Ppp2r2a	2.8E+06	1.5E+08	3.8E+07	1.3E+08	1.4E+08	54.3	3.4	1.1
Hnrnrm	5.7E+07	2.4E+08	1.8E+07	7.8E+08	5.5E+07	4.2	42.9	4.3
Fam129b	7.3E+06	3.1E+08	4.7E+07	1.6E+08	8.1E+07	42.8	3.4	3.8
Nup155	1.3E+07	5.7E+08	2.1E+07	5.5E+07	1.6E+07	43.3	2.6	36.0
Actn4	1.7E+07	5.0E+08	7.5E+06	1.2E+08	5.9E+07	29.0	16.3	8.4
Lap3	1.1E+07	2.8E+08	4.8E+06	9.6E+07	3.5E+07	25.0	19.8	8.0
Eif3f	4.3E+07	1.8E+09	3.7E+08	8.7E+08	6.6E+08	41.9	2.3	2.8
Dctn1	5.9E+07	8.8E+08	8.2E+06	2.2E+08	3.1E+08	14.9	27.2	2.8
Hnrnph1	1.2E+08	3.1E+08	4.1E+06	1.5E+08	1.5E+07	2.6	37.7	20.5
Atp1a1	9.6E+06	2.7E+08	1.9E+07	1.9E+08	4.0E+07	28.3	10.1	6.7
Spr	1.4E+08	3.6E+08	1.8E+07	6.4E+08	1.2E+07	2.5	35.3	29.3
Tagln	7.2E+06	2.7E+07	8.0E+06	2.7E+08	0.0E+00	3.7	33.5	∞
Kif5b	9.2E+07	8.3E+08	7.0E+06	1.9E+08	5.0E+08	9.0	27.7	1.7
Dhx9	2.8E+06	8.3E+07	2.1E+07	1.3E+08	0.0E+00	29.5	6.2	∞
Glg1	2.6E+07	7.8E+08	2.5E+07	1.4E+08	7.7E+07	30.1	5.5	10.1
Rps25	7.9E+07	5.1E+08	2.8E+08	7.4E+09	4.5E+08	6.4	26.8	1.1
Ikbkap	1.5E+07	3.2E+08	7.0E+06	7.2E+07	3.6E+07	21.6	10.2	8.9
Hook3	1.8E+07	4.6E+08	7.0E+06	3.9E+07	1.4E+08	25.3	5.5	3.4
Rpl27a	8.5E+07	2.1E+08	7.9E+07	2.0E+09	1.1E+08	2.4	25.8	1.9
Ap3b1	3.2E+07	9.3E+07	3.8E+06	9.5E+07	1.9E+07	2.9	25.1	5.0
Sf3b3	1.7E+08	4.8E+08	1.8E+07	4.2E+08	1.7E+08	2.9	23.5	2.8
Smc3	3.0E+07	6.2E+07	2.5E+06	5.8E+07	1.5E+07	2.1	23.5	4.1
Prpf8	1.4E+07	1.5E+08	1.3E+07	1.9E+08	7.5E+06	10.3	14.5	19.5
Ncln	7.3E+06	1.6E+08	4.0E+07	8.3E+07	3.2E+07	22.3	2.1	5.1
Pcbp1	4.9E+07	1.6E+08	7.2E+07	1.4E+09	7.7E+07	3.3	19.8	2.1
Usp9x	1.9E+07	2.4E+08	6.0E+06	6.0E+07	4.5E+07	12.4	10.0	5.3
Ipo7	3.3E+08	8.7E+08	1.6E+07	2.9E+08	1.3E+08	2.6	18.6	6.8
Ctps1	9.5E+07	6.5E+08	3.1E+07	4.2E+08	1.5E+08	6.8	13.4	4.3
Aacs	5.9E+07	6.2E+08	3.4E+07	3.2E+08	7.4E+07	10.5	9.5	8.3
Prdx4	2.8E+08	7.6E+08	1.1E+08	1.9E+09	7.7E+07	2.7	17.2	9.9
Ipo9	2.9E+07	2.5E+08	7.5E+06	7.5E+07	8.2E+06	8.6	10.0	30.5
Cand1	1.0E+08	1.2E+09	9.8E+07	6.8E+08	1.4E+08	11.1	6.9	8.3
Larp7	3.4E+06	3.2E+07	6.6E+06	5.5E+07	0.0E+00	9.4	8.2	∞
Tgm2	2.4E+07	3.0E+08	3.4E+07	1.7E+08	2.7E+07	12.5	5.1	11.3
Mrpl28	3.0E+06	4.0E+07	3.3E+07	1.3E+08	0.0E+00	13.2	3.8	∞

Gene names	T1 MT	T1 WT	T2 MT	T2 WT	T1 No TNF	T1 Fold change	T2 Fold change	Fold change with No TNF
Eef1b	5.5E+07	5.9E+08	3.1E+07	1.9E+08	2.7E+07	10.8	6.1	21.8
Gclm	1.5E+07	6.9E+07	8.8E+06	1.1E+08	0.0E+00	4.5	12.4	∞
Slc25a5	5.2E+08	1.2E+09	2.7E+07	3.9E+08	1.8E+08	2.3	14.5	6.7
Tuba4a	2.8E+07	3.5E+08	6.3E+06	2.7E+07	8.3E+06	12.6	4.2	41.6
Itgav	1.0E+08	6.8E+08	6.3E+06	6.6E+07	1.4E+08	6.5	10.3	4.9
Vcl	1.6E+09	5.5E+09	1.1E+08	1.4E+09	2.6E+09	3.4	12.4	2.1
Myh10	7.9E+08	1.7E+09	4.5E+07	6.0E+08	8.0E+08	2.1	13.3	2.1
Wdr18	1.8E+07	8.6E+07	1.4E+07	1.4E+08	7.3E+07	4.8	10.5	1.2
Lepre1	7.4E+07	4.7E+08	1.4E+07	1.2E+08	7.5E+07	6.3	8.7	6.2
Acly	1.7E+08	2.1E+09	6.9E+08	1.5E+09	7.8E+08	12.8	2.2	2.8
Dync1h1	1.4E+09	7.5E+09	2.0E+08	1.8E+09	2.1E+09	5.6	9.2	3.6
Ap2m1	1.3E+08	7.7E+08	1.4E+07	1.2E+08	2.7E+08	6.2	8.6	2.9
Copa	3.3E+08	1.3E+09	4.1E+07	4.4E+08	3.3E+08	3.9	10.7	4.0
Itga3	1.7E+07	1.6E+08	2.6E+06	1.3E+07	1.4E+08	9.3	5.1	1.1
Mta2	2.0E+07	1.9E+08	5.5E+07	2.5E+08	1.8E+08	9.4	4.6	1.1
Mov10	1.0E+08	5.9E+08	1.6E+07	1.4E+08	1.1E+08	5.7	8.4	5.5
Cul4b	2.8E+07	6.0E+07	8.1E+06	9.4E+07	1.7E+07	2.2	11.5	3.6
Eif6	2.7E+08	6.8E+08	4.6E+07	5.1E+08	5.9E+07	2.6	11.1	11.6
Pc	2.8E+07	2.3E+08	4.1E+07	2.0E+08	7.7E+07	8.4	5.0	3.0
Ywhab	4.4E+08	1.1E+09	1.1E+08	1.1E+09	2.2E+08	2.4	10.8	4.9
Ilk	5.0E+06	5.2E+07	1.1E+07	2.9E+07	9.5E+06	10.4	2.7	5.5
Copg1	8.6E+07	8.1E+08	5.9E+07	2.0E+08	1.5E+08	9.5	3.5	5.4
Nup93	4.8E+07	4.4E+08	4.3E+07	1.6E+08	5.3E+07	9.1	3.8	8.2
Ruvbl2	3.5E+08	9.1E+08	1.2E+08	1.3E+09	2.0E+08	2.6	10.3	4.6
Sucla2	3.9E+07	2.9E+08	1.7E+07	9.2E+07	1.3E+08	7.4	5.4	2.2
Ddb1	5.0E+07	3.7E+08	1.9E+07	9.7E+07	1.1E+08	7.4	5.2	3.3
Eftud2	1.1E+08	7.2E+08	3.1E+07	1.7E+08	1.2E+08	6.7	5.5	6.1
Cad	5.9E+08	2.4E+09	1.1E+08	8.8E+08	7.0E+08	4.1	7.8	3.4
Acaca	4.9E+07	4.1E+08	5.7E+07	1.9E+08	1.6E+08	8.3	3.4	2.5
Mcm2	1.4E+08	1.3E+09	1.6E+08	3.2E+08	2.9E+08	9.2	2.1	4.5
Hk1	7.3E+07	6.2E+08	1.1E+08	3.0E+08	2.7E+08	8.4	2.8	2.3
Tln1	8.8E+08	3.1E+09	1.2E+08	9.0E+08	1.4E+09	3.5	7.6	2.3
Dak	2.7E+07	6.2E+07	6.8E+06	5.8E+07	5.0E+06	2.3	8.6	12.4
Upf1	1.7E+08	1.3E+09	1.6E+08	4.3E+08	3.5E+08	7.9	2.7	3.8
Acat1	1.1E+07	4.3E+07	3.6E+07	2.4E+08	9.0E+06	4.1	6.5	4.8
Ap2a2	5.0E+07	2.5E+08	2.7E+07	1.5E+08	5.5E+07	5.1	5.3	4.6
Luc7l3	2.0E+07	5.6E+07	5.8E+06	4.4E+07	6.3E+06	2.8	7.5	8.8
Mcm3	2.5E+08	2.0E+09	3.7E+08	9.0E+08	5.9E+08	7.9	2.4	3.4

Gene names	T1 MT	T1 WT	T2 MT	T2 WT	T1 No TNF	T1 Fold change	T2 Fold change	Fold change with No TNF
Pfkl	9.3E+07	4.7E+08	2.1E+07	1.1E+08	7.5E+07	5.1	5.1	6.3
Atxn10	5.9E+07	3.6E+08	1.6E+08	6.5E+08	3.1E+08	6.1	4.1	1.2
Fdps	1.8E+08	8.1E+08	1.9E+07	1.1E+08	3.0E+08	4.4	5.7	2.7
Itgb1	5.4E+08	3.1E+09	1.4E+08	5.8E+08	1.5E+09	5.9	4.1	2.0
Hm13	7.0E+07	2.1E+08	1.7E+07	1.2E+08	1.2E+07	3.1	6.9	18.2
Ruvbl1	2.2E+08	1.7E+09	1.9E+08	4.5E+08	4.6E+08	7.5	2.3	3.7
Nomo1	1.3E+08	5.0E+08	3.7E+07	2.2E+08	2.4E+08	4.0	5.8	2.1
Ipo5	2.4E+08	1.0E+09	1.7E+08	8.7E+08	5.0E+08	4.3	5.2	2.0
Atp2a2	1.1E+08	4.2E+08	3.1E+07	1.7E+08	7.7E+07	3.8	5.5	5.5
Me2	4.5E+07	2.7E+08	1.3E+07	4.2E+07	8.4E+07	6.0	3.2	3.2
Srpr	2.4E+07	1.3E+08	3.1E+07	1.2E+08	1.9E+07	5.2	3.9	6.9
Fam49b	4.2E+07	1.6E+08	1.9E+07	1.0E+08	2.1E+07	3.7	5.5	7.3
Hadha	1.9E+08	8.2E+08	9.2E+07	4.4E+08	2.4E+08	4.3	4.8	3.4
Myh9	1.3E+10	2.9E+10	7.8E+08	5.3E+09	2.0E+10	2.1	6.8	1.4
Ranbp1	3.1E+08	7.5E+08	8.3E+07	5.4E+08	2.9E+08	2.4	6.6	2.6
Ap2b1	8.6E+07	4.5E+08	1.4E+08	5.1E+08	2.4E+08	5.3	3.6	1.9
Oxct1	4.6E+07	2.3E+08	6.3E+06	2.5E+07	3.1E+07	5.0	3.9	7.6
Eif3l	2.0E+08	1.3E+09	2.6E+08	6.4E+08	4.1E+08	6.5	2.4	3.2
Ddx56	3.8E+06	2.2E+07	1.6E+07	5.3E+07	0.0E+00	5.6	3.3	∞
Eif3c	2.3E+08	1.1E+09	1.6E+08	6.5E+08	2.9E+08	4.8	4.1	3.8
Rad23b	4.4E+07	2.9E+08	1.2E+07	2.7E+07	2.7E+07	6.7	2.2	10.7
Mrto4	6.6E+07	1.8E+08	3.5E+07	2.1E+08	6.0E+07	2.8	6.1	3.1
Ddx21	1.1E+08	5.8E+08	1.0E+08	3.2E+08	1.8E+08	5.5	3.2	3.2
Dnm2	1.1E+08	3.6E+08	9.8E+06	5.1E+07	5.5E+07	3.4	5.2	6.5
Eif3e	3.0E+08	1.8E+09	4.6E+08	1.1E+09	6.6E+08	6.2	2.3	2.8
Copb2	5.6E+08	2.9E+09	2.6E+08	8.4E+08	7.8E+08	5.1	3.2	3.7
Lars	8.3E+07	4.5E+08	5.2E+07	1.5E+08	6.4E+07	5.4	2.9	7.0
Xpo1	6.4E+07	2.8E+08	1.1E+07	4.1E+07	3.9E+07	4.4	3.8	7.2
Uba1	6.1E+08	3.7E+09	6.5E+08	1.4E+09	6.9E+08	6.0	2.1	5.3
Rad50	6.4E+07	3.3E+08	2.4E+07	7.0E+07	3.4E+07	5.1	2.9	9.6
Flnb	2.5E+09	5.4E+09	1.9E+08	1.1E+09	1.9E+09	2.2	5.8	2.9
Ywhaz	3.1E+09	6.5E+09	2.0E+08	1.2E+09	7.3E+08	2.1	5.9	8.9
Myof	6.1E+08	2.0E+09	1.7E+08	7.6E+08	5.9E+08	3.3	4.6	3.4
Rfc2	3.5E+07	1.8E+08	3.1E+07	8.6E+07	2.2E+07	5.1	2.8	8.4
Epb41l2	4.1E+07	8.2E+07	1.2E+07	6.9E+07	2.0E+07	2.0	5.8	4.0
Flna	1.8E+10	4.1E+10	1.7E+09	9.3E+09	1.3E+10	2.3	5.5	3.2
Dnaja3	2.9E+07	1.4E+08	1.3E+07	4.0E+07	2.8E+07	4.8	3.0	5.0
Snd1	4.9E+08	2.8E+09	3.7E+08	7.6E+08	8.5E+08	5.6	2.0	3.3

Gene names	T1 MT	T1 WT	T2 MT	T2 WT	T1 No TNF	T1 Fold change	T2 Fold change	Fold change with No TNF
Aars	8.5E+08	4.7E+09	1.6E+09	3.2E+09	1.1E+09	5.5	2.0	4.1
Gls	1.7E+08	5.7E+08	1.0E+08	4.3E+08	6.1E+07	3.3	4.2	9.4
Mthfd1l	2.5E+08	1.3E+09	1.3E+08	3.0E+08	4.8E+08	5.0	2.4	2.6
Ywhaq	4.3E+08	9.3E+08	8.4E+07	4.3E+08	1.5E+08	2.2	5.1	6.4
Naa15	4.1E+07	1.8E+08	4.7E+06	1.3E+07	0.0E+00	4.3	2.7	∞
Smc4	3.2E+08	1.4E+09	2.2E+08	5.4E+08	3.7E+08	4.4	2.4	3.8
Pgk1	4.4E+08	1.5E+09	5.3E+07	1.8E+08	7.6E+08	3.3	3.4	1.9
Mdh2	4.3E+08	1.4E+09	4.7E+07	1.6E+08	3.8E+08	3.2	3.5	3.7
Cltc	1.5E+09	4.4E+09	3.6E+08	1.3E+09	7.0E+08	2.9	3.7	6.3
Aldh18a1	2.7E+08	8.4E+08	1.5E+08	5.4E+08	2.9E+08	3.1	3.5	2.9
Hsd17b4	2.2E+08	4.6E+08	2.2E+08	9.6E+08	2.2E+08	2.1	4.5	2.1
Mrpl37	1.2E+07	5.2E+07	5.9E+07	1.3E+08	3.3E+07	4.4	2.2	1.6
Cops3	6.4E+07	2.4E+08	3.5E+07	9.5E+07	1.8E+08	3.7	2.7	1.3
Atp5a1	5.4E+08	2.1E+09	2.3E+08	5.7E+08	1.9E+08	3.9	2.5	11.3
Cct6a	4.8E+08	2.1E+09	1.1E+09	2.3E+09	1.3E+09	4.3	2.1	1.5
Tubb5	6.5E+09	2.5E+10	4.5E+09	1.1E+10	4.1E+09	3.8	2.5	6.0
Tuba1b	2.4E+10	1.0E+11	1.5E+10	3.1E+10	2.2E+10	4.2	2.1	4.7
Dnajc7	1.9E+08	4.4E+08	2.9E+07	1.2E+08	1.7E+08	2.3	3.9	2.6
Snx2	2.2E+07	7.4E+07	4.5E+07	1.3E+08	6.0E+06	3.3	2.9	12.4
Hdlbp	2.8E+08	1.1E+09	3.1E+08	7.6E+08	2.5E+08	3.7	2.5	4.1
Lamp2	6.2E+08	2.5E+09	2.2E+08	4.8E+08	1.6E+09	4.0	2.2	1.6
Copb1	2.9E+08	1.0E+09	1.4E+08	3.6E+08	2.6E+08	3.5	2.6	4.0
Lrpprc	1.7E+08	5.1E+08	1.2E+08	3.6E+08	1.1E+08	3.0	3.1	4.5
Akr1b1	4.8E+08	1.1E+09	7.8E+07	2.8E+08	4.6E+08	2.4	3.6	2.5
Tes	1.0E+08	2.3E+08	1.1E+07	3.9E+07	5.1E+07	2.2	3.7	4.6
Cyp20a1	1.0E+07	2.8E+07	5.7E+06	1.7E+07	0.0E+00	2.7	3.0	∞
Tubb4b	2.3E+10	5.3E+10	8.4E+09	2.7E+10	1.1E+10	2.3	3.1	4.8
Paics	1.6E+08	5.0E+08	5.9E+07	1.4E+08	4.1E+08	3.1	2.3	1.2
Ssr1	3.2E+08	1.1E+09	8.5E+07	1.7E+08	1.9E+08	3.4	2.0	5.8
Eef1g	2.8E+09	6.6E+09	1.3E+09	3.7E+09	1.4E+09	2.3	2.9	4.9
Ehd1	3.7E+08	9.8E+08	4.0E+08	1.0E+09	3.5E+08	2.7	2.6	2.8
Nsun2	4.3E+08	1.1E+09	1.6E+08	4.2E+08	3.7E+08	2.5	2.6	3.0
Mtap	1.2E+08	2.8E+08	2.0E+07	5.8E+07	2.3E+07	2.3	2.9	12.4
Psm14	2.3E+08	7.0E+08	1.6E+08	3.5E+08	1.3E+08	3.0	2.1	5.3
Fkbp5	5.2E+07	1.2E+08	4.7E+07	1.0E+08	8.0E+07	2.3	2.1	1.5
Anxa4	3.9E+08	8.1E+08	5.9E+07	1.4E+08	7.5E+07	2.0	2.4	10.7
Cdk1	7.7E+08	1.5E+09	2.8E+08	6.1E+08	1.4E+08	2.0	2.2	10.9
Pak2	8.9E+07	1.0E+08	3.6E+07	1.4E+08	2.5E+07	1.1	3.8	4.1

Gene names	T1 MT	T1 WT	T2 MT	T2 WT	T1 No TNF	T1 Fold change	T2 Fold change	Fold change with No TNF
Pbk	2.4E+07	3.7E+07	3.4E+07	6.9E+07	1.1E+07	1.5	2.0	3.4

^a Protein hits observed in the Miz1 K-CLASP study. The peptide intensity observed for each sample (WT: N-biotin Miz1 peptide crosslinking in TNF treated lysates, MT: N-biotin mutant Miz1 peptide crosslinking in TNF treated lysates, No TNF: N-biotin Miz1 peptide crosslinking in TNF untreated lysates) for the two trials (T1: trial 1, T2: trial 2) is shown. T1 and T2 fold changes were calculated by dividing the peptide intensity observed in the N-biotin Miz1 peptide crosslinking in TNF treated sample by the peptide intensity observed for the N-biotin mutant Miz1 peptide crosslinking in TNF treated sample. Fold change with no TNF was calculated by dividing the peptide intensity observed in the N-biotin Miz1 peptide crosslinking in TNF treated sample by the peptide intensity observed for the N-biotin Miz1 peptide crosslinking in TNF untreated sample. Infinity (∞) signifies that no peptides were observed in either the N-biotin mutant Miz1 peptide crosslinking sample or the N-biotin Miz1 peptide crosslinking in TNF untreated lysate sample. The K-CLASP hit kinases are yellow colored.

APPENDIX B – CHAPTER 3 SUPPORTING INFORMATION

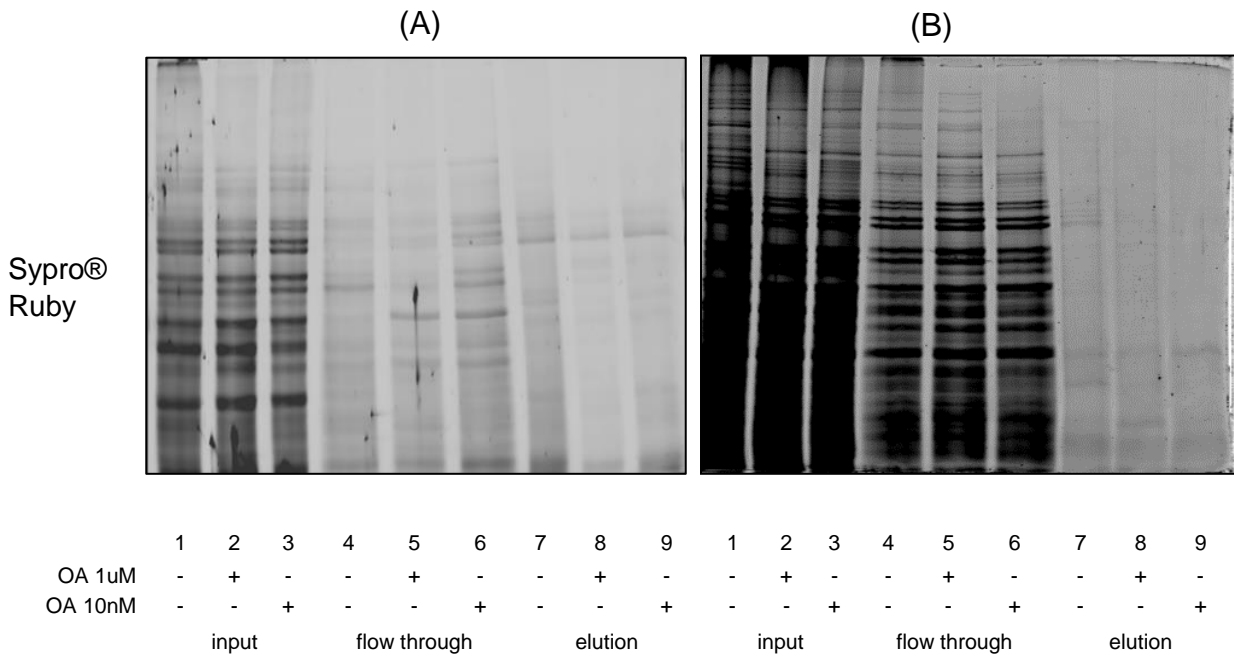


Figure B.1: Replicates of gel images (A-B) from K-BIPS with OA mediated phosphatase inactivation. Biotinylation was carried out with ATP-biotin and HeLa lysates treated with OA. Biotinylated proteins were purified using streptavidin resin after reaction and fractions from purification (input before streptavidin purification, flow through and elution) were separated by SDS-PAGE and visualized by SYPRO®Ruby stain. Control reaction was carried out with HeLa lysates not treated with OA. Trial A shown as Figure 3.5.

Table B.1: Full listing of the 71 hits from K-BIPS with OA mediated phosphatase inactivation^a

Gene names	T1-OA	T1+OA	T2-OA	T2+OA	T1 Fold change	T2 Fold change
SMC1A	2.2E+03	0.0E+00	5.3E+02	0.0E+00	∞	∞
STAR	1.1E+02	0.0E+00	2.0E+02	0.0E+00	∞	∞
C1QBP	2.5E+03	3.7E+02	6.7E+01	0.0E+00	6.8	∞
EIF2S1	7.2E+02	2.1E+02	3.8E+02	0.0E+00	3.4	∞
TRMT10C	2.2E+02	0.0E+00	3.2E+02	1.6E+02	∞	2.1
EPB41	6.4E+02	3.5E+02	3.4E+02	0.0E+00	1.8	∞
DDX60L	4.0E+03	0.0E+00	3.9E+02	2.3E+02	∞	1.7
HSPD1	1.7E+03	1.1E+03	6.8E+01	0.0E+00	1.5	∞
BBS1	3.8E+02	2.6E+02	2.0E+02	0.0E+00	1.5	∞
DAP3	1.3E+04	1.6E+02	8.6E+02	2.4E+02	80.7	3.6
MRPL44	1.2E+04	2.1E+02	4.5E+02	1.8E+02	58.3	2.5
TUBA1B	5.7E+05	1.0E+04	3.8E+04	2.3E+04	57.4	1.6
TUBB	8.3E+04	1.7E+03	6.6E+03	2.4E+03	48.2	2.7
LRPPRC	1.6E+04	4.5E+02	4.2E+03	8.2E+02	35.9	5.1
EIF3A	1.1E+04	3.6E+02	9.6E+02	4.2E+02	29.3	2.3
NCL	2.9E+04	1.3E+03	2.9E+03	8.0E+02	22.6	3.6
PHGDH	5.6E+04	3.5E+03	2.8E+04	2.9E+03	15.8	9.5
GCN1L1	2.0E+04	1.0E+03	1.3E+03	8.6E+02	19.8	1.5
HSP90AB1	1.7E+05	9.6E+03	2.0E+04	1.1E+04	17.7	1.8
TUBA4A	1.2E+04	7.3E+02	9.3E+02	5.3E+02	16.3	1.8
EIF4A3	1.7E+04	1.2E+03	1.1E+03	6.3E+02	14.4	1.7
EZR	2.9E+03	2.1E+02	6.9E+02	3.9E+02	13.6	1.8
DDX1	7.1E+03	5.4E+02	7.7E+02	3.8E+02	13.2	2.0
HLA-B	1.1E+03	4.8E+02	2.3E+03	1.9E+02	2.4	12.2
DHX9	1.5E+04	1.3E+03	1.0E+03	4.7E+02	11.8	2.1
PCNA	2.6E+03	2.2E+02	3.7E+02	1.9E+02	11.9	1.9
ZNF83	7.8E+03	6.8E+02	4.7E+02	2.7E+02	11.5	1.7
KATNAL2	1.5E+04	1.4E+03	2.0E+03	1.2E+03	11.0	1.7
ACADVL	3.0E+03	1.3E+03	2.8E+03	2.8E+02	2.3	10.0
TOM1L2	5.8E+03	9.4E+02	7.2E+02	1.4E+02	6.1	5.1
EXTL3	3.1E+03	4.1E+02	8.3E+02	3.0E+02	7.6	2.8
HSP90B1	1.7E+03	2.8E+02	7.9E+02	2.0E+02	6.2	4.0
VDAC2	2.9E+04	7.6E+03	5.8E+04	9.6E+03	3.8	6.0
CANX	3.4E+04	7.3E+03	2.2E+04	5.1E+03	4.7	4.4
VDAC1	5.3E+04	1.9E+04	1.3E+05	2.1E+04	2.8	6.0
GTF2H4	1.3E+03	2.2E+02	2.5E+02	9.1E+01	5.8	2.7

Gene names	T1-OA	T1+OA	T2-OA	T2+OA	T1 Fold change	T2 Fold change
KIAA1755	5.3E+02	1.5E+02	4.9E+02	1.0E+02	3.6	4.7
MCM3	4.4E+04	7.6E+03	1.5E+04	5.8E+03	5.8	2.5
SERPINB6	7.4E+04	1.7E+04	1.2E+04	3.6E+03	4.4	3.3
RALGAPA1	1.8E+03	9.7E+02	3.4E+03	6.0E+02	1.9	5.6
TNFRSF21	3.4E+03	1.5E+03	6.5E+03	1.3E+03	2.4	5.0
HORMAD1	1.5E+03	9.2E+02	9.5E+02	1.7E+02	1.6	5.5
KPNB1	3.7E+04	8.2E+03	1.8E+04	7.0E+03	4.5	2.6
HADHA	1.8E+04	6.3E+03	1.4E+04	3.6E+03	2.8	3.9
CAD	1.4E+03	6.1E+02	2.0E+03	4.8E+02	2.3	4.1
C3orf17	1.1E+03	4.0E+02	8.4E+02	2.5E+02	2.9	3.4
HADHB	5.0E+04	1.9E+04	1.3E+04	4.3E+03	2.7	3.1
WDR87	1.2E+03	4.6E+02	1.1E+03	3.6E+02	2.7	3.1
RNF207	4.9E+02	1.4E+02	3.4E+02	1.7E+02	3.5	2.0
IMMT	7.0E+02	2.6E+02	1.0E+03	3.8E+02	2.7	2.7
ARFGEF2	1.2E+03	3.4E+02	4.7E+02	3.1E+02	3.6	1.5
SERPINB1	1.1E+05	3.2E+04	1.8E+04	1.1E+04	3.3	1.7
OR5H2	2.2E+03	9.4E+02	8.6E+02	3.3E+02	2.4	2.6
C2orf78	4.8E+02	2.8E+02	4.9E+02	1.5E+02	1.7	3.2
RYR2	4.3E+03	1.4E+03	2.3E+03	1.3E+03	3.0	1.8
RDH13	3.1E+03	9.9E+02	6.8E+02	4.4E+02	3.2	1.5
RPL27	7.4E+03	2.6E+03	1.2E+03	7.4E+02	2.9	1.6
BDP1	7.0E+02	4.7E+02	1.2E+03	3.9E+02	1.5	3.0
LDHA	1.8E+04	9.3E+03	1.6E+04	6.4E+03	1.9	2.5
APMAP	3.8E+03	2.5E+03	1.8E+03	6.5E+02	1.5	2.8
EEF2	3.6E+04	1.3E+04	1.4E+04	8.7E+03	2.7	1.6
MSN	3.4E+05	1.3E+05	2.4E+05	1.5E+05	2.6	1.5
KIF20B	2.1E+03	1.4E+03	5.6E+02	2.4E+02	1.5	2.3
TPP1	3.1E+03	1.7E+03	6.8E+02	3.4E+02	1.8	2.0
PML	1.4E+02	7.0E+01	1.2E+02	7.5E+01	2.0	1.6
CALR	7.1E+02	3.7E+02	6.1E+02	3.7E+02	1.9	1.7
ZNF618	1.8E+03	1.2E+03	2.6E+03	1.3E+03	1.5	2.0
PPIA	1.0E+03	6.5E+02	7.4E+02	4.3E+02	1.6	1.7
PKM	4.5E+04	3.0E+04	3.7E+04	2.1E+04	1.5	1.7
TCF20	2.0E+03	1.2E+03	2.2E+03	1.5E+03	1.6	1.5
HSPA6	3.4E+04	2.2E+04	4.5E+03	2.9E+03	1.6	1.5

^a Protein hits observed in the K-BIPS study with OA mediated phosphatase inactivation. The TMT reporter intensity observed for each sample (-OA: Without okadaic acid, +OA: With okadaic acid) for the two trials (T1: trial 1, T2: trial 2) is shown. Fold change for each trial was calculated by dividing the TMT reporter intensity observed in the okadaic acid untreated sample (phosphatase active) by the TMT reporter intensity

observed for the okadaic acid treated sample (phosphatase inactive). Infinity (∞) signifies that no TMT reporters were observed in the okadaic acid treated sample, making a numeric ratio calculation impossible. The known substrates of the inhibited phosphatases are green colored. The K-BIPS hits that are not previously known substrates, but known to interact with the inhibited phosphatases are blue colored.

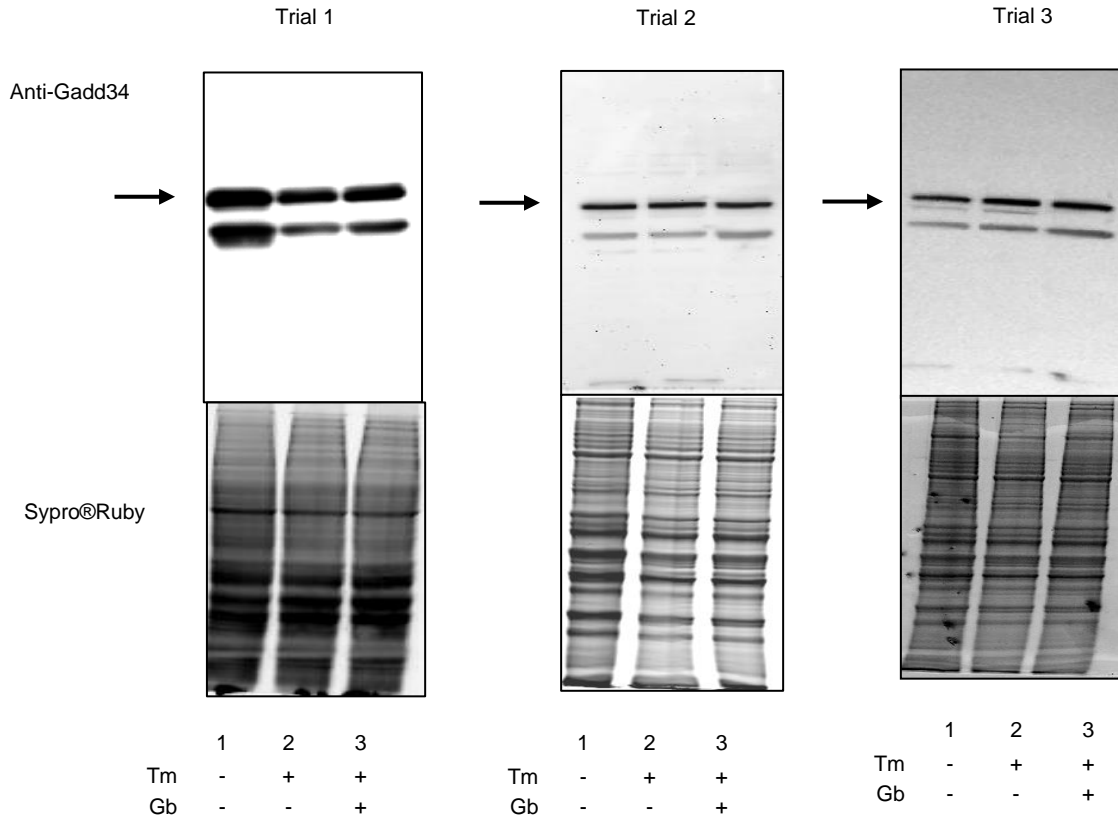
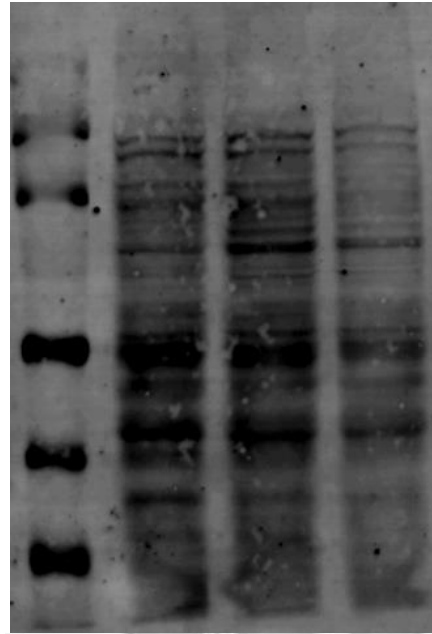


Figure B.2: Replicates of gel images from assessment of Gadd34 expression. Gadd34 expression was probed with Western blot (Top gel) in untreated cells (Lane 1), cells treated with only Tm (Lane 2) and cell treated with both Tm and Gb (Lane 3). The bottom Sypro-Ruby stained gel shows equal protein loading. The arrow points to the band corresponding Gadd34. A cropped image of Trial 1 is shown in Figure 3.8. Trial 2 and 3 were performed by N.Chinthaka.

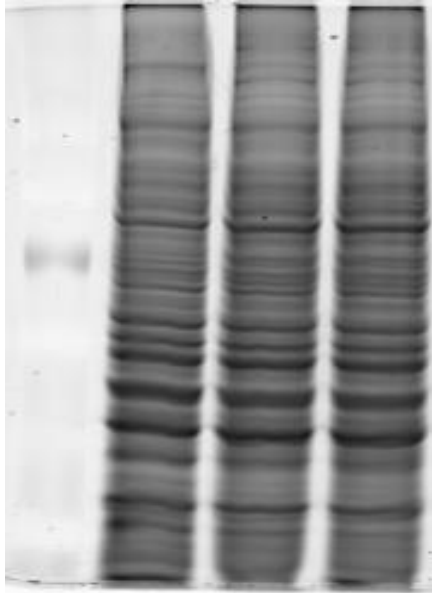
(A)

170
130
95
72
SA-
Cy5
55
43
34



Sypro
@Ruby

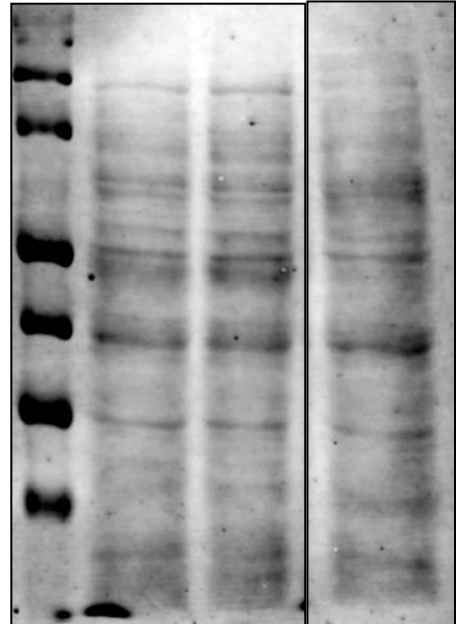
170
130
95
72
55
43
34



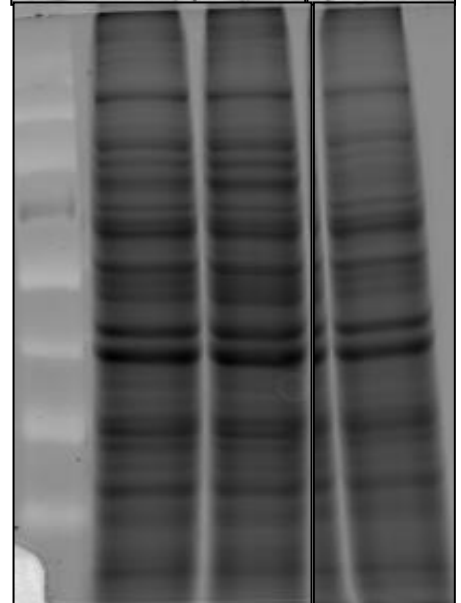
	1	2	3
Tm	-	+	+
Gb	-	-	+

(B)

170
130
95
72
55
43
34
26



170
130
95
72
55
43
34
26



	1	2	3
Tm	-	+	+
Gb	-	-	+

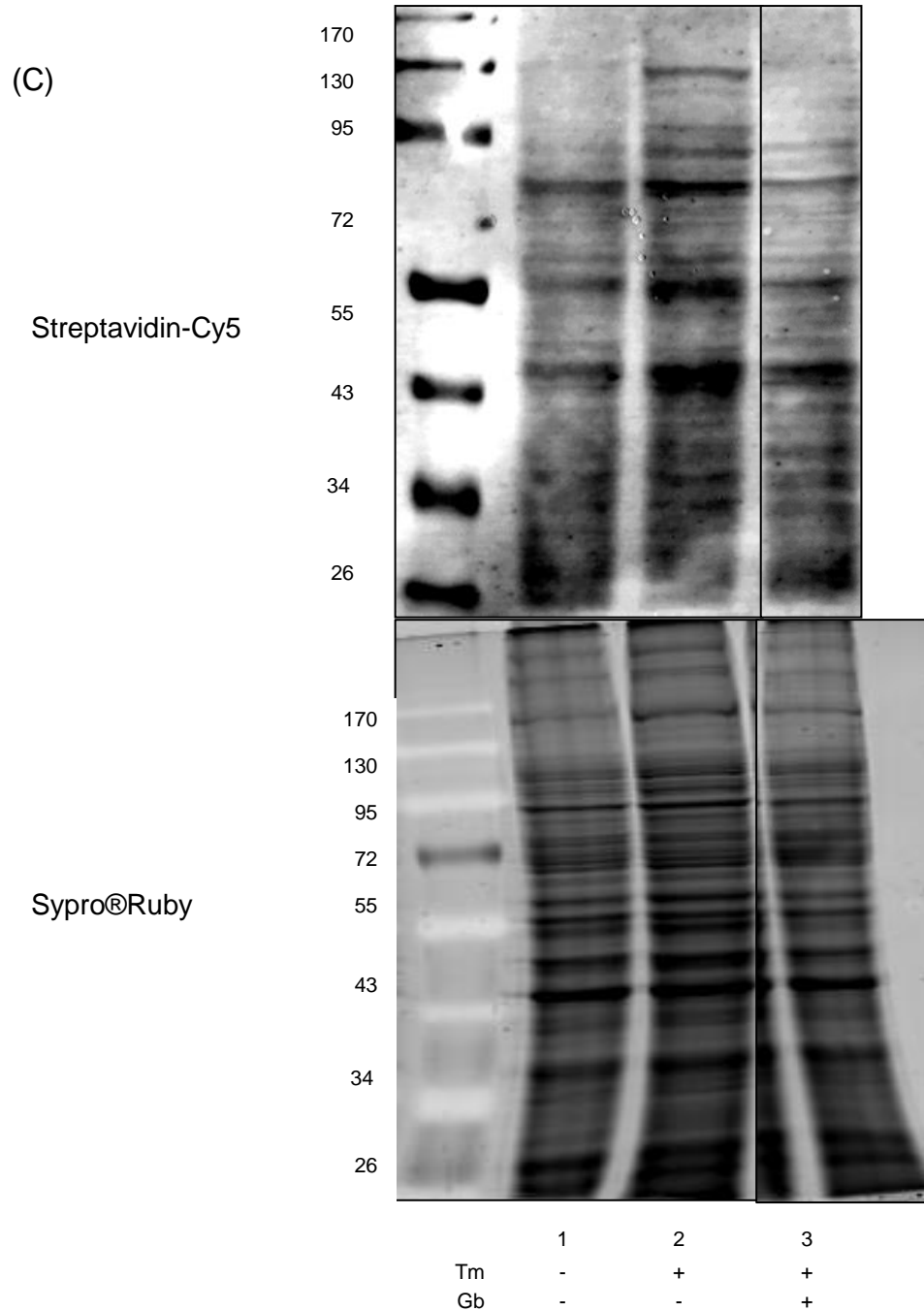


Figure B.3: Replicates of gel images (A-C) from biotinylation reactions using PP1-Gadd34 inactivated lysates. Biotinylation was carried out with HeLa lysates treated with Tm and Gb. Biotinylated proteins were separated by SDS-PAGE and visualized by Streptavidin-Cy5 (top) and SYPRO® Ruby stain (bottom). Control reactions were carried out with HeLa untreated with both Tm and Gb and lysates treated only with Tm. Trial A shown as Figure 3.9.

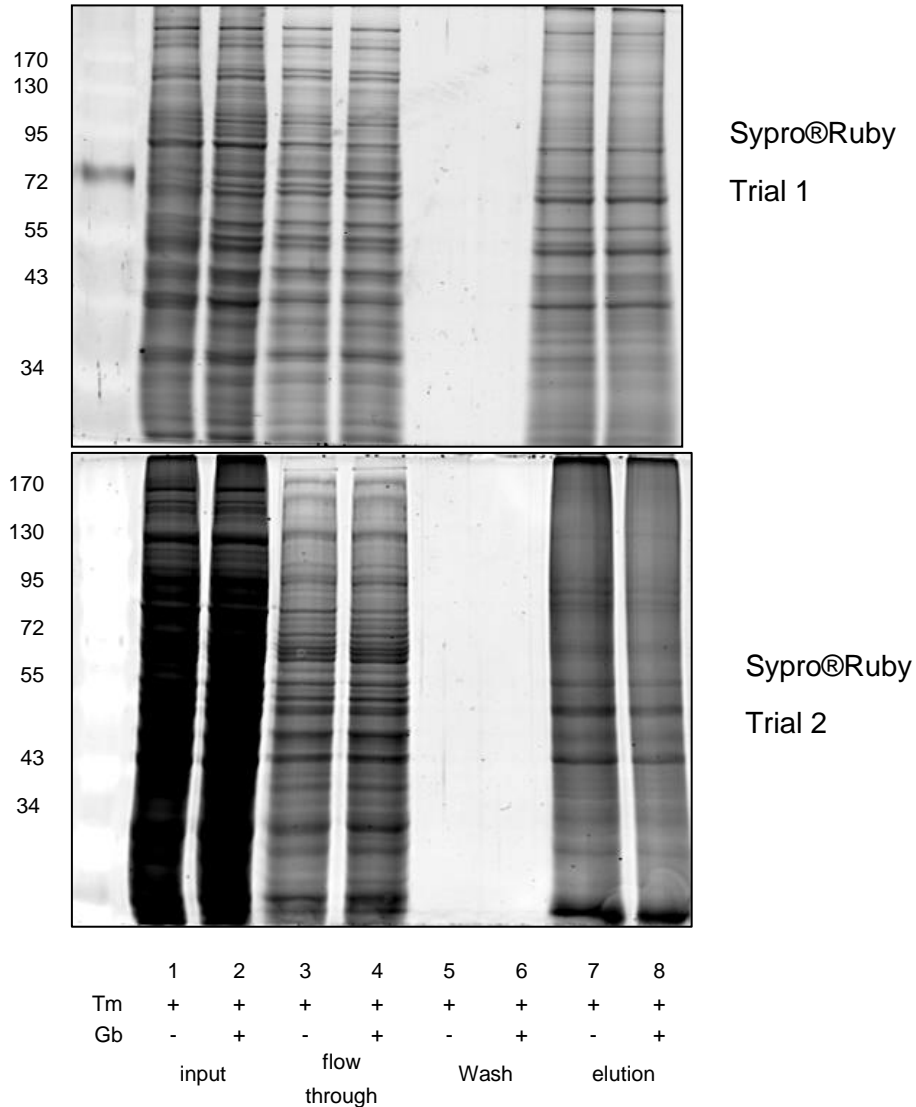


Figure B.4: Replicates of gel images from K-BIPS with PP1-Gadd34 phosphatase inactivation. Biotinylation was carried out with lysates treated with Tm and Gb and with lysates treated only with Tm. After reaction, biotin tagged proteins were purified by Streptavidin resin and separated on SDS-PAGE. The input before streptavidin purification, flow through and elution was also loaded on gel along with the eluted proteins. Then total proteins were visualized with Sypro®Ruby stain. The gels were used for LC-MS/MS analysis.

Table B.2: Full listing of the 130 hits from K-BIPS with PP1-Gadd34 phosphatase inactivation^a

Gene names	T1- Gb	T1 + Gb	T2 -Gb	T2 +Gb	T1 ratio	T2 ratio
RPS12	5.5E+07	0.0E+00	6.5E+06	0.0E+00	∞	∞
FHOD1	5.5E+06	0.0E+00	1.7E+07	0.0E+00	∞	∞
ARF1	2.1E+07	0.0E+00	1.7E+06	0.0E+00	∞	∞
STK3	5.6E+06	0.0E+00	1.5E+07	0.0E+00	∞	∞
IST1	1.2E+07	0.0E+00	6.4E+06	0.0E+00	∞	∞
SNRPF	1.9E+06	0.0E+00	6.4E+06	0.0E+00	∞	∞
EIF4G3	4.7E+06	0.0E+00	2.5E+06	0.0E+00	∞	∞
SLC9A3R1	5.5E+07	1.7E+06	3.1E+06	0.0E+00	31.3	∞
RELA	1.1E+08	5.7E+06	4.4E+06	0.0E+00	20.0	∞
TIMM50	2.6E+07	1.8E+06	2.0E+07	0.0E+00	14.5	∞
FAM120A	3.3E+07	2.3E+06	2.7E+07	0.0E+00	14.0	∞
FDPS	4.8E+08	3.8E+07	2.3E+07	0.0E+00	12.8	∞
PTMA	1.6E+07	1.7E+06	4.7E+06	0.0E+00	9.0	∞
GPI	3.2E+07	3.9E+06	4.2E+06	0.0E+00	8.1	∞
PRDX4	5.7E+07	1.0E+07	1.3E+07	0.0E+00	5.7	∞
AIMP2	1.9E+07	0.0E+00	8.4E+07	1.5E+07	∞	5.6
CTBP2	3.0E+07	6.2E+06	4.8E+06	0.0E+00	4.9	∞
FMR1	1.7E+07	3.6E+06	6.9E+06	0.0E+00	4.7	∞
TIAL1	1.9E+07	4.7E+06	1.0E+07	0.0E+00	4.1	∞
HMGB1P1	1.4E+06	4.4E+05	4.6E+06	0.0E+00	3.1	∞
MAPK1	2.0E+08	6.9E+07	1.1E+07	0.0E+00	2.9	∞
ITPR1	6.2E+06	0.0E+00	3.9E+06	1.5E+06	∞	2.5
PPP2R4	1.0E+08	0.0E+00	8.3E+06	3.3E+06	∞	2.5
STARD7	1.7E+07	0.0E+00	7.4E+06	3.1E+06	∞	2.4
VPS26B	1.1E+07	0.0E+00	1.2E+07	5.1E+06	∞	2.4
CAPN2	1.6E+06	0.0E+00	2.6E+08	1.1E+08	∞	2.3
VPS13A	3.5E+05	0.0E+00	9.9E+06	4.4E+06	∞	2.3
SNX2	3.0E+07	0.0E+00	1.5E+07	6.5E+06	∞	2.2
NARS	7.4E+05	0.0E+00	2.0E+07	9.2E+06	∞	2.2
ERLIN1	8.3E+06	0.0E+00	6.2E+06	2.9E+06	∞	2.1
CKAP4	2.4E+06	0.0E+00	9.2E+07	4.4E+07	∞	2.1
PUF60	4.8E+07	0.0E+00	4.0E+07	2.0E+07	∞	2.0
TNPO2	1.5E+07	0.0E+00	3.9E+06	2.0E+06	∞	2.0
CAPRIN1	1.3E+08	0.0E+00	1.7E+08	8.7E+07	∞	2.0
MYO18A	2.2E+06	1.1E+06	1.9E+07	0.0E+00	2.0	∞
IGF2BP3	1.1E+07	5.7E+06	2.2E+06	0.0E+00	1.9	∞
SYNCRIP	9.4E+06	0.0E+00	2.5E+08	1.4E+08	∞	1.8

Gene names	T1- Gb	T1 + Gb	T2 -Gb	T2 +Gb	T1 ratio	T2 ratio
DAP3	7.2E+06	0.0E+00	1.0E+07	5.9E+06	∞	1.7
PITPNA	5.5E+05	0.0E+00	2.0E+08	1.2E+08	∞	1.7
DNAJB11	4.8E+07	0.0E+00	1.5E+07	8.9E+06	∞	1.7
TIMM44	3.3E+07	1.9E+07	1.7E+06	0.0E+00	1.7	∞
RRM2	7.3E+07	0.0E+00	1.1E+08	6.6E+07	∞	1.6
ATP6V0D1	3.4E+07	0.0E+00	1.1E+08	7.0E+07	∞	1.5
THUMPD1	1.3E+06	0.0E+00	4.6E+06	3.0E+06	∞	1.5
CSNK2A3	1.5E+07	0.0E+00	1.3E+07	9.0E+06	∞	1.5
RNF213	2.1E+05	0.0E+00	6.0E+07	4.3E+07	∞	1.4
MRPS9	5.6E+08	0.0E+00	1.3E+07	9.5E+06	∞	1.4
ANP32E	1.1E+07	0.0E+00	6.7E+07	4.9E+07	∞	1.4
WDR5	5.9E+07	0.0E+00	2.2E+07	1.6E+07	∞	1.4
PSMC3	7.8E+07	6.2E+07	1.3E+07	0.0E+00	1.3	∞
KHDRBS1	5.4E+07	0.0E+00	3.5E+07	2.7E+07	∞	1.3
SMG9	5.9E+06	0.0E+00	7.5E+06	5.8E+06	∞	1.3
NUP37	5.8E+07	0.0E+00	2.7E+07	2.1E+07	∞	1.3
COPS5	9.0E+07	0.0E+00	1.4E+08	1.1E+08	∞	1.3
STRAP	5.7E+08	9.6E+06	1.9E+08	6.7E+07	59.1	2.8
GOT2	3.0E+08	6.2E+06	1.4E+08	1.0E+08	48.4	1.4
ARHGDI1	8.2E+07	2.3E+06	4.6E+06	3.6E+06	35.2	1.3
GAPVD1	4.8E+07	1.4E+06	1.2E+07	9.0E+06	34.7	1.3
EEF1D	1.4E+09	4.1E+07	6.3E+08	3.8E+08	33.9	1.7
DYNC1LI2	2.6E+07	7.7E+05	1.4E+07	1.1E+07	34.1	1.3
G3BP1	1.6E+08	6.3E+06	1.6E+08	1.1E+08	25.7	1.5
ACOT7	9.0E+08	4.3E+07	4.9E+07	2.6E+07	20.8	1.9
UBE2Z	5.0E+08	2.7E+07	1.6E+07	5.1E+06	18.4	3.0
PARVA	1.5E+08	8.4E+06	2.6E+08	1.1E+08	17.4	2.3
PSAT1	6.0E+08	3.5E+07	9.3E+07	5.9E+07	17.3	1.6
RPL10A	6.9E+07	4.2E+06	1.5E+08	1.1E+08	16.5	1.5
PPA1	3.7E+08	2.4E+07	6.6E+07	4.2E+07	15.2	1.6
PDHB	2.4E+08	1.6E+07	6.7E+07	3.6E+07	14.7	1.8
RBBP7	9.8E+07	8.7E+06	6.3E+07	2.6E+07	11.3	2.5
FXR1	1.0E+07	1.1E+06	1.1E+07	4.3E+06	9.8	2.6
ALDOC	4.7E+08	4.9E+07	2.3E+07	8.4E+06	9.4	2.7
ST13	9.5E+07	1.1E+07	5.6E+07	1.8E+07	8.6	3.1
NACA	3.2E+08	3.2E+07	1.0E+09	7.8E+08	10.1	1.3
CAPG	5.4E+08	1.5E+08	4.8E+06	6.4E+05	3.7	7.5
ACTR2	2.7E+08	2.9E+07	3.6E+07	2.4E+07	9.6	1.5
PLXNB2	5.4E+07	5.6E+06	2.2E+07	1.8E+07	9.6	1.3

Gene names	T1- Gb	T1 + Gb	T2 -Gb	T2 +Gb	T1 ratio	T2 ratio
NAP1L4	2.2E+07	3.1E+06	1.1E+07	2.8E+06	6.9	3.8
PICALM	5.3E+08	1.4E+08	1.5E+07	2.2E+06	3.9	6.8
TALDO1	5.3E+08	5.8E+07	1.8E+08	1.2E+08	9.2	1.5
GNB2	8.4E+07	9.2E+06	1.5E+08	1.2E+08	9.1	1.3
VPS26A	3.6E+08	4.1E+07	2.1E+08	1.3E+08	8.7	1.6
SH3GL1	4.5E+07	5.5E+06	1.6E+07	8.6E+06	8.1	1.8
ALDOA	5.5E+09	1.2E+09	1.9E+08	4.3E+07	4.5	4.5
VIM	6.2E+08	8.9E+07	5.2E+09	2.6E+09	7.0	2.0
SEH1L	5.9E+07	8.6E+06	1.9E+07	9.1E+06	6.8	2.1
PTPN12	1.9E+07	2.8E+06	1.2E+07	5.7E+06	6.6	2.1
TWF1	2.3E+08	3.2E+07	8.6E+07	6.5E+07	7.1	1.3
NDRG1	8.6E+08	1.3E+08	5.4E+07	3.2E+07	6.6	1.7
HNRNPAB	8.7E+06	1.3E+06	5.4E+07	4.1E+07	6.6	1.3
EIF3M	7.6E+08	1.4E+08	2.0E+07	8.3E+06	5.4	2.5
HSD17B4	6.4E+08	1.1E+08	1.4E+08	6.5E+07	5.6	2.1
TUBA4A	1.4E+08	3.9E+07	2.0E+07	4.8E+06	3.6	4.1
NDC1	5.4E+06	8.9E+05	4.5E+06	3.1E+06	6.1	1.5
HM13	1.9E+07	3.3E+06	5.9E+06	3.9E+06	5.8	1.5
PRKAR2A	5.1E+07	8.4E+06	3.4E+07	2.7E+07	6.0	1.3
PSMD13	4.2E+08	9.1E+07	4.5E+06	1.7E+06	4.6	2.6
RAN	1.2E+09	6.8E+08	3.7E+07	7.2E+06	1.8	5.1
MAP2K3	7.4E+07	1.6E+07	3.8E+07	2.7E+07	4.7	1.4
SEPHS1	6.5E+07	2.4E+07	1.4E+07	4.3E+06	2.7	3.3
NAP1L1	1.6E+08	3.6E+07	1.7E+08	1.1E+08	4.6	1.5
VAT1	8.5E+07	2.2E+07	2.0E+08	9.2E+07	3.8	2.2
GALE	1.8E+08	4.1E+07	3.6E+07	2.4E+07	4.5	1.5
CALU	2.2E+07	7.0E+06	3.9E+08	1.3E+08	3.1	2.9
ANXA2	1.4E+10	3.0E+09	6.4E+09	5.0E+09	4.5	1.3
RPL26L1	1.5E+07	3.8E+06	1.3E+07	8.0E+06	4.0	1.6
SMARCC1	2.5E+07	1.3E+07	6.5E+06	2.0E+06	1.9	3.3
ENO1	9.2E+08	3.0E+08	3.7E+08	1.7E+08	3.0	2.2
GMPS	1.2E+08	3.2E+07	1.9E+08	1.2E+08	3.6	1.6
DNAJA1	1.3E+08	3.7E+07	4.9E+07	2.8E+07	3.4	1.7
SFN	1.3E+08	3.8E+07	1.4E+07	8.5E+06	3.5	1.6
PSMC2	1.3E+08	5.9E+07	6.5E+07	2.3E+07	2.3	2.8
EIF3G	5.6E+07	1.9E+07	5.8E+07	3.1E+07	3.0	1.8
RPLP0	3.9E+09	1.1E+09	7.8E+09	5.7E+09	3.4	1.4
PPP2R1B	1.7E+07	6.8E+06	6.5E+06	2.9E+06	2.5	2.2
MDH1	2.1E+08	7.0E+07	3.7E+08	2.1E+08	3.0	1.7

Gene names	T1- Gb	T1 + Gb	T2 -Gb	T2 +Gb	T1 ratio	T2 ratio
EIF2S1	1.2E+09	5.1E+08	5.4E+08	2.3E+08	2.4	2.3
UBE3A	2.9E+06	8.7E+05	2.3E+07	1.7E+07	3.3	1.3
UBQLN2	2.0E+06	1.6E+06	1.1E+07	3.3E+06	1.3	3.3
BZW1	6.8E+07	2.0E+07	3.3E+07	2.6E+07	3.3	1.3
SFPQ	6.0E+08	1.8E+08	4.0E+07	3.1E+07	3.3	1.3
PRKAR1A	2.4E+07	7.4E+06	5.1E+07	3.9E+07	3.2	1.3
PGAM1	6.0E+07	3.2E+07	8.9E+06	3.6E+06	1.9	2.5
PDIA6	2.0E+08	1.1E+08	2.8E+08	1.1E+08	1.8	2.5
SF3A1	2.3E+07	1.1E+07	2.2E+07	9.7E+06	2.1	2.2
NUDC	2.7E+08	1.1E+08	2.5E+07	1.5E+07	2.5	1.7
sept7	9.4E+05	4.4E+05	1.5E+08	7.2E+07	2.1	2.0
LAP3	2.6E+07	1.1E+07	3.3E+07	1.9E+07	2.3	1.7
CFL1	1.9E+08	9.7E+07	3.3E+07	1.6E+07	2.0	2.0
SUCLG2	4.1E+06	2.0E+06	1.4E+07	7.3E+06	2.1	1.9
FKBP10	2.7E+07	1.0E+07	3.2E+07	2.4E+07	2.6	1.3

^a Protein hits observed in the K-BIPS study with PP1-Gadd34 inactivation. The peptide intensity observed for each sample (-Gb: Without guanabenz, +Gb: With guanabenz) for the two trials (T1: trial 1, T2: trial 2) is shown. Fold change for each trial was calculated by dividing the peptide intensity observed in the guanabenz untreated sample (PP1-Gadd34 active) sample by the peptide intensity observed for the guanabenz treated sample (PP1-Gadd34 inactive). Infinity (∞) signifies that no peptides were observed in the guanabenz treated sample, making a numeric ratio calculation impossible. EIF2S1, the known substrate of PP1-Gadd34 is green colored.

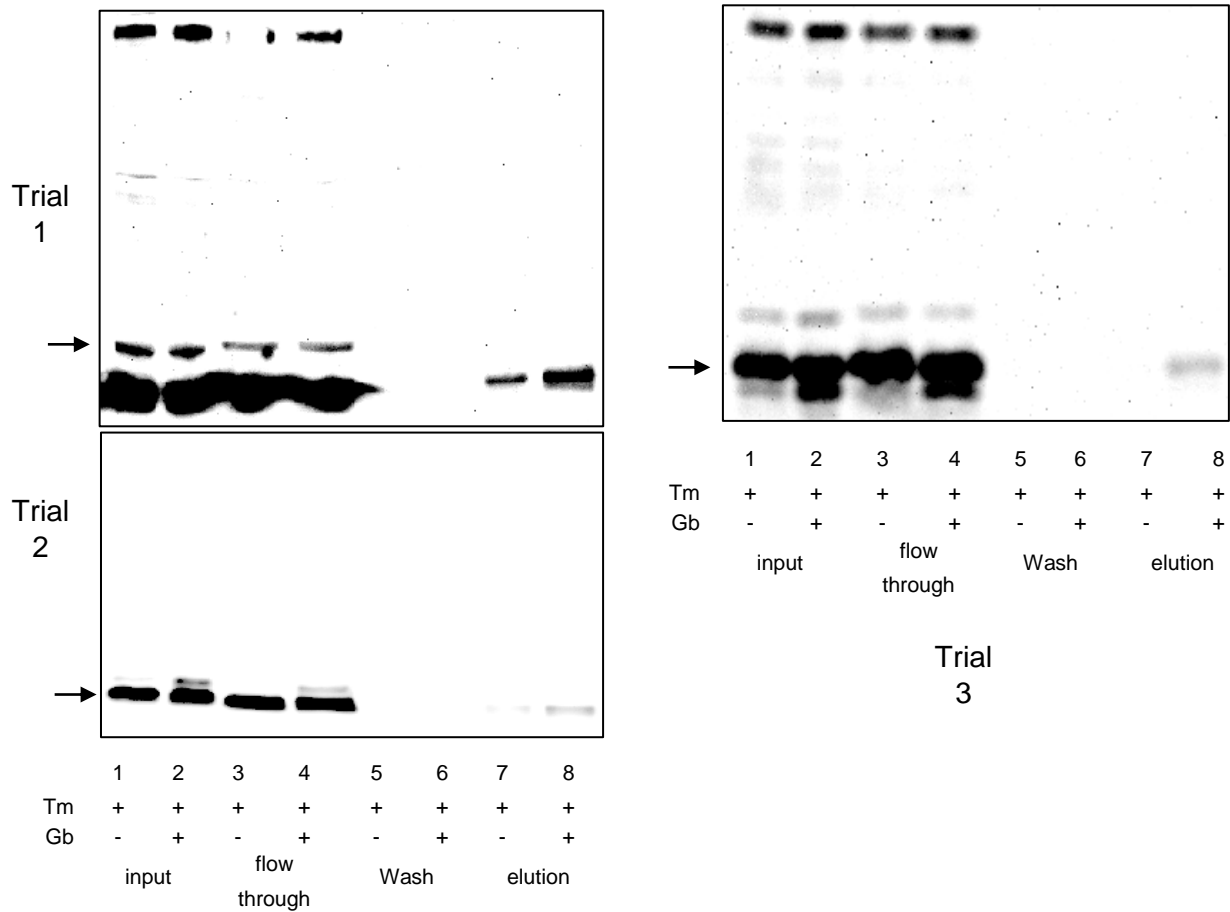


Figure B.5: Full gel images from streptavidin enrichment of COPS5 from biotinylated PP1-Gadd34 active and PP1-Gadd34 inactive lysates. Biotinylation was carried out with HeLa lysates treated with Tm and Gb or with lysates treated with only Tm. Biotinylated proteins were then enriched with streptavidin resin and the input, flow through, wash and elution were separated by SDS-PAGE and visualized with a COPS5 antibody. The arrow indicates the band corresponding to COPS5. Trial 2 is shown in Figure 3.11.

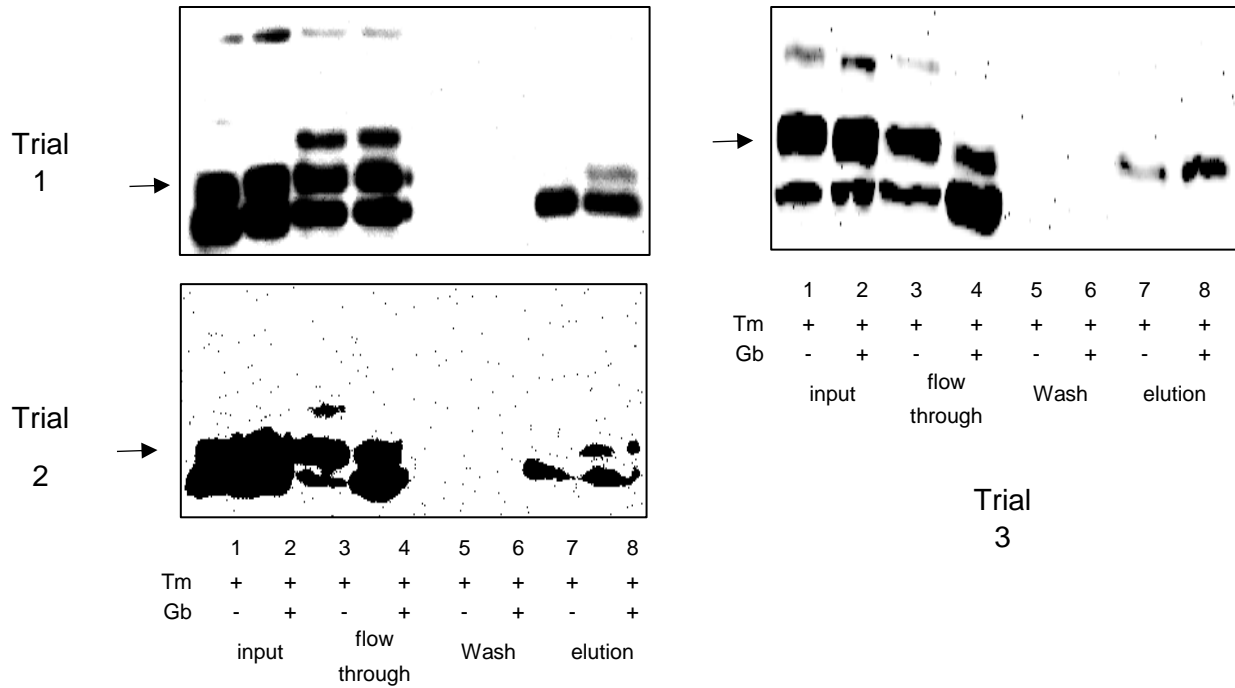


Figure B.6: Full gel images from streptavidin enrichment of WDR5 from biotinylated PP1-Gadd34 active and PP1-Gadd34 inactive lysates. Biotinylation was carried out with HeLa lysates treated with Tm and Gb or with lysates treated with only Tm. Biotinylated proteins were then enriched with streptavidin resin and the input, flow through, wash and elution were separated by SDS-PAGE and visualized by a WDR5 specific antibody by Western blot. The arrow indicates the band corresponding to WDR5. Trial 3 is shown in Figure 3.11.

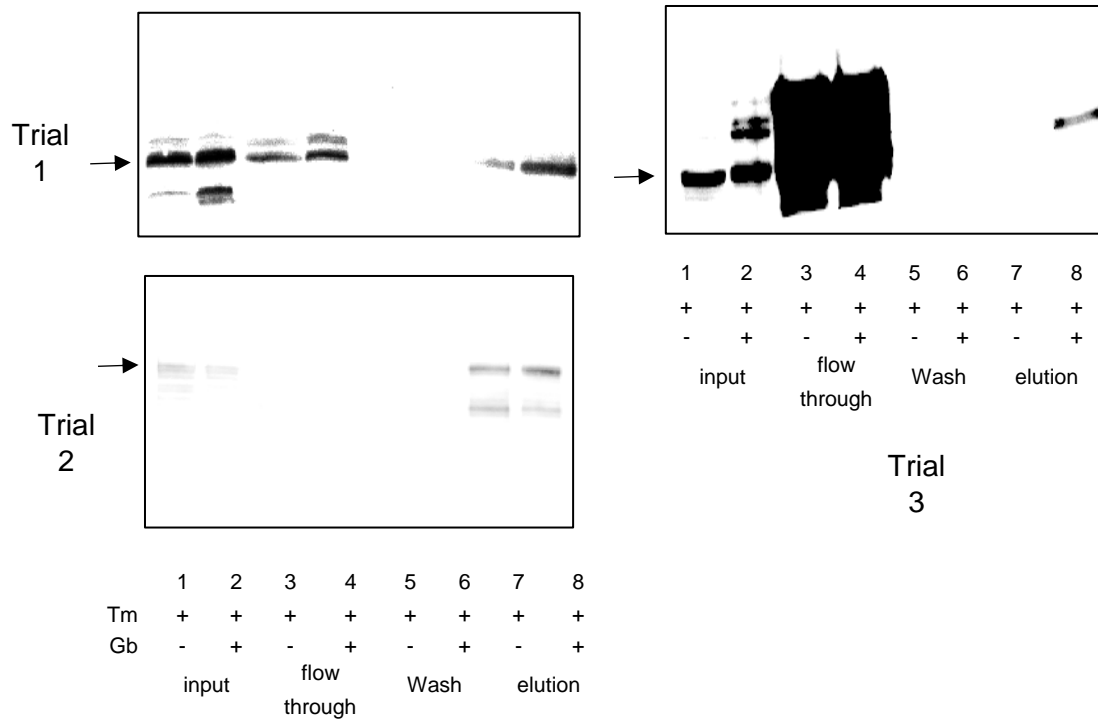


Figure B.7: Full gel images from streptavidin enrichment of CAPRIN1 from biotinylated PP1-Gadd34 active and PP1-Gadd34 inactive lysates. Biotinylation was carried out with HeLa lysates treated with Tm and Gb or with lysates treated with only Tm. Biotinylated proteins were then enriched with streptavidin resin and the input, flow through, wash and elution were separated by SDS-PAGE and visualized by a CAPRIN1 specific antibody by Western blot. The arrow indicates the band corresponding to CAPRIN1. Trial 1 shown in Figure 3.11. Trial 2 was performed by N.Chinthaka.

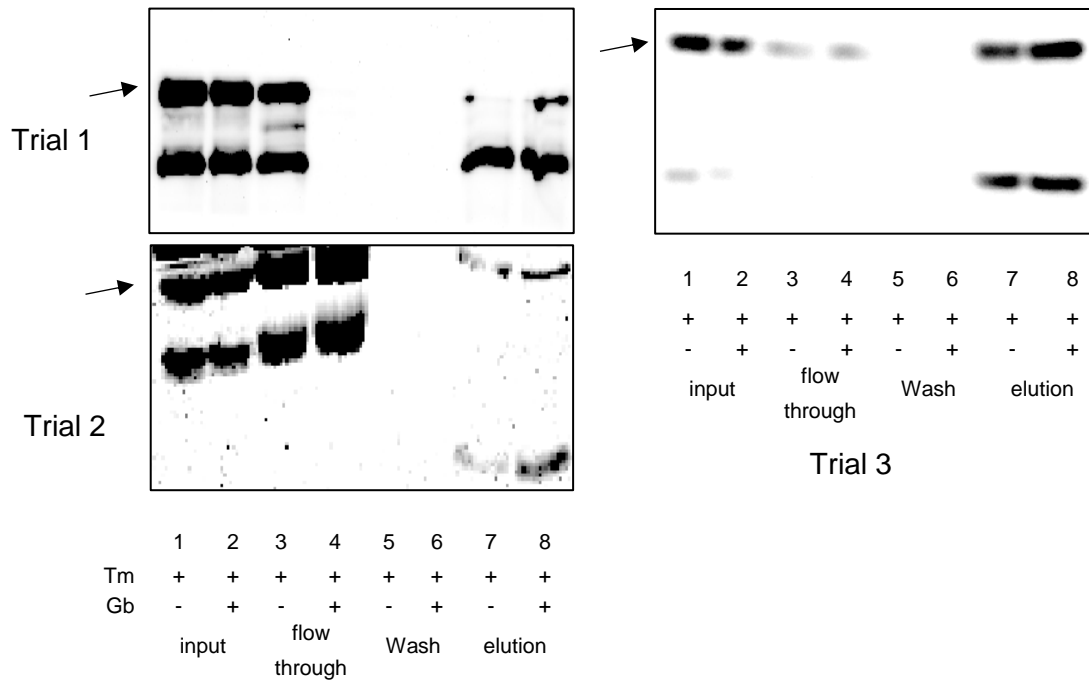


Figure B.8: Full gel images from streptavidin enrichment of G3BP1 from biotinylated PP1-Gadd34 active and PP1-Gadd34 inactive lysates. Biotinylation was carried out with HeLa lysates treated with Tm and Gb or with lysates treated with only Tm. Biotinylated proteins were then enriched with streptavidin resin and the input, flow through, wash and elution were separated by SDS-PAGE and visualized by a G3BP1 specific antibody by Western blot. The arrow indicates the band corresponding to G3BP1. Trial 1 shown in Figure 3.11. Trial 2 and 3 were carried out by N.Chinthaka.

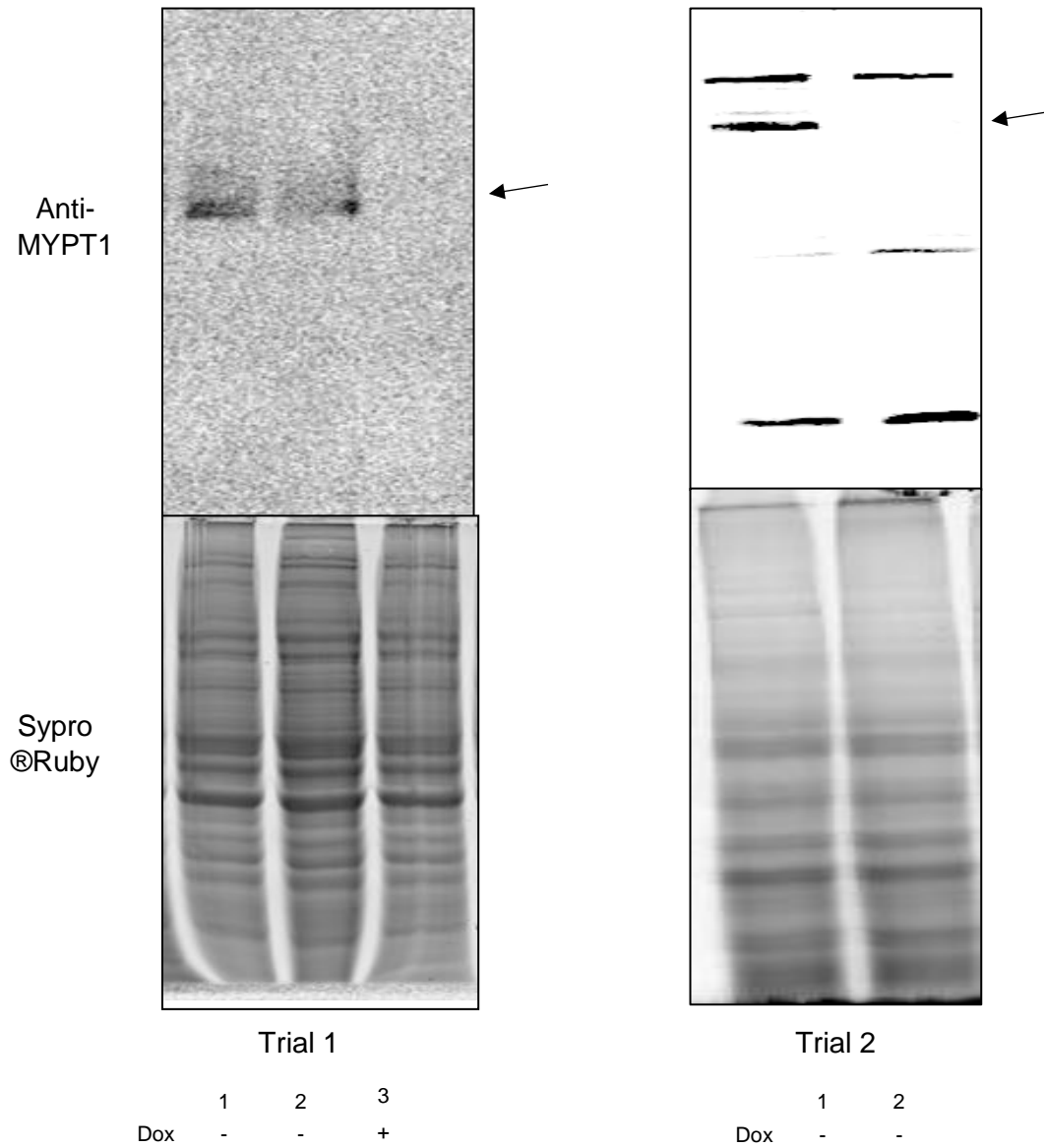
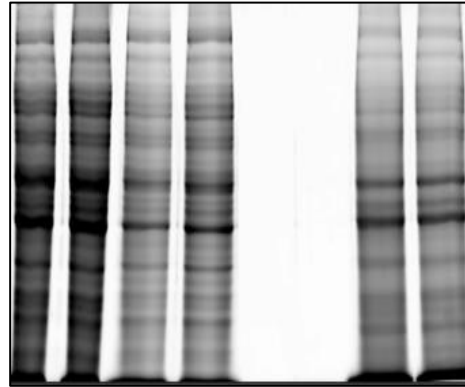
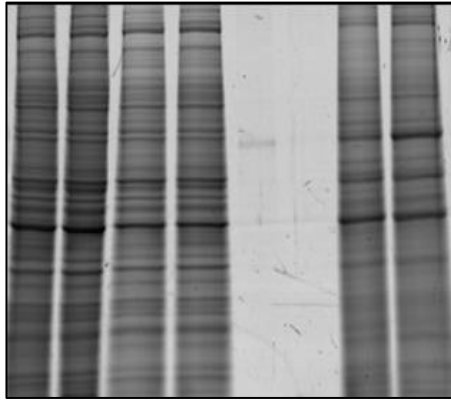
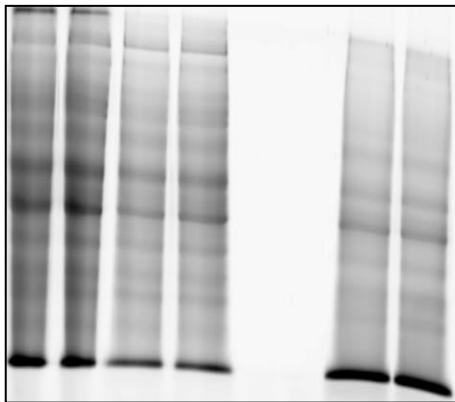


Figure B.9: Assessment of MYPT1 knockdown in L6 myoblasts treated with and without doxycycline. L6 myoblast lysates were separated on SDS-PAGE. Total proteins were visualized with Sypro®Ruby stain and MYPT1 was probed with an anti-MYPT1 antibody. Arrow points to MYPT1. Trial 1 is shown in Figure 3.12.



	1	2	3	4	5	6	7	8
Dox	-	+	-	+	-	+	-	+
	input		flow through		Wash		elution	



	1	2	3	4	5	6	7	8
Dox	-	+	-	+	-	+	-	+
	input		flow through		Wash		elution	

Figure B.10: Replicates of gel images from K-BIPS with PP1-MYPT1 phosphatase inactivation. Biotinylation was carried out with L6 lysates treated with doxycycline (Dox) and without Dox. Biotin tagged proteins were purified by streptavidin and separated on SDS-PAGE. The input before streptavidin resin, flow through, and the last wash were also separated on SDS-PAGE. Total proteins were then visualized by Sypro®Ruby stain. All three gels were used in LC-MS/MS analysis.

Table B.3: The 14 K-BIPS hits enriched in all three trials from the study with PP1-MYPT1 phosphatase inactivation^a

Gene	T1 -Dox	T2 -Dox	T3 -Dox	T1 +Dox	T2 +Dox	T3 +Dox	t-test	T1 Ratio	T2 Ratio	T3 Ratio	Average Ratio
Copg2	2.3E +08	7.2E +07	2.3E +08	1.7E +08	0.0E +00	1.6E +08	0.01	1.3	∞	1.4	∞
Cnp	2.7E +08	2.1E +08	3.9E +08	9.9E +07	0.0E +00	2.2E +08	0.01	2.7	∞	1.8	∞
Akt1	2.7E +07	3.1E +07	6.2E +07	0.0E +00	0.0E +00	4.3E +07	0.02	∞	∞	1.4	∞
Nptn	1.7E +08	1.6E +08	2.2E +08	2.2E +07	1.2E +07	1.4E +08	0.04	7.4	12.9	1.5	7.3
Aldh9a1	1.2E +09	3.0E +08	2.0E +08	1.0E +09	1.7E +08	2.2E +07	0.01	1.2	1.8	9.1	4.0
Actr2	3.2E +09	5.2E +08	1.0E +09	2.5E +09	7.3E +07	5.8E +08	0.03	1.3	7.2	1.8	3.4
Cops4	2.2E +09	2.4E +08	3.2E +08	2.0E +09	4.3E +07	1.6E +08	0.00	1.1	5.5	2.0	2.9
Pdia3	3.0E +10	7.0E +09	1.1E +10	2.0E +10	2.0E +09	4.2E +09	0.03	1.5	3.5	2.6	2.5
Fxr1	1.2E +09	5.0E +08	7.2E +08	9.1E +08	1.6E +08	2.6E +08	0.01	1.4	3.2	2.7	2.4
Fkbp9	3.6E +08	3.0E +08	4.6E +08	1.7E +08	1.0E +08	3.3E +08	0.02	2.1	3.1	1.4	2.2
anxa1	4.0E +10	2.7E +09	4.9E +09	3.8E +10	1.0E +09	1.9E +09	0.03	1.1	2.7	2.6	2.1
Glud1	4.1E +09	6.2E +08	1.1E +09	3.4E +09	2.4E +08	5.1E +08	0.03	1.2	2.6	2.2	2.0
Bre	2.3E +08	2.2E +07	1.2E +08	2.0E +08	6.8E +06	8.3E +07	0.04	1.1	3.2	1.4	1.9
Pdia6	1.3E +10	2.3E +09	3.9E +09	1.1E +10	1.1E +09	2.4E +09	0.01	1.1	2.1	1.6	1.6

^a Protein hits observed in all three trials in the K-BIPS study with PP1-MYPT1 inactivation. The peptide intensity observed for each sample (-Dox: Without doxycycline, +Dox: With doxycycline) for the three trials (T1: trial 1, T2: trial 2, T3: trial 3) is shown. Fold change for each trial was calculated by dividing the peptide intensity observed in the doxycycline untreated sample (PP1-MYPT1 active) sample by the peptide intensity observed for the doxycycline treated sample (PP1-MYPT1 inactive). Infinity (∞) signifies that no peptides were observed in the doxycycline treated sample, making a numeric ratio calculation impossible.

Table B.4: The 161 K-BIPS hits enriched in at least two trials from the study with PP1-MYPT1 phosphatase inactivation^a

Gene Name	T1 -Dox	T2 -Dox	T3 -Dox	T1 +Dox	T2 +Dox	T3 +Dox	T1 Ratio	T2 Ratio	T3 Ratio
SHTN1	2.2E+0 8	6.2E+0 7	4.0E+0 7	0.0E+0 0	2.3E+0 7	0.0E+0 0	∞	2.7	∞
Rnpep	1.8E+0 9	2.2E+0 7	8.6E+0 7	1.2E+0 9	0.0E+0 0	0.0E+0 0	1.5	∞	∞
Mlt4	8.1E+0 6	3.7E+0 7	5.5E+0 7	0.0E+0 0	0.0E+0 0	5.7E+0 7	∞	∞	1.0
Mogs	5.4E+0 8	0.0E+0 0	4.6E+0 7	0.0E+0 0	0.0E+0 0	0.0E+0 0	∞	0.0	∞
Plcg1	2.5E+0 8	1.8E+0 7	1.8E+0 7	2.9E+0 8	0.0E+0 0	0.0E+0 0	0.9	∞	∞
Fcgrt	7.9E+0 6	8.0E+0 7	1.7E+0 7	0.0E+0 0	0.0E+0 0	1.0E+0 8	∞	∞	0.2
Fh	5.8E+0 9	5.8E+0 7	1.4E+0 8	4.1E+0 9	0.0E+0 0	0.0E+0 0	1.4	∞	∞
Gsk3a	1.6E+0 8	1.6E+0 8	4.9E+0 7	1.4E+0 8	0.0E+0 0	0.0E+0 0	1.2	∞	∞
Mif	4.4E+0 8	2.4E+0 8	6.4E+0 7	0.0E+0 0	0.0E+0 0	1.4E+0 8	∞	∞	0.5
Rab8b	1.2E+0 7	4.2E+0 7	1.6E+0 7	0.0E+0 0	0.0E+0 0	1.6E+0 7	∞	∞	1.0
Grpel1	7.0E+0 7	9.7E+0 6	6.0E+0 6	0.0E+0 0	0.0E+0 0	6.7E+0 7	∞	∞	0.1
Adprh	1.2E+0 8	1.7E+0 5	2.1E+0 7	0.0E+0 0	0.0E+0 0	7.5E+0 7	∞	∞	0.3
Atg5	7.1E+0 7	1.5E+0 7	2.4E+0 7	7.0E+0 7	0.0E+0 0	0.0E+0 0	1.0	∞	∞
Ssu72	0.0E+0 0	3.4E+0 7	1.9E+0 7	0.0E+0 0	0.0E+0 0	0.0E+0 0	0.0	∞	∞
Exosc9	1.1E+0 8	2.1E+0 7	6.0E+0 6	2.1E+0 8	0.0E+0 0	0.0E+0 0	0.5	∞	∞
Med4	2.2E+0 6	1.7E+0 7	2.5E+0 7	0.0E+0 0	0.0E+0 0	4.7E+0 7	∞	∞	0.5
Nucb1	7.4E+0 8	5.8E+0 6	2.9E+0 7	7.2E+0 8	0.0E+0 0	0.0E+0 0	1.0	∞	∞
Ndufs2	3.6E+0 8	7.2E+0 6	4.8E+0 7	3.3E+0 8	0.0E+0 0	0.0E+0 0	1.1	∞	∞
Pex14	0.0E+0 0	2.0E+0 7	7.6E+0 7	1.4E+0 7	0.0E+0 0	0.0E+0 0	0.0	∞	∞
Emc10	2.7E+0 7	3.1E+0 7	3.2E+0 7	0.0E+0 0	0.0E+0 0	0.0E+0 0	∞	∞	∞
Snx17	0.0E+0 0	4.8E+0 7	7.7E+0 7	0.0E+0 0	0.0E+0 0	0.0E+0 0	0.0	∞	∞
Pdcd10	3.4E+0 7	0.0E+0 0	1.4E+0 8	0.0E+0 0	1.6E+0 8	0.0E+0 0	∞	0.0	∞
Entpd5	5.4E+0 6	6.3E+0 7	2.2E+0 8	0.0E+0 0	0.0E+0 0	2.0E+0 8	∞	∞	1.1
Fam3c	6.2E+0 7	0.0E+0 0	5.2E+0 7	0.0E+0 0	0.0E+0 0	0.0E+0 0	∞	0.0	∞

Gene Name	T1 -Dox	T2 -Dox	T3 -Dox	T1 +Dox	T2 +Dox	T3 +Dox	T1 Ratio	T2 Ratio	T3 Ratio
Akr7a2	5.8E+0 8	1.7E+0 8	2.2E+0 7	3.0E+0 8	0.0E+0 0	0.0E+0 0	1.9	∞	∞
Xab2	1.1E+0 8	9.1E+0 5	8.5E+0 7	0.0E+0 0	0.0E+0 0	0.0E+0 0	∞	∞	∞
Gde1	6.6E+0 6	0.0E+0 0	1.8E+0 7	0.0E+0 0	0.0E+0 0	0.0E+0 0	∞	0.0	∞
Haus1	3.6E+0 7	0.0E+0 0	1.8E+0 7	0.0E+0 0	0.0E+0 0	0.0E+0 0	∞	0.0	∞
Ola1	2.2E+0 9	1.9E+0 7	7.5E+0 7	3.0E+0 9	0.0E+0 0	1.1E+0 7	0.7	∞	6.9
Tmem214	5.3E+0 7	0.0E+0 0	1.1E+0 8	0.0E+0 0	0.0E+0 0	2.5E+0 7	∞	0.0	4.5
Emc2	2.3E+0 7	2.7E+0 8	9.4E+0 8	8.7E+0 6	2.3E+0 8	3.3E+0 8	2.6	1.1	2.9
Ostc	0.0E+0 0	1.1E+0 8	1.8E+0 8	0.0E+0 0	2.0E+0 7	8.0E+0 7	0.0	5.2	2.3
Otub1	1.4E+0 8	1.7E+0 8	3.5E+0 8	2.1E+0 7	2.0E+0 7	6.1E+0 7	6.4	8.5	5.8
Aasdhpt	0.0E+0 0	1.1E+0 7	2.5E+0 7	0.0E+0 0	0.0E+0 0	6.4E+0 6	0.0	∞	3.8
Acad11	0.0E+0 0	2.7E+0 8	2.5E+0 8	0.0E+0 0	7.4E+0 6	8.6E+0 6	0.0	36.7	29.1
Cul3	6.1E+0 8	0.0E+0 0	1.6E+0 7	2.3E+0 8	0.0E+0 0	0.0E+0 0	2.7	0.0	∞
Nek7	2.8E+0 5	3.0E+0 8	7.0E+0 8	0.0E+0 0	5.2E+0 7	3.6E+0 8	∞	5.7	1.9
Macf1	5.8E+0 8	2.3E+0 8	4.1E+0 8	1.2E+0 8	1.0E+0 8	4.5E+0 8	4.9	2.2	0.9
Ppm1g	1.0E+0 8	4.2E+0 7	7.8E+0 7	2.6E+0 8	1.9E+0 7	1.2E+0 7	0.4	2.2	6.6
Trip12	2.9E+0 7	0.0E+0 0	4.2E+0 7	5.0E+0 6	0.0E+0 0	0.0E+0 0	5.8	0.0	∞
Prkci	0.0E+0 0	7.1E+0 6	3.4E+0 7	0.0E+0 0	0.0E+0 0	2.7E+0 6	0.0	∞	12.5
Bin1	0.0E+0 0	1.0E+0 8	2.0E+0 7	0.0E+0 0	4.8E+0 7	4.7E+0 6	0.0	2.1	4.2
Ptk2	4.5E+0 7	3.0E+0 7	5.4E+0 7	5.5E+0 7	0.0E+0 0	1.3E+0 7	0.8	∞	4.1
Atic	3.3E+0 9	4.5E+0 8	3.5E+0 8	4.7E+0 9	2.6E+0 7	8.1E+0 7	0.7	17.1	4.4
Kif3c	3.8E+0 8	3.0E+0 7	1.2E+0 8	0.0E+0 0	3.7E+0 7	5.9E+0 7	∞	0.8	2.1
Kif1b	2.8E+0 7	0.0E+0 0	7.1E+0 7	5.2E+0 6	0.0E+0 0	2.9E+0 7	5.4	0.0	2.5
Got2	1.8E+1 0	3.1E+0 9	9.9E+0 9	1.1E+1 0	1.3E+0 9	2.9E+0 9	1.5	2.3	3.4
Ldha	4.3E+0 9	1.8E+0 9	3.3E+0 9	7.9E+0 8	8.8E+0 8	2.4E+0 9	5.4	2.0	1.4
Cat	2.8E+0 9	1.2E+0 8	1.9E+0 8	2.0E+0 9	0.0E+0 0	4.5E+0 7	1.4	∞	4.2

Gene Name	T1 -Dox	T2 -Dox	T3 -Dox	T1 +Dox	T2 +Dox	T3 +Dox	T1 Ratio	T2 Ratio	T3 Ratio
Gstp1	1.1E+0 7	3.0E+0 8	3.5E+0 8	0.0E+0 0	1.1E+0 8	3.5E+0 8	∞	2.6	1.0
Scd2	0.0E+0 0	2.3E+0 7	1.9E+0 8	0.0E+0 0	0.0E+0 0	3.2E+0 7	0.0	∞	5.9
Acox1	4.1E+0 8	2.1E+0 7	3.5E+0 7	1.9E+0 8	6.8E+0 6	2.2E+0 7	2.1	3.2	1.6
App	1.2E+0 8	9.6E+0 6	0.0E+0 0	4.0E+0 7	0.0E+0 0	4.4E+0 7	2.9	∞	0.0
Ppia	0.0E+0 0	1.0E+0 8	7.6E+0 8	0.0E+0 0	3.5E+0 7	2.7E+0 8	0.0	2.9	2.8
Aldh3a1	3.8E+0 8	3.2E+0 9	6.3E+0 9	2.2E+0 7	1.1E+0 9	1.6E+0 9	17.8	2.8	3.9
Apeh	9.7E+0 8	0.0E+0 0	3.3E+0 6	2.3E+0 8	0.0E+0 0	0.0E+0 0	4.2	0.0	∞
Spn	0.0E+0 0	8.6E+0 7	1.6E+0 8	0.0E+0 0	0.0E+0 0	4.4E+0 7	0.0	∞	3.6
Pgk1	8.7E+1 0	1.2E+0 8	1.0E+0 9	8.0E+1 0	5.5E+0 6	3.3E+0 8	1.1	21.6	3.0
Acly	9.2E+0 9	7.1E+0 8	4.0E+0 9	6.1E+0 9	1.6E+0 8	1.8E+0 9	1.5	4.4	2.2
Nup62	9.5E+0 8	1.4E+0 7	8.2E+0 7	3.7E+0 8	0.0E+0 0	7.0E+0 7	2.6	∞	1.2
Mat2a	6.4E+0 9	2.8E+0 8	5.4E+0 8	6.5E+0 9	0.0E+0 0	5.5E+0 7	1.0	∞	9.7
Itga1	1.1E+0 8	7.3E+0 6	0.0E+0 0	2.6E+0 7	0.0E+0 0	0.0E+0 0	4.2	∞	0.0
Cpt2	2.4E+0 8	4.8E+0 7	5.7E+0 7	1.2E+0 8	2.2E+0 7	4.4E+0 7	2.1	2.1	1.3
Ptpn1	2.4E+0 8	1.3E+0 8	2.2E+0 7	7.3E+0 7	7.7E+0 7	0.0E+0 0	3.3	1.6	∞
Xdh	1.5E+0 6	4.5E+0 7	2.9E+0 8	0.0E+0 0	4.7E+0 7	5.6E+0 7	∞	1.0	5.2
Rpn2	2.9E+0 8	1.7E+0 9	3.4E+0 9	8.6E+0 7	4.1E+0 8	1.9E+0 9	3.4	4.2	1.8
Hibadh	4.2E+0 8	0.0E+0 0	8.1E+0 7	2.0E+0 7	0.0E+0 0	0.0E+0 0	21.1	0.0	∞
Rnh1	2.4E+0 8	3.0E+0 8	2.5E+0 8	3.9E+0 7	5.3E+0 7	2.3E+0 8	6.2	5.6	1.1
Serpnb2	5.2E+0 6	3.2E+0 8	5.1E+0 8	0.0E+0 0	1.3E+0 8	6.1E+0 8	∞	2.4	0.8
Lta4h	3.2E+0 9	3.3E+0 8	1.4E+0 9	4.1E+0 9	4.3E+0 7	7.3E+0 7	0.8	7.6	18.9
Ezr	7.9E+0 9	9.5E+0 7	6.7E+0 7	3.9E+0 9	1.3E+0 7	1.6E+0 8	2.0	7.0	0.4
Uqcrc2	8.8E+0 6	3.9E+0 8	8.2E+0 8	7.7E+0 7	1.2E+0 8	2.3E+0 8	0.1	3.2	3.5
Gpc1	9.7E+0 7	1.9E+0 8	4.3E+0 8	2.3E+0 7	2.6E+0 7	5.8E+0 8	4.3	7.2	0.8
Ywhab	2.6E+0 7	3.3E+0 9	2.5E+0 9	4.7E+0 6	1.4E+0 9	1.5E+0 9	5.5	2.3	1.7

Gene Name	T1 -Dox	T2 -Dox	T3 -Dox	T1 +Dox	T2 +Dox	T3 +Dox	T1 Ratio	T2 Ratio	T3 Ratio
Ldlr	4.1E+0 7	1.0E+0 8	2.5E+0 8	8.6E+0 5	2.5E+0 7	2.3E+0 8	47.7	4.1	1.1
Ak1	0.0E+0 0	2.9E+0 7	4.5E+0 7	0.0E+0 0	0.0E+0 0	2.0E+0 7	0.0	∞	2.2
Ldhb	1.5E+1 0	8.9E+0 6	0.0E+0 0	1.6E+0 9	0.0E+0 0	0.0E+0 0	9.6	∞	0.0
Pfkm	1.7E+0 9	1.1E+0 8	6.9E+0 8	7.9E+0 8	2.1E+0 7	8.6E+0 8	2.2	5.3	0.8
St13	2.6E+0 9	2.4E+0 8	9.9E+0 7	1.3E+0 9	1.1E+0 7	2.1E+0 8	2.1	22.3	0.5
Rab4b	0.0E+0 0	1.5E+0 8	2.6E+0 7	0.0E+0 0	3.9E+0 7	0.0E+0 0	0.0	3.9	∞
Lum	1.2E+0 9	5.4E+0 8	6.0E+0 8	3.5E+0 7	2.5E+0 8	4.2E+0 7	33.9	2.2	14.1
Ap1b1	5.2E+0 8	2.8E+0 7	4.1E+0 8	4.8E+0 8	1.1E+0 7	1.4E+0 8	1.1	2.5	3.0
Nckap1	4.9E+0 8	4.7E+0 7	4.1E+0 8	2.1E+0 8	1.3E+0 7	2.5E+0 8	2.3	3.7	1.6
Casp3	2.0E+0 7	7.1E+0 7	8.7E+0 7	0.0E+0 0	1.5E+0 6	8.1E+0 7	∞	46.1	1.1
Actb	1.1E+0 9	1.1E+0 9	1.6E+0 9	4.1E+0 7	3.3E+0 8	1.7E+0 9	26.3	3.4	0.9
Chp1	0.0E+0 0	9.6E+0 7	9.1E+0 7	0.0E+0 0	4.0E+0 7	1.5E+0 7	0.0	2.4	6.0
Rhoa	2.2E+0 7	1.8E+0 9	4.9E+0 8	0.0E+0 0	3.6E+0 8	1.2E+0 9	∞	5.1	0.4
Pafah1b1	2.7E+0 9	9.3E+0 7	1.4E+0 8	1.5E+0 9	0.0E+0 0	3.4E+0 7	1.8	∞	4.1
Eif4e	2.8E+0 7	8.4E+0 6	1.8E+0 8	0.0E+0 0	1.5E+0 7	7.2E+0 6	∞	0.6	25.4
Eif2b3	1.3E+0 8	3.4E+0 7	5.9E+0 7	2.4E+0 7	0.0E+0 0	6.6E+0 7	5.5	∞	0.9
Nagk	1.9E+0 8	0.0E+0 0	2.1E+0 7	1.5E+0 7	0.0E+0 0	0.0E+0 0	12.9	0.0	∞
Stim1	3.0E+0 7	0.0E+0 0	2.6E+0 6	1.3E+0 7	0.0E+0 0	0.0E+0 0	2.3	0.0	∞
Arpc2	1.5E+0 7	1.0E+0 8	5.1E+0 8	7.3E+0 6	1.1E+0 7	4.5E+0 8	2.1	9.3	1.1
Pgls	1.6E+0 8	3.9E+0 8	4.3E+0 8	1.8E+0 8	1.1E+0 8	7.5E+0 7	0.9	3.6	5.8
Slc25a11	5.7E+0 7	0.0E+0 0	3.2E+0 8	0.0E+0 0	0.0E+0 0	9.0E+0 7	∞	0.0	3.5
Aldh6a1	4.5E+0 7	2.4E+0 8	1.6E+0 8	0.0E+0 0	1.0E+0 8	1.0E+0 8	∞	2.3	1.6
Rabggtb	4.0E+0 8	0.0E+0 0	5.5E+0 7	6.6E+0 7	0.0E+0 0	0.0E+0 0	6.1	0.0	∞
Tomm34	0.0E+0 0	1.6E+0 7	5.8E+0 7	8.0E+0 7	0.0E+0 0	7.4E+0 6	0.0	∞	7.8
Aldh16a1	2.0E+0 8	5.6E+0 8	1.9E+0 9	9.8E+0 6	2.7E+0 8	6.4E+0 8	20.3	2.1	3.0

Gene Name	T1 -Dox	T2 -Dox	T3 -Dox	T1 +Dox	T2 +Dox	T3 +Dox	T1 Ratio	T2 Ratio	T3 Ratio
Dnajc10	2.0E+0 8	3.4E+0 8	1.4E+0 9	1.9E+0 7	1.0E+0 7	1.5E+0 9	10.7	34.1	0.9
Wdr18	0.0E+0 0	3.0E+0 7	1.4E+0 8	4.1E+0 6	0.0E+0 0	1.6E+0 7	0.0	∞	8.4
C1galt1c1	1.6E+0 7	0.0E+0 0	6.7E+0 7	0.0E+0 0	0.0E+0 0	2.1E+0 7	∞	0.0	3.2
Gmps	4.1E+0 9	6.4E+0 7	1.0E+0 8	4.3E+0 9	2.4E+0 7	2.1E+0 7	0.9	2.7	4.8
Golim4	1.6E+0 7	5.8E+0 8	1.3E+0 9	0.0E+0 0	2.3E+0 8	8.3E+0 8	∞	2.5	1.5
Slc30a7	5.6E+0 7	1.1E+0 8	2.7E+0 7	3.8E+0 8	4.1E+0 7	0.0E+0 0	0.1	2.5	∞
Ufm1	0.0E+0 0	8.8E+0 7	1.8E+0 7	0.0E+0 0	2.3E+0 7	0.0E+0 0	0.0	3.8	∞
Mlec	0.0E+0 0	3.1E+0 8	9.4E+0 8	0.0E+0 0	1.2E+0 8	4.6E+0 8	0.0	2.6	2.1
Aip	5.3E+0 8	8.4E+0 7	1.0E+0 8	1.3E+0 8	7.3E+0 7	2.0E+0 7	4.0	1.1	5.0
Tmed9	5.4E+0 5	1.6E+0 9	1.2E+0 9	0.0E+0 0	6.9E+0 8	1.4E+0 9		2.3	0.8
Spc25	6.6E+0 5	2.8E+0 7	8.9E+0 8	5.2E+0 7	0.0E+0 0	3.3E+0 8	0.0	∞	2.7
Herc4	2.7E+0 8	2.5E+0 7	4.7E+0 7	7.7E+0 7	0.0E+0 0	5.3E+0 7	3.5	∞	0.9
Uxs1	0.0E+0 0	4.1E+0 7	7.7E+0 7	0.0E+0 0	1.1E+0 7	3.2E+0 6	0.0	3.6	23.9
Ctps2	1.4E+0 9	0.0E+0 0	1.2E+0 6	6.1E+0 8	0.0E+0 0	0.0E+0 0	2.3	0.0	∞
Emc3	5.9E+0 7	1.0E+0 8	3.4E+0 8	0.0E+0 0	3.6E+0 7	5.4E+0 6	∞	2.8	63.6
Ccdc47	1.7E+0 8	3.4E+0 7	6.4E+0 8	1.7E+0 8	1.6E+0 7	2.2E+0 8	1.0	2.1	3.0
Tars	1.9E+1 0	3.5E+0 7	1.0E+0 8	1.4E+1 0	1.4E+0 7	3.9E+0 7	1.3	2.5	2.7
Abhd6	1.4E+0 7	1.6E+0 8	1.5E+0 8	0.0E+0 0	9.8E+0 6	1.5E+0 8	∞	16.3	1.0
Eci2	0.0E+0 0	1.9E+0 8	2.3E+0 8	0.0E+0 0	7.7E+0 7	1.0E+0 8	0.0	2.5	2.2
Tmx2	0.0E+0 0	2.8E+0 7	2.4E+0 8	4.1E+0 6	8.9E+0 6	5.9E+0 7	0.0	3.1	4.0
Pelo	2.5E+0 8	1.5E+0 8	4.5E+0 8	1.1E+0 8	3.9E+0 7	1.2E+0 8	2.3	3.9	3.9
Ubr5	2.1E+0 7	3.8E+0 6	0.0E+0 0	9.9E+0 6	0.0E+0 0	0.0E+0 0	2.1	∞	0.0
Rcn2	5.6E+0 7	7.2E+0 7	4.3E+0 7	2.0E+0 7	3.2E+0 7	1.4E+0 8	2.8	2.3	0.3
Kif2c	3.4E+0 7	0.0E+0 0	1.6E+0 8	0.0E+0 0	4.5E+0 7	4.5E+0 7	∞	0.0	3.5
Dpysl3	4.4E+0 8	1.9E+0 8	4.2E+0 8	3.8E+0 8	4.7E+0 7	8.8E+0 7	1.2	4.0	4.7


Gene Name	T1 -Dox	T2 -Dox	T3 -Dox	T1 +Dox	T2 +Dox	T3 +Dox	T1 Ratio	T2 Ratio	T3 Ratio
Eif2ak2	0.0E+0 0	4.2E+0 7	8.1E+0 7	0.0E+0 0	0.0E+0 0	1.6E+0 7	0.0	∞	5.1
Tpm3	1.0E+0 7	1.1E+0 9	9.4E+0 8	0.0E+0 0	3.7E+0 8	9.8E+0 8	∞	3.0	1.0
Gbp2	1.1E+0 8	1.2E+0 8	7.0E+0 7	6.0E+0 7	2.5E+0 7	2.9E+0 7	1.9	4.7	2.4
Aldh7a1	3.0E+0 9	5.8E+0 8	1.6E+0 8	3.5E+0 9	2.8E+0 7	2.7E+0 7	0.9	20.4	6.0
Leprel4	2.0E+0 7	2.6E+0 8	5.1E+0 8	3.8E+0 6	1.1E+0 8	4.4E+0 8	5.3	2.4	1.2
Hsph1	5.5E+0 9	8.9E+0 8	1.2E+0 9	3.3E+0 9	2.6E+0 8	5.2E+0 8	1.7	3.4	2.3
Gsn	0.0E+0 0	2.7E+0 7	2.3E+0 8	1.1E+0 7	1.1E+0 7	9.1E+0 7	0.0	2.4	2.5
Lap3	8.5E+0 8	2.2E+0 9	3.0E+0 9	3.5E+0 8	7.5E+0 8	1.8E+0 9	2.4	2.9	1.7
Cops3	2.0E+0 9	1.9E+0 8	1.0E+0 8	1.9E+0 9	6.0E+0 7	4.8E+0 7	1.0	3.3	2.1
Nup35	0.0E+0 0	3.2E+0 7	1.2E+0 7	0.0E+0 0	7.7E+0 6	0.0E+0 0	0.0	4.2	∞
Pycr2	3.2E+0 8	2.5E+0 8	5.8E+0 8	2.0E+0 7	8.3E+0 7	1.0E+0 9	16.0	3.0	0.6
Hgh1	7.5E+0 6	1.7E+0 8	6.0E+0 8	1.2E+0 8	7.7E+0 6	1.3E+0 8	0.1	22.6	4.5
Capg	9.7E+0 8	4.0E+0 8	6.4E+0 8	1.0E+0 9	8.9E+0 7	2.7E+0 8	0.9	4.5	2.3
Tsg101	4.4E+0 8	3.0E+0 7	3.9E+0 7	1.9E+0 8	3.7E+0 6	5.3E+0 6	2.3	8.3	7.4
Cops8	0.0E+0 0	1.8E+0 8	1.7E+0 7	0.0E+0 0	9.8E+0 6	3.5E+0 6	0.0	17.9	4.7
Gpi	1.1E+0 9	3.9E+0 6	3.6E+0 7	1.1E+0 9	0.0E+0 0	1.2E+0 7	1.1	∞	3.1
Sars	9.4E+0 8	4.1E+0 6	1.8E+0 6	4.5E+0 8	0.0E+0 0	2.4E+0 7	2.1	∞	0.1
Asah1	2.8E+0 7	1.3E+0 8	4.2E+0 8	0.0E+0 0	2.4E+0 7	4.3E+0 8	∞	5.4	1.0
Pds5b	8.8E+0 6	0.0E+0 0	1.3E+0 7	1.0E+0 6	0.0E+0 0	0.0E+0 0	8.8	0.0	∞
Rbbp7	1.3E+1 0	6.2E+0 8	1.4E+0 9	8.9E+0 9	2.4E+0 8	7.2E+0 8	1.4	2.6	2.0
Apob	3.3E+0 7	1.7E+0 8	1.8E+0 8	0.0E+0 0	4.1E+0 7	1.6E+0 8	∞	4.2	1.1
Ehd3	5.0E+0 8	3.9E+0 8	5.0E+0 8	1.2E+0 8	8.0E+0 7	7.0E+0 8	4.1	4.9	0.7
Ppp4r1	2.2E+0 8	7.5E+0 7	5.0E+0 7	7.4E+0 7	1.8E+0 7	2.9E+0 7	2.9	4.1	1.7
Khdrbs1	5.0E+0 8	3.5E+0 7	9.4E+0 7	4.2E+0 8	1.4E+0 7	2.5E+0 7	1.2	2.6	3.8
Pi4k2a	5.6E+0 8	0.0E+0 0	3.0E+0 8	1.4E+0 8	0.0E+0 0	1.4E+0 6	4.0	0.0	215.0

Gene Name	T1 -Dox	T2 -Dox	T3 -Dox	T1 +Dox	T2 +Dox	T3 +Dox	T1 Ratio	T2 Ratio	T3 Ratio
Arpc1a	1.4E+0 7	0.0E+0 0	6.8E+0 7	0.0E+0 0	0.0E+0 0	2.6E+0 7	∞	0.0	2.6
Arl6ip5	1.2E+0 8	9.9E+0 7	1.4E+0 8	2.6E+0 7	6.5E+0 7	5.1E+0 7	4.6	1.5	2.8
Wnk1	5.4E+0 7	3.6E+0 7	0.0E+0 0	0.0E+0 0	1.3E+0 7	0.0E+0 0	∞	2.7	0.0
Cul5	2.0E+0 8	3.1E+0 7	2.5E+0 7	6.8E+0 7	1.5E+0 7	1.3E+0 8	3.0	2.1	0.2
Ccs	0.0E+0 0	3.7E+0 7	6.8E+0 7	0.0E+0 0	0.0E+0 0	2.7E+0 7	0.0	∞	2.5
Prpf19	3.8E+0 9	3.4E+0 8	2.3E+0 8	1.7E+0 9	1.1E+0 8	3.3E+0 8	2.3	3.0	0.7
Htra1	7.9E+0 6	1.8E+0 8	5.4E+0 8	9.0E+0 5	7.6E+0 7	4.6E+0 8	8.8	2.4	1.2
Lepre1	4.0E+0 8	1.3E+0 9	1.6E+0 9	1.0E+0 8	3.7E+0 8	4.8E+0 8	3.8	3.5	3.3
Clic4	7.1E+0 6	8.3E+0 8	3.6E+0 9	3.3E+0 6	2.1E+0 8	1.6E+0 9	2.2	3.9	2.3
Actn1	8.2E+0 9	2.3E+0 6	5.2E+0 8	7.7E+0 9	0.0E+0 0	1.1E+0 8	1.1	∞	4.8
Nap111	7.4E+0 9	3.4E+0 8	1.0E+0 9	2.8E+0 9	5.0E+0 7	7.3E+0 8	2.6	6.8	1.4


^aProtein hits enriched in at least two replicates (at least 2 fold enrichment in at least two replicates) in the K-BIPS study with PP1-MYPT1 phosphatase inactivation. The peptide intensity observed for each sample (-Dox: Without doxycycline, +Dox: With doxycycline) for the three trials (T1: trial 1, T2: trial 2, T3: trial 3) is shown. Fold change for each trial was calculated by dividing the peptide intensity observed in the doxycycline untreated sample (PP1-MYPT1 active) sample by the peptide intensity observed for the doxycycline treated sample (PP1-MYPT1 inactive). Infinity (∞) signifies that no peptides were observed in the doxycycline treated sample, making a numeric ratio calculation impossible.


APPENDIX C - COPYRIGHT PERMISSIONS

C1. Reprint authorization for Dedigama-Arachchige, P. M.; Pflum, M. K., K-CLASP: A tool to identify phosphosite specific kinases and interacting proteins. *ACS Chem Biol* 2016.



Copyright Clearance Center



[Home](#)
[Create Account](#)
[Help](#)




ACS Publications
Most Trusted. Most Cited. Most Read.

Title: K-CLASP: A Tool to Identify Phosphosite Specific Kinases and Interacting Proteins

Author: Pavithra M. Dedigama-Arachchige, Mary Kay H. Pflum

Publication: ACS Chemical Biology

Publisher: American Chemical Society

Date: Oct 1, 2016

Copyright © 2016, American Chemical Society

LOGIN

If you're a copyright.com user, you can login to RightsLink using your copyright.com credentials. Already a RightsLink user or want to [learn more?](#)

Quick Price Estimate

Permission for this particular request is granted for print and electronic formats, and translations, at no charge. Figures and tables may be modified. Appropriate credit should be given. Please print this page for your records and provide a copy to your publisher. Requests for up to 4 figures require only this record. Five or more figures will generate a printout of additional terms and conditions. Appropriate credit should read: "Reprinted with permission from {COMPLETE REFERENCE CITATION}. Copyright {YEAR} American Chemical Society." Insert appropriate information in place of the capitalized words.

I would like to... ?	<input type="text" value="reuse in a Thesis/Dissertation"/>	This service provides permission for reuse only. If you do not have a copy of the article you are using, you may copy and paste the content and reuse according to the terms of your agreement. Please be advised that obtaining the content you license is a separate transaction not involving Rightslink.
Requestor Type ?	<input type="text" value="Author (original work)"/>	
Portion ?	<input type="text" value="Full article"/>	
Format ?	<input type="text" value="Print"/>	
Will you be translating? ?	<input type="text" value="No"/>	
Select your currency	<input type="text" value="USD - \$"/>	
Quick Price	<input type="button" value="Click Quick Price"/>	

To request permission for a type of use not listed, please contact [the publisher](#) directly.

Copyright © 2016 Copyright Clearance Center, Inc. All Rights Reserved. [Privacy statement](#). [Terms and Conditions](#).
Comments? We would like to hear from you. E-mail us at customer@copyright.com



RightsLink®

[Home](#)
[Create Account](#)
[Help](#)


ACS Publications
Most Trusted. Most Cited. Most Read.

Title: K-CLASP: A Tool to Identify Phosphosite Specific Kinases and Interacting Proteins
Author: Pavithra M. Dedigama-Arachchige, Mary Kay H. Pflum
Publication: ACS Chemical Biology
Publisher: American Chemical Society
Date: Oct 1, 2016

Copyright © 2016, American Chemical Society

[LOGIN](#)

If you're a [copyright.com](#) user, you can login to RightsLink using your [copyright.com](#) credentials. Already a [RightsLink](#) user or want to [learn more?](#)

PERMISSION/LICENSE IS GRANTED FOR YOUR ORDER AT NO CHARGE

This type of permission/license, instead of the standard Terms & Conditions, is sent to you because no fee is being charged for your order. Please note the following:

- Permission is granted for your request in both print and electronic formats, and translations.
- If figures and/or tables were requested, they may be adapted or used in part.
- Please print this page for your records and send a copy of it to your publisher/graduate school.
- Appropriate credit for the requested material should be given as follows: "Reprinted (adapted) with permission from (COMPLETE REFERENCE CITATION). Copyright (YEAR) American Chemical Society." Insert appropriate information in place of the capitalized words.
- One-time permission is granted only for the use specified in your request. No additional uses are granted (such as derivative works or other editions). For any other uses, please submit a new request.

[BACK](#)
[CLOSE WINDOW](#)

Copyright © 2016 [Copyright Clearance Center, Inc.](#) All Rights Reserved. [Privacy statement](#). [Terms and Conditions](#).

Comments? We would like to hear from you. E-mail us at customercare@copyright.com

C2.Reprint authorization for Figure 2.1 from Maly, D. J.; Allen, J. A.; Shokat, K. M., A mechanism-based cross-linker for the identification of kinase-substrate pairs. *J Am Chem Soc* 2004, 126 (30), 9160-1



RightsLink®

Home

Create Account

Help



ACS Publications
Most Trusted. Most Cited. Most Read.

Title: A Mechanism-Based Cross-Linker for the Identification of Kinase-Substrate Pairs
Author: Dustin J. Maly, Jasmina A. Allen, Kevan M. Shokat
Publication: Journal of the American Chemical Society
Publisher: American Chemical Society
Date: Aug 1, 2004

Copyright © 2004, American Chemical Society

LOGIN

If you're a [copyright.com user](#), you can login to RightsLink using your [copyright.com credentials](#). Already a [RightsLink user](#) or want to [learn more?](#)

PERMISSION/LICENSE IS GRANTED FOR YOUR ORDER AT NO CHARGE

This type of permission/license, instead of the standard Terms & Conditions, is sent to you because no fee is being charged for your order. Please note the following:

- Permission is granted for your request in both print and electronic formats, and translations.
- If figures and/or tables were requested, they may be adapted or used in part.
- Please print this page for your records and send a copy of it to your publisher/graduate school.
- Appropriate credit for the requested material should be given as follows: "Reprinted (adapted) with permission from (COMPLETE REFERENCE CITATION). Copyright (YEAR) American Chemical Society." Insert appropriate information in place of the capitalized words.
- One-time permission is granted only for the use specified in your request. No additional uses are granted (such as derivative works or other editions). For any other uses, please submit a new request.

If credit is given to another source for the material you requested, permission must be obtained from that source.

BACK

CLOSE WINDOW

Copyright © 2016 [Copyright Clearance Center, Inc.](#) All Rights Reserved. [Privacy statement.](#) [Terms and Conditions.](#)

Comments? We would like to hear from you. E-mail us at customer@copyright.com

C3. Reprint authorization for Figure 2.3 from Riel-Mehan, M. M.; Shokat, K. M., A crosslinker based on a tethered electrophile for mapping kinase-substrate networks.

Chem Biol 2014, 21 (5), 585-90.



Copyright Clearance Center



[Home](#)
[Account Info](#)
[Help](#)




Title: A Crosslinker Based on a Tethered Electrophile for Mapping Kinase-Substrate Networks

Author: Megan M. Riel-Mehan, Kevan M. Shokat

Publication: Chemistry & Biology

Publisher: Elsevier

Date: 22 May 2014

Copyright © 2014 Elsevier Ltd. All rights reserved.

Logged in as:
Pavithra Dedigama Arachchige

Account #:
3001063706

LOGOUT

Order Completed

Thank you for your order.

This Agreement between Pavithra M Dedigama Arachchige ("You") and Elsevier ("Elsevier") consists of your license details and the terms and conditions provided by Elsevier and Copyright Clearance Center.

Your confirmation email will contain your order number for future reference.

Printable details.

License Number	4007721194057
License date	Dec 14, 2016
Licensed Content Publisher	Elsevier
Licensed Content Publication	Chemistry & Biology
Licensed Content Title	A Crosslinker Based on a Tethered Electrophile for Mapping Kinase-Substrate Networks
Licensed Content Author	Megan M. Riel-Mehan, Kevan M. Shokat
Licensed Content Date	22 May 2014
Licensed Content Volume	21
Licensed Content Issue	5
Licensed Content Pages	6
Type of Use	reuse in a thesis/dissertation
Portion	figures/tables/illustrations
Number of figures/tables/illustrations	1
Format	both print and electronic
Are you the author of this Elsevier article?	No
Will you be translating?	No
Order reference number	
Original figure numbers	Figure 2A
Title of your thesis/dissertation	DEVELOPMENT OF TOOLS FOR PHOSPHOSITE-SPECIFIC KINASE IDENTIFICATION AND DISCOVERY OF PHOSPHATASE SUBSTRATES
Expected completion date	Jan 2017
Estimated size (number of pages)	200
Elsevier VAT number	GB 494 6272 12
Requestor Location	Pavithra M Dedigama Arachchige 5201 DETROIT, MI 48201 United States Attn: Pavithra M Dedigama Arachchige
Total	0.00 USD

[ORDER MORE](#)

[CLOSE WINDOW](#)

Copyright © 2016 Copyright Clearance Center, Inc. All Rights Reserved. [Privacy statement](#). [Terms and Conditions](#).
Comments? We would like to hear from you. E-mail us at customer@copyright.com

C4. Reprint authorization for Figure 3.1 from Soulsby, M.; Bennett, A. M., Physiological signaling specificity by protein tyrosine phosphatases. *Physiology* 2009, 24, 281



RightsLink®

Home

Create Account

Help



Title: Physiological Signaling Specificity by Protein Tyrosine Phosphatases

Author: Matthew Soulsby, Anton M. Bennett

Publication: Physiology

Publisher: The American Physiological Society

Date: Oct 1, 2009

Copyright © 2009, Copyright © 2009 the American Physiological Society

LOGIN

If you're a [copyright.com](#) user, you can login to RightsLink using your [copyright.com](#) credentials. Already a [RightsLink](#) user or want to [learn more?](#)

Permission Not Required

Permission is not required for this type of use.

BACK

CLOSE WINDOW

Copyright © 2016 [Copyright Clearance Center, Inc.](#) All Rights Reserved. [Privacy statement](#). [Terms and Conditions](#).

Comments? We would like to hear from you. E-mail us at customercare@copyright.com

C4. Reprint authorization for Figure 3.3 for Senevirathne, C.; Pflum, M. K., Biotinylated phosphoproteins from kinase-catalyzed biotinylation are stable to phosphatases: implications for phosphoproteomics. *Chembiochem* 2013, 14 (3), 381-7.

Pavithra Dedigama <pavithradedigama@gmail.com>
to rightsDE

Dec 9 (5 days ago) ☆

Hi,

I am a Ph.D. student in Prof. Mary Kay Pflum's lab at Wayne State University, Detroit. I would like to use Figure 4 from the following Pflum lab publication for my thesis. I was not able to find a link for copyright permissions. I would be grateful if I can get the permission to use the mentioned figure in my thesis.

Senevirathne, C.; Pflum, M. K., Biotinylated phosphoproteins from kinase-catalyzed biotinylation are stable to phosphatases: implications for phosphoproteomics. *Chembiochem* 2013, 14 (3), 381-7.

Thank You.

Rights DE <RIGHTS-and-LICENCES@wiley-vch.de>
to me

Dec 12 (2 days ago) ☆

Dear Pavithra,

We hereby grant permission for the requested use expected that due credit is given to the original source.

Any third party material is expressly excluded from this permission. If any of the material you wish to use appears within our work with credit to another source, authorization from that source must be obtained.
Credit must include the following components:

- Journals: Author(s) Name(s): Title of the Article. Name of the Journal. Publication year. Volume. Page(s). Copyright Wiley-VCH Verlag GmbH & Co. KGaA. Reproduced with permission.

This permission does not include the right to grant others permission to photocopy or otherwise reproduce this material except for accessible versions made by non-profit organizations serving the blind, visually impaired and other persons with print disabilities (VIPs).

Kind regards

Bettina Loycke
Senior Rights Manager
Rights & Licenses

Wiley-VCH Verlag GmbH & Co. KGaA
Boschstraße 12
69469 Weinheim
Germany
www.wiley-vch.de

REFERENCES

1. Prabakaran, S.; Lippens, G.; Steen, H.; Gunawardena, J., Post-translational modification: nature's escape from genetic imprisonment and the basis for dynamic information encoding. *Wiley Interdiscip Rev Syst Biol Med* **2012**, *4* (6), 565-83.
2. Ubersax, J. A.; Ferrell, J. E., Jr., Mechanisms of specificity in protein phosphorylation. *Nat Rev Mol Cell Biol* **2007**, *8* (7), 530-41.
3. Hunter, T., Protein kinases and phosphatases: the yin and yang of protein phosphorylation and signaling. *Cell* **1995**, *80* (2), 225-36.
4. Johnson, L. N.; Lowe, E. D.; Noble, M. E.; Owen, D. J., The Eleventh Datta Lecture. The structural basis for substrate recognition and control by protein kinases. *FEBS Lett* **1998**, *430* (1-2), 1-11.
5. Cohen, P., The regulation of protein function by multisite phosphorylation--a 25 year update. *Trends Biochem Sci* **2000**, *25* (12), 596-601.
6. Lonze, B. E.; Ginty, D. D., Function and regulation of CREB family transcription factors in the nervous system. *Neuron* **2002**, *35* (4), 605-23.
7. Moll, U. M.; Petrenko, O., The MDM2-p53 interaction. *Mol Cancer Res* **2003**, *1* (14), 1001-8.
8. Ozer, R. S.; Halpain, S., Phosphorylation-dependent localization of microtubule-associated protein MAP2c to the actin cytoskeleton. *Mol Biol Cell* **2000**, *11* (10), 3573-87.
9. Nardoizzi, J. D.; Lott, K.; Cingolani, G., Phosphorylation meets nuclear import: a review. *Cell Commun Signal* **2010**, *8*, 32.

10. Kolch, W., Meaningful relationships: the regulation of the Ras/Raf/MEK/ERK pathway by protein interactions. *Biochem J* **2000**, *351 Pt 2*, 289-305.
11. Chang, F.; Steelman, L. S.; Lee, J. T.; Shelton, J. G.; Navolanic, P. M.; Blalock, W. L.; Franklin, R. A.; McCubrey, J. A., Signal transduction mediated by the Ras/Raf/MEK/ERK pathway from cytokine receptors to transcription factors: potential targeting for therapeutic intervention. *Leukemia* **2003**, *17 (7)*, 1263-93.
12. Yu, L. G.; Packman, L. C.; Weldon, M.; Hamlett, J.; Rhodes, J. M., Protein phosphatase 2A, a negative regulator of the ERK signaling pathway, is activated by tyrosine phosphorylation of putative HLA class II-associated protein I (PHAPI)/pp32 in response to the antiproliferative lectin, jacalin. *J Biol Chem* **2004**, *279 (40)*, 41377-83.
13. (a) Kohno, M.; Pouyssegur, J., Targeting the ERK signaling pathway in cancer therapy. *Ann Med* **2006**, *38 (3)*, 200-11; (b) Leicht, D. T.; Balan, V.; Kaplun, A.; Singh-Gupta, V.; Kaplun, L.; Dobson, M.; Tzivion, G., Raf kinases: function, regulation and role in human cancer. *Biochim Biophys Acta* **2007**, *1773 (8)*, 1196-212; (c) Roberts, P. J.; Der, C. J., Targeting the Raf-MEK-ERK mitogen-activated protein kinase cascade for the treatment of cancer. *Oncogene* **2007**, *26 (22)*, 3291-310.
14. Zhang, Z. Y.; Lee, S. Y., PTP1B inhibitors as potential therapeutics in the treatment of type 2 diabetes and obesity. *Expert Opin Investig Drugs* **2003**, *12 (2)*, 223-33.
15. Cookson, M. R.; Dauer, W.; Dawson, T.; Fon, E. A.; Guo, M.; Shen, J., The roles of kinases in familial Parkinson's disease. *J Neurosci* **2007**, *27 (44)*, 11865-8.
16. Rafiqi, F. H.; Zuber, A. M.; Glover, M.; Richardson, C.; Fleming, S.; Jovanovic, S.; Jovanovic, A.; O'Shaughnessy, K. M.; Alessi, D. R., Role of the WNK-activated SPAK kinase in regulating blood pressure. *EMBO Mol Med* **2010**, *2 (2)*, 63-75.

17. Minami, K.; Tambe, Y.; Watanabe, R.; Isono, T.; Haneda, M.; Isobe, K.; Kobayashi, T.; Hino, O.; Okabe, H.; Chano, T.; Inoue, H., Suppression of viral replication by stress-inducible GADD34 protein via the mammalian serine/threonine protein kinase mTOR pathway. *J Virol* **2007**, *81* (20), 11106-15.
18. (a) He, R. J.; Yu, Z. H.; Zhang, R. Y.; Zhang, Z. Y., Protein tyrosine phosphatases as potential therapeutic targets. *Acta Pharmacol Sin* **2014**, *35* (10), 1227-46; (b) Zhang, J.; Yang, P. L.; Gray, N. S., Targeting cancer with small molecule kinase inhibitors. *Nat Rev Cancer* **2009**, *9* (1), 28-39.
19. Wu, P.; Nielsen, T. E.; Clausen, M. H., FDA-approved small-molecule kinase inhibitors. *Trends Pharmacol Sci* **2015**, *36* (7), 422-39.
20. (a) Wu, P.; Nielsen, T. E.; Clausen, M. H., Small-molecule kinase inhibitors: an analysis of FDA-approved drugs. *Drug Discov Today* **2016**, *21* (1), 5-10; (b) Cho, H., Protein tyrosine phosphatase 1B (PTP1B) and obesity. *Vitam Horm* **2013**, *91*, 405-24.
21. Shim, S. M.; Lee, W. J.; Kim, Y.; Chang, J. W.; Song, S.; Jung, Y. K., Role of S5b/PSMD5 in proteasome inhibition caused by TNF-alpha/NFkappaB in higher eukaryotes. *Cell Rep* **2012**, *2* (3), 603-15.
22. Manning, G.; Whyte, D. B.; Martinez, R.; Hunter, T.; Sudarsanam, S., The protein kinase complement of the human genome. *Science* **2002**, *298* (5600), 1912-34.
23. Zheng, J.; Knighton, D. R.; ten Eyck, L. F.; Karlsson, R.; Xuong, N.; Taylor, S. S.; Sowadski, J. M., Crystal structure of the catalytic subunit of cAMP-dependent protein kinase complexed with MgATP and peptide inhibitor. *Biochemistry* **1993**, *32* (9), 2154-61.

24. (a) Bossemeyer, D., Protein kinases--structure and function. *FEBS Lett* **1995**, 369 (1), 57-61; (b) Chico, L. K.; Van Eldik, L. J.; Watterson, D. M., Targeting protein kinases in central nervous system disorders. *Nat Rev Drug Discov* **2009**, 8 (11), 892-909.
25. Adams, J. A., Kinetic and catalytic mechanisms of protein kinases. *Chem Rev* **2001**, 101 (8), 2271-90.
26. Hornbeck, P. V.; Zhang, B.; Murray, B.; Kornhauser, J. M.; Latham, V.; Skrzypek, E., PhosphoSitePlus, 2014: mutations, PTMs and recalibrations. *Nucleic Acids Res* **2015**, 43 (Database issue), D512-20.
27. Ross, K. E.; Arighi, C. N.; Ren, J.; Huang, H.; Wu, C. H., Construction of protein phosphorylation networks by data mining, text mining and ontology integration: analysis of the spindle checkpoint. *Database (Oxford)* **2013**, 2013, bat038.
28. Fernandes, N. D.; Sun, Y.; Price, B. D., Activation of the kinase activity of ATM by retinoic acid is required for CREB-dependent differentiation of neuroblastoma cells. *J Biol Chem* **2007**, 282 (22), 16577-84.
29. David, S.; Kalb, R. G., Serum/glucocorticoid-inducible kinase can phosphorylate the cyclic AMP response element binding protein, CREB. *FEBS Lett* **2005**, 579 (6), 1534-8.
30. (a) Litchfield, D. W., Protein kinase CK2: structure, regulation and role in cellular decisions of life and death. *Biochem J* **2003**, 369 (Pt 1), 1-15; (b) Nolen, B.; Taylor, S.; Ghosh, G., Regulation of protein kinases; controlling activity through activation segment conformation. *Mol Cell* **2004**, 15 (5), 661-75; (c) Aggen, J. B.; Nairn, A. C.; Chamberlin, R., Regulation of protein phosphatase-1. *Chem Biol* **2000**, 7 (1), R13-23.

31. Johnson, S. A.; Hunter, T., Kinomics: methods for deciphering the kinome. *Nat Methods* **2005**, 2 (1), 17-25.
32. Green, K. D.; Pflum, M. K., Kinase-catalyzed biotinylation for phosphoprotein detection. *J Am Chem Soc* **2007**, 129 (1), 10-1.
33. (a) Eckstein, F., Nucleoside phosphorothioates. *Annu Rev Biochem* **1985**, 54, 367-402; (b) Cassel, D.; Glaser, L., Resistance to phosphatase of thiophosphorylated epidermal growth factor receptor in A431 membranes. *Proc Natl Acad Sci U S A* **1982**, 79 (7), 2231-5.
34. Sun, I. Y.; Johnson, E. M.; Allfrey, V. G., Affinity purification of newly phosphorylated protein molecules. Thiophosphorylation and recovery of histones H1, H2B, and H3 and the high mobility group protein HMG-1 using adenosine 5'-O-(3-thiotriphosphate) and cyclic AMP-dependent protein kinase. *J Biol Chem* **1980**, 255 (2), 742-7.
35. (a) Kwon, S. W.; Kim, S. C.; Jaunbergs, J.; Falck, J. R.; Zhao, Y., Selective enrichment of thiophosphorylated polypeptides as a tool for the analysis of protein phosphorylation. *Mol Cell Proteomics* **2003**, 2 (4), 242-7; (b) Jeong, S.; Nikiforov, T. T., Kinase assay based on thiophosphorylation and biotinylation. *Biotechniques* **1999**, 27 (6), 1232-8.
36. (a) Lee, S. E.; Elphick, L. M.; Kramer, H. B.; Jones, A. M.; Child, E. S.; Anderson, A. A.; Bonnac, L.; Suwaki, N.; Kessler, B. M.; Gouverneur, V.; Mann, D. J., The chemoselective one-step alkylation and isolation of thiophosphorylated cdk2 substrates in the presence of native cysteine. *Chembiochem* **2011**, 12 (4), 633-40; (b) Carlson, S. M.; Chouinard, C. R.; Labadorf, A.; Lam, C. J.; Schmelzle, K.; Fraenkel, E.; White, F. M.,

Large-scale discovery of ERK2 substrates identifies ERK-mediated transcriptional regulation by ETV3. *Sci Signal* **2011**, 4 (196), rs11.

37. Blethrow, J. D.; Glavy, J. S.; Morgan, D. O.; Shokat, K. M., Covalent capture of kinase-specific phosphopeptides reveals Cdk1-cyclin B substrates. *Proc Natl Acad Sci U S A* **2008**, 105 (5), 1442-7.

38. Freeman, R.; Finder, T.; Gill, R.; Willner, I., Probing protein kinase (CK2) and alkaline phosphatase with CdSe/ZnS quantum dots. *Nano Lett* **2010**, 10 (6), 2192-6.

39. Song, H.; Kerman, K.; Kraatz, H. B., Electrochemical detection of kinase-catalyzed phosphorylation using ferrocene-conjugated ATP. *Chem Commun (Camb)* **2008**, (4), 502-4.

40. Martic, S.; Gabriel, M.; Turowec, J. P.; Litchfield, D. W.; Kraatz, H. B., Versatile strategy for biochemical, electrochemical and immunoarray detection of protein phosphorylations. *J Am Chem Soc* **2012**, 134 (41), 17036-45.

41. (a) Villamor, J. G.; Kaschani, F.; Colby, T.; Oeljeklaus, J.; Zhao, D.; Kaiser, M.; Patricelli, M. P.; van der Hoorn, R. A., Profiling protein kinases and other ATP binding proteins in Arabidopsis using Acyl-ATP probes. *Mol Cell Proteomics* **2013**, 12 (9), 2481-96; (b) Deng, X.; Dzamko, N.; Prescott, A.; Davies, P.; Liu, Q.; Yang, Q.; Lee, J. D.; Patricelli, M. P.; Nomanbhoy, T. K.; Alessi, D. R.; Gray, N. S., Characterization of a selective inhibitor of the Parkinson's disease kinase LRRK2. *Nat Chem Biol* **2011**, 7 (4), 203-5.

42. (a) Wang, Z.; Levy, R.; Fernig, D. G.; Brust, M., Kinase-catalyzed modification of gold nanoparticles: a new approach to colorimetric kinase activity screening. *J Am Chem Soc* **2006**, 128 (7), 2214-5; (b) Wang, Z.; Lee, J.; Cossins, A. R.; Brust, M., Microarray-

based detection of protein binding and functionality by gold nanoparticle probes. *Anal Chem* **2005**, *77* (17), 5770-4.

43. (a) Senevirathne, C.; Green, K. D.; Pflum, M. K., Kinase-Catalyzed Biotinylation. *Curr Protoc Chem Biol* **2012**, *4* (1), 83-100; (b) Senevirathne, C.; Embogama, D. M.; Anthony, T. A.; Fouda, A. E.; Pflum, M. K., The generality of kinase-catalyzed biotinylation. *Bioorg Med Chem* **2016**, *24* (1), 12-9.

44. Senevirathne, C.; Pflum, M. K., Biotinylated phosphoproteins from kinase-catalyzed biotinylation are stable to phosphatases: implications for phosphoproteomics. *Chembiochem* **2013**, *14* (3), 381-7.

45. Embogama, D. M.; Pflum, M. K., K-BILDS: A kinase substrate discovery tool. *Chembiochem* **2016**.

46. Fouda, A. E.; Pflum, M. K., A Cell-Permeable ATP Analogue for Kinase-Catalyzed Biotinylation. *Angew Chem Int Ed Engl* **2015**, *54* (33), 9618-21.

47. Green, K. D.; Pflum, M. K., Exploring kinase cosubstrate promiscuity: monitoring kinase activity through dansylation. *Chembiochem* **2009**, *10* (2), 234-7.

48. (a) Suwal, S.; Pflum, M. K., Phosphorylation-dependent kinase-substrate cross-linking. *Angew Chem Int Ed Engl* **2010**, *49* (9), 1627-30; (b) Garre, S.; Senevirathne, C.; Pflum, M. K., A comparative study of ATP analogs for phosphorylation-dependent kinase-substrate crosslinking. *Bioorg Med Chem* **2014**, *22* (5), 1620-5.

49. Parang, K.; Kohn, J. A.; Saldanha, S. A.; Cole, P. A., Development of photo-crosslinking reagents for protein kinase-substrate interactions. *FEBS Lett* **2002**, *520* (1-3), 156-60.

50. Dedigama-Arachchige, P. M.; Pflum, M. K., K-CLASP: A tool to identify phosphosite specific kinases and interacting proteins. *ACS Chem Biol* **2016**.
51. Flint, A. J.; Tiganis, T.; Barford, D.; Tonks, N. K., Development of "substrate-trapping" mutants to identify physiological substrates of protein tyrosine phosphatases. *Proc Natl Acad Sci U S A* **1997**, *94* (5), 1680-5.
52. Mann, M.; Ong, S. E.; Gronborg, M.; Steen, H.; Jensen, O. N.; Pandey, A., Analysis of protein phosphorylation using mass spectrometry: deciphering the phosphoproteome. *Trends in biotechnology* **2002**, *20* (6), 261-8.
53. Xue, L.; Tao, W. A., Current technologies to identify protein kinase substrates in high throughput. *Frontiers in biology* **2013**, *8* (2), 216-227.
54. Xue, Y.; Zhou, F.; Zhu, M.; Ahmed, K.; Chen, G.; Yao, X., GPS: a comprehensive www server for phosphorylation sites prediction. *Nucleic Acids Res* **2005**, *33* (Web Server issue), W184-7.
55. Hjerrild, M.; Gammeltoft, S., Phosphoproteomics toolbox: computational biology, protein chemistry and mass spectrometry. *FEBS Lett* **2006**, *580* (20), 4764-70.
56. Hutti, J. E.; Jarrell, E. T.; Chang, J. D.; Abbott, D. W.; Storz, P.; Toker, A.; Cantley, L. C.; Turk, B. E., A rapid method for determining protein kinase phosphorylation specificity. *Nat Methods* **2004**, *1* (1), 27-9.
57. (a) Shenoy, S.; Choi, J. K.; Bagrodia, S.; Copeland, T. D.; Maller, J. L.; Shalloway, D., Purified maturation promoting factor phosphorylates pp60c-src at the sites phosphorylated during fibroblast mitosis. *Cell* **1989**, *57* (5), 763-74; (b) Delpire, E.; Gagnon, K. B., Genome-wide analysis of SPAK/OSR1 binding motifs. *Physiol Genomics*

2007, 28 (2), 223-31; (c) Meggio, F.; Marin, O.; Pinna, L. A., Substrate specificity of protein kinase CK2. *Cell Mol Biol Res* **1994**, 40 (5-6), 401-9.

58. (a) Huang, H. D.; Lee, T. Y.; Tzeng, S. W.; Horng, J. T., KinasePhos: a web tool for identifying protein kinase-specific phosphorylation sites. *Nucleic Acids Res* **2005**, 33 (Web Server issue), W226-9; (b) Ellis, J. J.; Kobe, B., Predicting protein kinase specificity: Predikin update and performance in the DREAM4 challenge. *PLoS One* **2011**, 6 (7), e21169.

59. Kreegipuu, A.; Blom, N.; Brunak, S.; Jarv, J., Statistical analysis of protein kinase specificity determinants. *FEBS Lett* **1998**, 430 (1-2), 45-50.

60. Li, L.; Shakhnovich, E. I.; Mirny, L. A., Amino acids determining enzyme-substrate specificity in prokaryotic and eukaryotic protein kinases. *Proc Natl Acad Sci U S A* **2003**, 100 (8), 4463-8.

61. Maly, D. J.; Allen, J. A.; Shokat, K. M., A mechanism-based cross-linker for the identification of kinase-substrate pairs. *J Am Chem Soc* **2004**, 126 (30), 9160-1.

62. Statsuk, A. V.; Maly, D. J.; Seeliger, M. A.; Fabian, M. A.; Biggs, W. H., 3rd; Lockhart, D. J.; Zarrinkar, P. P.; Kuriyan, J.; Shokat, K. M., Tuning a three-component reaction for trapping kinase substrate complexes. *J Am Chem Soc* **2008**, 130 (51), 17568-74.

63. Riel-Mehan, M. M.; Shokat, K. M., A crosslinker based on a tethered electrophile for mapping kinase-substrate networks. *Chem Biol* **2014**, 21 (5), 585-90.

64. Maller, J. L.; Kemp, B. E.; Krebs, E. G., In vivo phosphorylation of a synthetic peptide substrate of cyclic AMP-dependent protein kinase. *Proc Natl Acad Sci U S A* **1978**, 75 (1), 248-51.

65. Geiger, T.; Wehner, A.; Schaab, C.; Cox, J.; Mann, M., Comparative proteomic analysis of eleven common cell lines reveals ubiquitous but varying expression of most proteins. *Mol Cell Proteomics* **2012**, *11* (3), M111 014050.
66. Montojo, J.; Zuberi, K.; Rodriguez, H.; Kazi, F.; Wright, G.; Donaldson, S. L.; Morris, Q.; Bader, G. D., GeneMANIA Cytoscape plugin: fast gene function predictions on the desktop. *Bioinformatics* **2010**, *26* (22), 2927-8.
67. Hornbeck, P. V.; Kornhauser, J. M.; Tkachev, S.; Zhang, B.; Skrzypek, E.; Murray, B.; Latham, V.; Sullivan, M., PhosphoSitePlus: a comprehensive resource for investigating the structure and function of experimentally determined post-translational modifications in man and mouse. *Nucleic Acids Res* **2012**, *40* (Database issue), D261-70.
68. Cline, M. S.; Smoot, M.; Cerami, E.; Kuchinsky, A.; Landys, N.; Workman, C.; Christmas, R.; Avila-Campilo, I.; Creech, M.; Gross, B.; Hanspers, K.; Isserlin, R.; Kelley, R.; Killcoyne, S.; Lotia, S.; Maere, S.; Morris, J.; Ono, K.; Pavlovic, V.; Pico, A. R.; Vailaya, A.; Wang, P. L.; Adler, A.; Conklin, B. R.; Hood, L.; Kuiper, M.; Sander, C.; Schmulevich, I.; Schwikowski, B.; Warner, G. J.; Ideker, T.; Bader, G. D., Integration of biological networks and gene expression data using Cytoscape. *Nat Protoc* **2007**, *2* (10), 2366-82.
69. Bjorbaek, C.; Zhao, Y.; Moller, D. E., Divergent functional roles for p90rsk kinase domains. *The Journal of biological chemistry* **1995**, *270* (32), 18848-52.
70. Pearce, L. R.; Komander, D.; Alessi, D. R., The nuts and bolts of AGC protein kinases. *Nature reviews. Molecular cell biology* **2010**, *11* (1), 9-22.
71. (a) Yang, L.; McKnight, G. S., Hypothalamic PKA regulates leptin sensitivity and adiposity. *Nat Commun* **2015**, *6*, 8237; (b) Gangoda, L.; Doerflinger, M.; Lee, Y. Y.;

- Rahimi, A.; Etemadi, N.; Chau, D.; Milla, L.; O'Connor, L.; Puthalakath, H., Cre transgene results in global attenuation of the cAMP/PKA pathway. *Cell Death Dis* **2012**, *3*, e365; (c)
- Miller, R. A.; Chu, Q.; Xie, J.; Foretz, M.; Viollet, B.; Birnbaum, M. J., Biguanides suppress hepatic glucagon signalling by decreasing production of cyclic AMP. *Nature* **2013**, *494* (7436), 256-60.
72. Myeku, N.; Clelland, C. L.; Emrani, S.; Kukushkin, N. V.; Yu, W. H.; Goldberg, A. L.; Duff, K. E., Tau-driven 26S proteasome impairment and cognitive dysfunction can be prevented early in disease by activating cAMP-PKA signaling. *Nat Med* **2016**, *22* (1), 46-53.
73. Ashe, M. P.; De Long, S. K.; Sachs, A. B., Glucose depletion rapidly inhibits translation initiation in yeast. *Mol Biol Cell* **2000**, *11* (3), 833-48.
74. Burnett, B. G.; Munoz, E.; Tandon, A.; Kwon, D. Y.; Sumner, C. J.; Fischbeck, K. H., Regulation of SMN protein stability. *Mol Cell Biol* **2009**, *29* (5), 1107-15.
75. Liu, J.; Yan, J.; Jiang, S.; Wen, J.; Chen, L.; Zhao, Y.; Lin, A., Site-specific ubiquitination is required for relieving the transcription factor Miz1-mediated suppression on TNF-alpha-induced JNK activation and inflammation. *Proceedings of the National Academy of Sciences of the United States of America* **2012**, *109* (1), 191-6.
76. Do-Umehara, H. C.; Chen, C.; Urich, D.; Zhou, L.; Qiu, J.; Jang, S.; Zander, A.; Baker, M. A.; Eilers, M.; Sporn, P. H.; Ridge, K. M.; Sznajder, J. I.; Budinger, G. R.; Mutlu, G. M.; Lin, A.; Liu, J., Suppression of inflammation and acute lung injury by Miz1 via repression of C/EBP-delta. *Nat Immunol* **2013**, *14* (5), 461-9.
77. Lawrence, T., The nuclear factor NF-kappaB pathway in inflammation. *Cold Spring Harb Perspect Biol* **2009**, *1* (6), a001651.

78. Bader, G. D.; Hogue, C. W., An automated method for finding molecular complexes in large protein interaction networks. *BMC Bioinformatics* **2003**, *4*, 2.
79. Bondar, T.; Kalinina, A.; Khair, L.; Kopanja, D.; Nag, A.; Bagchi, S.; Raychaudhuri, P., Cul4A and DDB1 associate with Skp2 to target p27Kip1 for proteolysis involving the COP9 signalosome. *Mol Cell Biol* **2006**, *26* (7), 2531-9.
80. Waters, M. G.; Serafini, T.; Rothman, J. E., 'Coatomer': a cytosolic protein complex containing subunits of non-clathrin-coated Golgi transport vesicles. *Nature* **1991**, *349* (6306), 248-51.
81. Zhao, C.; Slevin, J. T.; Whiteheart, S. W., Cellular functions of NSF: not just SNAPs and SNAREs. *FEBS Lett* **2007**, *581* (11), 2140-9.
82. UniProt, C., UniProt: a hub for protein information. *Nucleic Acids Res* **2015**, *43* (Database issue), D204-12.
83. Warthaka, M.; Karwowska-Desaulniers, P.; Pflum, M. K., Phosphopeptide modification and enrichment by oxidation-reduction condensation. *ACS Chem Biol* **2006**, *1* (11), 697-701.
84. Sambrook, J. a. R., D, *Molecular Cloning: A Laboratory Manual*. Third edition ed.; Cold Spring Harbor Press: New York, 2011.
85. Shevchenko, A.; Tomas, H.; Havlis, J.; Olsen, J. V.; Mann, M., In-gel digestion for mass spectrometric characterization of proteins and proteomes. *Nat Protoc* **2006**, *1* (6), 2856-60.
86. Stoker, A. W., Protein tyrosine phosphatases and signalling. *The Journal of endocrinology* **2005**, *185* (1), 19-33.

87. Tonks, N. K., Protein tyrosine phosphatases: from genes, to function, to disease. *Nature reviews. Molecular cell biology* **2006**, 7 (11), 833-46.
88. Zhang, Q.; Claret, F. X., Phosphatases: the new brakes for cancer development? *Enzyme research* **2012**, 2012, 659649.
89. Goldstein, B. J., Protein-tyrosine phosphatase 1B (PTP1B): a novel therapeutic target for type 2 diabetes mellitus, obesity and related states of insulin resistance. *Current drug targets. Immune, endocrine and metabolic disorders* **2001**, 1 (3), 265-75.
90. Jiang, Z. X.; Zhang, Z. Y., Targeting PTPs with small molecule inhibitors in cancer treatment. *Cancer metastasis reviews* **2008**, 27 (2), 263-72.
91. Jackson, M. D.; Denu, J. M., Molecular reactions of protein phosphatases--insights from structure and chemistry. *Chem Rev* **2001**, 101 (8), 2313-40.
92. Soulsby, M.; Bennett, A. M., Physiological signaling specificity by protein tyrosine phosphatases. *Physiology (Bethesda)* **2009**, 24, 281-9.
93. Camps, M.; Nichols, A.; Arkininstall, S., Dual specificity phosphatases: a gene family for control of MAP kinase function. *FASEB journal : official publication of the Federation of American Societies for Experimental Biology* **2000**, 14 (1), 6-16.
94. Adhikary, S.; Peukert, K.; Karsunky, H.; Beuger, V.; Lutz, W.; Elsasser, H. P.; Moroy, T.; Eilers, M., Miz1 is required for early embryonic development during gastrulation. *Molecular and cellular biology* **2003**, 23 (21), 7648-57.
95. Andersen, J. N.; Mortensen, O. H.; Peters, G. H.; Drake, P. G.; Iversen, L. F.; Olsen, O. H.; Jansen, P. G.; Andersen, H. S.; Tonks, N. K.; Moller, N. P., Structural and evolutionary relationships among protein tyrosine phosphatase domains. *Mol Cell Biol* **2001**, 21 (21), 7117-36.

96. Yip, S. C.; Saha, S.; Chernoff, J., PTP1B: a double agent in metabolism and oncogenesis. *Trends in biochemical sciences* **2010**, *35* (8), 442-9.
97. Eto, M., Regulation of cellular protein phosphatase-1 (PP1) by phosphorylation of the CPI-17 family, C-kinase-activated PP1 inhibitors. *J Biol Chem* **2009**, *284* (51), 35273-7.
98. Blanchetot, C.; Chagnon, M.; Dube, N.; Halle, M.; Tremblay, M. L., Substrate-trapping techniques in the identification of cellular PTP targets. *Methods* **2005**, *35* (1), 44-53.
99. Wu, J.; Katrekar, A.; Honigberg, L. A.; Smith, A. M.; Conn, M. T.; Tang, J.; Jeffery, D.; Mortara, K.; Sampang, J.; Williams, S. R.; Buggy, J.; Clark, J. M., Identification of substrates of human protein-tyrosine phosphatase PTPN22. *J Biol Chem* **2006**, *281* (16), 11002-10.
100. Rusin, S. F.; Schlosser, K. A.; Adamo, M. E.; Kettenbach, A. N., Quantitative phosphoproteomics reveals new roles for the protein phosphatase PP6 in mitotic cells. *Sci Signal* **2015**, *8* (398), rs12.
101. Hilger, M.; Bonaldi, T.; Gnad, F.; Mann, M., Systems-wide analysis of a phosphatase knock-down by quantitative proteomics and phosphoproteomics. *Mol Cell Proteomics* **2009**, *8* (8), 1908-20.
102. Zhang, X.; Ma, D.; Caruso, M.; Lewis, M.; Qi, Y.; Yi, Z., Quantitative phosphoproteomics reveals novel phosphorylation events in insulin signaling regulated by protein phosphatase 1 regulatory subunit 12A. *J Proteomics* **2014**, *109*, 63-75.
103. (a) Olsen, J. V.; Blagoev, B.; Gnad, F.; Macek, B.; Kumar, C.; Mortensen, P.; Mann, M., Global, in vivo, and site-specific phosphorylation dynamics in signaling networks. *Cell*

2006, 127 (3), 635-48; (b) Schweppe, D. K.; Rigas, J. R.; Gerber, S. A., Quantitative phosphoproteomic profiling of human non-small cell lung cancer tumors. *J Proteomics* **2013**, 91, 286-96.

104. Bodenmiller, B.; Mueller, L. N.; Mueller, M.; Domon, B.; Aebersold, R., Reproducible isolation of distinct, overlapping segments of the phosphoproteome. *Nat Methods* **2007**, 4 (3), 231-7.

105. Haystead, T. A.; Sim, A. T.; Carling, D.; Honnor, R. C.; Tsukitani, Y.; Cohen, P.; Hardie, D. G., Effects of the tumour promoter okadaic acid on intracellular protein phosphorylation and metabolism. *Nature* **1989**, 337 (6202), 78-81.

106. Cohen, P.; Klumpp, S.; Schelling, D. L., An improved procedure for identifying and quantitating protein phosphatases in mammalian tissues. *FEBS Lett* **1989**, 250 (2), 596-600.

107. Peng, A.; Lewellyn, A. L.; Schieman, W. P.; Maller, J. L., Repo-man controls a protein phosphatase 1-dependent threshold for DNA damage checkpoint activation. *Curr Biol* **2010**, 20 (5), 387-96.

108. Novoa, I.; Zeng, H.; Harding, H. P.; Ron, D., Feedback inhibition of the unfolded protein response by GADD34-mediated dephosphorylation of eIF2alpha. *J Cell Biol* **2001**, 153 (5), 1011-22.

109. Yamamoto, H.; Saitoh, Y.; Fukunaga, K.; Nishimura, H.; Miyamoto, E., Dephosphorylation of microtubule proteins by brain protein phosphatases 1 and 2A, and its effect on microtubule assembly. *J Neurochem* **1988**, 50 (5), 1614-23.

110. Kotlo, K.; Xing, Y.; Lather, S.; Grillon, J. M.; Johnson, K.; Skidgel, R. A.; Solaro, R. J.; Danziger, R. S., PR65A phosphorylation regulates PP2A complex signaling. *PLoS One* **2014**, *9* (1), e85000.
111. Potapova, T. A.; Sivakumar, S.; Flynn, J. N.; Li, R.; Gorbsky, G. J., Mitotic progression becomes irreversible in prometaphase and collapses when Wee1 and Cdc25 are inhibited. *Mol Biol Cell* **2011**, *22* (8), 1191-206.
112. Canals, D.; Roddy, P.; Hannun, Y. A., Protein phosphatase 1alpha mediates ceramide-induced ERM protein dephosphorylation: a novel mechanism independent of phosphatidylinositol 4, 5-biphosphate (PIP2) and myosin/ERM phosphatase. *J Biol Chem* **2012**, *287* (13), 10145-55.
113. Sheldon, K. L.; Maldonado, E. N.; Lemasters, J. J.; Rostovtseva, T. K.; Bezrukov, S. M., Phosphorylation of voltage-dependent anion channel by serine/threonine kinases governs its interaction with tubulin. *PLoS One* **2011**, *6* (10), e25539.
114. Kono, Y.; Maeda, K.; Kuwahara, K.; Yamamoto, H.; Miyamoto, E.; Yonezawa, K.; Takagi, K.; Sakaguchi, N., MCM3-binding GANP DNA-primase is associated with a novel phosphatase component G5PR. *Genes Cells* **2002**, *7* (8), 821-34.
115. Shin, Y. H.; Choi, Y.; Erdin, S. U.; Yatsenko, S. A.; Kloc, M.; Yang, F.; Wang, P. J.; Meistrich, M. L.; Rajkovic, A., Hormad1 mutation disrupts synaptonemal complex formation, recombination, and chromosome segregation in mammalian meiosis. *PLoS Genet* **2010**, *6* (11), e1001190.
116. Kuroda, F.; Moss, J.; Vaughan, M., Regulation of brefeldin A-inhibited guanine nucleotide-exchange protein 1 (BIG1) and BIG2 activity via PKA and protein phosphatase 1gamma. *Proc Natl Acad Sci U S A* **2007**, *104* (9), 3201-6.

117. Marx, S. O.; Reiken, S.; Hisamatsu, Y.; Gaburjakova, M.; Gaburjakova, J.; Yang, Y. M.; Rosembliit, N.; Marks, A. R., Phosphorylation-dependent regulation of ryanodine receptors: a novel role for leucine/isoleucine zippers. *J Cell Biol* **2001**, *153* (4), 699-708.
118. Redpath, N. T.; Price, N. T.; Severinov, K. V.; Proud, C. G., Regulation of elongation factor-2 by multisite phosphorylation. *Eur J Biochem* **1993**, *213* (2), 689-99.
119. Rodrigues, N. T.; Lekomtsev, S.; Jananji, S.; Kriston-Vizi, J.; Hickson, G. R.; Baum, B., Kinetochore-localized PP1-Sds22 couples chromosome segregation to polar relaxation. *Nature* **2015**, *524* (7566), 489-92.
120. Trotta, A.; Konert, G.; Rahikainen, M.; Aro, E. M.; Kangasjarvi, S., Knock-down of protein phosphatase 2A subunit B'gamma promotes phosphorylation of CALRETICULIN 1 in *Arabidopsis thaliana*. *Plant Signal Behav* **2011**, *6* (11), 1665-8.
121. Pelech, S.; Cohen, P., The protein phosphatases involved in cellular regulation. 1. Modulation of protein phosphatases-1 and 2A by histone H1, protamine, polylysine and heparin. *Eur J Biochem* **1985**, *148* (2), 245-51.
122. Chatr-Aryamontri, A.; Breitkreutz, B. J.; Oughtred, R.; Boucher, L.; Heinicke, S.; Chen, D.; Stark, C.; Breitkreutz, A.; Kolas, N.; O'Donnell, L.; Reguly, T.; Nixon, J.; Ramage, L.; Winter, A.; Sellam, A.; Chang, C.; Hirschman, J.; Theesfeld, C.; Rust, J.; Livstone, M. S.; Dolinski, K.; Tyers, M., The BioGRID interaction database: 2015 update. *Nucleic Acids Res* **2015**, *43* (Database issue), D470-8.
123. Morrow, P. W.; Tung, H. Y.; Hemmings, H. C., Jr., Rapamycin causes activation of protein phosphatase-2A1 and nuclear translocation of PCNA in CD4+ T cells. *Biochem Biophys Res Commun* **2004**, *323* (2), 645-51.

124. Peng, B.; Lei, N.; Chai, Y.; Chan, E. K.; Zhang, J. Y., CIP2A regulates cancer metabolism and CREB phosphorylation in non-small cell lung cancer. *Mol Biosyst* **2015**, *11* (1), 105-14.
125. Gene Ontology, C., Gene Ontology Consortium: going forward. *Nucleic Acids Res* **2015**, *43* (Database issue), D1049-56.
126. Ceulemans, H.; Bollen, M., Functional diversity of protein phosphatase-1, a cellular economizer and reset button. *Physiol Rev* **2004**, *84* (1), 1-39.
127. Mkaddem, S. B.; Werts, C.; Goujon, J. M.; Bens, M.; Pedruzzi, E.; Ogier-Denis, E.; Vandewalle, A., Heat shock protein gp96 interacts with protein phosphatase 5 and controls toll-like receptor 2 (TLR2)-mediated activation of extracellular signal-regulated kinase (ERK) 1/2 in post-hypoxic kidney cells. *J Biol Chem* **2009**, *284* (18), 12541-9.
128. Schmitz, M. H.; Held, M.; Janssens, V.; Hutchins, J. R.; Hudecz, O.; Ivanova, E.; Goris, J.; Trinkle-Mulcahy, L.; Lamond, A. I.; Poser, I.; Hyman, A. A.; Mechtler, K.; Peters, J. M.; Gerlich, D. W., Live-cell imaging RNAi screen identifies PP2A-B55alpha and importin-beta1 as key mitotic exit regulators in human cells. *Nat Cell Biol* **2010**, *12* (9), 886-93.
129. (a) Prevost, M.; Chamousset, D.; Nasa, I.; Freele, E.; Morrice, N.; Moorhead, G.; Trinkle-Mulcahy, L., Quantitative fragmentome mapping reveals novel, domain-specific partners for the modular protein RepoMan (recruits PP1 onto mitotic chromatin at anaphase). *Mol Cell Proteomics* **2013**, *12* (5), 1468-86; (b) Chamousset, D.; De Wever, V.; Moorhead, G. B.; Chen, Y.; Boisvert, F. M.; Lamond, A. I.; Trinkle-Mulcahy, L., RRP1B targets PP1 to mammalian cell nucleoli and is associated with Pre-60S ribosomal subunits. *Mol Biol Cell* **2010**, *21* (23), 4212-26.

130. Regad, T.; Bellodi, C.; Nicotera, P.; Salomoni, P., The tumor suppressor Pml regulates cell fate in the developing neocortex. *Nat Neurosci* **2009**, *12* (2), 132-40.
131. Wang, M.; Herrmann, C. J.; Simonovic, M.; Szklarczyk, D.; von Mering, C., Version 4.0 of PaxDb: Protein abundance data, integrated across model organisms, tissues, and cell-lines. *Proteomics* **2015**, *15* (18), 3163-8.
132. Brush, M. H.; Weiser, D. C.; Shenolikar, S., Growth arrest and DNA damage-inducible protein GADD34 targets protein phosphatase 1 alpha to the endoplasmic reticulum and promotes dephosphorylation of the alpha subunit of eukaryotic translation initiation factor 2. *Mol Cell Biol* **2003**, *23* (4), 1292-303.
133. (a) Hetz, C., The unfolded protein response: controlling cell fate decisions under ER stress and beyond. *Nat Rev Mol Cell Biol* **2012**, *13* (2), 89-102; (b) Wang, M.; Kaufman, R. J., The impact of the endoplasmic reticulum protein-folding environment on cancer development. *Nat Rev Cancer* **2014**, *14* (9), 581-97.
134. Hetz, C.; Chevet, E.; Harding, H. P., Targeting the unfolded protein response in disease. *Nat Rev Drug Discov* **2013**, *12* (9), 703-19.
135. Tsaytler, P.; Harding, H. P.; Ron, D.; Bertolotti, A., Selective inhibition of a regulatory subunit of protein phosphatase 1 restores proteostasis. *Science* **2011**, *332* (6025), 91-4.
136. Jackson, R. J.; Hellen, C. U.; Pestova, T. V., The mechanism of eukaryotic translation initiation and principles of its regulation. *Nat Rev Mol Cell Biol* **2010**, *11* (2), 113-27.
137. (a) Song, Z. T.; Sun, L.; Lu, S. J.; Tian, Y.; Ding, Y.; Liu, J. X., Transcription factor interaction with COMPASS-like complex regulates histone H3K4 trimethylation for

specific gene expression in plants. *Proc Natl Acad Sci U S A* **2015**, *112* (9), 2900-5; (b) Oono, K.; Yoneda, T.; Manabe, T.; Yamagishi, S.; Matsuda, S.; Hitomi, J.; Miyata, S.; Mizuno, T.; Imaizumi, K.; Katayama, T.; Tohyama, M., JAB1 participates in unfolded protein responses by association and dissociation with IRE1. *Neurochem Int* **2004**, *45* (5), 765-72.

138. Kedersha, N.; Panas, M. D.; Achorn, C. A.; Lyons, S.; Tisdale, S.; Hickman, T.; Thomas, M.; Lieberman, J.; McInerney, G. M.; Ivanov, P.; Anderson, P., G3BP-Caprin1-USP10 complexes mediate stress granule condensation and associate with 40S subunits. *J Cell Biol* **2016**, *212* (7), 845-60.

139. (a) Kawai, T.; Lal, A.; Yang, X.; Galban, S.; Mazan-Mamczarz, K.; Gorospe, M., Translational control of cytochrome c by RNA-binding proteins TIA-1 and HuR. *Mol Cell Biol* **2006**, *26* (8), 3295-307; (b) Anderson, P.; Kedersha, N., Stress granules: the Tao of RNA triage. *Trends Biochem Sci* **2008**, *33* (3), 141-50.

140. Ruggieri, A.; Dazert, E.; Metz, P.; Hofmann, S.; Bergeest, J. P.; Mazur, J.; Bankhead, P.; Hiet, M. S.; Kallis, S.; Alvisi, G.; Samuel, C. E.; Lohmann, V.; Kaderali, L.; Rohr, K.; Frese, M.; Stoecklin, G.; Bartenschlager, R., Dynamic oscillation of translation and stress granule formation mark the cellular response to virus infection. *Cell Host Microbe* **2012**, *12* (1), 71-85.

141. Kobayashi, T.; Winslow, S.; Sunesson, L.; Hellman, U.; Larsson, C., PKC α binds G3BP2 and regulates stress granule formation following cellular stress. *PLoS One* **2012**, *7* (4), e35820.

142. Szegezdi, E.; Logue, S. E.; Gorman, A. M.; Samali, A., Mediators of endoplasmic reticulum stress-induced apoptosis. *EMBO Rep* **2006**, *7* (9), 880-5.

143. Wu, H.; Wei, L.; Fan, F.; Ji, S.; Zhang, S.; Geng, J.; Hong, L.; Fan, X.; Chen, Q.; Tian, J.; Jiang, M.; Sun, X.; Jin, C.; Yin, Z. Y.; Liu, Q.; Zhang, J.; Qin, F.; Lin, K. H.; Yu, J. S.; Deng, X.; Wang, H. R.; Zhao, B.; Johnson, R. L.; Chen, L.; Zhou, D., Integration of Hippo signalling and the unfolded protein response to restrain liver overgrowth and tumorigenesis. *Nat Commun* **2015**, *6*, 6239.
144. (a) Varjosalo, M.; Sacco, R.; Stukalov, A.; van Drogen, A.; Planyavsky, M.; Hauri, S.; Aebersold, R.; Bennett, K. L.; Colinge, J.; Gstaiger, M.; Superti-Furga, G., Interlaboratory reproducibility of large-scale human protein-complex analysis by standardized AP-MS. *Nat Methods* **2013**, *10* (4), 307-14; (b) Wang, B.; Means, C. K.; Yang, Y.; Mamonova, T.; Bisello, A.; Altschuler, D. L.; Scott, J. D.; Friedman, P. A., Ezrin-anchored protein kinase A coordinates phosphorylation-dependent disassembly of a NHERF1 ternary complex to regulate hormone-sensitive phosphate transport. *J Biol Chem* **2012**, *287* (29), 24148-63; (c) Li, H.; Cai, Z.; Chen, J. H.; Ju, M.; Xu, Z.; Sheppard, D. N., The cystic fibrosis transmembrane conductance regulator Cl(-) channel: a versatile engine for transepithelial ion transport. *Sheng Li Xue Bao* **2007**, *59* (4), 416-30.
145. Shackelford, T. J.; Claret, F. X., JAB1/CSN5: a new player in cell cycle control and cancer. *Cell Div* **2010**, *5*, 26.
146. Pinheiro, A. S.; Marsh, J. A.; Forman-Kay, J. D.; Peti, W., Structural signature of the MYPT1-PP1 interaction. *J Am Chem Soc* **2011**, *133* (1), 73-80.
147. Martinez-Lemus, L. A.; Hill, M. A.; Meininger, G. A., The plastic nature of the vascular wall: a continuum of remodeling events contributing to control of arteriolar diameter and structure. *Physiology* **2009**, *24*, 45-57.

148. (a) Xia, D.; Stull, J. T.; Kamm, K. E., Myosin phosphatase targeting subunit 1 affects cell migration by regulating myosin phosphorylation and actin assembly. *Exp Cell Res* **2005**, *304* (2), 506-17; (b) Matsumura, F.; Hartshorne, D. J., Myosin phosphatase target subunit: Many roles in cell function. *Biochem Biophys Res Commun* **2008**, *369* (1), 149-56; (c) Eto, M.; Kirkbride, J. A.; Brautigan, D. L., Assembly of MYPT1 with protein phosphatase-1 in fibroblasts redirects localization and reorganizes the actin cytoskeleton. *Cell Motil Cytoskeleton* **2005**, *62* (2), 100-9.
149. Birukova, A. A.; Smurova, K.; Birukov, K. G.; Usatyuk, P.; Liu, F.; Kaibuchi, K.; Ricks-Cord, A.; Natarajan, V.; Alieva, I.; Garcia, J. G.; Verin, A. D., Microtubule disassembly induces cytoskeletal remodeling and lung vascular barrier dysfunction: role of Rho-dependent mechanisms. *J Cell Physiol* **2004**, *201* (1), 55-70.
150. Serrano, I.; McDonald, P. C.; Lock, F.; Muller, W. J.; Dedhar, S., Inactivation of the Hippo tumour suppressor pathway by integrin-linked kinase. *Nat Commun* **2013**, *4*, 2976.
151. Kiss, A.; Lontay, B.; Becsi, B.; Markasz, L.; Olah, E.; Gergely, P.; Erdodi, F., Myosin phosphatase interacts with and dephosphorylates the retinoblastoma protein in THP-1 leukemic cells: its inhibition is involved in the attenuation of daunorubicin-induced cell death by calyculin-A. *Cell Signal* **2008**, *20* (11), 2059-70.
152. Yamashiro, S.; Yamakita, Y.; Totsukawa, G.; Goto, H.; Kaibuchi, K.; Ito, M.; Hartshorne, D. J.; Matsumura, F., Myosin phosphatase-targeting subunit 1 regulates mitosis by antagonizing polo-like kinase 1. *Dev Cell* **2008**, *14* (5), 787-97.
153. Li, J.; Liu, X.; Liao, J.; Tian, J.; Wang, J.; Wang, X.; Zhang, J.; Xu, X., MYPT1 sustains centromeric cohesion and the spindle-assembly checkpoint. *J Genet Genomics* **2013**, *40* (11), 575-8.

154. Geetha, T.; Langlais, P.; Caruso, M.; Yi, Z., Protein phosphatase 1 regulatory subunit 12A and catalytic subunit delta, new members in the phosphatidylinositide 3 kinase insulin-signaling pathway. *J Endocrinol* **2012**, *214* (3), 437-43.
155. Xue, G.; Hemmings, B. A., PKB/Akt-dependent regulation of cell motility. *J Natl Cancer Inst* **2013**, *105* (6), 393-404.
156. Xiao, L.; Gong, L. L.; Yuan, D.; Deng, M.; Zeng, X. M.; Chen, L. L.; Zhang, L.; Yan, Q.; Liu, J. P.; Hu, X. H.; Sun, S. M.; Liu, J.; Ma, H. L.; Zheng, C. B.; Fu, H.; Chen, P. C.; Zhao, J. Q.; Xie, S. S.; Zou, L. J.; Xiao, Y. M.; Liu, W. B.; Zhang, J.; Liu, Y.; Li, D. W., Protein phosphatase-1 regulates Akt1 signal transduction pathway to control gene expression, cell survival and differentiation. *Cell Death Differ* **2010**, *17* (9), 1448-62.
157. Lee, J. H.; Ragolia, L., AKT phosphorylation is essential for insulin-induced relaxation of rat vascular smooth muscle cells. *Am J Physiol Cell Physiol* **2006**, *291* (6), C1355-65.
158. Fang, X.; Yu, S. X.; Lu, Y.; Bast, R. C., Jr.; Woodgett, J. R.; Mills, G. B., Phosphorylation and inactivation of glycogen synthase kinase 3 by protein kinase A. *Proc Natl Acad Sci U S A* **2000**, *97* (22), 11960-5.
159. Sit, S. T.; Manser, E., Rho GTPases and their role in organizing the actin cytoskeleton. *J Cell Sci* **2011**, *124* (Pt 5), 679-83.
160. Chen, Y.; Yang, Z.; Meng, M.; Zhao, Y.; Dong, N.; Yan, H.; Liu, L.; Ding, M.; Peng, H. B.; Shao, F., Cullin mediates degradation of RhoA through evolutionarily conserved BTB adaptors to control actin cytoskeleton structure and cell movement. *Mol Cell* **2009**, *35* (6), 841-55.

161. Wu, J. T.; Lin, H. C.; Hu, Y. C.; Chien, C. T., Neddylation and deneddylation regulate Cul1 and Cul3 protein accumulation. *Nat Cell Biol* **2005**, 7 (10), 1014-20.
162. (a) Martin, D. S.; Wang, X., The COP9 signalosome and vascular function: intriguing possibilities? *Am J Cardiovasc Dis* **2015**, 5 (1), 33-52; (b) Leck, Y. C.; Choo, Y. Y.; Tan, C. Y.; Smith, P. G.; Hagen, T., Biochemical and cellular effects of inhibiting Nedd8 conjugation. *Biochem Biophys Res Commun* **2010**, 398 (3), 588-93.
163. Mitra, S. K.; Hanson, D. A.; Schlaepfer, D. D., Focal adhesion kinase: in command and control of cell motility. *Nat Rev Mol Cell Biol* **2005**, 6 (1), 56-68.

ABSTRACT**DEVELOPMENT OF TOOLS FOR PHOSPHOSITE-SPECIFIC KINASE IDENTIFICATION AND DISCOVERY OF PHOSPHATASE SUBSTRATES**

by

PAVITHRA DEDIGAMA ARACHCHIGE**May 2017****Advisor:** Dr. Mary Kay Pflum**Major:** Chemistry (Biochemistry)**Degree:** Doctor of Philosophy

Phosphorylation is a ubiquitous post translational modification implicated in many diseases, such as cancer. The phosphorylation status of cellular proteins is regulated by the activity of kinases and phosphatases. The biological significance of many phosphorylation events remain unknown because the methods to determine which kinase or phosphatase is responsible for phosphorylation are limited. Previously, we established kinase-catalyzed labeling where kinases accept γ -modified ATP analogs, such as ATP-arylazide and ATP-biotin, to label phosphoproteins. To study substrates of kinases and phosphatases, here we developed two new methods using kinase-catalyzed labeling. As one application, we developed K-CLASP (Kinase-catalyzed CrossLinking And Streptavidin Purification) to identify the in-cellulo kinase of a phosphorylated site on a protein. In this case, we used ATP-arylazide to mediate crosslinking between a biotin tagged peptide carrying a phosphosite of interest and the respective kinase. Using Protein kinase A (PKA) and its known peptide substrate kemptide, we demonstrated that K-CLASP is capable of identifying PKA as the kinase responsible for kemptide phosphorylation in cell lysates. Then we used K-CLASP to identify the kinases that

phosphorylate S178 of the Miz1 protein in a collaboration project. For phosphatase substrate identification, we developed K-BIPS (Kinase-catalyzed Biotinylation to Identify Phosphatase Substrates). In prior work, we observed that labeling of phosphoproteins by ATP-biotin is reduced when phosphatases are inactive. The phosphatase dependency of biotinylation is due to the presence of already existing phosphorylation, which prevents ATP-biotin labeling. Therefore, in K-BIPS, ATP-biotin labeling is carried out after the inactivation of a particular phosphatase. The loss in biotinylation can then be analyzed to reveal substrates. To establish K-BIPS as a viable method, we carried out ATP-biotin labeling in lysates treated with the general phosphatase inhibitor okadaic acid. Many known phosphatase substrates were observed validating our method. Then as further applications, we used K-BIPS to explore substrates of PP1-Gadd34 and PP1-MYPT1 phosphatase complexes. The results demonstrate that K-BIS-Phos is a feasible method for phosphatase substrate identification. In summary, we have developed two chemical tools based on kinase-catalyzed labeling that will enhance our understanding of phosphorylation events mediated by kinases and phosphatases.

AUTOBIOGRAPHICAL STATEMENT

PAVITHRA DEDIGAMA ARACHCHIGE

Education

- ❖ **Wayne State University, Detroit, MI (August, 2011-Present)**
Ph.D. Department of Chemistry, Major in Biochemistry. GPA: 3.94. Advisor: Mary Kay Pflum. Dissertation: Development of tools for phosphosite-specific kinase identification and discovery of phosphatase substrates.
- ❖ **University of Colombo, Sri Lanka (August, 2006-August, 2010)**
Bachelor of Science (B.Sc). Major in Biochemistry and Molecular Biology. GPA: 3.5, First Class Honors. Dissertation: : “Real Time PCR based High Resolution Melting Analysis to detect JAK2 mutation”

Publications

- ❖ **Dedigama-Arachchige, P. M.**; Chinthaka, N.; Pflum, M. K., K-BIPS, A method for phosphatase substrate identification. Manuscript in preparation.
- ❖ **Dedigama-Arachchige, P. M.**; Zhang, X.; Yi, Z.; Pflum, M. K., Identification of PP1-MYPT1 substrates in L6 myoblasts. Manuscript in preparation.
- ❖ Garre, S.; Faner, T.; **Dedigama-Arachchige, P. M.**; Pflum, M. K., “Kinase-catalyzed Crosslinking and Immunoprecipitation (K-CLIP) is a Kinase-substrate Identification Tool: Application to p53” Manuscript in preparation.
- ❖ **Dedigama-Arachchige, P. M.**; Pflum, M. K., K-CLASP: A tool to identify phosphosite specific kinases and interacting proteins. *ACS Chem Biol*, 2016, In press
- ❖ Anthony, T. M.; **Dedigama-Arachchige, P. M.**; Embogama, D. M.; Faner, T. R.; Fouda, A. E.; Pflum, M.K. ATP analogs in protein kinase research. *Kinomics: Approaches and Applications*, Martic, S.; Kraatz, H. B., Eds. VCH-Wiley: 2014 (All authors contributed equally to this work)

Presentations

- ❖ **Dedigama-Arachchige, P.M & Pflum, M.K.** *Exploiting kinase-catalyzed labeling to unravel the cellular phosphorylation network.* **Gordon Research Conference – Bioorganic Chemistry, Andover, NH. June 2016**
- ❖ **Dedigama-Arachchige, P.M & Pflum, M.K.** *Exploiting kinase-catalyzed labeling to unravel the cellular phosphorylation network.* **47th Central Regional Meeting (CERM) –American Chemical Society. Covington, KY. May 2016**
- ❖ **Dedigama-Arachchige, P.M & Pflum, M.K.** *Exploiting kinase cosubstrate promiscuity to identify phosphatase substrates.* **7th Annual Midwest Graduate Research Symposium, University of Toledo. April 2016**